Author/s:
Sharma, Ashish Kumar

Title:
Evaluation of renal bone disease: advancing our understanding of associations and diagnostic challenges

Date:
2020

Persistent Link:
https://hdl.handle.net/11343/241795

Evaluation of renal bone disease: advancing our understanding of associations and diagnostic challenges

ASHISH KUMAR SHARMA

ORCID identifier 0000-0002-4205-1098

Doctor of Philosophy

April 2020

Department of Medicine (RMH)
Faculty of Medicine, Dentistry and Health Sciences

Department of Nephrology, The Royal Melbourne Hospital

Submitted in total fulfilment for the degree of
Doctor of Philosophy

ABSTRACT

In patients with chronic kidney disease (CKD), disordered mineral metabolism, deterioration in bone quality and extra-skeletal calcification constitute the clinical syndrome known as chronic kidney disease – mineral and bone disorder (CKD–MBD). Renal osteodystrophy (ROD) is the skeletal component of CKD-MBD, and refers to abnormalities of bone turnover, mineralisation, volume, linear growth or strength. The erosion of bone quality in CKD confers an excess fracture risk through stages of CKD, is not attenuated by kidney transplantation and can be associated with persistent hyperparathyroidism in kidney transplant recipients (KTRs). The currently available tools in clinical practice have limited utility in evaluating ROD and add to diagnostic and therapeutic uncertainty in this area. The mechanisms of bone loss after transplantation and their relationship with changes in bone structure and markers of mineral metabolism are poorly understood. Tackling these challenges requires an enhanced understanding of the pathophysiology of ROD and development of tools for accurate evaluation of renal bone disease.

The advent of high-resolution (HR) imaging and newer biomarkers has provided greater insight and generated research interest in CKD-MBD. HR imaging studies of bone microarchitecture have highlighted the contribution of cortical bone structure to overall bone strength and its association with hyperparathyroidism and bone fragility in KTRs and patients with CKD. HR magnetic resonance imaging (MRI) using customised processing techniques has proven to be an excellent non-invasive tool for studying bone microarchitecture.

My research explored prevalent bone and mineral metabolism abnormalities and the role of various contemporary imaging modalities, in particular MRI, in evaluation of ROD. **Chapter 2**, a cross-sectional study of histological abnormalities of bone in a relatively young cohort of potential KTRs, highlights severe deterioration of cortical microarchitecture but predominantly normal trabecular parameters, reinforcing the importance of comprehensive cortical bone evaluation in patients with CKD. **Chapter 3** describes a proof-of-concept evaluation of bone microarchitecture in patients with CKD using MRI with findings correlated to those obtained by bone biopsy and other bone imaging techniques (Dual-energy X-ray absorptiometry, DXA; peripheral quantitative computed tomography, pQCT; trabecular bone score, TBS), to highlight advantages of MRI as a diagnostic tool in ROD. MRI demonstrated significant and relevant associations with important bone biopsy and DXA parameters but could not establish a reliable relationship with bone turnover. No associations were observed with bone turnover markers. This study also underlined the inherent heterogeneity of bone microarchitecture at differing skeletal sites and the pitfalls of assessing these and comparing imaging modalities with vastly different resolutions and protocols. The study described in **Chapter 4** monitored changes in bone density and microarchitecture in KTRs over one year after transplantation using MRI, DXA, pQCT and TBS and biomarkers. Trabecular bone structure and connectivity deteriorated independent of changes in BMD but associated with PTH levels, complemented by significant reduction in TBS. Unlike in other contemporary studies, there was no progressive deterioration in cortical bone. **Chapter 5** describes an exploration of mineral metabolism and clinical outcomes after transplantation in a large cohort of KTRs, focusing on the impact of discontinuation of cinacalcet on these parameters. Persistent post-transplantation hyperparathyroidism and hypercalcaemia, consistent with available data, was demonstrated, but the clinical significance of these mineral metabolism

markers was unclear. Historically, aluminium deposition in bone was recognised as a major cause of adynamic bone disease but is now less relevant due to increasingly rare use and phasing out of aluminium-containing phosphate binders in clinical practice. However, many centres continue to routinely screen dialysis patients for aluminium levels. The study in **Chapter 6** examined the utility of routine testing of serum aluminium levels in the haemodialysis population in our centre via a retrospective audit of tests performed on 755 patients over four years. Only 0.5% of 2058 test results matched criteria for toxic aluminium levels, with no evidence of clinical toxicity and progressive reduction in the proportion of elevated aluminium levels over the years. This led to cessation of routine testing of aluminium levels in our dialysis unit.

In conclusion, clinical studies presented in this thesis add to the increasing body of literature about the bone abnormalities prevalent in CKD and highlight the novel use of MRI in assessing bone quality in CKD and in KTRs. Overall, non-invasive HR imaging, particularly MRI, has the potential to close the vast gap between screening of BMD using DXA and comprehensive diagnosis by bone biopsy. This needs validation in large trials with hard clinical endpoints and should be viewed in the context of a plethora of technical caveats and issues of high cost and availability. The utility of MRI (and other HR imaging) would be enhanced by more accurate and reliable non-invasive markers of bone turnover and mineralisation. These challenges are significant, but not insurmountable. A coordinated, multidisciplinary, patient-focused effort is needed from the nephrology research community to address the unmet needs of patients with ROD and CKD-MBD.

GENERAL DECLARATION

I hereby declare that

1. this thesis comprises only my original work towards the degree of a Doctor of Philosophy, except where indicated in the preface
2. due acknowledgement has been made in the text to methodology and materials
3. the thesis is fewer than 100,000 words in length, exclusive of tables, bibliographies and appendices.

Signed:

Dr Ashish Kumar Sharma

Department of Medicine (RMH), University of Melbourne

Department of Nephrology, The Royal Melbourne Hospital

Parkville, Australia.

April 2020

PREFACE

The author performed the work described in this thesis except where due credit is given. Collaborators' contributions are detailed below.

Chapters 2 and 3 – Bone Histomorphometry and micro-CT

The studies described in these chapters required undertaking iliac crest bone biopsies and their assessment using both conventional histomorphometry and micro-CT-based evaluation of bone microarchitecture. Professor Stephen Holt and Dr Emma Tully (The Royal Melbourne Hospital) performed the biopsies; Professor Grahame Elder, Dr Paul Baldock and Ms Sindhu Mohanty (Osteoporosis and Bone Biology Division, Garvan Institute of Medical Research) undertook and reported the histomorphometry assessments.

Chapters 2 and 4 – MRI distal tibia

The MRI scans described in these chapters were performed at The Royal Melbourne Hospital as per protocol. The acquired images were then processed, analysed and reported by A/Prof Chamith Rajapakse and his team at the Departments of Radiology and Orthopaedic Surgery, University of Pennsylvania, PA, USA. Ms Susan Harvey performed the DXA and pQCT scans.

Publications

This thesis includes seven original papers published in peer-reviewed journals. My principal supervisor completed a "Declaration for a thesis with publication" form, and my co-authors completed Co-author authorisation forms that have been submitted separately online. Copies of the original publications are included in the Appendix. This thesis contains no material that

has been accepted for the award of any other degree or diploma at any university or equivalent institution.

The publication status of each manuscript included within this thesis is listed in the following table. Each manuscript contains individual reference sections and journal page numbers, which have not been reformatted for this thesis.

Thesis Chapter	Publication title	Publication status	Candidate's contribution
1	**Sharma AK** et al. Emerging role of high-resolution imaging in the detection of renal osteodystrophy	*Nephrology* 2016; 21(10):801-11	90%
1	**Sharma AK** and Toussaint ND. Is there a practical role for a virtual bone biopsy using high-resolution imaging of bone in patients with chronic kidney disease?	*Nephrology* 2017. 22: 27-30.	90%
2	**Sharma AK** et al. Deterioration of Cortical Bone Microarchitecture: Critical Component of Renal Osteodystrophy Evaluation	*American Journal of Nephrology* 2018. **47**(6): p. 376-384	75%
3	**Sharma AK** et al. Magnetic resonance imaging based assessment of bone	*Bone* 2018. **114**: p. 14-21	80%

	microstructure as a non-invasive alternative to histomorphometry in patients with chronic kidney disease		
4	**Sharma AK** et al. Changes in bone microarchitecture following kidney transplantation – beyond bone mineral density	*Clinical Transplantation* 2018. **32**(9): p. e13347	85%
5	**Sharma AK** et al. Assessing the utility of testing aluminum levels in dialysis patients	*Hemodialysis International* 2015;19(2):256-62	80%
6	**Sharma AK**, et al. Impact of cinacalcet pre-transplantation on mineral metabolism in renal transplant recipients	*Nephrology* 2016; 21(1):46-54	75%

ACKNOWLEDGEMENTS

The work presented in this thesis was primarily carried out in the Department of Nephrology at The Royal Melbourne Hospital, and would not have been possible without the support of the staff members and the participation of many patients. I would also like to acknowledge and thank the Department of Nephrology, The Royal Melbourne Hospital for providing me with a scholarship for two years to support my research work. I also want to extend my thanks to the MRI team at Department of Radiology, The Royal Melbourne Hospital, for setting up and conducting the MRI scans.

This thesis would not have materialised without the expertise, guidance and support of many individuals. I wish to acknowledge and thank the following people for their contributions towards this work.

Associate Professor Nigel D Toussaint (Principal Supervisor), for giving me the opportunity to undertake this PhD. I owe him my never-ending gratitude for his infinite patience, dedication, mentorship and unstinting support, not only with respect to my research but my well-being. His work ethic and commitment to clinical research in the field of bone and mineral metabolism has provided me with the foundation and passion for ongoing research in this field.

Associate Professor Rosemary Masterson (Co-supervisor), for the opportunity to undertake this project. I am grateful for her support, mentorship and invaluable suggestions. Her

insightful contributions to various publications presented in this thesis greatly added to the clarity of the overall message.

Professor Stephen G Holt, for the opportunity to undertake this project and for his expertise and guidance in completing it. I am grateful for his encouragement and kindness towards me within and outside the purview of this project.

Professor Grahame Elder, for sharing his expertise in the field of CKD-MBD and bone histomorphometry, for his meticulous approach to research work and insightful contributions to some of the publications in this thesis. I am also grateful to him for handling my endless queries and enhancing my knowledge.

Associate Professor Chamith Rajapakse, for applying his vast expertise in the niche field of evaluation of bone microarchitecture by MRI to patients with CKD and for his technical and moral support.

Professor Peter R Ebeling, for his role in the conception of this project and for his support, advice and contribution as a co-author.

Dr Patricia L Robertson, for her work, support and advice related to MRI scans.

Dr Paul Baldock, for his work, support and advice on bone histomorphometry.

Ms Susan Harvey, not only for her help with conducting DXA and pQCT scans, but for her cheerful and ever-present support of this project.

Dr Sven-Jean Tan and **Dr Michael Cai**, my PhD colleagues, for their kindness and encouragement and for helping me negotiate my initial steps into my research endeavours.

Dr Campbell Aitken provided professional editing assistance in line with Preparation of Graduate Research Theses Rules and the Institute of Professional Editors' *Guidelines for editing research theses*.

Finally, I thank my family for accepting my commitment to this work and for their unfailing support during the project. I thank my parents and my parent in-laws for their abiding love and blessings for all my endeavours and my young daughter **Aarna** for her unconditional love and for giving me perspective throughout this long journey. My greatest thanks are to my wife **Kalpana** for her infinite patience, never-ending encouragement and love, without which none of this would have been possible.

TABLE OF CONTENTS

ABBREVIATIONS AND ACRONYMS

aBMD	areal BMD
Al	Aluminium
ALP	Alkaline phosphatase
ANZSN	Australian and New Zealand Society of Nephrology
AUC	Area under the curve
β-CTx	Beta-cross linked telopeptide
BFR	Bone formation rate
BMD	Bone mineral density
BMP	Bone morphogenic protein
BVF	Bone volume fraction
bALP	Bone-specific alkaline phosphatase
calcitriol	1,25-dihydroxyvitamin D
CKD	Chronic kidney disease
CT	Computed tomography
CTX	C-terminal telopeptides of type I collagen
CV	Coefficients of variance
dkk-1	Dickkopf1
DXA	Dual-energy X-ray absorptiometry
EI	Erosion index
ESKD	End-stage kidney disease
FEA	Finite element analysis
FGF-23	Fibroblast growth factor 23
GFR	Glomerular filtration rate
HD	Haemodialysis
HR	High resolution
HR-pQCT	High-resolution peripheral quantitative computed tomography
iPTH	Intact parathyroid hormone
KDIGO	Kidney Disease Improving Global Outcomes
KTR	Kidney transplant recipient
MAR	Mineral apposition rate

MBD	Mineral and bone disorder
Micro-CT	Micro-computed tomography
MRI	Magnetic resonance imaging
NTX	N-terminal telopeptides of type I collagen
OPG	Osteoprotegerin
OR	Odds ratio
pQCT	peripheral quantitative computed tomography
PTH	Parathyroid hormone
P1NP	Procollagen type 1 N-terminal propeptide
QCT	Quantitative computed tomography
RF	Radiofrequency
RMH	The Royal Melbourne Hospital
RO	Reverse osmosis
ROC	Receiver operating characteristic
ROD	Renal osteodystrophy
ROI	Region of interest
$1,25[OH]_2D$	Serum 1,25-dihydroxyvitamin D
25(OH)D	Serum 25-hydroxyvitamin D
SHPT	Secondary hyperparathyroidism
SNR	Signal to noise ratio
S/C	Surface to curve ratio
TBS	Trabecular bone score
TMV	Turnover, mineralisation and volume
TRAP5b	Tartrate-resistant acid phosphatase 5b
3D	Three-dimensional
2D	Two-dimensional
USA	United States of America
UTE	Ultrashort-echo-time
vBMD	Volumetric BMD

LIST OF PUBLICATIONS

The following manuscripts, resulting directly from the work presented in this thesis, were published during my PhD candidature.

1. **AK Sharma,** ND Toussaint, GJ Elder, R Masterson, SG Holt, PL Robertson, PR Ebeling, P Baldock, RC Miller and CS Rajapakse. Magnetic resonance imaging based assessment of bone microstructure as a non-invasive alternative to histomorphometry in patients with chronic kidney disease. *Bone* 2018; **114**: 14-21.
2. **AK Sharma,** ND Toussaint, GJ Elder, CS Rajapakse, SG Holt, P Baldock, PL Robertson, PR Ebeling, OR Sorci and R Masterson. Changes in bone microarchitecture following kidney transplantation – beyond bone mineral density. *Clinical Transplantation* 2018; **32**(9): e13347.
3. **AK Sharma,** ND Toussaint, R Masterson, SG Holt, CS Rajapakse, PR Ebeling, ST Mohanty, P Baldock and GJ Elder. Deterioration of cortical bone microarchitecture: critical component of renal osteodystrophy evaluation. *American Journal of Nephrology*, 2018; **47**(6): 376-384
4. **AK Sharma** and ND Toussaint. Is there a practical role for a virtual bone biopsy using high-resolution imaging of bone in patients with chronic kidney disease? *Nephrology* 2017; **22**: 27-30.
5. **AK Sharma**, R Masterson, SG Holt, ND Toussaint. Emerging role of high-resolution imaging in the detection of renal osteodystrophy. *Nephrology* 2016; **21**(10): 801-11.

6. **AK Sharma**, R Masterson, SG Holt, SJ Tan, PD Hughes, M Chu, P Jayadeva and ND Toussaint. Impact of cinacalcet pre-transplantation on mineral metabolism in renal transplant recipients. *Nephrology*. 2016; **21**(1):46-54.
7. **AK Sharma**, ND Toussaint, J Pickering, T Beeston, ER Smith and SG Holt. Assessing the utility of testing aluminum levels in dialysis patients. *Hemodialysis International*. 2015; **19**(2):256-62.

LIST OF CONFERENCE PRESENTATIONS

The following conference abstracts, directly related to the work in this thesis, were presented at national or international scientific meetings during my PhD candidature.

1. **Sharma AK**, ND Toussaint, SG Holt, AJ Johncola, CS Rajapakse, R Masterson, GJ Elder and P Baldock. Deterioration of cortical bone microarchitecture in renal osteodystrophy – under-represented in the 'Turnover Mineralisation Volume' (TMV) classification?
    a. Abstract & Poster – Kidney Week, American Society of Nephrology, New Orleans, USA, October 31 – November 5, 2017
    b. Mini-oral & Abstract – 53rd Annual Scientific Meeting of the Australian and New Zealand Society of Nephrology (ANZSN), Darwin, NT, Australia, September 2-6, 2017
2. **Sharma AK,** NT Toussaint, SG Holt, Kiara Honma, C Rajapakse and R Masterson. Bone disease after kidney transplantation – looking beyond bone mineral density.
    a. Abstract & Poster – Kidney Week, American Society of Nephrology, New Orleans, USA, October 31 – November 5, 2017
3. **AK Sharma, ND** Toussaint, GJ Elder, SG Holt, PL Robertson, PR Ebeling, P Baldock, CS Rajapakse and R Masterson. High-resolution magnetic resonance imaging to assess bone microarchitecture in patients with chronic kidney disease.
    a. Mini-oral & Abstract – 15th Asian Pacific Congress of Nephrology and 52nd Annual Scientific Meeting of the ANZSN, Perth, WA, Australia, September 17 – 21, 2016
    b. Royal Melbourne Hospital Research Week 2016

4. **Sharma AK** and Toussaint ND. Is there a practical role for a virtual bone biopsy using high-resolution imaging of bone in patients with chronic kidney disease?
    a. Oral presentation – CKD-MBD Controversies and Directions: a workgroup of members of the ANZSN and Australian and New Zealand Bone and Mineral Society (ANZBMS), Canberra, ACT, Australia, September 6, 2015
5. **AK Sharma**, R Masterson, SJ Tan, PD Hughes, SG Holt and ND Toussaint. Impact of cinacalcet pre-transplantation on mineral metabolism in renal transplant recipients.
    a. Poster & Abstract – Kidney Week 2014, American Society of Nephrology, Philadelphia, PA, USA, November 11-16, 2014
    b. Poster & Abstract – 50th Annual Scientific Meeting of the ANZSN, Melbourne, VIC, Australia, August 25-27, 2014
6. **AK Sharma**, ND Toussaint, J Pickering, T Beeston, ER Smith, SG Holt. Assessing the utility of testing aluminium levels in dialysis patients.
    a. Poster & Abstract – Kidney Week 2014, American Society of Nephrology, Philadelphia, PA, USA, November 11-16, 2014
    b. Poster & Abstract – 50th Annual Scientific Meeting of the ANZSN, Melbourne, VIC, Australia, August 25-27, 2014

CHAPTER 1: INTRODUCTION AND LITERATURE REVIEW

The research presented in this chapter has been published in the following articles.

AK Sharma, R Masterson, SG Holt, ND Toussaint. Emerging role of high-resolution imaging in the detection of renal osteodystrophy. *Nephrology*. 2016; **21**(10):801-11.

AK Sharma and ND Toussaint. Is there a practical role for a virtual bone biopsy using high-resolution imaging of bone in patients with chronic kidney disease? *Nephrology*, 2017. 22: 27-30.

Author affiliations

Ashish K SHARMA[1,2], Rosemary Masterson[1,2], Stephen G HOLT[1,2], Nigel D TOUSSAINT[1,2]

[1]*The Royal Melbourne Hospital, Parkville, Victoria, Australia;*

[2]*Department of Medicine (RMH), The University of Melbourne, Melbourne, Australia*

Chronic kidney disease – mineral and bone disorder and renal osteodystrophy

Chronic kidney disease (CKD) is a public health problem affecting 10–15% of the global population, and is associated with adverse outcomes including progressive loss of kidney function, disorders of mineral metabolism, fractures, cardiovascular disease and reduced life expectancy [1-8]. Although estimates of CKD prevalence vary between countries, the prevalence and associated burden of CKD is rising worldwide [9].

In people with normal kidney function, the interaction of parathyroid hormone (PTH), 1,25-dihydroxyvitamin D (calcitriol), and fibroblast growth factor 23 (FGF-23) and their actions on bone, kidney, intestine and parathyroid glands are responsible for maintaining normal serum calcium and phosphate levels. The kidneys have a central role in regulation of these hormones and calcium and phosphate homeostasis. Early deterioration in kidney function is accompanied by decrease in renal synthesis of 1,25-dihydroxyvitamin D and characteristic compensatory increase in FGF-23 and PTH levels to maintain normal calcium and phosphate levels. Progression of kidney disease and a further decrease in glomerular filtration rate (GFR) results in an overwhelming of these compensatory mechanisms and disruption of bone and mineral metabolism. The resultant abnormalities in bone turnover, mineralisation and volume [10, 11] deleteriously affect all levels of bone structure and material hierarchy, collectively referred to as bone quality [12-14]. This deterioration in bone quality culminates in compromised bone strength and greater susceptibility to fracture [14, 15], a common and serious clinical outcome of CKD. Moreover, mineral and bone abnormalities in CKD are associated with significant extra-skeletal calcification and increased burden of cardiovascular disease [16]. The altered biochemical milieu due to disordered mineral metabolism,

deterioration in bone quality and extra-skeletal calcification constitute the clinical syndrome known as chronic kidney disease – mineral and bone disorder (CKD–MBD) [17]. Renal osteodystrophy (ROD), as currently defined, is the skeletal component of CKD–MBD and refers to abnormalities of bone turnover, mineralisation, volume, linear growth, or strength encountered in CKD [18].

Evolution of renal osteodystrophy – from bystander to central player?

The earliest known accounts of bone disease associated with CKD date from 1883, when Clement Lucas described "rickets of adolescents" in a case series of adolescents presenting with clinical features consistent with rickets and albuminuria [19]. This was ascribed to malnutrition and "defective diet". Von Recklinghausen, a German pathologist, made a more robust association of bone disorder with CKD in 1890, describing osteitis fibrosis cystica and osteomalacia in hyperparathyroidism [20, 21]. Subsequently, in the first quarter of the twentieth century, various researchers described cases of rickets attributed to renal insufficiency, interstitial nephritis or hyperparathyroidism [22-24]. In 1942, S H Liu and H I Chu proposed "renal osteodystrophy" as a "suitable generic name for osseous disorders simulating rickets, osteomalacia or osteitis fibrosis cystica, but originating from chronic renal insufficiency", conceding that the "exact nature of the pathological process in the skeleton is still undetermined" [25, 26]. They described abnormal calcium and phosphate balance in five patients with varying degrees of CKD. In these patients, hypocalcaemia and phosphate retention was unresponsive to treatment with vitamin D but responded favourably to dihydrotachysterol, a synthetic vitamin D analogue. They also noted a decrease in phosphate following iron intake (prescribed for anaemia) in a pregnant woman.

During the 1950s and earlier, bone changes related to CKD were mostly attributed to secondary hyperparathyroidism (SHPT), deranged calcium and phosphate metabolism and defective production of vitamin D by the kidney. The corresponding bone abnormalities were noted to be osteitis fibrosa related to secondary hyperparathyroidism and defective mineralisation or osteomalacia [27-29], the latter thought to occur earlier in the course of CKD. In the second half of the twentieth century, the discovery and use of tetracycline as a bone marker to define dynamic bone formation [30, 31] was another important development, sparking further interest and providing more insight into the pathophysiology of ROD.

With the advent of dialysis in 1960 [32-34] and resultant improved life expectancy of patients with CKD, there came increased recognition of bone abnormalities. In 1966, Pendras and Erikson published a comprehensive account of their clinical experience with a cohort of 22 patients on haemodialysis [35]. Notably, nine of 19 patients (three patients died) had ROD characterised by elevated alkaline phosphatase (ALP), bone tenderness, rib fractures and, in one case, fracture of the hip. Moreover, response to therapy with vitamin D in these patients was unpredictable. Johnson *et al.* reported gross skeletal and soft tissue radiological manifestations of CKD in a series of 33 patients undergoing "periodic haemodialysis" for up to 15–36 hours per week [36]. The lesions included those related to bone resorption or "hypomineralisation" and frequently soft tissue calcification, with partial reversibility seen in the latter with the use of phosphate binders. In 1971, calcitriol was identified as the physiologically active metabolite of vitamin D [37] synthesised in the kidney, and was used successfully to reverse histological manifestations of hyperparathyroidism [38]. The prevailing heterogeneity of bone abnormalities during this period was further underlined by

histomorphometric findings of a mixture of features of osteoclastic resorption and osteomalacia (mixed uraemic osteodystrophy) [39].

Another significant bone abnormality identified in the 1970s was related to aluminium toxicity due to contamination of the dialysate water and heavy use of aluminium-based phosphate binders. This was also associated with the finding of dialysis encephalopathy syndrome [40-42]. Bone abnormalities due to aluminium manifested in the form of osteomalacia, which was unresponsive to calcitriol therapy [43]. This was noted to occur either in the presence of stainable aluminium in the bone or just as a low bone turnover condition without significant aluminium staining, the latter defined as adynamic bone disease [44]. Over the subsequent decade the incidence of aluminum bone disease significantly decreased, due to improved dialysis water purification and the decline in prescription of aluminium-based phosphate binders to patients with CKD. Since the era of aluminum toxicity, histomorphometric studies in ROD demonstrated a consistent trend of increasing proportion of low-turnover bone disease and a decrease in mineralisation abnormalities in CKD patients [45-48], in contrast to the predominance of hyperparathyroidism-related osteitis fibrosa in earlier decades. There has also been an increase in understanding of bone changes corresponding to different stages of CKD, and low-turnover bone disease has been shown to occur in earlier stages of CKD prior to progression to end-stage kidney disease (ESKD) [48-50]. Over the years, several systems have been proposed to classify the various bone abnormalities but were limited by the uniquely complex pathophysiology and inherent heterogeneity of ROD and the difficulty in extrapolating the classification to clinical practice. The more commonly used of these histological classifications was Sherrard's, in 1993, which divided renal bone disorders into mild, osteitis fibrosa, mixed, osteomalacia, and aplastic or

adynamic bone disease [51]. ROD in the current era is classified by quantifiable histomorphometric parameters of turnover, mineralisation and volume (TMV) following a standardised nomenclature for static and dynamic measurements [18, 52].

Traditionally, “renal osteodystrophy” was used as an umbrella term to non-uniformly describe skeletal phenotypes, histological findings and abnormalities of mineral metabolism associated with bone disease. The constellation of bone, mineral, and cardiovascular disorders recognised to be highly prevalent in the setting of CKD is now better encapsulated in the more contemporary designation of CKD–MBD, with ROD referring to its skeletal component [17]. Nevertheless, over the last two decades, the perception of ROD has evolved to include strong epidemiological links between bone metabolism and vascular calcification and a substantially increased risk of cardiovascular morbidity and mortality associated with CKD [7, 16, 53-55]. There is increasing evidence that this is mediated in part by bone-derived substances like FGF-23, Wnt inhibitors (sclerostin and DKK1), osteoprotegerin, osteocalcin and bone morphogenic protein which have distant effects in the setting of CKD [56-60]. This has led to a growing conceptual shift about the role of the skeleton in CKD – from being passively affected by metabolic derangement in CKD to an active inducer or mediator of cardiovascular pathology [53, 59], in addition to the well-known increase in fracture risk with declining GFR in people with CKD [61, 62]. While causality between bone abnormalities and vascular calcification and subsequent cardiovascular outcomes in CKD remains to be firmly established [63], ROD is no longer a mere bystander.

Renal bone disease – why should we care?

Disruption of bone and mineral metabolism and altered biochemical milieu invariably causes erosion in bone quality in patients with CKD. The accumulation of CKD-related bone fragility is likely additive to the traditional risk factors for fractures in the general population. This is reflected in numerous epidemiological studies describing an increased prevalence of fractures in patients with CKD compared to age and gender-matched individuals in the general population [3, 61, 62, 64-66]. The overall risk of sustaining a hip fracture in patients on dialysis is 4–17 times higher than among their age and gender-matched counterparts in the general population [64, 65, 67]. The fracture risk increases in a graded manner with decreasing GFR, while being higher in all stages of CKD than in the general population, independent of traditional risk factors for fracture [61, 62, 68-72]. In elderly patients treated for osteoporosis, creatinine clearance of less than 65 ml/min is an independent risk factor for falls (odds ratio [OR] 1.69) as well as hip (OR 1.57), radial (OR 1.79) and vertebral (OR 1.31) fractures, compared to individuals with creatinine clearance of equal to or more than 65 ml/min [68]. Demographic risk factors for fractures among patients with CKD include increasing age, female gender, Caucasian race, duration of dialysis, diabetes, low body mass, prior kidney transplant and narcotic and psychoactive medications [65, 73, 74]. Higher frequency of fractures in individuals with CKD is also associated with increased adverse outcomes following the fracture. In patients with CKD who sustain fractures, incidence of hospitalisation, morbidity and mortality related to fractures is demonstrably higher than in those without CKD [3, 65, 75-77]. This risk remains significant and is only partially attenuated in competing risk analysis taking excess mortality in CKD into account and adjusting for other likely confounders [78]. Several recent studies of contemporary fracture epidemiology have noted declining rates of hip fracture and associated mortality among dialysis patients since

2003–05 [75, 79-81]. Although these reports are encouraging, the contemporary rates of hip fractures remain high compared to those in the early 1990s and are still many-fold higher than those in the general population [75, 79].

Kidney transplantation is the optimal treatment for ESKD but does not attenuate susceptibility to fracture. Indeed, fracture risk has been reported at up to 34% higher in the first two years post-transplantation than in the preceding period on dialysis [82], with a fracture incidence up to 22.5% over the first five years post-transplantation [83]. In addition, kidney transplant recipients (KTRs) have higher rates of hospitalisation and mortality after fracture than people in the general population [84]. Although reductions in bone mineral density (BMD) after transplantation have been reported extensively, there is a paucity of post-transplant data regarding modifiable risk factors for fracture [85]. Disorders of mineral metabolism, known associates of increased morbidity and mortality in patients with advanced kidney disease [86, 87], also contribute to post-transplantation bone disease. Successful renal transplantation improves calcitriol synthesis with a trend towards normalisation of calcium and phosphate levels, but hyperparathyroidism can persist in up to 50% of renal transplant recipients at one year after transplantation [88, 89]. Hyperparathyroidism and hypercalcemia post-transplantation have been associated with poorer graft outcomes [90, 91], soft tissue and vascular calcification [92], and increased incidence of fractures [93].

Post-transplant bone disease is multifactorial, and includes effects of immunosuppressive therapy, changes in mineral metabolism and the consequences of post-transplant impairment of renal function superimposed on pre-existing ROD [94]. The diagnosis and management of post-transplant bone disease is therefore difficult, with limited validation of available

diagnostic tools to evaluate changes in bone structure or predict fracture risk. Although accelerated loss of BMD in the first year after transplantation has been described as the hallmark of post-transplant bone disease [95-97], recent studies have demonstrated a more conservative estimate of early BMD loss, with long-term values nearer to average for age and gender [98]. The focus of contemporary research has been on change in bone microarchitecture post-kidney transplantation and its relationship to bone fragility and biomarkers [99-103]. A few studies based on histomorphometry have addressed this issue [103-106], and more recently, studies involving non-invasive imaging, such as high-resolution peripheral quantitative computed tomography (HR-pQCT) [100], high-resolution magnetic resonance imaging (MRI) [99, 107] and the Trabecular Bone Score (TBS) [108-111], have focused on defining changes in bone microarchitecture. These are welcome steps in the right direction, but there is a need for further, larger studies given the magnitude of the problem and its potentially devastating consequences.

Evaluating renal osteodystrophy in current clinical practice

Chronic kidney disease affects the entire hierarchical structure of bone, with a varying extent and combination of abnormalities in bone remodelling, collagen crosslinking and mineralisation. The uniqueness and complexity of ROD and its significant additive effect on fracture risk associated with normal ageing underline the need for validated approaches to fracture risk stratification and appropriate prevention and management strategies in patients with CKD. This requires an enhanced understanding of pathophysiology of ROD, its relationship to fracture risk, and development of tools for accurate evaluation and screening of renal bone disease. The currently available tools in routine clinical practice of nephrology include BMD measurement with dual-energy X-ray absorptiometry (DXA), using biomarkers

like PTH, ALP or bone turnover markers, and histomorphometric analysis of iliac crest bone biopsies.

Bone mineral density and dual-energy X-ray absorptiometry

In patients without CKD, osteoporotic fractures are a significant cause of morbidity and mortality [112, 113] and areal BMD (aBMD) is a strong predictor of fracture risk [114]. However, the utility of aBMD measurement in patients with advanced CKD remains unproven and is controversial. DXA is the most widely used, inexpensive, noninvasive screening technique for evaluating BMD with low radiation exposure. Cross-sectional studies assessing the ability of DXA-derived aBMD to discriminate between CKD patients with and without fracture have mostly provided inconsistent results [115-123], and BMD measurement in CKD 4-5 for assessing ROD has not been considered useful in the past [17]. More recent longitudinal studies have reported that low DXA-measured BMD is predictive of future fracture risk in patients with CKD stages 3–5 [124-127]. These results have prompted a revised Kidney Disease Improving Global Outcomes (KDIGO) guideline recommendation to include BMD measurement to assess fracture risk in patients with CKD 3-5D with evidence of CKD-MBD and/or risk factors for osteoporosis if results will influence treatment decisions [128].

Notwithstanding the recent encouraging results for utility of BMD measurements, DXA has several technical limitations when used in the CKD cohort. Areal BMD measurement is unable to distinguish individual trabecular or cortical BMD, which is a significant potential confounder in ROD, given the differential effects of secondary hyperparathyroidism with cortical thinning but relatively preserved trabecular bone mass. Additionally, measurements may be skewed by degenerative bone changes in the spine and extra-skeletal calcification,

especially in the aorta, which can overestimate the spinal bone density score [129]. Lastly, although BMD is an estimate of bone mass, it provides no information about other determinants of bone quality or turnover, which are also significant contributors to bone fragility in CKD.

Bone biomarkers in chronic kidney disease

Bone turnover is an important determinant of bone quality. Both low and high-turnover bone disease are prevalent in patients with CKD [47, 130] and may cause deterioration in bone quality [131]. The availability and development of reliable and accurate biomarkers to non-invasively diagnose extremes of bone turnover, therefore, has an important role in the diagnosis of ROD.

Parathyroid hormone is the most commonly used surrogate marker of bone turnover in the clinical assessment of patients with CKD. Both very low and very high PTH levels correlate with bone turnover consistent with bone histomorphometry [130], but between these extremes the predictive value is weak. Racial differences [47] and hyporesponsiveness of bone to PTH also influence the predictive ability of PTH to define bone turnover status. Adding to the confounding effects of the above, there is significant biologic variation of PTH in patients with CKD, with studies reporting high intraindividual coefficients of variance (CV) for PTH and other biomarkers [132, 133]. Despite these limitations of PTH as a marker of bone turnover, histomorphometry studies exploring the efficacy of bone biomarkers in predicting bone turnover have yet to provide a superior replacement. Bone-specific alkaline phosphatase (bALP), an ectoenzyme of osteoblast, is essential for the mineralisation of osteoid and has shown promise as a marker of turnover or bone formation. One of the largest

bone biopsy studies conducted in dialysis patients found that PTH and bALP levels (or combinations thereof) allowed discrimination of low from non-low and high from non-high turnover, with an area under the receiver operating characteristic (ROC) curve more than 0.70 but less than 0.80 [130].

Other markers of bone turnover can be broadly categorised into markers of bone formation and bone resorption. Osteocalcin and procollagen type 1 N-terminal propeptide (P1NP) are markers of osteoblast function and bone formation. Bone resorption markers include tartrate-resistant acid phosphatase 5b (TRAP5b) and N and C-terminal telopeptides of type I collagen (NTX and CTX) for monitoring osteoclast number and function respectively. However, these serum markers are not widely used clinically because of analytical and biological variability, and in patients with CKD, variable renal clearances and undefined reference ranges (e.g. osteocalcin, CTX and P1NP) make these markers difficult to interpret. Despite this, and partly owing to their independence from kidney function, bALP, TRAP5b and P1NP (trimeric) have emerged as potentially useful markers of bone turnover, and further studies are needed to explore and validate their use.

The last decade has also witnessed an increase in studies using high-resolution imaging modalities to assess bone microarchitecture in CKD. A by-product of these studies is the emerging potential of bone biomarkers to aid in assessment of ROD and to play a role in fracture risk stratification of CKD patients in combination with these techniques. Some cross-sectional and prospective imaging studies in CKD and KTRs have noted strong associations between levels of bone turnover markers and changes in bone mass and architecture which are potentially useful in determining prevalent fractures, predicting bone loss and fracture

risk [100, 124, 134-137]. In a prospective study involving 485 patients on haemodialysis, Iimori *et al.* [124] reported a higher fracture risk with higher bALP, and both low and high PTH levels, as well as low hip BMD. In another study including 143 consecutive KTRs, PTH greater than 130pg/ml at three months after transplantation was an independent predictor of new fractures in the five years post-transplantation [93]. In contrast, other imaging studies have shown inconsistent, absent or only weak correlations between biomarkers and bone microarchitecture [138-140].

Novel circulating biomarkers of bone function include FGF-23 and the Wnt inhibitors (sclerostin and dickkopf1 [dkk-1]). In a prospective trial of patients on haemodialysis, baseline levels of FGF-23 predicted changes in aBMD at the spine and baseline TRAP5b, with sclerostin predicting loss of total vBMD at the hip as measured by quantitative computed tomography (QCT) [134] . In a cross-sectional study of bone histomorphometry in 60 dialysis patients, low sclerostin levels were found to predict high bone turnover better than PTH in adjusted analyses [141]. Low PTH levels, however, were more predictive of low bone turnover. Serum levels of dkk-1 did not correlate with PTH or any histomorphometric parameter. These novel markers display promise but need further development and exploration in larger trials.

Bone biopsy

Bone biopsy is typically performed at the iliac crest after double tetracycline labelling to allow assessment of bone formation rate over time [142, 143], and is currently the only test capable of accurately distinguishing between high, normal and low bone turnover, and of defining mineralisation abnormalities. Histomorphometric analysis of bone biopsy yields information about its structure, static and dynamic formation parameters and mineralisation status, thus

providing the most detailed information about the bone. The complexity of ROD, combined with the limited utility of available diagnostic modalities as stand-alone screening tools for ROD, has put the onus of a definitive diagnosis on bone biopsy. However, bone biopsy and its analysis have their own set of caveats.

Bone biopsy is invasive, requires expertise to perform, process and interpret, and is rarely performed routinely in clinical nephrology practice. Biopsy is performed on the iliac crest because it is a safe and convenient anatomic location. However, the iliac crest is not weight bearing, has a thinner cortex than bones in the axial skeleton, and the trabecular bone in the iliac crest has higher bone turnover. Therefore, histomorphometric analysis of biopsies performed at the iliac crest may not be representative of the whole skeleton [144], in particular of the more fracture-prone, load-bearing bones. In fact, even at the iliac crest, contiguous bone biopsies in the same patient with ROD have been reported to show up to 24% variability in trabecular bone parameters [145]. Recent studies have also reported variability in cortical bone architecture at various sites [146]. Although histomorphometry studies in patients with CKD have described skeletal microstructural and mechanical abnormalities, the few studies designed to examine links between bone histology and fracture have provided mixed results [147, 148]. Despite these shortcomings, bone biopsy captures a comprehensive snapshot of bone microarchitecture, turnover and mineralisation and continues to be the gold standard for the diagnosis of ROD.

Application of high-resolution imaging in renal osteodystrophy

Over the last two decades, the emergence of bone quality as the determinant of bone strength and the need to look beyond BMD for factors contributing to fracture risk has led to

the development and improvement of non-invasive imaging methods for assessing bone microarchitecture. Bone microarchitecture is an important component of bone strength, and methods to assess it may not only improve estimates of bone strength and fracture prediction but enable clarification of the pathophysiology of – and monitoring of response to therapy in – ROD [12, 149].

Nuts and bolts of high-resolution imaging

Bone trabeculae measure 50–400 µm in thickness [150]; therefore, any imaging system applied to *in vivo* non-invasive imaging of bone structure requires a high enough spatial resolution in this range. High-resolution (HR) imaging enables imaging of trabecular and cortical bone micro-structure. Currently used *in vivo* HR imaging modalities – HR-pQCT and HR-MRI – measure and quantify cortical and trabecular geometry, microarchitecture and strength [151-153]. The structural parameters obtained by HR imaging include trabecular thickness, separation and number. Topological analysis of trabeculae (rod and plates) can also be performed and their connectivity assessed. In addition, cortical bone thickness and porosity can be estimated. The structural parameters measured by both these modalities have been validated against the reference standard measurements of bone structure obtained by micro-computed tomography in *ex vivo* and *in vivo* studies [154-157]. The description of these parameters follows the same nomenclature as classical bone histomorphometry, which – along with the potential of such imaging to revolutionise assessment of bone microarchitecture – led some clinicians to refer to the process as a "virtual bone biopsy" [158, 159].

Finite element modelling is an established method applied in engineering which can add to the information obtained by HR imaging through the extraction of information regarding biomechanical properties of bone. Finite element analysis (FEA), a computer-based simulation of stresses and strains induced by the mechanical loading of a structure, can be applied to three-dimensional HR-pQCT and MRI data to measure the strength of whole bone or its compartments [160]. In addition to correlating bone strength with its microarchitecture, bone mechanical properties assessed by FEA may provide information about skeletal fragility and fracture risk independent of BMD or architecture measurements, and represents another potential method of assessing bone vulnerability [161].

High-resolution peripheral quantitative computed tomography

Quantitative CT has a resolution of approximately 300 μm and can be applied to central skeletal sites (hip, spine) on whole-body CT scanners and peripheral sites (radius, tibia) using dedicated smaller scanners manufactured for this purpose. QCT can discriminate bone into cortical and trabecular compartments, providing separate measurements of total and compartmental volumetric BMD (vBMD) and cortical thickness and area [162]. Peripheral QCT, with lower radiation exposure than central QCT, has been more commonly used in studies involving the ESKD population. HR-pQCT, owing to a significantly higher resolution and increased versatility, represents a significant advancement over pQCT and has become the preferred tool to quantify bone microarchitecture in research over the last decade.

HR-pQCT uses a dedicated extremity scanner currently available from a single manufacturer (XtremeCT; Scanco Medical AG, Brüttisellen, Switzerland) to measure total, cortical or trabecular vBMD and bone structure parameters from ultra-distal radius or distal tibia using

the endplate as the reference. The region of interest (ROI) spans 9.02 mm and is located 9.5 mm and 22.5 mm proximally from the endplates of the radius and tibia respectively. The image contrast is generated by the attenuation of X-rays by mineralised tissues, with 110 consecutive slices acquired in a scan time of three minutes with an isotropic voxel size of 60 to 82 μm [152, 163]. This entails an effective patient radiation exposure of less than 5 μSV, which is comparable to DXA and several orders of magnitude lower than a standard clinical CT [164]. Image analysis and post-processing is carried out using the manufacturer's standard protocol. The algorithm includes semiautomatic contouring of the periosteal perimeter by the operator, followed by an automated segmentation into cortical and trabecular compartments by a "thresholding" technique and subsequent morphometric and densitometric analysis. A hydroxyapatite calibration phantom provided is used to independently determine compartment-specific vBMD by converting attenuation values of tomographic images to hydroxyapatite mineral densities [152]. HR-pQCT is an accurate method for bone image acquisition and analysis, with high reproducibility [152, 165, 166] for measuring vBMD (root mean square CV <1%) and morphometric parameters (CV 0.9-5%), but has technical limitations that need to be considered when interpreting results. High frequency of motion artefacts, limitation in identifying the "transitional or cortico-trabecular zone" of the bone [167, 168], issues with having a fixed ROI in growing children or when comparing individuals of different races, ages or gender, and accurate image registration in longitudinal studies are some potential pitfalls associated with this method [153]. Currently, HR-pQCT scans are limited to peripheral sites, although second generation scanners (XtremeCT II; Scanco Medical AG, Brüttisellen, Switzerland) potentially allow for *in vivo* measurements of the knee [169] .

Magnetic resonance imaging

Mechanisms of image generation in HR-MRI and CT differ completely. MRI is a noninvasive imaging technique that does not require the use of ionising radiation and is therefore well suited both for clinical screening and scientific studies. MRI utilises the inherent magnetic spin of the hydrogen protons (free hydrogen in water) in the tissues by subjecting them to a strong magnetic field and specialized sequences of radiofrequency (RF) pulses to generate three-dimensional (3D) images of bone structure. In MRI, bone appears dark due to its relatively low water content, and is therefore depicted with a negative contrast against the intense background signal emanating from the bone marrow and surrounding soft tissues. HR-MRI is performed using clinical scanners and customised pulse sequences, coils and post-processing software, achieving a spatial resolution of 150-300 μm. This involves a complex cascade of steps, generally including customised RF sequences, ROI selection, image acquisition and registration, correction of motion artefacts, and image processing including bone/marrow segmentation and structural analysis, yielding trabecular and cortical bone parameters [151, 152]. Like HR-pQCT, the 3D MRI data can be subjected to FEA to estimate the mechanical competence of the bone and its interrelationship with structural measurements [99, 170]. Most MRI studies have successfully used similar processes for bone imaging with reproducible results [171], albeit with significant heterogeneity in the techniques used.

Magnetic resonance imaging of bone architecture has proven technically challenging to execute, optimise and standardise, despite the wide availability of MRI scanners in clinical practice. Marrow heterogeneity, propensity for the bone/marrow interface to generate artefacts, achievable signal-to-noise ratio (SNR) while striving for high spatial resolution, and the dependence on sophisticated post-processing have limited the use of MRI largely to

peripheral skeletal sites (distal radius, distal tibia, calcaneus). The increased availability of high-field MRI and significant progress in pulse sequence and coil development and processing and analysis techniques have overcome these limitations to a great extent [155-157]. Bone microarchitecture of the proximal femur, a site of high fracture incidence in CKD, is technically challenging to assess both by HR-pQCT (potentially higher radiation exposure) and MRI (the deep-seated site causing SNR limitation and signal attenuation by surrounding tissues). However, studies in recent years have demonstrated the feasibility of assessing both trabecular and cortical microarchitecture of the proximal femur [172-174] and linking it to bone strength parameters [175]. In a study published in 2017, Rajapakse *et al.* described a reproducible FEA method using MRI to estimate mechanical parameters that relate to hip fracture resistance [176]. This method is an attractive future proposition, and particularly relevant to a population with advanced CKD and high rates of hip fractures [61, 62, 65, 67, 76]. Lastly, MRI using ultrashort-echo-time imaging techniques has been applied to quantify the water content of cortical bone [177] as a potential surrogate measure of cortical porosity, which is an important determinant of bone strength [178].

Multiple *in vivo* clinical studies performed in non-CKD cohorts have reported the utility of HR-MRI in demonstrating the association between bone structure and fracture discrimination [179, 180], structural and mechanical implications of therapeutic interventions longitudinally on bone microarchitecture [170, 181-185], and differential diagnosis in metabolic bone disease [107, 186, 187]. However, there have been no prospective studies of the role of HR-MRI in fracture prediction, and the technique has not been validated against bone histomorphometry. Moreover, despite the advances in MRI techniques over the last decade, there have been very few studies of its role in ROD.

HR-pQCT in chronic kidney disease

Most studies using conventional pQCT are cross-sectional and highlight the predominant loss of cortical vBMD and cortical thickness in patients on haemodialysis [188-190] and peritoneal dialysis [191] as well as kidney transplant recipients [192]. Two prospective studies involving pre-dialysis [193] and haemodialysis [194] patients explored the relationship of radial BMD with biochemical markers over time. They reported significant loss in cortical vBMD and cortical area at the radius in haemodialysis patients and progressive loss in both cortical and trabecular BMD in the pre-dialysis cohort. More recent studies, however, have utilized HR-pQCT as the modality of choice.

Multiple cross-sectional studies have demonstrated the utility of HR-pQCT to quantify disruption of cortical and trabecular microarchitecture [135, 136, 139, 140, 195-197], provide discrimination for fracture status [136, 138, 196, 197] and explore potential relationships between bone microarchitecture and turnover markers [135, 136] or vascular calcification [198, 199] in patients with CKD. While HR-pQCT has generally outperformed DXA, some studies have demonstrated the ability of DXA to discriminate for and predict fracture risk as equivalent to HR-pQCT [127, 136, 196] while others have reported limitations [138]. Jamal *et al* compared the ability for fracture discrimination of HR-pQCT with DXA in 211 participants with stage 3-5 CKD [196] by ROC curve analyses. BMD by DXA at the ultradistal radius, with an area under the curve (AUC) of 0.80, best discriminated between patients with and without fractures with no improvement by the addition of HR-pQCT measurements. After two-year follow up of this cohort (n= 131) there was a decrease in BMD and worsening of both cortical and trabecular bone microarchitecture with the changes being significantly greater in those with incident fractures compared to those without. BMD by DXA at the ultra-distal radius was

the strongest predictor of incident fractures (AUC 0.74, 95% CI 0.65-0.83), [127]. HR-pQCT parameters also exhibited similar prognostic ability with the AUCs for cortical measures generally being higher than those for trabecular parameters. This is the first study to describe the prognostic significance of DXA and HR-pQCT related to fracture risk in CKD. In general, in studies which included both DXA and HR-pQCT, DXA performed better in pre-dialysis patients compared to those receiving dialysis in keeping with known limitations and utility of aBMD measurement in more advanced CKD population. The other notable finding in these studies was the consistent greater discriminating ability of aBMD measurements at the distal radius and femoral neck, both sites rich in cortical bone, perhaps reflective of cortical bone loss in CKD.

Three prospective studies have highlighted the prevalence and importance of deterioration in cortical bone architecture, likely related to hyperparathyroidism in patients with CKD. Nickolas *et al* monitored changes in bone microarchitecture and its relationship with bone biomarkers in 53 patients with CKD stages 2 to 5D (9 on HD) for a median follow up of 1.5 years [137]. They demonstrated a significant loss of cortical bone - reduced cortical area, density, and thickness and increased cortical porosity – related to elevated levels of PTH and bone turnover markers, but no significant deterioration in trabecular parameters. This was accompanied by a decline in DXA-derived aBMD at the ultra-distal radius and total hip unrelated to remodeling markers. Similar progressive loss of cortical bone related to hyperparathyroidism and elevated bone turnover markers, albeit one year after kidney transplantation, was also highlighted by Iyer *et al.* [100], who measured BMD by DXA and bone microarchitecture by HR-pQCT at baseline, 3, 6, and 12 months in 47 renal transplant recipients on early corticosteroid withdrawal immunosuppressive protocol. Moreover, these

changes were linked to significant reductions in estimated bone strength. Nishiyama *et al* [101] explored the changes in cortical porosity following renal transplantation in 31 recipients over one year utilising three different fully automated image registration methods to best detect endocortical bone loss. The baseline-index method, in which exactly the same region was analyzed in the baseline and follow-up scans to account for and include potential endocortical "trabecularisation" [168], showed the greatest increase in porosity and had the strongest relationship with changes by PTH and bone turnover markers.

MRI in chronic kidney disease

There have been few studies of the use of HR-MRI in the CKD population to date. Link *et al.* [107] reported that MRI measures of trabecular structure of the calcaneus and BMD of the spine (by QCT) in a mixed cohort of pre- and post-kidney transplant patients and 20 control subjects, discriminated between patients with and without fractures. In addition, MRI trabecular parameters were significantly lower in patients than healthy controls, but no changes were observed in DXA-derived hip BMD in the three groups. Wehrli *et al.* [187] evaluated the role of HR-MRI in assessing bone microstructure in 17 young adults on maintenance haemodialysis compared with age, gender and BMI-matched healthy controls. This study reported significantly lower cortical thickness and cross-sectional area in dialysis patients than in controls. There was also evidence of trabecular disruption, including reduced trabecular number and an increased erosion index; however, differences did not achieve statistical significance. Rajapakse *et al.* [99], in 2012, applied FEA to HR-MRI images to assess cortical and trabecular bone strength in addition to structural parameters in a prospective study involving 49 renal transplant recipients. They demonstrated a decrease in stiffness and

failure strength in the distal tibia over six months post-transplantation without corresponding changes in the conventional structural parameters.

Promise of a virtual bone biopsy

The unique and complex pathophysiology of ROD and the lack of accurate diagnostic tools makes bone abnormalities in CKD challenging to interpret and manage. Non-invasive HR imaging has the potential to fill, at least partially, the significant gap between screening of BMD using DXA and comprehensive diagnosis by bone biopsy. HR-pQCT and MRI, in conjunction with accurate and appropriate bone turnover markers, can potentially be used to screen for bone fragility, predict fracture and help in developing therapeutic interventions and monitoring treatment effect in the CKD population. The euphoria surrounding the potential of HR imaging, while not unfounded, has to be viewed in the context of potential hurdles in its implementation into mainstream clinical practice. A plethora of technical caveats, relative lack of standardisation of reference and technical parameters, limitation of imaging to peripheral sites and high costs are some of the challenges which currently restrict the use of these modalities to research settings. Moreover, both techniques need validation in large multi-centre prospective trials to determine their utility in guiding clinical decision-making and improving outcomes in the CKD population. Lastly, more accurate and reliable non-invasive markers of bone turnover and mineralisation, validated against bone histology, are required. These challenges are significant but not insurmountable, and once met, may fulfill the vision of a “virtual bone biopsy”.

Aims of thesis

People with CKD have a significantly higher risk of bone disease and all-cause mortality than the general population. As renal function declines, patients develop characteristic biochemical abnormalities, including decreased synthesis of vitamin D, hyperphosphataemia, hypocalcaemia, and increased secretion of PTH. These abnormalities lead to the development of CKD–MBD, a systemic disorder which encompasses intimately related abnormalities of mineral homeostasis, bone turnover and mineralisation, and vascular and soft tissue calcification. Bone microarchitecture is invariably adversely affected in CKD, leading to reduced bone quality and a high susceptibility to fracture.

Renal osteodystrophy, although a well-recognised entity for many decades, has a disproportionately small body of evidence relating to its diagnosis and treatment. Major gaps still exist in our knowledge about management of ROD in the clinical setting. Inability to accurately identify the type of ROD by non-invasive means, lack of CKD-specific screening tools for assessing fracture risk, and limited supportive evidence for appropriate therapy has hampered our ability to institute preventative treatment in this high-risk group of patients. Currently available diagnostic tools in routine clinical practice have limited utility in assisting with management of ROD and therefore add to diagnostic and therapeutic uncertainty in this area. Bone biopsy captures a comprehensive snapshot of bone microarchitecture, turnover and mineralisation but has many limitations and is not a practical test for routine clinical practice. Micro-CT is an *ex vivo* ultra-HR, non-destructive method to acquire direct three-dimensional (3D) measurements of bone microarchitecture and images a much larger volume of interest than two-dimensional (2D) histology. Although equipped with the resolution to

measure the size of cortical pores, micro-CT has not been previously utilised to study cortical porosity in biopsies of patients with CKD.

Over the last two decades, important advances in non-invasive HR imaging and identification of novel biomarkers have enhanced our knowledge of bone microarchitecture in patients with CKD and provided new insights into the pathophysiology and progression of CKD-MBD. High-resolution MRI, using customised processing techniques, has proved to be an excellent non-invasive tool to study bone microarchitecture in the non-CKD population but remains relatively untested in patients with CKD. Large histomorphometry studies have also indicated a changing pattern of histological abnormalities in the bone in patients with CKD over the last few decades. Traditionally described histological patterns of renal bone disease have given way to a newer classification according to the KDIGO TMV system in a major, and advantageous, shift in approach towards defining ROD. The TMV classification provides clinically relevant descriptors, but fails to emphasise the importance of assessment of cortical microarchitecture, which is described as an adjunct to trabecular bone measurements. Our increased understanding of the important contribution of cortical bone structure to overall bone strength – and the more recent findings of cortical thinning and increased cortical porosity in patients with CKD – suggest a need to emphasise the evaluation of cortical microarchitecture as a key parameter in addition to trabecular changes within the TMV classification.

Aim 1: To study histological abnormalities of bone, particularly cortical bone structure, in a relatively young cohort of patients with ESKD at the time of kidney transplantation by utilising micro-CT as a novel tool in addition to traditional histomorphometry. (Chapter 2)

Accurate and reliable screening methods to assess abnormalities of bone turnover and skeletal structure associated with ROD will be invaluable in clinical practice given the wide prevalence of bone disease in patients with CKD, including KTRs. HR-MRI using customised processing techniques has proved to be an excellent non-invasive tool to study bone microarchitecture in research. Moreover, it is radiation free and can be performed widely on commercially available scanners.

Aim 2: To evaluate bone microarchitecture in patients with CKD using HR-MRI and correlate findings to those obtained by bone biopsy and other contemporary bone imaging techniques (DXA, pQCT, TBS) and highlight the advantages of MRI as a diagnostic tool in renal bone disease. (Chapter 3)

Renal osteodystrophy and CKD–MBD are almost universal findings in ESKD and may persist after kidney transplantation. Histological abnormalities in bone structure and turnover existing at the time of transplantation contribute significantly to post-transplant bone disease, in addition to the risk factors for bone disease unique to KTRs (e.g. immunosuppressive medications). There is a paucity of data on changes in bone structure and histomorphometry after kidney transplantation, with mechanisms of underlying bone loss poorly understood.

Aim 3: To monitor and compare longitudinal changes in bone density and microarchitecture (using MRI, DXA, pQCT and TBS), and bone turnover markers over one year after transplantation in kidney transplant recipients. (Chapter 4)

Post-transplant mineral and bone disorders are common, with persistent SHPT seen in up to 50% of KTRs one year after transplantation. Bone disease related to ongoing SHPT is associated with a heightened risk of fractures, cardiovascular calcification and graft failure, and is sometimes treated with parathyroidectomy or calcimimetic agents. In Australia, the calcimimetic agent cinacalcet was approved for financial reimbursement (on the Pharmaceutical Benefits Scheme) in late 2007 for treatment of SHPT in patients with ESKD on dialysis, but not for use in KTRs, and is therefore discontinued in most patients at the time of transplantation. Few researchers have reported biochemical profiles and other clinical outcomes in patients discontinuing cinacalcet at the time of kidney transplantation.

Aim 4: To assess the impact of discontinuation of cinacalcet at the time of transplantation on mineral metabolism and clinical outcomes in a large cohort of kidney transplant recipients over 5 years post transplantation via a retrospective audit (Chapter 5)

In the 1970s, aluminium toxicity emerged as a major cause of encephalopathy and anaemia in patients receiving haemodialysis, but is now rare in the era of modern dialysis water systems. Aluminium deposition in bone was also recognised as a major cause of adynamic bone disease and added another dimension to the pathophysiology of ROD. Although studies demonstrated a correlation between high serum aluminium levels and aluminium bone disease, the reference range of serum levels predictive of bone disease has not been established. Aluminium-containing phosphate binder use decreased with the advent of calcium-based agents, and subsequently was almost completely phased out with increasing use of non-calcium containing binders. However, many centres continue to routinely screen dialysis patients for aluminium levels.

Aim 5: To assess the utility of routine testing of serum aluminium levels in the haemodialysis population in our centre via a retrospective audit of aluminium levels tested in 755 patients over 4 years. *(Chapter 6)*

Overall, the work presented in this thesis was designed to increase knowledge and further research in the field of CKD-MBD, and in particular ROD, within the Australian nephrology community.

References

1. Hill, N.R., et al., *Global Prevalence of Chronic Kidney Disease - A Systematic Review and Meta-Analysis.* PLoS One, 2016. **11**(7): p. e0158765.
2. Levin, A., et al., *Global kidney health 2017 and beyond: a roadmap for closing gaps in care, research, and policy.* Lancet, 2017. **390**(10105): p. 1888-1917.
3. Tentori, F., et al., *High rates of death and hospitalization follow bone fracture among hemodialysis patients.* Kidney Int, 2014. **85**(1): p. 166-73.
4. Pimentel, A., et al., *Fractures in patients with CKD-diagnosis, treatment, and prevention: a review by members of the European Calcified Tissue Society and the European Renal Association of Nephrology Dialysis and Transplantation.* Kidney Int, 2017. **92**(6): p. 1343-1355.
5. Go, A.S., et al., *Chronic kidney disease and the risks of death, cardiovascular events, and hospitalization.* N Engl J Med, 2004. **351**(13): p. 1296-305.
6. Consortium, C.P., *Association of estimated glomerular filtration rate and albuminuria with all-cause and cardiovascular mortality in general population cohorts: a collaborative meta-analysis.* Lancet, 2010. **375**(9731): p. 2073-81.
7. Gansevoort, R.T., et al., *Chronic kidney disease and cardiovascular risk: epidemiology, mechanisms, and prevention.* Lancet, 2013. **382**(9889): p. 339-52.
8. *Global, regional, and national age-sex specific all-cause and cause-specific mortality for 240 causes of death, 1990-2013: a systematic analysis for the Global Burden of Disease Study 2013.* Lancet, 2015. **385**(9963): p. 117-71.
9. Jager, K.J. and S.D.S. Fraser, *The ascending rank of chronic kidney disease in the global burden of disease study.* Nephrol Dial Transplant, 2017. **32**(suppl_2): p. ii121-ii128.
10. Hruska, K.A. and S.L. Teitelbaum, *Renal osteodystrophy.* N Engl J Med, 1995. **333**(3): p. 166-74.
11. Parfitt, A.M., *A structural approach to renal bone disease.* J Bone Miner Res, 1998. **13**(8): p. 1213-20.
12. Seeman, E. and P.D. Delmas, *Bone quality--the material and structural basis of bone strength and fragility.* N Engl J Med, 2006. **354**(21): p. 2250-61.
13. Malluche, H.H., D.S. Porter, and D. Pienkowski, *Evaluating bone quality in patients with chronic kidney disease.* Nat Rev Nephrol, 2013. **9**(11): p. 671-80.

14. Bouxsein, M.L., *Bone quality: where do we go from here?* Osteoporosis international, 2003. **14**(5): p. 118-127.
15. Felsenberg, D. and S. Boonen, *The bone quality framework: determinants of bone strength and their interrelationships, and implications for osteoporosis management.* Clin Ther, 2005. **27**(1): p. 1-11.
16. London, G.M., et al., *Arterial media calcification in end-stage renal disease: impact on all-cause and cardiovascular mortality.* Nephrol Dial Transplant, 2003. **18**(9): p. 1731-40.
17. *KDIGO clinical practice guideline for the diagnosis, evaluation, prevention, and treatment of Chronic Kidney Disease-Mineral and Bone Disorder (CKD-MBD).* Kidney Int Suppl, 2009. **76**(113): p. S1-130.
18. Moe, S., et al., *Definition, evaluation, and classification of renal osteodystrophy: a position statement from Kidney Disease: Improving Global Outcomes (KDIGO).* Kidney Int, 2006. **69**(11): p. 1945-53.
19. Clement Lucas, R., *On a Form of Late Rickets Associated with Albuminuria, Rickets of Adolescents.* The Lancet, 1883. **121**(3119): p. 993-994.
20. Malluche, H.H. and M.C. Monier-Faugere, *Renal osteodystrophy: what's in a name? Presentation of a clinically useful new model to interpret bone histologic findings.* Clin Nephrol, 2006. **65**(4): p. 235-42.
21. Ott, S.M., *Renal Osteodystrophy-Time for Common Nomenclature.* Curr Osteoporos Rep, 2017. **15**(3): p. 187-193.
22. Barber, H., *The bone deformities of renal dwarfism.* The Lancet, 1920. **195**(5027): p. 18-19.
23. Barber, H., *Renal dwarfism.* QJM: Quarterly Journal of Medicine, 1921(55): p. 205-213.
24. Brockman, E., *Some observations on the bone changes in renal rickets.* British Journal of Surgery, 1927. **14**(56): p. 634-645.
25. Liu, S. and H. Chu, *Treatment of renal osteodystrophy with dihydrotachysterol (AT 10) and iron.* Science, 1942. **95**(2467): p. 388-389.
26. Liu, S. and H. Chu, *Studies of calcium and phosphorus metabolism with special reference to pathogenesis and effects of dihydrotachysterol (AT 10) and iron.* Medicine, 1943. **22**(2): p. 103-162.

27. Pollak, V.E., et al., *Chronic renal disease with secondary hyperparathyroidism.* AMA Arch Intern Med, 1959. **103**(2): p. 200-18.
28. Stanbury, S.W. and G.A. Lumb, *Parathyroid function in chronic renal failure. A statistical survey of the plasma biochemistry in azotaemic renal osteodystrophy.* Q J Med, 1966. **35**(137): p. 1-23.
29. Stanbury, S.W., *Bone disease in uremia.* Am J Med, 1968. **44**(5): p. 714-24.
30. Milch, R.A., D.P. Rall, and J.E. Tobie, *Bone localization of the tetracyclines.* J Natl Cancer Inst, 1957. **19**(1): p. 87-93.
31. Frost, H.M., *Tetracycline-based histological analysis of bone remodeling.* Calcif Tissue Res, 1969. **3**(3): p. 211-37.
32. Quinton, W., D. Dillard, and B.H. Scribner, *Cannulation of blood vessels for prolonged hemodialysis.* Trans Am Soc Artif Intern Organs, 1960. **6**(1): p. 104-13.
33. Scribner, B.H., et al., *The treatment of chronic uremia by means of intermittent hemodialysis: a preliminary report.* Trans Am Soc Artif Intern Organs, 1960. **6**(1): p. 114-22.
34. Scribner, B.H., et al., *The technique of continuous hemodialysis.* ASAIO Journal, 1960. **6**(1): p. 88-103.
35. Pendras, J.P. and R.V. Erickson, *Hemodialysis: a successful therapy for chronic uremia.* Ann Intern Med, 1966. **64**(2): p. 293-311.
36. Johnson, C., et al., *Roentgenographic manifestations of chronic renal disease treated by periodic hemodialysis.* Am J Roentgenol Radium Ther Nucl Med, 1967. **101**(4): p. 915-26.
37. Lawson, D.E., et al., *Identification of 1,25-dihydroxycholecalciferol, a new kidney hormone controlling calcium metabolism.* Nature, 1971. **230**(5291): p. 228-30.
38. Brickman, A.S., et al., *1,25-dihydroxycholecalciferol. Effect on skeletal lesions and plasma parathyroid hormone levels in uremic osteodystrophy.* Arch Intern Med, 1974. **134**(5): p. 883-8.
39. Ritz, E., et al., *Skeletal abnormalities in chronic renal insufficiency before and during maintenance hemodialysis.* Kidney Int, 1973. **4**(2): p. 116-27.
40. Parsons, V., et al., *Aluminium in bone from patients with renal failure.* Br Med J, 1971. **4**(5782): p. 273-5.

41. Alfrey, A.C., G.R. LeGendre, and W.D. Kaehny, *The dialysis encephalopathy syndrome. Possible aluminum intoxication.* N Engl J Med, 1976. **294**(4): p. 184-8.
42. Parkinson, I.S., et al., *Fracturing dialysis osteodystrophy and dialysis encephalopathy. An epidemiological survey.* Lancet, 1979. **1**(8113): p. 406-9.
43. Pierides, A.M., et al., *Variable response to long-term 1alpha-hydroxycholecalciferol in haemodialysis osteodystrophy.* Lancet, 1976. **1**(7969): p. 1092-5.
44. Ott, S.M., et al., *The prevalence of bone aluminum deposition in renal osteodystrophy and its relation to the response to calcitriol therapy.* N Engl J Med, 1982. **307**(12): p. 709-13.
45. Malluche, H.H., H. Mawad, and M.C. Monier-Faugere, *The importance of bone health in end-stage renal disease: out of the frying pan, into the fire?* Nephrol Dial Transplant, 2004. **19 Suppl 1**(suppl 1): p. i9-13.
46. Barreto, F.d.C., et al., *Osteoporosis in hemodialysis patients revisited by bone histomorphometry: a new insight into an old problem.* Kidney Int, 2006. **69**(10): p. 1852-1857.
47. Malluche, H.H., H.W. Mawad, and M.C. Monier-Faugere, *Renal osteodystrophy in the first decade of the new millennium: analysis of 630 bone biopsies in black and white patients.* J Bone Miner Res, 2011. **26**(6): p. 1368-76.
48. Drueke, T.B. and Z.A. Massy, *Changing bone patterns with progression of chronic kidney disease.* Kidney Int, 2016. **89**(2): p. 289-302.
49. Malluche, H.H., et al., *Bone histology in incipient and advanced renal failure.* Kidney Int, 1976. **9**(4): p. 355-62.
50. Graciolli, F.G., et al., *The complexity of chronic kidney disease-mineral and bone disorder across stages of chronic kidney disease.* Kidney Int, 2017. **91**(6): p. 1436-1446.
51. Sherrard, D.J., et al., *The spectrum of bone disease in end-stage renal failure-an evolving disorder.* Kidney Int, 1993. **43**: p. 436-436.
52. Dempster, D.W., et al., *Standardized nomenclature, symbols, and units for bone histomorphometry: a 2012 update of the report of the ASBMR Histomorphometry Nomenclature Committee.* J Bone Miner Res, 2013. **28**(1): p. 2-17.
53. Reiss, A.B., et al., *CKD, arterial calcification, atherosclerosis and bone health: Inter-relationships and controversies.* Atherosclerosis, 2018. **278**: p. 49-59.

54. Chen, J., et al., *Coronary Artery Calcification and Risk of Cardiovascular Disease and Death Among Patients With Chronic Kidney Disease.* JAMA Cardiol, 2017. **2**(6): p. 635-643.
55. Toussaint, N.D., et al., *Associations between vascular calcification, arterial stiffness and bone mineral density in chronic kidney disease.* Nephrol Dial Transplant, 2008. **23**(2): p. 586-93.
56. Faul, C., et al., *FGF23 induces left ventricular hypertrophy.* J Clin Invest, 2011. **121**(11): p. 4393-408.
57. Kendrick, J., et al., *FGF-23 associates with death, cardiovascular events, and initiation of chronic dialysis.* J Am Soc Nephrol, 2011. **22**(10): p. 1913-22.
58. Isakova, T., et al., *Fibroblast growth factor 23 and risks of mortality and end-stage renal disease in patients with chronic kidney disease.* JAMA, 2011. **305**(23): p. 2432-9.
59. Vervloet, M.G., et al., *Bone: a new endocrine organ at the heart of chronic kidney disease and mineral and bone disorders.* The Lancet Diabetes & Endocrinology, 2014. **2**(5): p. 427-436.
60. Morena, M., et al., *Osteoprotegerin and sclerostin in chronic kidney disease prior to dialysis: potential partners in vascular calcifications.* Nephrol Dial Transplant, 2015. **30**(8): p. 1345-56.
61. Naylor, K.L., et al., *The three-year incidence of fracture in chronic kidney disease.* Kidney Int, 2014. **86**(4): p. 810-8.
62. Kim, S.M., et al., *Hip Fracture in Patients With Non-Dialysis-Requiring Chronic Kidney Disease.* J Bone Miner Res, 2016. **31**(10): p. 1803-1809.
63. Vervloet, M. and M. Cozzolino, *Vascular calcification in chronic kidney disease: different bricks in the wall?* Kidney Int, 2017. **91**(4): p. 808-817.
64. Alem, A.M., et al., *Increased risk of hip fracture among patients with end-stage renal disease.* Kidney Int, 2000. **58**(1): p. 396-9.
65. Coco, M. and H. Rush, *Increased incidence of hip fractures in dialysis patients with low serum parathyroid hormone.* Am J Kidney Dis, 2000. **36**(6): p. 1115-21.
66. Hansen, D., et al., *Risk of fracture in adults on renal replacement therapy: a Danish national cohort study.* Nephrol Dial Transplant, 2016. **31**(10): p. 1654-62.
67. Wakasugi, M., et al., *Increased risk of hip fracture among Japanese hemodialysis patients.* J Bone Miner Metab, 2013. **31**(3): p. 315-321.

68. Dukas, L., E. Schacht, and H.B. Stähelin, *In elderly men and women treated for osteoporosis a low creatinine clearance of< 65 ml/min is a risk factor for falls and fractures.* Osteoporosis Int, 2005. **16**(12): p. 1683-1690.
69. Nickolas, T.L., D.J. McMahon, and E. Shane, *Relationship between moderate to severe kidney disease and hip fracture in the United States.* J Am Soc Nephrol, 2006. **17**(11): p. 3223-3232.
70. Ensrud, K.E., et al., *Renal function and risk of hip and vertebral fractures in older women.* Arch Intern Med, 2007. **167**(2): p. 133-9.
71. Dooley, A.C., N.S. Weiss, and B. Kestenbaum, *Increased risk of hip fracture among men with CKD.* Am J Kidney Dis, 2008. **51**(1): p. 38-44.
72. LaCroix, A.Z., et al., *Cystatin-C, renal function, and incidence of hip fracture in postmenopausal women.* J Am Geriatr Soc, 2008. **56**(8): p. 1434-41.
73. Jadoul, M., et al., *Incidence and risk factors for hip or other bone fractures among hemodialysis patients in the Dialysis Outcomes and Practice Patterns Study.* Kidney Int, 2006. **70**(7): p. 1358-1366.
74. Stehman-Breen, C.O., et al., *Risk factors for hip fracture among patients with end-stage renal disease.* Kidney Int, 2000. **58**(5): p. 2200-2205.
75. Nair, S.S., et al., *Temporal trends in the incidence, treatment, and outcomes of hip fracture in older patients initiating dialysis in the United States.* Clin J Am Soc Nephrol, 2013. **8**(8): p. 1336-42.
76. Lin, Z.-Z., et al., *Epidemiology and mortality of hip fracture among patients on dialysis: Taiwan National Cohort Study.* Bone, 2014. **64**: p. 235-239.
77. Daya, N., et al., *Kidney Function and Fracture Risk: The Atherosclerosis Risk in Communities (ARIC) Study.* Am J Kidney Dis, 2016. **67**(2): p. 218-226.
78. Perez-Saez, M.J., et al., *Increased hip fracture and mortality in chronic kidney disease individuals: the importance of competing risks.* Bone, 2015. **73**: p. 154-9.
79. Arneson, T.J., et al., *Trends in hip fracture rates in US hemodialysis patients, 1993-2010.* Am J Kidney Dis, 2013. **62**(4): p. 747-54.
80. Kim, S.M., et al., *Declining Rates of Hip Fracture in End-Stage Renal Disease: Analysis From the 2003-2011 Nationwide Inpatient Sample.* J Bone Miner Res, 2017. **32**(11): p. 2297-2303.

81. Wakasugi, M., et al., *Hip Fracture Trends in Japanese Dialysis Patients, 2008-2013.* Am J Kidney Dis, 2018. **71**(2): p. 173-181.
82. Ball, A.M., *Risk of Hip Fracture Among Dialysis and Renal Transplant Recipients.* JAMA, 2002. **288**(23): p. 3014-3018.
83. Nikkel, L.E., et al., *Risk of fractures after renal transplantation in the United States.* Transplantation, 2009. **87**(12): p. 1846-51.
84. Abbott, K.C., et al., *Hospitalizations for fractures after renal transplantation in the United States.* Ann Epidemiol, 2001. **11**(7): p. 450-7.
85. Naylor, K.L., et al., *Fracture risk in kidney transplant recipients: a systematic review.* Transplantation, 2013. **95**(12): p. 1461-70.
86. Block, G.A., et al., *Mineral metabolism, mortality, and morbidity in maintenance hemodialysis.* J Am Soc Nephrol, 2004. **15**(8): p. 2208-2218.
87. Ganesh, S.K., et al., *Association of elevated serum PO4, Ca× PO4 product, and parathyroid hormone with cardiac mortality risk in chronic hemodialysis patients.* J Am Soc Nephrol, 2001. **12**(10): p. 2131-2138.
88. Evenepoel, P., et al., *Natural history of parathyroid function and calcium metabolism after kidney transplantation: a single-centre study.* Nephrol Dial Transplant, 2004. **19**(5): p. 1281-7.
89. Torres, A., V. Lorenzo, and E. Salido, *Calcium metabolism and skeletal problems after transplantation.* J Am Soc Nephrol, 2002. **13**(2): p. 551-558.
90. Gwinner, W., et al., *Early calcification of renal allografts detected by protocol biopsies: causes and clinical implications.* Am J Transplant, 2005. **5**(8): p. 1934-41.
91. Schwarz, A., et al., *Risk factors for chronic allograft nephropathy after renal transplantation: a protocol biopsy study.* Kidney Int, 2005. **67**(1): p. 341-8.
92. Mazzaferro, S., et al., *Progression of coronary artery calcification in renal transplantation and the role of secondary hyperparathyroidism and inflammation.* Clin J Am Soc Nephrol, 2009. **4**(3): p. 685-90.
93. Perrin, P., et al., *Persistent hyperparathyroidism is a major risk factor for fractures in the five years after kidney transplantation.* Am J Transplant, 2013. **13**(10): p. 2653-63.
94. Malluche, H.H., M.C. Monier-Faugere, and J. Herberth, *Bone disease after renal transplantation.* Nat Rev Nephrol, 2010. **6**(1): p. 32-40.

95. Julian, B.A., et al., *Rapid loss of vertebral mineral density after renal transplantation.* N Engl J Med, 1991. **325**(8): p. 544-50.
96. Almond, M.K., et al., *Loss of regional bone mineral density in the first 12 months following renal transplantation.* Nephron, 1994. **66**(1): p. 52-7.
97. Brandenburg, V.M., et al., *Early rapid loss followed by long-term consolidation characterizes the development of lumbar bone mineral density after kidney transplantation.* Transplantation, 2004. **77**(10): p. 1566-71.
98. Naylor, K.L., et al., *Long-term changes in bone mineral density in kidney transplant recipients.* Transplantation, 2014. **98**(12): p. 1279-85.
99. Rajapakse, C.S., et al., *Micro-MR imaging-based computational biomechanics demonstrates reduction in cortical and trabecular bone strength after renal transplantation.* Radiology, 2012. **262**(3): p. 912-20.
100. Iyer, S.P., et al., *Kidney transplantation with early corticosteroid withdrawal: paradoxical effects at the central and peripheral skeleton.* J Am Soc Nephrol, 2014. **25**(6): p. 1331-41.
101. Nishiyama, K.K., et al., *Longitudinal HR-pQCT and image registration detects endocortical bone loss in kidney transplantation patients.* J Bone Miner Res, 2015. **30**(3): p. 554-61.
102. Bonani, M., et al., *Effect of Twice-Yearly Denosumab on Prevention of Bone Mineral Density Loss in De Novo Kidney Transplant Recipients: A Randomized Controlled Trial.* Am J Transplant, 2016. **16**(6): p. 1882-91.
103. Evenepoel, P., et al., *Bone histomorphometry in de novo renal transplant recipients indicates a further decline in bone resorption 1 year posttransplantation.* Kidney Int, 2017. **91**(2): p. 469-476.
104. Monier-Faugere, M.C., et al., *High prevalence of low bone turnover and occurrence of osteomalacia after kidney transplantation.* J Am Soc Nephrol, 2000. **11**(6): p. 1093-9.
105. Cruz, E.A., et al., *Histologic evolution of bone disease 6 months after successful kidney transplantation.* Am J Kidney Dis, 2004. **44**(4): p. 747-56.
106. Kodras, K. and M. Haas, *Effect of kidney transplantation on bone.* Eur J Clin Invest, 2006. **36 Suppl 2**: p. 63-75.

107. Link, T.M., et al., *Changes in calcaneal trabecular bone structure assessed with high-resolution MR imaging in patients with kidney transplantation.* Osteoporos Int, 2002. **13**(2): p. 119-29.
108. Luckman, M., et al., *Spine Trabecular Bone Score as an Indicator of Bone Microarchitecture at the Peripheral Skeleton in Kidney Transplant Recipients.* Clin J Am Soc Nephrol, 2017. **12**(4): p. 644-652.
109. Naylor, K.L., et al., *Trabecular bone score in kidney transplant recipients.* Osteoporos Int, 2016. **27**(3): p. 1115-1121.
110. Perez-Saez, M.J., et al., *Bone Density, Microarchitecture, and Tissue Quality Long-term After Kidney Transplant.* Transplantation, 2017. **101**(6): p. 1290-1294.
111. Perez-Saez, M.J., et al., *Bone density, microarchitecture, and material strength in chronic kidney disease patients at the time of kidney transplantation.* Osteoporos Int, 2017. **28**(9): p. 2723-2727.
112. Kanis, J.A., et al., *The burden of osteoporotic fractures: a method for setting intervention thresholds.* Osteoporos Int, 2001. **12**(5): p. 417-27.
113. Johnell, O. and J.A. Kanis, *An estimate of the worldwide prevalence and disability associated with osteoporotic fractures.* Osteoporos Int, 2006. **17**(12): p. 1726-33.
114. Johnell, O., et al., *Predictive value of BMD for hip and other fractures.* J Bone Miner Res, 2005. **20**(7): p. 1185-94.
115. Atsumi, K., et al., *Risk factors for vertebral fractures in renal osteodystrophy.* Am J Kidney Dis, 1999. **33**(2): p. 287-93.
116. Stehman-Breen, C.O., et al., *Racial differences in bone mineral density and bone loss among end-stage renal disease patients.* Am J Kidney Dis, 1999. **33**(5): p. 941-946.
117. Jamal, S.A., et al., *Bone density and heel ultrasound testing do not identify patients with dialysis-dependent renal failure who have had fractures.* Am J Kidney Dis, 2002. **39**(4): p. 843-849.
118. Urena, P., et al., *Bone mineral density, biochemical markers and skeletal fractures in haemodialysis patients.* Nephrol Dial Transplant, 2003. **18**(11): p. 2325-31.
119. Negri, A., et al., *Bone mineral density: serum markers of bone turnover and their relationships in peritoneal dialysis.* Peritoneal Dialysis International, 2004. **24**(2): p. 163-168.

120. Ersoy, F.F., et al., *Bone mineral density and its correlation with clinical and laboratory factors in chronic peritoneal dialysis patients.* J Bone Miner Metab, 2006. **24**(1): p. 79-86.
121. Jassal, S.K., D. von Muhlen, and E. Barrett-Connor, *Measures of renal function, BMD, bone loss, and osteoporotic fracture in older adults: the Rancho Bernardo study.* J Bone Miner Res, 2007. **22**(2): p. 203-10.
122. Jamal, S.A., S.L. West, and T.L. Nickolas, *The clinical utility of FRAX to discriminate fracture status in men and women with chronic kidney disease.* Osteoporos Int, 2014. **25**(1): p. 71-6.
123. Lima, G.A., et al., *Bone Density Is Directly Associated With Glomerular Filtration and Metabolic Acidosis but Do Not Predict Fragility Fractures in Men With Moderate Chronic Kidney Disease.* J Clin Densitom, 2016. **19**(2): p. 146-53.
124. Iimori, S., et al., *Diagnostic usefulness of bone mineral density and biochemical markers of bone turnover in predicting fracture in CKD stage 5D patients--a single-center cohort study.* Nephrol Dial Transplant, 2012. **27**(1): p. 345-51.
125. Yenchek, R.H., et al., *Bone mineral density and fracture risk in older individuals with CKD.* Clin J Am Soc Nephrol, 2012. **7**(7): p. 1130-6.
126. Naylor, K.L., et al., *Comparison of fracture risk prediction among individuals with reduced and normal kidney function.* Clin J Am Soc Nephrol, 2015. **10**(4): p. 646-653.
127. West, S.L., et al., *Bone mineral density predicts fractures in chronic kidney disease.* J Bone Miner Res, 2015. **30**(5): p. 913-9.
128. Ketteler, M., et al., *Executive summary of the 2017 KDIGO Chronic Kidney Disease-Mineral and Bone Disorder (CKD-MBD) Guideline Update: what's changed and why it matters.* Kidney Int, 2017. **92**(1): p. 26-36.
129. Adams, J.E., *Advances in bone imaging for osteoporosis.* Nat Rev Endocrinol, 2013. **9**(1): p. 28-42.
130. Sprague, S.M., et al., *Diagnostic Accuracy of Bone Turnover Markers and Bone Histology in Patients With CKD Treated by Dialysis.* Am J Kidney Dis, 2016. **67**(4): p. 559-66.
131. Malluche, H.H., et al., *Differences in bone quality in low- and high-turnover renal osteodystrophy.* J Am Soc Nephrol, 2012. **23**(3): p. 525-32.

132. Gardham, C., et al., *Variability of parathyroid hormone and other markers of bone mineral metabolism in patients receiving hemodialysis.* Clin J Am Soc Nephrol, 2010. **5**(7): p. 1261-7.
133. Cavalier, E., P. Delanaye, and O. Moranne, *Variability of new bone mineral metabolism markers in patients treated with maintenance hemodialysis: implications for clinical decision making.* Am J Kidney Dis, 2013. **61**(5): p. 847-8.
134. Malluche, H.H., et al., *Bone mineral density and serum biochemical predictors of bone loss in patients with CKD on dialysis.* Clin J Am Soc Nephrol, 2014. **9**(7): p. 1254-62.
135. Negri, A.L., et al., *Evaluation of bone microarchitecture by high-resolution peripheral quantitative computed tomography (HR-pQCT) in hemodialysis patients.* Osteoporos Int, 2012. **23**(10): p. 2543-50.
136. Nickolas, T.L., et al., *Discriminants of prevalent fractures in chronic kidney disease.* J Am Soc Nephrol, 2011. **22**(8): p. 1560-72.
137. Nickolas, T.L., et al., *Rapid cortical bone loss in patients with chronic kidney disease.* J Bone Miner Res, 2013. **28**(8): p. 1811-20.
138. Cejka, D., et al., *Bone microarchitecture in hemodialysis patients assessed by HR-pQCT.* Clin J Am Soc Nephrol, 2011. **6**(9): p. 2264-71.
139. Pelletier, S., et al., *Bone microarchitecture is more severely affected in patients on hemodialysis than in those receiving peritoneal dialysis.* Kidney Int, 2012. **82**(5): p. 581-588.
140. Trombetti, A., et al., *Alterations of bone microstructure and strength in end-stage renal failure.* Osteoporos Int, 2013. **24**(5): p. 1721-32.
141. Cejka, D., et al., *Sclerostin and Dickkopf-1 in renal osteodystrophy.* Clin J Am Soc Nephrol, 2011. **6**(4): p. 877-82.
142. Malluche, H.H. and M.C. Monier-Faugere, *The role of bone biopsy in the management of patients with renal osteodystrophy.* J Am Soc Nephrol, 1994. **4**(9): p. 1631-42.
143. Torres, P.U., et al., *When, How, and Why a Bone Biopsy Should Be Performed in Patients With Chronic Kidney Disease.* Seminars in Nephrology, 2014. **34**(6): p. 612-625.
144. Thomsen, J.S., E.N. Ebbesen, and L. Mosekilde, *Static histomorphometry of human iliac crest and vertebral trabecular bone: a comparative study.* Bone, 2002. **30**(1): p. 267-74.
145. Chavassieux, P.M., M.E. Arlot, and P.J. Meunier, *Intersample variation in bone histomorphometry: comparison between parameter values measured on two*

contiguous transiliac bone biopsies. Calcified Tissue International, 1985. **37**(4): p. 345-350.

146. Tong, X., et al., *Iliac crest histomorphometry and skeletal heterogeneity in men.* Bone Rep, 2017. **6**: p. 9-16.
147. Dempster, D., et al., *Relationships between bone structure in the iliac crest and bone structure and strength in the lumbar spine.* Osteoporosis Int, 1993. **3**(2): p. 90-96.
148. Eventov, I., et al., *Osteopenia, hematopoiesis, and bone remodelling in iliac crest and femoral biopsies: a prospective study of 102 cases of femoral neck fractures.* Bone, 1991. **12**(1): p. 1-6.
149. Dempster, D.W., *Bone microarchitecture and strength.* Osteoporos Int, 2003. **14 Suppl 5**: p. S54-6.
150. Clarke, B., *Normal bone anatomy and physiology.* Clin J Am Soc Nephrol, 2008. **3 Suppl 3**(Supplement 3): p. S131-9.
151. Wehrli, F.W., *Structural and functional assessment of trabecular and cortical bone by micro magnetic resonance imaging.* J Magn Reson Imaging, 2007. **25**(2): p. 390-409.
152. Krug, R., et al., *High-resolution imaging techniques for the assessment of osteoporosis.* Radiologic Clinics of North America, 2010. **48**(3): p. 601-621.
153. Geusens, P., et al., *High-resolution in vivo imaging of bone and joints: a window to microarchitecture.* Nat Rev Rheumatol, 2014. **10**(5): p. 304-13.
154. Liu, X.S., et al., *High-resolution peripheral quantitative computed tomography can assess microstructural and mechanical properties of human distal tibial bone.* J Bone Miner Res, 2010. **25**(4): p. 746-756.
155. Phan, C.M., et al., *Trabecular Bone Structure of the Calcaneus: Comparison of MR Imaging at 3.0 and 1.5 T with Micro-CT as the Standard of Reference.* Radiology, 2006. **239**(2): p. 488-496.
156. Krug, R., et al., *Assessment of trabecular bone structure comparing magnetic resonance imaging at 3 Tesla with high-resolution peripheral quantitative computed tomography ex vivo and in vivo.* Osteoporosis Int, 2008. **19**(5): p. 653-661.
157. Liu, X.S., et al., *Accuracy of high-resolution in vivo micro magnetic resonance imaging for measurements of microstructural and mechanical properties of human distal tibial bone.* J Bone Miner Res, 2010. **25**(9): p. 2039-50.

158. Wehrli, F.W., et al., *Role of magnetic resonance for assessing structure and function of trabecular bone.* Top Magn Reson Imaging, 2002. **13**(5): p. 335-55.
159. Nickolas, T.L., S. Shirazian, and E. Shane, *High-resolution computed tomography imaging: a virtual bone biopsy.* Kidney Int, 2010. **77**(11): p. 1046.
160. van Rietbergen, B. and K. Ito, *A survey of micro-finite element analysis for clinical assessment of bone strength: the first decade.* J Biomech, 2015. **48**(5): p. 832-41.
161. Boutroy, S., et al., *Finite element analysis based on in vivo HR-pQCT images of the distal radius is associated with wrist fracture in postmenopausal women.* J Bone Miner Res, 2008. **23**(3): p. 392-399.
162. Adams, J.E., *Quantitative computed tomography.* Eur J Radiol, 2009. **71**(3): p. 415-24.
163. Manske, S.L., et al., *Human trabecular bone microarchitecture can be assessed independently of density with second generation HR-pQCT.* Bone, 2015. **79**: p. 213-21.
164. Damilakis, J., et al., *Radiation exposure in X-ray-based imaging techniques used in osteoporosis.* Eur Radiol, 2010. **20**(11): p. 2707-14.
165. Boutroy, S., et al., *In vivo assessment of trabecular bone microarchitecture by high-resolution peripheral quantitative computed tomography.* J Clin Endocrinol Metab, 2005. **90**(12): p. 6508-15.
166. Khosla, S., et al., *Effects of sex and age on bone microstructure at the ultradistal radius: a population-based noninvasive in vivo assessment.* J Bone Miner Res, 2006. **21**(1): p. 124-131.
167. Zebaze, R. and E. Seeman, *Cortical bone: a challenging geography.* J Bone Miner Res, 2015. **30**(1): p. 24-9.
168. Zebaze, R.M., et al., *Intracortical remodelling and porosity in the distal radius and post-mortem femurs of women: a cross-sectional study.* Lancet, 2010. **375**(9727): p. 1729-36.
169. Kroker, A., et al., *Quantitative in vivo assessment of bone microarchitecture in the human knee using HR-pQCT.* Bone, 2017. **97**: p. 43-48.
170. Al Mukaddam, M., et al., *Effects of testosterone and growth hormone on the structural and mechanical properties of bone by micro-MRI in the distal tibia of men with hypopituitarism.* J Clin Endocrinol Metab, 2014. **99**(4): p. 1236-44.
171. Gomberg, B., et al., *Reproducibility and error sources of μ-MRI-based trabecular bone structural parameters of the distal radius and tibia.* Bone, 2004. **35**(1): p. 266-276.

172. Krug, R., et al., *Feasibility of in vivo structural analysis of high-resolution magnetic resonance images of the proximal femur.* Osteoporos Int, 2005. **16**(11): p. 1307-14.
173. Chang, G., et al., *Feasibility of three-dimensional MRI of proximal femur microarchitecture at 3 tesla using 26 receive elements without and with parallel imaging.* J Magn Reson Imaging, 2014. **40**(1): p. 229-38.
174. Gomberg, B.R., P.K. Saha, and F.W. Wehrli, *Method for cortical bone structural analysis from magnetic resonance images.* Acad Radiol, 2005. **12**(10): p. 1320-32.
175. Chang, G., et al., *Finite element analysis applied to 3-T MR imaging of proximal femur microarchitecture: lower bone strength in patients with fragility fractures compared with control subjects.* Radiology, 2014. **272**(2): p. 464-74.
176. Rajapakse, C.S., et al., *Patient-specific Hip Fracture Strength Assessment with Microstructural MR Imaging-based Finite Element Modeling.* Radiology, 2017. **283**(3): p. 854-861.
177. Techawiboonwong, A., et al., *Cortical bone water: in vivo quantification with ultrashort echo-time MR imaging.* Radiology, 2008. **248**(3): p. 824-33.
178. Bala, Y., R. Zebaze, and E. Seeman, *Role of cortical bone in bone fragility.* Curr Opin Rheumatol, 2015. **27**(4): p. 406-13.
179. Majumdar, S., et al., *Trabecular bone architecture in the distal radius using magnetic resonance imaging in subjects with fractures of the proximal femur. Magnetic Resonance Science Center and Osteoporosis and Arthritis Research Group.* Osteoporos Int, 1999. **10**(3): p. 231-9.
180. Wehrli, F.W., et al., *Digital topological analysis of in vivo magnetic resonance microimages of trabecular bone reveals structural implications of osteoporosis.* J Bone Miner Res, 2001. **16**(8): p. 1520-31.
181. Benito, M., et al., *Deterioration of trabecular architecture in hypogonadal men.* J Clin Endocrinol Metab, 2003. **88**(4): p. 1497-502.
182. Benito, M., et al., *Effect of testosterone replacement on trabecular architecture in hypogonadal men.* J Bone Miner Res, 2005. **20**(10): p. 1785-91.
183. Zhang, X.H., et al., *In Vivo μMRI-Based Finite Element and Morphological Analyses of Tibial Trabecular Bone in Eugonadal and Hypogonadal Men Before and After Testosterone Treatment.* J Bone Miner Res, 2008. **23**(9): p. 1426-1434.

184. Chesnut, C.H., 3rd, et al., *Effects of salmon calcitonin on trabecular microarchitecture as determined by magnetic resonance imaging: results from the QUEST study.* J Bone Miner Res, 2005. **20**(9): p. 1548-61.
185. Folkesson, J., et al., *Longitudinal evaluation of the effects of alendronate on MRI bone microarchitecture in postmenopausal osteopenic women.* Bone, 2011. **48**(3): p. 611-21.
186. Link, T.M., et al., *Changes in calcaneal trabecular bone structure after heart transplantation: an MR imaging study.* Radiology, 2000. **217**(3): p. 855-62.
187. Wehrli, F.W., et al., *Quantitative high-resolution magnetic resonance imaging reveals structural implications of renal osteodystrophy on trabecular and cortical bone.* J Magn Reson Imaging, 2004. **20**(1): p. 83-9.
188. Russo, C.R., et al., *Volumetric bone density and geometry assessed by peripheral quantitative computed tomography in uremic patients on maintenance hemodialysis.* Osteoporos Int, 1998. **8**(5): p. 443-8.
189. Hasegawa, K., Y. Hasegawa, and A. Nagano, *Estimation of bone mineral density and architectural parameters of the distal radius in hemodialysis patients using peripheral quantitative computed tomography.* Journal of biomechanics, 2004. **37**(5): p. 751-756.
190. Jamal, S.A., et al., *Cortical pQCT measures are associated with fractures in dialysis patients.* J Bone Miner Res, 2006. **21**(4): p. 543-8.
191. Negri, A.L., et al., *Evaluation of cortical bone by peripheral quantitative computed tomography in continuous ambulatory peritoneal dialysis patients.* Hemodial Int, 2006. **10**(4): p. 351-5.
192. Negri, A., et al. *Evaluation of cortical bone by peripheral quantitative computed tomography in renal transplant recipients*. Transplant Proc. 2005. **37**(2): p. 1020-1022.
193. Obatake, N., et al., *Annual change in bone mineral density in predialysis patients with chronic renal failure: significance of a decrease in serum 1,25-dihydroxy-vitamin D.* J Bone Miner Metab, 2007. **25**(1): p. 74-9.
194. Fujimori, A., et al., *Relationship between Biochemical Markers and Radial Cortical Bone Changes in Hemodialysis Patients.* Nephron Clinical Practice, 2011. **118**(4): p. c375-c379.
195. Bacchetta, J., et al., *Early impairment of trabecular microarchitecture assessed with HR-pQCT in patients with stage II-IV chronic kidney disease.* J Bone Miner Res, 2010. **25**(4): p. 849-57.

196. Jamal, S., et al., *Bone mineral density by DXA and HR pQCT can discriminate fracture status in men and women with stages 3 to 5 chronic kidney disease.* Osteoporos Int, 2012. **23**(12): p. 2805-13.
197. Nickolas, T.L., et al., *Bone mass and microarchitecture in CKD patients with fracture.* J Am Soc Nephrol, 2010. **21**(8): p. 1371-80.
198. Cejka, D., et al., *Inverse association between bone microarchitecture assessed by HR-pQCT and coronary artery calcification in patients with end-stage renal disease.* Bone, 2014. **64**: p. 33-8.
199. Pelletier, S., et al., *Serum sclerostin: the missing link in the bone-vessel cross-talk in hemodialysis patients?* Osteoporos Int, 2015. **26**(8): p. 2165-74.

CHAPTER 2: DETERIORATION OF CORTICAL BONE MICROARCHITECTURE: CRITICAL COMPONENT OF RENAL OSTEODYSTROPHY EVALUATION

The research presented in this chapter has been published in the following article.

AK Sharma, ND Toussaint, R Masterson, SG Holt, CS Rajapakse, PR Ebeling, ST Mohanty, P Baldock and GJ Elder. Deterioration of cortical bone microarchitecture: critical component of renal osteodystrophy evaluation. *American Journal of Nephrology* 2018; **47**(6):376-384.

Author affiliations

Ashish K SHARMA[1,2], Nigel D TOUSSAINT[1,2], Rosemary MASTERSON[1,2], Stephen G HOLT[1,2], Chamith S RAJAPAKSE[3], Peter R EBELING[4], Sindhu T MOHANTY[5], Paul BALDOCK[5], Grahame J ELDER[5,6]

[1]*Department of Nephrology, The Royal Melbourne Hospital, Parkville, Australia*

[2]*Department of Medicine (RMH), University of Melbourne, Parkville, Australia*

[3]*Departments of Radiology and Orthopaedic Surgery, University of Pennsylvania, PA, USA*

[4]*Monash University, Clayton, Australia*

[5]*Osteoporosis and Bone Biology Division, Garvan Institute of Medical Research, Darlinghurst, Australia,*

[6]*Department of Renal Medicine, Westmead Hospital, Westmead, Australia*

Summary

Background: Cortical bone is a significant determinant of bone strength and its deterioration contributes to bone fragility. Thin cortices and increased cortical porosity have been noted in patients with chronic kidney disease (CKD), but the 'Turnover Mineralization Volume' (TMV) classification of renal osteodystrophy does not emphasize cortical bone as a key parameter. We aimed to assess trabecular and cortical bone microarchitecture by histomorphometry and micro-computed tomography (micro-CT) in patients with CKD G5 and 5D (dialysis).

Methods: Transiliac bone biopsies were performed in 14 patients undergoing kidney transplantation (n=12) and parathyroidectomy (n=2). Structural parameters analysed by histomorphometry and micro-CT included trabecular bone volume, thickness (TbTh), number (TbN) and separation and cortical thickness (CtTh) and porosity (CtPo). Indices of bone remodelling and mineralisation were obtained and relationships to bone biomarkers examined. Associations were determined by Spearman's or Pearson's rank correlation coefficients.

Results: By micro-CT, trabecular parameters were within normal ranges in most patients, but all patients showed very low CtTh (127±44 μm) and high CtPo (60.3±22.5%). CtPo was inversely related to TbN (r=-0.56; p=0.03) by micro-CT and to TbTh (r=-0.60; p=0.024) by histomorphometry and correlated to parathyroid hormone values (r=0.62; p=0.021). By histomorphometry, bone turnover was high in 50%, low in 21% and normal in 29%, while 36% showed abnormal patterns of mineralization. Significant positive associations were observed between osteoblast surface, osteoclast surface, mineralization surface and bone turnover markers.

Conclusions: Deterioration of cortical microarchitecture despite predominantly normal trabecular parameters, reinforces the importance of comprehensive cortical evaluation in patients with CKD.

Introduction

Bone structure can be divided into cortical and cancellous tissue compartments., with approximately 80% of the adult skeleton comprised of cortical bone and trabecular bone in the cancellous compartment comprising the remainder. The ratio of cortical to trabecular bone varies widely for bones at different anatomic locations and within the same bone at different sites. The two types of bone also differ in arrangement of microstructure, which is responsible for the difference in their functional attributes. Cortical bone is compact and dense and provides bulk and strength, whereas the more 'metabolically active' trabecular bone is a honeycomb-like network of plates and rods [1]. Trabecular bone provides larger surface area per matrix volume for remodelling to occur and is the site of earlier and more rapid bone loss. With ageing, cortical bone undergoes increased remodelling leading to widening of long bones, thinner cortices and increased remodelling spaces that are visualized as 'pores' [2, 3]. If excessive, these changes can potentially result in a marked increase in bone fragility and heightened fracture risk.

Current concept of 'bone quality' includes all levels of bone structure and material composition as determinants of bone strength [4, 5]. Although lower values of bone mineral density (BMD) measured by dual-energy X-ray absorptiometry (DXA) and trabecular bone loss have been traditionally associated with increased fracture risk, newer high-resolution imaging techniques have highlighted the important independent contribution of cortical bone to overall bone strength and fragility [6-9]. Studies in people with chronic kidney disease (CKD), including after renal transplantation, have highlighted their enhanced susceptibility to fracture compared with age and gender matched controls [10-13] with consequent increases in hospitalization and mortality [14]. For the classification of bone structural abnormalities in

patients with CKD, development of the Kidney Disease Improving Global Outcomes (KDIGO) 'Turnover Mineralization Volume' (TMV) system [15] has been the most notable advancement, because it provides clinically relevant descriptors. However, assessment of cortical microarchitecture is described as an adjunct to the trabecular bone measurements. The common findings of cortical thinning and increased cortical porosity in recent studies of patients with CKD [16, 17] and their potential contribution to bone fragility suggest a need to emphasize the evaluation of cortical microarchitecture as a key parameter in addition to trabecular changes within the TMV classification.

In this cross-sectional study, we describe trabecular and cortical microarchitecture obtained by classical histomorphometry and micro-computed tomography (micro-CT) of iliac crest biopsies in participants with CKD G5 and 5D (dialysis). Micro-CT is an *ex-vivo* ultra-high resolution, non-destructive method to acquire direct three-dimensional (3D) measurements of cortical and cancellous bone microarchitecture and images a much larger volume of interest than two-dimensional (2D) histology.

Materials and Methods

Study participants

Between December 2014 and January 2016, fourteen participants, planned for living donor kidney transplantation (n=12) and parathyroidectomy (n=2), underwent transiliac bone biopsies at the completion of their surgical procedure. Inclusion criteria were CKD G.5 and 5D and non-participation in another trial at the time of recruitment. The protocol was approved by the local ethics committee and all patients provided informed consent.

Biochemical measurements

Blood samples were obtained prior to surgery and analysed at The Royal Melbourne Hospital using standard laboratory analysis on an Elecsys Cobas autoanalyser system. Serum concentrations of intact parathyroid hormone (iPTH) were determined using Architect Intact PTH (Abbott Laboratories, USA) chemiluminescent microparticle immunoassay (CMIA). Osteocalcin (OC) and procollagen type 1 N-terminal propeptide (P1NP), markers of osteoblast activity, and beta-cross linked telopeptides (β-CTx), a marker of osteoclastic resorption, were assayed by an electrochemiluminescence immunoassay (Elecsys®, Roche, Switzerland). Serum 1,25-dihydroxyvitamin D ($1,25[OH]_2D$) was measured by radioimmunoassay (Immunodiagnostic Systems Ltd).

Bone histomorphometry

Participants underwent double tetracycline labelling for bone histomorphometry, consisting of three days of doxycycline hydrochloride (100 mg twice daily), followed by a tetracycline-free interval of 10 days and then tetracycline hydrochloride (500mg twice daily) for three days. Anterior iliac crest bone biopsies were obtained under general anaesthesia using a modified 7.5 mm Bordier trephine (Landanger) via a horizontal approach as described elsewhere [18]. The specimens were fixed in cold neutral buffered formalin (NBF) 10% for up to 48 hours and then dehydrated in 70% ethanol. The static and dynamic parameters were examined and reported as measurements in two dimensions using nomenclature established by the American Society for Bone and Mineral Research [19]. Normal ranges of bone histomorphometry [20, 21] and micro-CT [22, 23] derived parameters were defined from previously reported data and local experience. Final histomorphometry results were categorized according to the TMV classification [15] .

Microcomputed tomography

Micro-CT was performed by an experienced operator blinded to patient characteristics. Bone debris was first eliminated from the biopsy core (Figure 1A), and the complete biopsy core was scanned using a Skyscan Model 1172 Micro-CT scanner (Bruker, Aartselar, Belgium) at 50 kV, 200 mA with a 0.5-mm aluminium filter using a isotropic voxel size of 4.3 microns. Images were captured every 0.4˚ through 180˚ and then reconstructed and analyzed using NRecon software (version 1.6.10.5; Bruker, Belgium). The average scan time was 60 minutes per sample. CTAnalyser software (version 1.16.1.0; Bruker, Belgium) was applied to quantify bone volume and architecture. Boundaries of the cortical and cancellous compartments, indicated in Figures 1B and 1C, were determined by X-ray attenuation of voxels on a grey scale from 1; black, indicating empty space and no bone, to 255; white, indicating most dense bone. A range from 1-59 for the cancellous compartment and 60-255 for the cortical compartment produced the best binary images for analysis of each compartment in the bone biopsy samples and these threshold values were maintained across all samples to ensure integrity of the study.

Three-dimensional analysis was applied to calculate morphometric parameters within the total cancellous compartment of each biopsy core, including trabecular bone volume to tissue volume (BV/TV), trabecular number (TbN) and trabecular thickness (TbTh). Using the binary images created by thresholding at 60-255 to exclude denser (cortical) areas of the biopsy, the cancellous ROI was then inverted to measure cortical bone volume (C.BV) and cortical bone thickness (CTh). Within the cortical ROI, total cortical porosity was calculated as the volume of all open and closed pores as a percentage of the total C.BV. The cortical thickness and porosity represent the mean of the two cortices for 10 biopsy samples while in the remaining

four samples only the intact outer cortex was available for measurements. Analysis of the structure model index (SMI), which corresponds to the trabecular plate- or rod-like geometry, and the degree of anisotropy (DA), for which higher values indicate disruption of trabecular network connectivity, was performed according to manufacturer's specifications.

Statistical methods

Results are presented as mean (+/- standard deviation) for normally distributed continuous variables and as median (and interquartile range) for continuous variables with skewed distributions. Correlation analyses were conducted to investigate associations between parameters obtained by classical histomorphometry and those obtained by micro-CT as well as biomarkers. Pearson correlation coefficients were used to express the relationship between variables if both parameters were normally distributed. Spearman correlation coefficients were used if results of one or both parameters were not normally distributed. We compared the cortical structural parameters measured by micro-CT in subjects with or without high turnover and in subjects with or without normal mineralisation. A two-tailed *p* value <0.05 was considered statistically significant. Stata statistical software package (version 11.0, Stata Corporation, College Station, TX) was used for analysis.

Results

Participant characteristics

Demographic and biochemical parameters of the study cohort are shown in Table 1 and Table 2 respectively. The mean age of participants was 44.4+/-10.3 years and 64.3% were male. Glomerulonephritis (42.8%) was the most common cause of CKD. Nine (64.2%) participants were on renal replacement therapy (hemodialysis n=6; peritoneal dialysis n=3) for a median

duration of 8.5 (interquartile range [IQR] 0 – 32.75) months, and five underwent pre-emptive living donor renal transplantation. Potential bone modulating medications prescribed to participants are listed in Table 1. Median serum iPTH was 45.3 (24 - 66.5) pmol/L. Serum iPTH values were above the KDIGO (Kidney Disease Improving Global Outcomes) CKD - Mineral and Bone Disorder (MBD) Guidelines [24] target range of up to nine times the normal upper reference range of the assay in three patients, two of whom were undergoing parathyroidectomy. Median values of bone turnover markers were elevated, as expected for these markers in patients with CKD G5 and 5D. P1NP and β-CTx were approximately two times and OC was four times the normal upper reference value.

Bone trephine histomorphometry and micro-CT measures

On histomorphometry of the cancellous compartment, features of hyperparathyroidism and increased bone turnover were present in 50% (n=7) of participants, while 21.4% (n=3) had low or absent bone turnover and little or no evidence of bone resorption based on static indices of cellular activity; osteoblast, osteoclast and eroded surface to bone surface (Table 3). Features of osteomalacia, based on osteoid thickness, surface, volume and smeared or absent tetracycline label were present in 35.7% (n=5). The mean trabecular bone volume was within the normal range (Table 4) and was low or low normal in only 28.6% of participants. The mean cortical thickness was 868 ± 410 μm (normal range 800 – 1400 μm) and cortical porosity was 10.8 ± 8.2% (high >10%).

Quantitative histomorphometry by micro-CT was characterised by deterioration in cortical bone, with thin cortices (mean thickness 127 ± 44 μm) and high cortical porosity (60.3 ±

22.5%) in all participants. Trabecular parameters were relatively preserved (Table 4), with reduced trabecular bone volume in only 21.4% of participants.

Comparing results from micro-CT and histomorphometry, measures of cortical thickness showed no significant correlation but cortical porosity correlated significantly (0.56; p=0.036). Cortical porosity by micro-CT correlated to values of iPTH (r=0.62; *p*=0.02) and was negatively correlated to TbN by micro-CT (r=-0.56; p=0.03) and TbTh (r=-0.60; p=0.02) by histomorphometry. Cortical thickness and porosity by micro-CT showed no significant variation with histomorphometric parameters of mineralisation or with contemporaneous high or low turnover status. The median trabecular SMI value was negative at -0.8 (-7.7 to 0.7; normal range 1.15 ± 0.61), indicative of cavities, and anisotropy was increased with the mean DA 2.04 ± 0.8 (normal range 1.49 ± 0.18), indicating fewer trabeculae in directions of lower load and disruption of trabecular network connectivity. Histomorphometry parameters arranged by the TMV classification are presented in Table 3 and structural parameters by both techniques are listed in Table 4.

Bone biomarkers and histomorphometry

Bone turnover markers correlated significantly to all histomorphometric remodelling indices. P1NP was positively correlated to osteoblast surface (r=0.54; *p*=0.04), osteoclast surface (r=0.65; *p*=0.01) and mineralization surface (r=0.74; *p*=0.002). Similarly, β-CTx was positively correlated to osteoblast surface (r=0.61; *p*=0.02), osteoclast surface (r=0.66; *p*=0.009) and mineralization surface (r=0.77; *p*=0.001). There was also a positive correlation of osteocalcin to both osteoblast surface (r=0.65; *p*=0.01) and mineralization surface (r=0.75; *p*=0.003). Serum 25(OH)D values were associated with indices of resorption - osteoclast surface (r=0.62;

p=0.02) and osteoclast number (r=0.62; *p*=0.01) - and mineralization surface (r=0.64; *p*=0.01). Serum 1,25$(OH)_2$D values were associated with osteoid width (r=-0.86; *p*=0.001). There were no significant relationships of bone biomarkers to other structural parameters derived by histomorphometry or micro-CT.

Discussion

Cortical bone constitutes approximately 80% of the adult skeleton and its contribution to fracture resistance is well recognised. However, relatively few studies have endeavoured to use histomorphometry [25, 26] or micro-CT of bone trephine samples, or utilised non-invasive techniques [16, 17, 27] to assess cortical microarchitecture and porosity in patients with CKD G5, 5D or after kidney transplantation. In the current study, 50% of patients had changes consistent with high bone turnover on histomorphometry, accompanied by elevated PTH values, but all participants had markedly abnormal cortical microarchitecture assessed by micro-CT with relatively preserved trabecular structural parameters. This severe cortical bone loss is remarkable, given that patients in this study were relatively young (mean 44.4 ± 10.3 years) and healthy, with the majority undergoing transplantation, compared with older and non-transplantable patients with CKD G5 and 5D. However, these characteristics also limit the extrapolation of our results to a general dialysis population. Of note, the cortical abnormalities were not as prominent by histomorphometry and values for cortical thickness by micro-CT and histomorphometry were not significantly correlated. Differences in cortical thickness are unlikely to be due to the segmentation threshold used for delineation of cortex from the cancellous compartments by micro-CT, since the thresholding value was consistent throughout the samples. More likely, differences in thickness and porosity relate to the

limited portion of cortex assessed in 2D by histomorphometry versus the entire cortex assessed in 3D by micro-CT.

Physiological remodelling of bone with aging, or rapid unbalanced remodelling associated with metabolic disease plays a key role in the pathogenesis of cortical bone loss. Trabecular bone has a high surface to matrix volume ratio and provides a larger surface for initiation of remodelling compared with cortical bone. Interestingly, the bone turnover markers P1NP, β-CTx and osteocalcin correlated to histomorphometric remodelling indices in this study, despite the recognised difficulty of interpreting these markers due to rises that accompany deteriorating renal function. Serum 25(OH)D values also correlated to indices of resorption and mineralization. While vitamin D and its metabolites may have local actions in the bone environment that include the facilitation of mineral deposition and the enhancement of bone resorption [28], the basis of these associations is unclear.

Cortical bone, although traditionally described as being compact, is traversed by Haversian and Volkmann canals which provide the intracortical surface for remodelling. Over time, with fewer trabecular sites available for remodelling, there is increased bone loss from the cortical compartment. Increased remodelling at intracortical and endocortical surfaces, and uncoupling of bone formation from resorption, leads to incomplete refilling of cavities and widening of canals, and increases the available cortical surface area for the initiation of remodelling events. This results in 'trabecularisation' of the cortex and increased cortical porosity [3]. A small increase in cortical porosity disproportionately affects bone strength and may potentially contribute to bone fragility [9, 29]. This is significant given that more than 70% of all fractures occur at non-vertebral sites [30, 31] that are rich in both cortical and

trabecular bone. A number of studies have demonstrated a relationship of fracture to the deterioration of cortical architecture with aging and metabolic disease. [3, 6-8]

To our knowledge, this study is the first to report the role of micro-CT in assessing cortical porosity in patients with CKD. Data on cortical porosity in the CKD population is derived mainly from studies using HR-pQCT, an imaging modality prone to certain limitations in quantifying cortical bone structure [32]. For example, trabecularisation of cortical bone may cause potential measurement errors in segmentation between cortical and trabecular bone compartments, leading to overestimation of trabecular density or underestimation of cortical porosity [3, 33]. HR-pQCT does not have the requisite resolution to measure cortical pores smaller than 100 μm which constitute about 60% of total pores, and this leads to significant underestimation of total cortical porosity [29]. The average cortical porosity defined by HR-pQCT is approximately 3-7% [34] compared with a cortical void volume of 15-40% derived by direct measurements of cortical bone water identified in MRI studies [35, 36]. However, the very high mean cortical porosity in our study (mean 60.3 ± 22.5%), representing a higher number of larger 'pores,' is likely to reflect uncoupled, largely PTH-mediated cortical remodelling, and can only be partly attributed to identification of larger numbers of pores by micro-CT due to its higher resolution. In such a scenario, the relatively normal trabecular structure observed in our study may represent a differential action of PTH on trabecular and cortical bone compartments.

This study supports recent histomorphometric [25, 26, 37, 38] and imaging studies [16, 17, 27, 39, 40] that have reported changes in cortical bone microarchitecture in individuals with CKD. In a cross sectional study involving 38 dialysis patients, Adragao *et al.* [25] reported high

cortical porosity in 57% and reported a significant inverse relationship between femoral BMD and cortical porosity. The presence of high cortical porosity and reduced cortical thickness in dialysis patients was also reported by Malluche *et al.* [26] in a large histomorphometry study of 630 bone biopsies. Cortical porosity was related to hyper-resorption and high turnover, and varied with race, being present in 50% of white and 75% of black patients, while reduced cortical thickness was reported in 50% of white patients and 10% of black patients. In a recent *post-hoc* analysis of histomorphometry data from a randomized controlled trial [41], Araujo *et al.* [38] reported high cortical porosity in 85% of 52 hemodialysis patients at baseline and a subsequent increase in both PTH levels and cortical porosity in patients who were treated for low bone turnover. Similarly, imaging studies have described abnormal cortical bone microarchitecture [39], progressive cortical loss and increased cortical porosity to be associated with hyperparathyroidism in patients with CKD [16] including kidney transplant recipients [40]. In the TMV classification, measurement of cortical bone volume and thickness is described as additional information to that provided by the trabecular bone volume [15]. However, the current and aforementioned studies emphasize the importance of describing cortical microarchitecture as a central parameter of the TMV classification, together with the trabecular parameters.

Our study has some limitations including its cross-sectional nature and small sample size without a non-CKD control group. The sample size limits statistical robustness, and as a single center study with 13 of 14 patients being Caucasian, the generalisability of our findings to other centers and racial groups may be limited. Four patients in our cohort were on maintenance prednisolone therapy at the time of transplantation and this might have contributed to overall finding of abnormal bone structure in our patients. It is, however, hard

to delineate these manifestations from those due to ESKD in a small cohort. The thresholding method of segmentation between cortical and cancellous compartments used in our micro-CT analysis has known limitations. Inaccuracy in differentiating cortical and trabecular bone by thresholding can potentially result in overestimation of trabecular parameters, which may be reflected in our finding of relatively normal trabecular indices [33]. Some voxels being evaluated for cortical porosity may contain varying proportions of void volume and mineralized bone matrix. In such voxels, the photo-attenuation caused by mineralized bone may lead to underestimation of the void volume and cortical porosity [42]. These potential measurement errors, if applied to our study, may present a more severe picture of both cortical and trabecular architecture in our cohort. Despite these limitations, this study is one of relatively few to report cortical microstructure and the first to utilize micro-CT to measure cortical porosity and thickness from 3D sections in a CKD-G5 and 5D cohort.

In summary, this study highlights a marked deterioration of cortical bone microarchitecture in CKD. Cortical porosity has an established role in bone fragility, and a focus on cortical changes represents a significant shift in the assessment of renal osteodystrophy that may have diagnostic and treatment implications. In addition to the TMV classification of trabecular bone, assessment of the cortex (‘C’) requires emphasis, but to establish an association of cortical porosity and thickness to fractures in people with CKD, prospective studies are required. Such studies, using newer non-invasive means to assess the cortical and cancellous compartments that can be readily repeated over time, might lead to interventions using cortical bone as a therapeutic target.

References

1. Clarke, B., *Normal bone anatomy and physiology.* Clin J Am Soc Nephrol, 2008. 3(Supplement 3): p. S131-S139.
2. Seeman, E., *Pathogenesis of bone fragility in women and men.* The Lancet, 2002. 359(9320): p. 1841-1850.
3. Zebaze, R.M., et al., *Intracortical remodelling and porosity in the distal radius and post-mortem femurs of women: a cross-sectional study.* Lancet, 2010. 375(9727): p. 1729-36.
4. Seeman, E. and P.D. Delmas, *Bone quality--the material and structural basis of bone strength and fragility.* N Engl J Med, 2006. 354(21): p. 2250-61.
5. Malluche, H.H., D.S. Porter, and D. Pienkowski, *Evaluating bone quality in patients with chronic kidney disease.* Nat Rev Nephrol, 2013. 9(11): p. 671-80.
6. Nishiyama, K.K., et al., *Postmenopausal women with osteopenia have higher cortical porosity and thinner cortices at the distal radius and tibia than women with normal aBMD: an in vivo HR-pQCT study*. J Bone Miner Res, 2010. 25(4): p. 882-890.
7. Patsch, J.M., et al., *Increased cortical porosity in type 2 diabetic postmenopausal women with fragility fractures.* J Bone Miner Res, 2013. 28(2): p. 313-324.
8. Bala, Y., et al., *Cortical Porosity Identifies Women With Osteopenia at Increased Risk for Forearm Fractures.* J Bone Miner Res, 2014. 29(6): p. 1356-1362.
9. Bala, Y., R. Zebaze, and E. Seeman, *Role of cortical bone in bone fragility.* Curr Opin Rheumatol, 2015. 27(4): p. 406-413.
10. Alem, A.M., et al., *Increased risk of hip fracture among patients with end-stage renal disease.* Kidney Int, 2000. 58(1): p. 396-9.
11. Ball, A.M., *Risk of Hip Fracture Among Dialysis and Renal Transplant Recipients.* JAMA, 2002. 288(23): p. 3014-3018.
12. Naylor, K.L., et al., *The three-year incidence of fracture in chronic kidney disease.* Kidney Int, 2014. 86(4): p. 810-8.
13. Hansen, D., et al., *Risk of fracture in adults on renal replacement therapy: a Danish national cohort study.* Nephrol Dial Transplant, 2016. 31(10): p. 1654-62.
14. Tentori, F., et al., *High rates of death and hospitalization follow bone fracture among hemodialysis patients.* Kidney Int, 2014. 85(1): p. 166-73.

15. Moe, S., et al., *Definition, evaluation, and classification of renal osteodystrophy: a position statement from Kidney Disease: Improving Global Outcomes (KDIGO)*. Kidney Int, 2006. 69(11): p. 1945-53.
16. Nickolas, T.L., et al., *Rapid cortical bone loss in patients with chronic kidney disease.* J Bone Miner Res, 2013. 28(8): p. 1811-20.
17. Nishiyama, K.K., et al., *Longitudinal HR-pQCT and image registration detects endocortical bone loss in kidney transplantation patients.* J Bone Miner Res, 2015. 30(3): p. 554-61.
18. Hernandez, J.D., et al., *Technical approach to iliac crest biopsy.* Clin J Am Soc Nephrol, 2008. 3 Suppl 3(Supplement 3): p. S164-9.
19. Dempster, D.W., et al., *Standardized nomenclature, symbols, and units for bone histomorphometry: a 2012 update of the report of the ASBMR Histomorphometry Nomenclature Committee.* J Bone Miner Res, 2013. 28(1): p. 2-17.
20. Malluche, H.H. and M.-C. Faugere, *Atlas of mineralized bone histology.* 1986: Karger New York.
21. Malluche, H.H., et al., *Quantitative bone histology in 84 normal American subjects.* Calcified Tissue International, 1982. 34(1): p. 449-455.
22. Hildebrand, T., et al., *Direct three-dimensional morphometric analysis of human cancellous bone: microstructural data from spine, femur, iliac crest, and calcaneus.* J Bone Miner Res , 1999. 14(7): p. 1167-1174.
23. Kulak, C.A.M., et al., *Skeletal microstructural abnormalities in postmenopausal women with chronic obstructive pulmonary disease.* J Bone Miner Res, 2010. 25(9): p. 1931-1940.
24. Kidney Disease: Improving Global Outcomes (KDIGO) CKD-MBD Work Group. *KDIGO clinical practice guideline for the diagnosis, evaluation, prevention, and treatment of Chronic Kidney Disease-Mineral and Bone Disorder (CKD-MBD).* Kidney Int Suppl, 2009(113): p. S1-130.
25. Adragao, T., et al., *Femoral bone mineral density reflects histologically determined cortical bone volume in hemodialysis patients*. Osteoporosis Int, 2010. 21(4): p. 619-625.
26. Malluche, H.H., H.W. Mawad, and M.C. Monier-Faugere, *Renal osteodystrophy in the first decade of the new millennium: analysis of 630 bone biopsies in black and white patients.* J Bone Miner Res, 2011. 26(6): p. 1368-76.

27. Rajapakse, C.S., et al., *Micro-MR imaging-based computational biomechanics demonstrates reduction in cortical and trabecular bone strength after renal transplantation.* Radiology, 2012. 262(3): p. 912-20.
28. Eisman, J.A. and R. Bouillon, *Vitamin D: direct effects of vitamin D metabolites on bone: lessons from genetically modified mice.* Bonekey Rep, 2014. 3: p. 499.
29. Cooper, D.M.L., et al., *Cortical Bone Porosity: What Is It, Why Is It Important, and How Can We Detect It?* Curr Osteoporos Rep, 2016. 14(5): p. 187-198.
30. Roux, C., et al., *Burden of non-hip, non-vertebral fractures on quality of life in postmenopausal women.* Osteoporosis Int, 2012. 23(12): p. 2863-2871.
31. Rosengren, B.E., et al., *The 21st-Century Landscape of Adult Fractures: Cohort Study of a Complete Adult Regional Population.* J Bone Miner Res, 2015. 30(3): p. 535-542.
32. Geusens, P., et al., *High-resolution in vivo imaging of bone and joints: a window to microarchitecture.* Nat Rev Rheumatol, 2014. 10(5): p. 304-13.
33. Zebaze, R. and E. Seeman, *Cortical bone: a challenging geography.* J Bone Miner Res, 2015. 30(1): p. 24-29.
34. Burghardt, A.J., et al., *Reproducibility of direct quantitative measures of cortical bone microarchitecture of the distal radius and tibia by HR-pQCT.* Bone, 2010. 47(3): p. 519-528.
35. Techawiboonwong, A., et al., *Cortical bone water: in vivo quantification with ultrashort echo-time MR imaging.* Radiology, 2008. 248(3): p. 824-33.
36. Rajapakse, C.S., et al., *Volumetric Cortical Bone Porosity Assessment with MR Imaging: Validation and Clinical Feasibility.* Radiology, 2015. 276(2): p. 526-35.
37. Carvalho, C., et al., *Cortical bone analysis in a predialysis population: a comparison with a dialysis population.* J Bone Miner Metab, 2016: p. 1-9.
38. Araujo, M.J., et al., *The pitfall of treating low bone turnover: Effects on cortical porosity.* Bone, 2016. 91: p. 75-80.
39. Wehrli, F.W., et al., *Quantitative high-resolution magnetic resonance imaging reveals structural implications of renal osteodystrophy on trabecular and cortical bone.* J Magn Reson Imaging, 2004. 20(1): p. 83-9.
40. Iyer, S.P., et al., *Kidney transplantation with early corticosteroid withdrawal: paradoxical effects at the central and peripheral skeleton.* J Am Soc Nephrol, 2014. 25(6): p. 1331-41.

41. Barreto, D.V., et al., *Phosphate binder impact on bone remodeling and coronary calcification--results from the BRiC study.* Nephron Clin Pract, 2008. 110(4): p. c273-83.
42. Zebaze, R., et al., *A new method of segmentation of compact-appearing, transitional and trabecular compartments and quantification of cortical porosity from high resolution peripheral quantitative computed tomographic images*. Bone, 2013. 54(1): p. 8-20.

Figures

Figure 1. Representative micro-CT images of a biopsy obtained from a study subject showing stages in processing (A) Biopsy core with debris, (B) Three-dimensional longitudinal slice, and (C) Two-dimensional longitudinal slice. Trabecular bone, white arrows; Cortical bone, black arrows

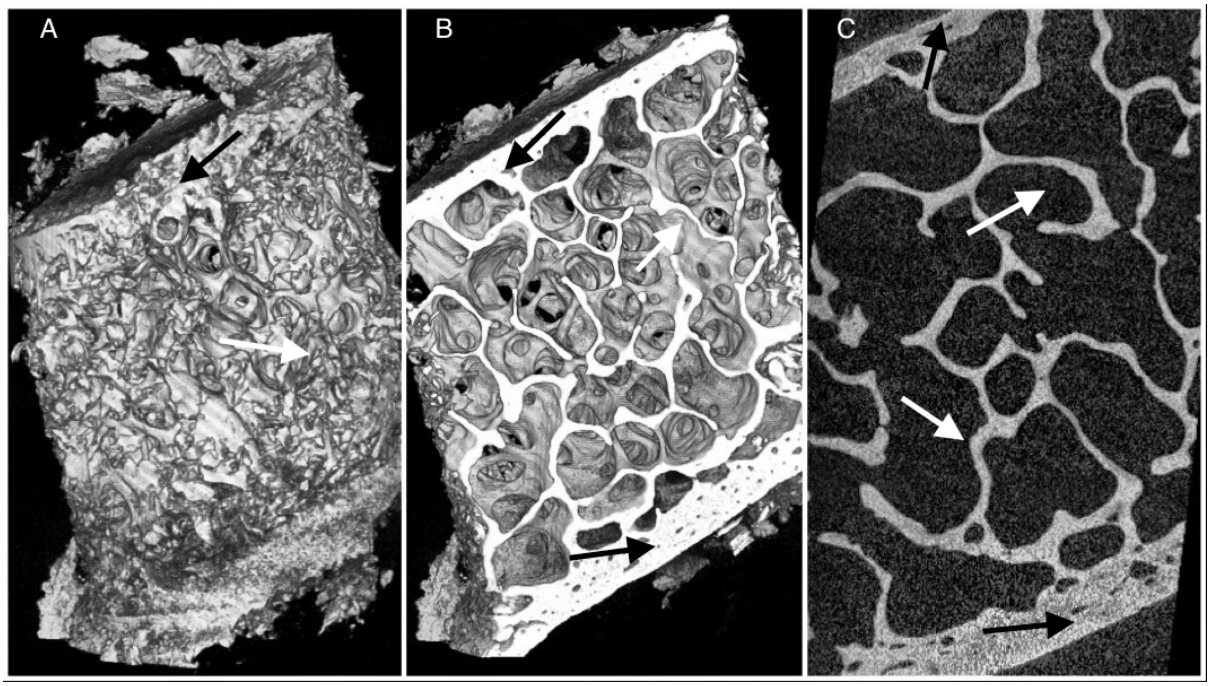

Tables

Table 1. Baseline demographic parameters (n = 14).

Variable	Values
Age at surgery (years)	44.4 ± 10.3
Gender (%Male)	64.2
Body Mass Index (kg/m^2)	27.1 ± 4.8
Cause of Chronic Kidney Disease (%)	
Glomerulonephritis	42.8
Diabetes mellitus	14.2
Polycystic kidney disease	14.2
Reflux nephropathy	21.4
Other	7.14
Dialysis: HD / PD / None (%)	42.8 / 21.4 / 35.7
Parathyroidectomy (%)	7.14
Bone Modulating Therapy (%)	
Cinacalcet	7.14
Phosphate binder	57.1
Calcitriol	42.8
Cholecalciferol	21.4
Prednisolone	28.5

Abbreviations: HD, hemodialysis; PD peritoneal dialysis.

Table 2. Baseline biochemical parameters for kidney transplant recipients (KTRs) and patients undergoing parathyroidectomy (PTHx). Data presented as mean ± SD or median (interquartile range)

Biomarker	KTR (n=12)	PTHx (n=2)	Normal range
Calcium	2.44 ± 0.1	2.46 ± 0.3	2.10-2.60 mmol/L
Phosphate	2.07 ± 0.3	2.83 ± 0.2	0.75-1.50 mmol/L
Parathyroid hormone	38.4 (19 - 55)	246 ± 101.6	1.7-10.0 pmol/L
Alkaline phosphatase	78 (63 - 121.5)	290 ± 168.2	30-120 IU/L
25-hydroxyvitamin D	65.1 ± 21.6	77.5 ± 20.5	55-108 nmol/L
1,25-dihydroxyvitamin D	29 (20 - 70)	N/A[#]	50-190 nmol/L
Osteocalcin	149.2 (30.9 - 203.6)	895 ± 841.4	14-46 ng/ml
Beta-cross linked telopeptide	1.26 (0.82 - 2.48)	6.0 ± 0.0	Males 0.1-0.6 ng/ml Females* 0.05-0.8 ng/ml
Procollagen type 1 N-propeptide	123.6 (47.3 – 262.1)	1665 ± 657.6	Males 15 – 80 µg/L Females* 15 - 90 µg/L

* Premenopausal reference range.

[#]Patients undergoing parathyroidectomy were pre-loaded with calcitriol, which would influence these results.

Values of serum osteocalcin, beta-cross linked telopeptide and procollagen type 1 N- propeptide increase above the normal range in patients with reduced renal function.

Table 3. Parameters measured by histomorphometry arranged by the TMV classification (n=14). Data presented as mean ± SD or median (interquartile range)

TMV	Variable	Value	Normal range
Turnover*	Ob.S/BS (%)	6.5 (2.9-16.6)	5.3 ± 2.7%
	ES/BS (%)	2.8 (0.4-5.2)	0.4-3.4%
	Oc.S/BS (%)	3.4 (0.4-6.5)	0.5-2.5%
	sLS/BS (%)	16.4 (4.9-37.2)	0.5-10.5%
Mineralisation	OV/BV (%)	2.1 (0.8-9.2)	1.3-3.1%
	OS/BS (%)	11.6 (8.4-32.6)	7.1-13.9%
	O.Th (µm)	14.1 ± 9.1	9.2-14.9 µm
Volume	BV/TV (%)	27 ± 1.1	21-29%

Abbreviations: Ob.S/BS, Osteoblast surface/Bone surface; ES/BS, Eroded surface; Oc.S/BS, Osteoclast surface; sLS/BS, Single-labelled surface (Mineralising surface); OV/BV, Osteoid volume/Bone volume; OS/BS, Osteoid surface; O.Th, Osteoid thickness; BV/TV, Cancellous bone volume/Total volume

*In patients with features of hyperparathyroidism, the mineral apposition rate varied from 0.77-1.08 µm/day (normal range 0.6-0.8 µm/day) and bone formation rate from 0.09-0.62 mm3/mm2/day (normal range 0.03-0.09 mm3/mm2/day). No label was detected for patients with adynamic bone and patients with normal bone surfaces had indices in the intermediate range or smeared label for mixed uraemic osteodystrophy. Due to difficulty reading the doxycycline label in some biopsies, sLS/BS is provided.

Table 4. Microarchitectural parameters measured by 2D histomorphometry and micro-CT (n=14). Data presented as mean ± SD or median (interquartile range).

	Variable	Mean±SD	Normal Range
Histomorphometry	BV/TV (%)	27.1 ± 11.5	21-29%
	TbTh (µm)	157.6 ± 60.1	90-175
	TbN (1/mm)	1.83 ± 0.75	1.1-2.2
	TbSp (µm)	368.5 (273.3-566.4)	770
Micro-CT	BV/TV (%)	20.3 ± 7.0	15.6 ± 5.4%
	TbTh (µm)	110 ± 37.0	151 ± 27
	TbN (1/mm)	2.20 ± 1.44	1.4 ± 0.27
	TbSp (µm)	593 ± 203	770 ± 350
	Mean cortical thickness (µm)	127 ± 44	381 ± 120*
	Cortical porosity (%)	60.31 ± 22.53	4-10 %*

Abbreviations: BV/TV, trabecular bone volume; TbTh, trabecular thickness; TbN, trabecular number; TbSp, trabecular separation. *Average values only; cortical thickness and porosity vary by sex and age.

CHAPTER 3: MAGNETIC RESONANCE IMAGING BASED ASSESSMENT OF BONE MICROSTRUCTURE AS A NON-INVASIVE ALTERNATIVE FOR HISTOMORPHOMETRY IN PATIENTS WITH CHRONIC KIDNEY DISEASE

The research presented in this chapter has been published in the following article.

AK Sharma, ND Toussaint, GJ Elder, R Masterson, SG Holt, PL Robertson, PR Ebeling, P Baldock, RC Miller and CS Rajapakse. Magnetic resonance imaging based assessment of bone microstructure as a non-invasive alternative to histomorphometry in patients with chronic kidney disease. *Bone* 2018; **114**:14-21.

Author affiliations

Ashish K SHARMA[1,2], Nigel D TOUSSAINT[1,2], Grahame J ELDER[3,4], Rosemary MASTERSON[1,2], Stephen G HOLT[1,2], Patricia L ROBERTSON[2,5], Peter R EBELING[6], Paul BALDOCK[4], Rhiannon C. MILLER[7], Chamith S RAJAPAKSE[7]

[1]*Department of Nephrology, The Royal Melbourne Hospital, Parkville, Australia*

[2]*Department of Medicine (RMH), University of Melbourne, Parkville, Australia*

[3]*Department of Renal Medicine, Westmead Hospital, Westmead, Australia*

[4]*Osteoporosis and Bone Biology Division, Garvan Institute of Medical Research, Darlinghurst, Australia*

[5]*Department of Radiology, The Royal Melbourne Hospital, Parkville, Australia*

[6]*Monash University, Clayton, Australia*

[7]*Departments of Radiology and Orthopaedic Surgery, University of Pennsylvania, PA, USA*

Summary

Background: Chronic kidney disease (CKD) adversely affects bone microarchitecture and increases fracture risk. Historically, bone biopsy has been the 'gold standard' for evaluating renal bone disease but is invasive and infrequently performed. High-resolution magnetic resonance imaging (MRI) quantifies bone microarchitecture noninvasively. In patients with CKD, it has not been compared with results derived from bone biopsy or with imaging using dual energy X-ray absorptiometry (DXA).

Methods: Fourteen patients with end-stage kidney disease (ESKD) underwent MRI at the distal tibia, bone mineral density (BMD) by dual energy X-ray absorptiometry (DXA; hip and spine) and transiliac bone biopsies with histomorphometry and microcomputed tomography (micro-CT). All patients had biomarkers of mineral metabolism. Associations were determined by Spearman's or Pearson's rank correlation coefficients.

Results: MRI indices of trabecular network integrity, surface to curve ratio (S/C) and erosion index (EI), correlated to histomorphometric trabecular bone volume (S/C r=0.85, *p*=0.0003; EI r=-0.82, *p*=0.001), separation (S/C r=-0.58, *p*=0.039; EI r=0.79, *p*=0.0012) and thickness (S/C, r=0.65, *p*=0.017). MRI EI and trabecular thickness (TbTh) also correlated to micro-CT trabecular separation (EI r=0.63, *p*=0.02; TbTh r=-0.60, *p*=0.02). Significant correlations were observed between histomorphometric mineralization and turnover indices and various MRI parameters. MRI-derived trabecular parameters were also significantly related to femoral neck BMD.

Conclusions: This study highlights the heterogeneity of bone microarchitecture at differing skeletal sites. MRI demonstrates significant, relevant associations to important bone biopsy and DXA indices and warrants further investigation to assess its potential to non-invasively evaluate changes in bone structure and quality over time.

Keywords: renal osteodystrophy, bone biopsy, magnetic resonance imaging, micro computed tomography, bone mineral density, bone turnover

Introduction

Renal osteodystrophy (ROD) refers to changes in bone quality associated with chronic kidney disease (CKD), and has been defined by changes to histomorphometric parameters of turnover, mineralization, and volume (TMV) [1]. Progressive decline in renal function adversely affects bone microarchitecture, mineralization, collagen structure and marrow composition. This may result in deterioration in both cancellous and cortical bone architecture to varying degrees. Structural changes in ROD include alterations in thickness, number and spacing of trabecular bone and disruption to its orientation, connectivity, and the ratio of its plate-like to rod-like structure. Similarly, abnormal bone remodelling and turnover results in thinned cortices and increased cortical porosity. These trabecular and cortical changes may lead to a loss of overall bone volume and increased bone fragility [2, 3].

Patients with CKD have significantly more fractures than age- and gender-matched individuals without CKD [4]. The risk of sustaining a fracture increases progressively as the glomerular filtration rate (GFR) falls [5] and persists in the early years after transplantation [6]. Moreover, fractures in patients with CKD are associated with increased morbidity and mortality compared to the general population [7]. Whilst recent epidemiological studies have emphasized the increased fracture risks of CKD [8, 9], tools used in clinical practice to evaluate ROD, including dual-energy X-ray absorptiometry (DXA) to assess bone mineral density (BMD) and biochemical bone turnover markers, have more diagnostic limitations in patients with CKD than in the general population. Bone biopsy and quantitative histomorphometry, the 'gold standard' for diagnosis and classification of ROD, is invasive, expensive, requires expertise to perform, process and interpret and is rarely used in clinical practice. Furthermore, the microstructure of the non-weight bearing iliac crest may differ in strength

and structure from the peripheral skeleton, where clinically relevant fractures often occur. This has led to a search for reliable biomarkers and non-invasive high-resolution imaging modalities such as high-resolution peripheral computed tomography (HR-pQCT) [10, 11], to determine bone microarchitecture and to estimate bone strength *in-viv*o.

High-resolution magnetic resonance imaging (MRI), is a non-ionising and non-invasive method for quantification of bone microstructure *in-vivo* [12]. Clinical studies using MRI scans at peripheral anatomical sites have reported associations between bone structure and fracture in non-CKD cohorts [13]. Additionally, the long-term impact of therapeutic interventions on the structural and mechanical components of bone microarchitecture [14-16] can be evaluated using MRI. Despite these putative advantages, few studies have examined its role in ROD [17-20] or its utility in evaluating changes in cortical and trabecular microarchitecture in patients with CKD. Moreover, in patients with CKD, the relationship of structural parameters obtained by *in-vivo* MRI to those derived from bone biopsy has not been explored. If validated, MRI has the potential to assess bone microstructure and estimate structural manifestations of strength at any anatomical site, including common sites of fracture such as the hip, a site at which feasibility studies have proven encouraging [21, 22].

The aim of this study was to compare information on bone structure obtained from non-invasive MRI at the distal tibia, to parameters obtained from transiliac bone biopsies submitted to standard histomorphometry and microcomputed tomography (micro-CT). Micro-CT analyses a much larger volume of interest compared with two-dimensional (2D) histology and is a non-destructive method to acquire direct three-dimensional (3D) measurements of cortical and cancellous bone microarchitecture, providing greater structural

detail. In addition to comparing bone structure parameters, we also assessed the relationship of MRI to BMD obtained by DXA, the current standard of care in clinical practice, and to laboratory indices. For this study, we recruited patients with CKD stage 5 or 5D (on dialysis), who were likely on clinical grounds to have ROD, with a range of structural bone abnormalities.

Materials and Methods

Study participants

A total of 31 patients were approached, including 27 patients planned for living donor kidney transplantation and four patients on hemodialysis awaiting parathyroidectomy. Five transplant surgeries were rescheduled or cancelled for clinical or logistical reasons. Sixteen of the remaining 26 patients consented and were recruited between December 2014 and January 2016, with 14 undergoing living donor kidney transplantation and two undergoing parathyroidectomies. Fourteen of the patients underwent transiliac bone biopsies at completion of the surgical procedure whilst under general anesthesia (12 after renal transplantation and 2 after parathyroidectomy). Inclusion criteria were end-stage kidney disease (ESKD), no contraindications to MRI, and non-participation in another trial. The protocol was approved by the local ethics committee and all patients provided informed consent.

MRI

MRI images were obtained within a 2-week period preceding the surgery with a commercial 3.0-Tesla whole-body imager (Siemens Trio, Germany). Participants were imaged in a feet-first prone position. MRI acquisitions were performed at the left distal tibial metaphysis using

a 3D ‘fast spin echo’ pulse sequence readily available on any clinical MRI system requiring a scan time of 12 minutes. This was undertaken utilizing a commercially available eight-channel radiofrequency (RF) extremity coil used in clinical practice. MRI parameters include 0.273 mm x 0.273 mm x 0.6 mm voxel size, 70 mm x 70 mm x 19.2 mm field-of-view, 53ms repetition time, 16ms echo time, 12 averages, and echo train length of two. Raw MRI data was pre-processed via bone volume fraction (BVF) mapping and segmentation of the bone into trabecular and cortical compartments for structural measurements and topological analysis using published algorithms [12, 19]. In brief, segmentation was determined by delineating the periosteal and endosteal boundaries of the bone using an operator-guided semi-automatic algorithm using a custom-built software [19] and standard microarchitecture parameters were derived for trabecular and cortical bone (Table 1). Topological analysis of the trabecular network was performed as previously described and two composite parameters, reported to be sensitive to microstructural change were also calculated [23, 24]. The surface/curve ratio (S/C) is the ratio of all surface voxels to all curve voxels with the former representing plate like elements and the latter being a marker of rod like elements of the trabecular network. A higher S/C ratio indicates a higher ratio of trabecular plates to rods, which is a hallmark of trabecular network integrity. The other parameter is the erosion index (EI), the ratio of topological parameters expected to increase to those parameters likely to decrease with network erosion caused by osteoclastic resorption. A higher ratio is consistent with greater deterioration.

Micro-computed tomography

Transiliac bone biopsies were performed under general anesthesia at the end of the renal transplant or parathyroidectomy using a modified Bordier trephine [25]. Specimens were

fixed in cold neutral buffered formalin 10% for up to 48 hours and then dehydrated in 70% ethanol. The intact iliac crest cores were analysed using a Skyscan Model 1172 Micro-CT scanner (Bruker, Aartselar, Belgium) at 50 kV, 200 mA with a 0.5-mm aluminium filter using a pixel size of 4.3 microns. Scanned images were captured every 0.4° through 180°, reconstructed and analysed by NRecon (software version 1.6.10.5; Bruker, Belgium). CTAnalyser software (version 1.16.1.0; Bruker, Belgium) to quantify bone volume and architecture. Boundaries of the cortical and cancellous compartments were determined by X-ray attenuation of voxels on a grey scale from 1; black, indicating empty space and no bone, to 255; white, indicating most dense bone. A range from 1-59 for the cancellous compartment and 60-255 for the cortical compartment produced the best binary images for analysis of each compartment in the samples and these threshold values were maintained across all samples. Three-dimensional analysis was applied to calculate standard morphometric parameters within the total cancellous and cortical compartments of each biopsy core (Table 1). The cortical porosity was calculated as the volume of all open and closed 'pores' as a percentage of the total cortical bone volume, and cortical thickness represented the mean of two cortices for 10 biopsy samples, while in the remaining four samples only the intact outer cortex was available for measurements. Other derived parameters included structure model index (SMI), indicating trabecular plate or rod-like geometry, degree of anisotropy (DA) and connectivity density, which are surrogates for trabecular connectivity. Micro-CT nomenclature and units accord with published guidelines [26].

Bone histomorphometry

Histomorphometry was performed on the non-decalcified iliac crest biopsies following completion of the micro-CT examination. Prior to biopsy, participants had three days of

doxycycline hydrochloride (100 mg twice daily), followed by a tetracycline-free interval of 10-14 days and then tetracycline hydrochloride (500mg twice daily) for three days, with the biopsy performed three to five days later. Static parameters were reported as measurements in two dimensions using established nomenclature [27]. Bone turnover activity was assessed from static indices including osteoblast surface and number and osteoclast surface, number and perimeter/eroded fraction, in addition to tetracycline labelled perimeter/bone perimeter, mineral apposition rate and bone formation rate derived from the tetracycline labels. Normal ranges of bone histomorphometry, and micro-CT derived parameters were defined from previously reported data [28-31] and local experience. Final histomorphometry results were categorized according to the TMV classification [1].

DXA

Participants scheduled for kidney transplantation (n=14) underwent BMD measurements by DXA (QDR-4500 Discovery, Hologic, Waltham, MA), at the lumbar spine, femoral neck and total proximal femur. BMD values were expressed in g/cm^2 and as T- and Z-scores. All DXA scans were performed at one center by a single operator not involved in the care of study participants and blinded to other study measurements.

Biochemical measurements

All biochemical measurements were performed at The Royal Melbourne Hospital prior to surgery. These included serum levels of creatinine, calcium, phosphate, 25-hydroxyvitamin D (25(OH)D), intact parathyroid hormone (iPTH) and alkaline phosphatase (ALP). The estimated GFR (eGFR) was calculated according to the Chronic Kidney Disease Epidemiology Collaboration (CKD-EPI) formula for non-dialysis patients. All biochemical markers were

measured using standard assays and analyses were performed according to the manufacturer's instructions. Serum concentrations of iPTH were determined using Architect Intact PTH (Abbott Laboratories, USA) chemiluminescent microparticle immunoassay (CMIA).

Statistical methods

Results are presented as mean (+/- standard deviation [SD]) for normally distributed continuous variables and as median (and interquartile range) for continuous variables with skewed distributions. Correlation analyses were conducted to investigate associations between BMD and bone structural parameters, obtained at different anatomical locations using the different imaging techniques and histomorphometry, as well as biomarkers. Pearson correlation coefficients were used to express the relationship between variables if both parameters were normally distributed. Spearman correlation coefficients were used if results of one or both parameters were not normally distributed. Independent sample t-test or Mann-Whitney tests were used to explore associations between MRI parameters and TMV parameters. A two-tailed *p* value <0.05 was considered statistically significant. Stata statistical software package (version 11.0, Stata Corporation, College Station, TX) was used for analysis.

Results

Patient characteristics

The mean age of patients at the time of surgery was 46.0 ± 11.3 years with 62.5% being male. Glomerulonephritis was the predominant cause of ESKD in the cohort (37.5%) followed by reflux nephropathy (18.8%) and diabetes (18.8%). At the time of surgery 11 of 16 patients were on renal replacement therapy (hemodialysis [HD] n=7; peritoneal dialysis [PD] n=4) for a median duration of 20.5 months (5-34.2 months), whilst 5 of 16 were scheduled for

pre-emptive living donor renal transplantation. One patient, a 30-year-old female undergoing parathyroidectomy, had a history of a low trauma fracture. Another, 50-year female recipient of a kidney transplant had a prior history of parathyroidectomy. Potential bone modulating treatment used by participants in our cohort involved phosphate binders (n=8, 50%), prednisolone (n=4, 25%), calcimimetics (n=1, 6.3%) and calcitriol (n=5, 31.3%). Median serum iPTH was 45.3 (26.8-64.8) pmol/L, and in four patients, iPTH values were above the Kidney Disease Improving Global Outcomes (KDIGO) recommended target range of up to nine times the normal upper reference range of the iPTH assay.

Representative images illustrating trabecular and cortical compartments of study participants are shown for MRI in Figure 1 and micro-CT in Figure 2. Mean values of trabecular and cortical structural parameters assessed at the distal tibia by MRI and at the iliac crest by micro-CT and histomorphometry are presented in Table 1. Biochemical parameters of patients are outlined in Table 2.

Bone histomorphometry and micro-CT

Bone turnover (T) activity was assessed as low in 21%, normal in 29%, and high in 50% of participants. For patients with histomorphometry findings suggestive of hyperparathyroidism, the mineral apposition rate (MAR) varied from 0.77-1.08 µm/day (normal 0.6-0.8 µm/day) and bone formation rate (BFR) from 0.09-0.62 $mm^3/mm^2/day$ (normal 0.03- 0.09 $mm^3/mm^2/day$). Mineralization (M) was abnormal in 35.7%, based on histological features of increased osteoid surface, volume and seam width. Trabecular bone volume (V) was relatively preserved. By microCT, only 28.5% % of patients had BV/TV values >1 SD below the mean, and mean trabecular thickness, number and separation were also

within the normal range. However, cortical bone was characterised by thin cortices and increased cortical porosity (Table 1). Cortical porosity by 2D histomorphometry correlated to porosity by 3D micro-CT (r=0.56; *p*=0.03), but there was no significant relationship between cortical thickness measured by 2D histomorphometry and 3D micro-CT.

Associations of MRI and Bone Histology

Turnover

MRI parameters are static, and like static histomorphometric indices, are likely to reflect the cumulative impact on bone structure of changes in bone turnover over time. Significant negative associations were present between eroded surface (ES/BS) by histomorphometry and MRI-derived total bone area (r = -0.85, *p* = 0.004), trabecular bone area (r = -0.71, *p* = 0.03) and cortical bone area (r = -0.83, *p* = 0.005), Osteoclast surface (Oc.S/BS %) by histomorphometry was negatively correlated to MRI-derived cortical area (r = -0.67, *p* = 0.01). Unlike these static parameters, tetracycline labelling represents current bone turnover. Nevertheless, a significant positive association was detected between BFR and MRI derived trabecular volume (r = 0.56, *p* = 0.04), and negative associations were present between BFR and MRI derived trabecular number (r = -0.59, *p* = 0.03) and trabecular spacing (r = -0.58, *p* = 0.03). MAR correlated significantly with S/C (r = 0.56, *p* = 0.04) with a negative trend for EI (r = -0.53, *p* = 0.06). However, BFR and MAR were not reliably determined on all samples due to inconsistent uptake of the first doxycycline label, so these correlations should be interpreted with caution.

Mineralisation

There were no significant associations between MRI derived trabecular or cortical bone structure and osteoid thickness or volume used to assess mineralization. However, total bone area measured by MRI correlated to osteoid thickness (r = 0.71, *p* = 0.006) and osteoid volume (r = 0.59, *p* = 0.03). Positive correlations were observed between tetracycline labeled mineralizing surface to bone surface and MRI-derived BV/TV (r = 0.61, *p* = 0.02) and TbN (r = 0.64, *p* = 0.04), with a negative association to TbS (r = -0.63, *p* = 0.02).

Volume

When assessing volume, 3D techniques are superior to the 2D structural parameters provided by histological sections. Nevertheless, MRI derived S/C, indicating the plate to rod ratio of trabeculae at the distal tibia, correlated positively to histomorphometry at the iliac crest for trabecular bone volume (BV/TV, r = 0.85, *p* = 0.0003), trabecular thickness (TbTh, r = 0.65, *p* = 0.017) and negatively to trabecular separation (TbS, r = -0.58, *p* = 0.039) (Figure 3). MRI-derived EI, which increases with trabecular deterioration, correlated negatively to histomorphometric BV/TV (r = -0.82, *p* = 0.0006) and positively to TbS (r = 0.80, *p* = 0.001) at the iliac crest.

MRI parameters and microCT-derived bone trephine indices are listed in Table 1 and compared in Table 3. There were no significant correlations between microCT-derived BV/TV, trabecular parameters (TbTh, TbN, TbS) or cortical thickness (CtTh) with the same MRI parameter, possibly due to differences in microarchitecture between the different skeletal sites. However, lower microCT-derived cortical and trabecular thickness and increased microCT-derived trabecular number were inversely related to the MRI-derived S/C ratio, and

there was a positive association of increased trabecular separation by microCT and the MRI-derived erosion index (EI) (r = 0.63, p = 0.02), which increases with trabecular deterioration, (Table 3).

MRI, BMD and Biomarkers

Mean values of lumbar spine, femoral neck and total hip BMD determined by DXA are presented in Supplementary Table 1, and the correlations of these parameters with MRI indices are presented in Supplementary Table 2.

Seven out of 14 (50%) patients, aged 33 to 63 years, met the World Health Organization (WHO) criteria for osteopenia (T-Score -1.0 to -2.5) and two for osteoporosis (T-Score <-2.5) respectively at the femoral neck. Significant correlations were observed between BMD at the hip and trabecular microarchitecture at the distal tibia by MRI and iliac crest histomorphometry. All MRI-derived trabecular parameters differed significantly for the participants with a femoral neck T-scores ≤ -2.5 versus those with T-scores > -2.5 whereas total bone area and trabecular area differed significantly for those with T-scores within versus above the osteopenic range (Table 4). Similar relationships were not observed between MRI and T-scores at the total proximal femur or lumbar spine.

MRI-derived trabecular area correlated to values of ALP (r = 0.55, p = 0.03) and TbS correlated to values of 25(OH)D (r =-0.57, p = 0.03). There were no other significant associations between MRI indices and biomarkers.

Discussion

To our knowledge, this study is the first to explore relationships between non-invasive assessment of bone microarchitecture using MRI at a peripheral skeletal site and quantitative histomorphometry at the iliac crest in patients with CKD. The results of this study confirm the complex skeletal phenotype of ROD and provide some encouraging data for the potential utility of MRI. Our results are congruent with previous studies showing widespread bone loss and deranged bone microarchitecture in relatively young patients with CKD. We observed significant cortical bone loss with increased cortical porosity and trabecular network deterioration but preserved trabecular volume at the iliac crest; and demonstrated correlations between some structural parameters assessed by different imaging modalities at skeletal sites with varying load bearing profiles.

The relationships between parameters of trabecular network integrity at the tibia (S/C and EI with MRI), trabecular microarchitecture at the iliac crest and BMD at the hip, demonstrate the widespread and serious nature of bone deficits in CKD. This is clinically relevant because disruption of trabecular network connectivity, increased trabecular separation and decreased trabecular number are associated with aging and osteoporosis [32, 33] and have assisted in discriminating between participants with or without fractures in histomorphometric [34, 35] and HR-pQCT studies [36, 37]. Other structural measurements derived from tibial MRI correlated weakly with corresponding parameters evaluated by histomorphometry. On the other hand, MRI-derived trabecular measurements were predictive of BMD at the femoral neck. The inverse relationships observed between MRI derived cortical thickness and trabecular structural parameters by micro-CT are likely representative of 'trabecularisation' of endocortical bone. This can lead to inaccuracies in distinguishing the cancellous from the

cortical compartments in this 'transitional zone' [38] causing potential overestimation of trabecular parameters.

This study demonstrates that MRI may have utility beyond quantification of bone microarchitecture, especially if combined with BMD measurement and reliable markers of bone turnover. While we demonstrated significant correlations between MRI and histomorphometric bone turnover parameters, these should be viewed with caution given our small cohort and inconsistent uptake of doxycycline labels. It is also important to recognize that MRI or micro-CT parameters are static and represent a legacy of changes to bone accumulated over time, which may not be indicative of current, dynamic bone turnover.

There are few other studies that can be compared or contrasted with our results. Cohen *et al* [39] compared HR-pQCT to classical bone histomorphometry and micro-CT of iliac crest biopsies in 54 participants without secondary osteoporosis or metabolic bone disease. They demonstrated weak to modest but statistically significant correlations between structural parameters obtained by these modalities. In a recent study, Marques *et al* [40] compared HR-pQCT (radius and tibia) and bone histomorphometry in 31 CKD patients. They reported modest, statistically significant correlations between structural parameters at the two sites. Similar to those studies, our results suggest that structural parameters measured by MRI are weakly to modestly associated to their direct counterparts measured by histomorphometry. It is important that these relationships are interpreted in the context of technical and analytic differences in the measurement of similarly named parameters by MRI, micro-CT and histomorphometry, three modalities with very different image resolutions and processing algorithms.

This study highlights the variation in indices of bone structure by anatomical site. While iliac crest biopsy has an established role as the 'gold standard' for ROD diagnosis, other skeletal sites also need consideration as targets for systemic treatments that affect the whole skeleton. In fact, even at the iliac crest, contiguous bone biopsies in the same patient with ROD have been reported to show up to 24% variability in trabecular bone parameters [41]. Similar variation has also been demonstrated in measurements by micro-CT of biopsies obtained from the cadavers of postmenopausal women [42]. Recent studies have also reported variability in cortical bone architecture at various sites [43]. The current study also demonstrates poor within-patient correlation of cortical thickness and porosity measured by micro-CT and histomorphometry. These differences are likely due to the larger 3D sample size and higher resolution of micro-CT, versus the smaller, 2D sample assessed by classical histomorphometry. Although histomorphometry studies in patients with CKD have described skeletal microstructural and mechanical abnormalities [44], the few studies designed to examine links between bone histology and fracture have provided mixed results [45, 46]. By contrast, several studies using MRI have reported associations between microstructural parameters at peripheral sites and spinal [13] and hip fracture [47], although only one such study has been conducted in patients with CKD [17].

Our study has several limitations including its cross-sectional nature and small sample size without a normal control group. The sample size limits our ability to apply regression analyses to determine the ability of a combination of imaging and biomarkers to predict TMV parameters. Also, being a single-center study, the generalisability of our findings is limited. Despite these limitations, this is the first study to compare MRI measurements to histomorphometry plus micro-CT in patients with CKD and provides a 'proof of concept' for

larger studies. Notably, for MRI, this was achieved using a commercially available, routinely used RF coil, which is a significant step towards wider availability. It also compares multiple standards of care and experimental imaging modalities (DXA, micro-CT, MRI) at different skeletal sites with histomorphometry. Although this approach gives us a comprehensive comparison of modalities, the technical and analytic differences in the techniques and the inherent variations between structural and adaptive characteristics of different skeletal sites make interpretation challenging.

There is a heightened awareness of the increased fracture risk in the CKD population, with a knowledge gap related to the pathologic mechanisms leading to fractures and the unmet need for adequate screening tools to identify and stratify this risk [48, 49]. This has resulted in an increased number of studies evaluating the utility of non-invasive imaging techniques and biomarkers in renal bone disease. There is also declining expertise in bone biopsy handling and analysis, patients may be reluctant to undergo the procedure, and processing is time consuming [50]. Whilst MRI is expensive, it is a technique widely researched in the non-CKD population, and scanners and commercial hardware are readily available. MRI may be able to quantify bone microarchitecture, improve fracture risk stratification and monitor intervention in ROD.

Conclusion

In summary, our study compared new HR imaging technology to traditional bone histomorphometry. Despite technical and analytical differences and skeletal heterogeneity, we observed statistically significant correlations between parameters assessed by histomorphometry and MRI at different anatomical sites, while demonstrating associations

of MRI parameters to BMD and indices of bone remodelling. Validation of the role of MRI in CKD will require prospective trials, designed to assess its potential for fracture prediction and monitoring therapeutic intervention.

References

1. Moe, S., et al., *Definition, evaluation, and classification of renal osteodystrophy: a position statement from Kidney Disease: Improving Global Outcomes (KDIGO).* Kidney Int, 2006. **69**(11): p. 1945-53.
2. Epstein, F.H., K.A. Hruska, and S.L. Teitelbaum, *Renal osteodystrophy.* N Engl J Med, 1995. **333**(3): p. 166-175.
3. Parfitt, A.M., *Renal bone disease: a new conceptual framework for the interpretation of bone histomorphometry.* Curr Opin Nephrol Hypertens, 2003. **12**(4): p. 387-403.
4. Alem, A.M., et al., *Increased risk of hip fracture among patients with end-stage renal disease.* Kidney Int, 2000. **58**(1): p. 396-9.
5. Naylor, K.L., et al., *The three-year incidence of fracture in chronic kidney disease.* Kidney Int, 2014. **86**(4): p. 810-8.
6. Ball, A.M., *Risk of Hip Fracture Among Dialysis and Renal Transplant Recipients.* JAMA, 2002. **288**(23): p. 3014-3018.
7. Tentori, F., et al., *High rates of death and hospitalization follow bone fracture among hemodialysis patients.* Kidney Int, 2014. **85**(1): p. 166-73.
8. Nair, S.S., et al., *Temporal trends in the incidence, treatment, and outcomes of hip fracture in older patients initiating dialysis in the United States.* Clin J Am Soc Nephrol, 2013. **8**(8): p. 1336-42.
9. Hansen, D., et al., *Risk of fracture in adults on renal replacement therapy: a Danish national cohort study.* Nephrol Dial Transplant, 2016. **31**(10): p. 1654-62.
10. Iyer, S.P., et al., *Kidney transplantation with early corticosteroid withdrawal: paradoxical effects at the central and peripheral skeleton.* J Am Soc Nephrol, 2014. **25**(6): p. 1331-41.
11. Nickolas, T.L., et al., *Rapid cortical bone loss in patients with chronic kidney disease.* J Bone Miner Res, 2013. **28**(8): p. 1811-20.
12. Wehrli, F.W., *Structural and functional assessment of trabecular and cortical bone by micro magnetic resonance imaging.* J Magn Reson Imaging, 2007. **25**(2): p. 390-409.
13. Kijowski, R., et al., *Evaluation of trabecular microarchitecture in nonosteoporotic postmenopausal women with and without fracture.* J Bone Miner Res, 2012. **27**(7): p. 1494-1500.

14. Benito, M., et al., *Effect of testosterone replacement on trabecular architecture in hypogonadal men.* J Bone Miner Res, 2005. **20**(10): p. 1785-91.
15. Folkesson, J., et al., *Longitudinal evaluation of the effects of alendronate on MRI bone microarchitecture in postmenopausal osteopenic women.* Bone, 2011. **48**(3): p. 611-21.
16. Zhang, X.H., et al., *In Vivo μMRI-Based Finite Element and Morphological Analyses of Tibial Trabecular Bone in Eugonadal and Hypogonadal Men Before and After Testosterone Treatment.* J Bone Miner Res, 2008. **23**(9): p. 1426-1434.
17. Link, T.M., et al., *Changes in calcaneal trabecular bone structure assessed with high-resolution MR imaging in patients with kidney transplantation.* Osteoporos Int, 2002. **13**(2): p. 119-29.
18. Wehrli, F.W., et al., *Quantitative high-resolution magnetic resonance imaging reveals structural implications of renal osteodystrophy on trabecular and cortical bone.* J Magn Reson Imaging, 2004. **20**(1): p. 83-9.
19. Rajapakse, C.S., et al., *Micro-MR imaging-based computational biomechanics demonstrates reduction in cortical and trabecular bone strength after renal transplantation.* Radiology, 2012. **262**(3): p. 912-20.
20. Rajapakse, C.S., et al., *The Efficacy of Low-intensity Vibration to Improve Bone Health in Patients with End-stage Renal Disease Is Highly Dependent on Compliance and Muscle Response.* Academic Radiology, 2017.
21. Han, M., et al., *Variable flip angle three-dimensional fast spin-echo sequence combined with outer volume suppression for imaging trabecular bone structure of the proximal femur.* J Magn Reson Imaging, 2015. **41**(5): p. 1300-10.
22. Rajapakse, C.S., et al., *Patient-specific Hip Fracture Strength Assessment with Microstructural MR Imaging-based Finite Element Modeling.* Radiology, 2017. **283**(3): p. 854-861.
23. Wehrli, F.W., et al., *Digital topological analysis of in vivo magnetic resonance microimages of trabecular bone reveals structural implications of osteoporosis.* J Bone Miner Res, 2001. **16**(8): p. 1520-31.
24. Benito, M., et al., *Deterioration of trabecular architecture in hypogonadal men.* J Clin Endocrinol Metab, 2003. **88**(4): p. 1497-502.
25. Hernandez, J.D., et al., *Technical approach to iliac crest biopsy.* Clin J Am Soc Nephrol, 2008. **3 Suppl 3**(Supplement 3): p. S164-9.

26. Bouxsein, M.L., et al., *Guidelines for assessment of bone microstructure in rodents using micro–computed tomography.* J Bone Miner Res, 2010. **25**(7): p. 1468-1486.
27. Dempster, D.W., et al., *Standardized nomenclature, symbols, and units for bone histomorphometry: a 2012 update of the report of the ASBMR Histomorphometry Nomenclature Committee.* J Bone Miner Res, 2013. **28**(1): p. 2-17.
28. Malluche, H.H., et al., *Quantitative bone histology in 84 normal American subjects.* Calcified Tissue International, 1982. **34**(1): p. 449-455.
29. Malluche, H.H. and M.-C. Faugere, *Atlas of mineralized bone histology*. 1986: Karger New York.
30. Hildebrand, T., et al., *Direct three-dimensional morphometric analysis of human cancellous bone: microstructural data from spine, femur, iliac crest, and calcaneus.* J Bone Miner Res, 1999. **14**(7): p. 1167-1174.
31. Kulak, C.A.M., et al., *Skeletal microstructural abnormalities in postmenopausal women with chronic obstructive pulmonary disease.* J Bone Miner Res, 2010. **25**(9): p. 1931-1940.
32. Seeman, E. and P.D. Delmas, *Bone quality--the material and structural basis of bone strength and fragility.* N Engl J Med, 2006. **354**(21): p. 2250-61.
33. Akhter, M.P., et al., *Transmenopausal changes in the trabecular bone structure.* Bone, 2007. **41**(1): p. 111-6.
34. Kimmel, D.B., et al., *A comparison of iliac bone histomorphometric data in post-menopausal osteoporotic and normal subjects.* Bone Miner, 1990. **11**(2): p. 217-35.
35. Ito, M., et al., *Analysis of trabecular microarchitecture of human iliac bone using microcomputed tomography in patients with hip arthrosis with or without vertebral fracture.* Bone, 1998. **23**(2): p. 163-169.
36. Boutroy, S., et al., *In vivo assessment of trabecular bone microarchitecture by high-resolution peripheral quantitative computed tomography.* J Clin Endocrinol Metab, 2005. **90**(12): p. 6508-15.
37. Boutroy, S., et al., *Finite element analysis based on in vivo HR-pQCT images of the distal radius is associated with wrist fracture in postmenopausal women.* J Bone Miner Res, 2008. **23**(3): p. 392-399.
38. Zebaze, R.M., et al., *Intracortical remodelling and porosity in the distal radius and post-mortem femurs of women: a cross-sectional study.* Lancet, 2010. **375**(9727): p. 1729-36.

39. Cohen, A., et al., *Assessment of trabecular and cortical architecture and mechanical competence of bone by high-resolution peripheral computed tomography: comparison with transiliac bone biopsy.* Osteoporos Int, 2010. **21**(2): p. 263-73.
40. Marques, I.D., et al., *Biopsy vs. peripheral computed tomography to assess bone disease in CKD patients on dialysis: differences and similarities.* Osteoporos Int, 2017.
41. Chavassieux, P.M., M.E. Arlot, and P.J. Meunier, *Intersample variation in bone histomorphometry: comparison between parameter values measured on two contiguous transiliac bone biopsies.* Calcified Tissue International, 1985. **37**(4): p. 345-350.
42. Chappard, C., A. Marchadier, and C.L. Benhamou, *Side-to-side and within-side variability of 3D bone microarchitecture by conventional micro-computed tomography of paired iliac crest biopsies.* Bone, 2008. **43**(1): p. 203-8.
43. Tong, X., et al., *Iliac crest histomorphometry and skeletal heterogeneity in men.* Bone Rep, 2017. **6**: p. 9-16.
44. Malluche, H.H., et al., *Differences in bone quality in low- and high-turnover renal osteodystrophy.* J Am Soc Nephrol, 2012. **23**(3): p. 525-32.
45. Eventov, I., et al., *Osteopenia, hematopoiesis, and bone remodelling in iliac crest and femoral biopsies: a prospective study of 102 cases of femoral neck fractures.* Bone, 1991. **12**(1): p. 1-6.
46. Dempster, D., et al., *Relationships between bone structure in the iliac crest and bone structure and strength in the lumbar spine.* Osteoporosis Int, 1993. **3**(2): p. 90-96.
47. Link, T.M., et al., *In vivo high resolution MRI of the calcaneus: differences in trabecular structure in osteoporosis patients.* J Bone Miner Res, 1998. **13**(7): p. 1175-82.
48. Messa, P., *Skeletal fractures in patients on renal replacement therapy: how large still is the knowledge gap?* Nephrol Dial Transplant, 2016. **31**(10): p. 1554-6.
49. Moe, S.M. and T.L. Nickolas, *Fractures in Patients with CKD: Time for Action*. 2016, Am Soc Nephrol.
50. Evenepoel, P., et al., *Bone biopsy practice patterns across Europe: the European renal osteodystrophy initiative-a position paper.* Nephrol Dial Transplant, 2017. **32**(10): p. 1608-1613.

Tables

Table 1 – Bone microarchitecture parameters measured by MRI, micro-CT and histomorphometry

	Variable	Mean±SD	Normal Range[205-208]
MRI (Tibia)#			
	BV/TV (%)	10.4 +/- 2.2	
	TbTh (µm)	126 +/- 5.6	
	TbN (1/mm)	0.82 +/- 0.14	
	TbS (µm)	1120 +/- 23	
	Cortical thickness (µm)	2632 +/- 545	
	S/C	5.51 +/- 1.36	
	EI	0.91 +/- 0.25	
Transiliac biopsies			
Micro-CT	BV/TV (%)	20.3 ± 7.1	15.6 ± 5.4%
	TbTh (µm)	110 ± 37.0	150 ± 30 µm
	TbN (1/mm)	2.20 ± 1.44	1.4 ± 0.27/mm
	TbS (µm)	593 ± 203	770 ± 350
	Mean single cortical thickness (µm)	127 ± 44	381 ± 120*
	Cortical porosity (%)	60.3 ± 22.5	4-10 %*
	Structure Model Index	-0.8 (-7.7 to 0.7)^	1.15±0.61
	Degree of Anisotropy	2.04 ± 0.8	1.49±0.18
	Connectivity density (1/ µm3)	31 (-59 to 101)	-
Histomorphometry	BV/TV (%)	27.1 ± 11.6	21-29%
	TbTh (µm)	157.7 ± 60.2	90-175 µm
	TbN (1/mm)	1.83 ± 0.75	1.1-2.2/mm
	TbS (µm)	368.5 (273.3 – 566.4)	280-658 µm

Abbreviations: Trabecular bone volume (BV/TV %), trabecular thickness (TbTh), trabecular number (TbN), trabecular separation (TbS), surface to curve ratio (S/C), erosion index (EI). *Cortical thickness and porosity vary by age and sex. Thresholding and voxel size may differ from current study. ^Median (Range). #No validated normative data is currently available for structural parameters derived by MRI

Table 2 – Biochemical parameters of the study cohort (n = 16), median ± SD or median (IQR)

Biomarker	**Values**	**Normal range**
Calcium	2.45 ± 0.11	2.10-2.60 mmol/L
Phosphate	2.1 ± 0.46	0.75-1.50 mmol/L
Parathyroid hormone	45.3 (26.8-64.8)	1.7-10.0 pmol/L
Alkaline phosphatase	89.5 (67.5-131.8)	30-120 IU/L
25-Hydroxyvitamin D	65.2 ± 21.2	55-108 nmol/L

Table 3 – Correlations, Pearson's (r), between trabecular and cortical microarchitecture parameters measured by MRI and bone histomorphometry measured by micro-CT

Modalities		**MRI (Tibia)**						
	Parameters	**BV/TV**	**TbTh**	**TbN**	**TbS**	**CtTh**	**S/C**	**EI**
Micro-CT (Iliac crest)	**BV/TV**	0.25	0.30	0.24	-0.28	-0.43	0.30	-0.34
	TbTh	0.05	-0.09	-0.03	-0.06	0.06	-0.61*	0.43
	TbN	0.21	0.25	0.20	0.22	-0.24	0.60*	-0.47
	TbS	-0.52	-0.60*	-0.48	0.45	0.06	-0.51	0.63*
	CtTh	0.01	-0.01	0.01	-0.04	0.20	-0.62*	0.41
	SMI	0.25	0.18	0.23	-0.24	-	-0.11	0.11
	DA	0.28	0.35	0.30	-0.29	-	0.39	-0.53
	Conn. D (1/ µm3)	0.46	0.51	0.46	-0.45	-	0.49	-0.53

Abbreviations: Surface to curve ratio (S/C), erosion index (EI), trabecular bone volume (BV/TV %), trabecular thickness (TbTh), trabecular separation (TbS), cortical thickness (CtTh), Structural model index (SMI) – relative index of rods and plates or cavities if negative), Degree of anisotropy (DA), Connectivity density (Conn.D)

*p≤0.05**;** **p≤0.01

Table 4 – Associations of trabecular and cortical microarchitecture parameters measured by MRI (mean ± SD) with bone mineral density findings at the femoral neck (according to the WHO classification)

MRI parameter	Value in patients with osteopenia	Value in patients with osteoporosis
Surface to curve ratio	5.5 ± 0.85	3.6 ± 2.1*
Erosion Index	0.90 ± 0.1	1.3 ± 0.6
Bone volume (%)	11.0 ± 2.2	7.2 ± 0.8*
Trabecular thickness (mm)	0.13 ± 0.006	0.12 ± 0.0*
Trabecular number (1/mm)	0.86 ± 0.14	0.62 ± 0.1*
Trabecular separation (mm)	1.05 ± 0.2	1.5 ± 0.25**
Cortical thickness (mm)	2.7 ± 0.51	2.4 ± 0.46

*p≤0.05 compared to subjects without osteopenia or osteoporosis respectively

**p≤0.01 compared to subjects without osteopenia or osteoporosis respectively

Figures

Figure 1 - Intensity-inverted magnetic resonance images (MRI) of distal tibia of two study participants respectively showing (A) compact cortical bone and well-connected trabecular bone compartment; and (B) thinned and porous cortical bone and disconnected trabecular bone regions.

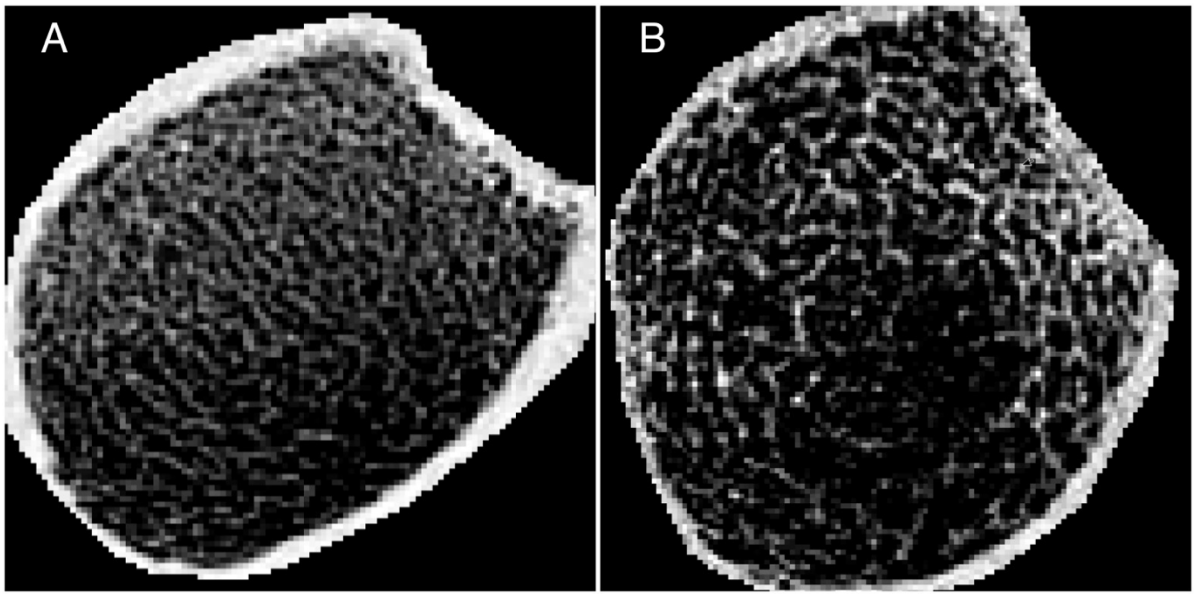

Figure 2 - Representative micro-CT images of a biopsy obtained from a study subject showing trabecular (white arrow) and cortical bone (black arrow) compartments in (A) biopsy core, (B) two-dimensional section, and (C) three-dimensional section.

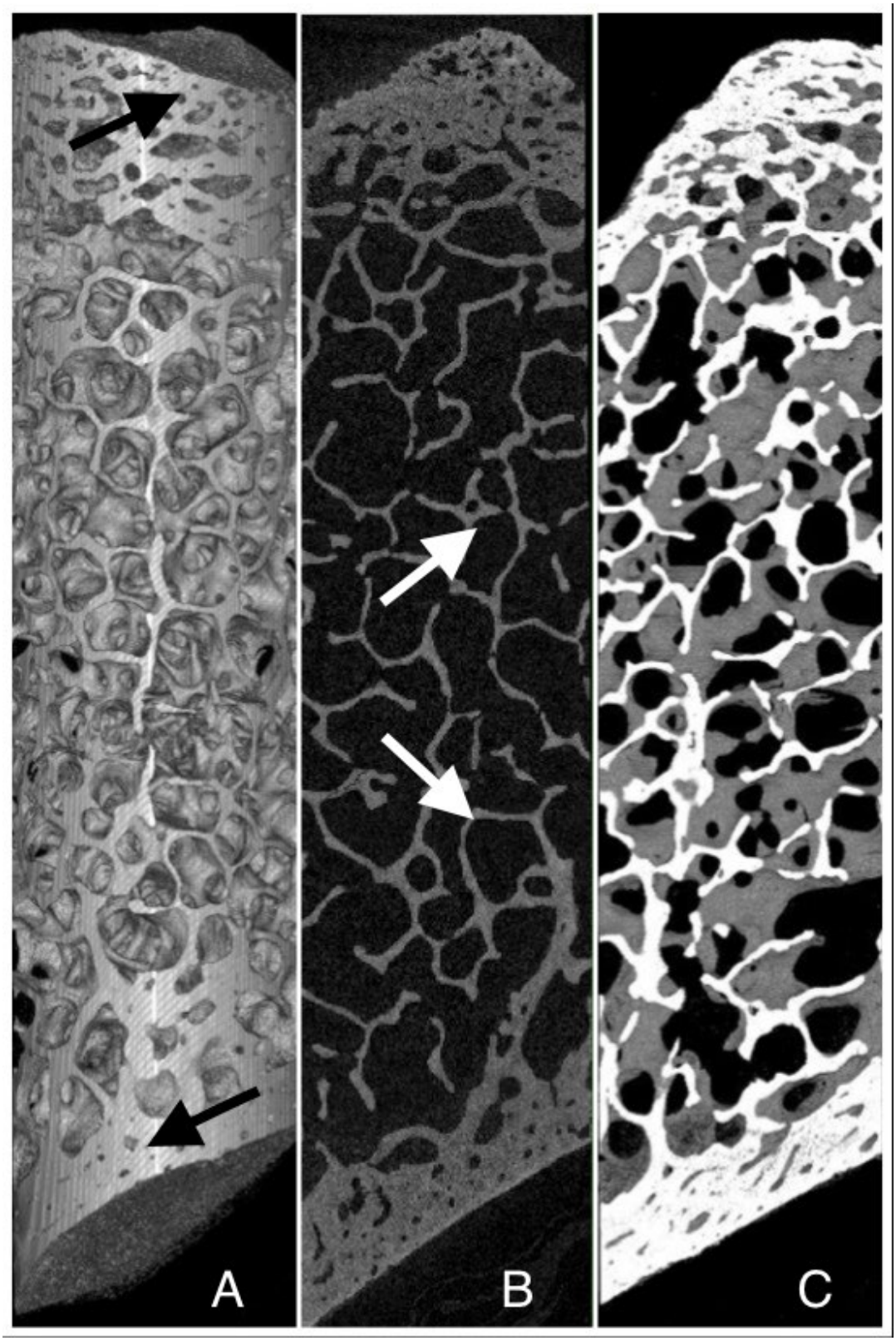

Figure 3 – Correlations, Pearson's (r), between trabecular topological parameters derived by MRI of distal tibia (MRI) with those at the iliac crest by 2D-histomorphometry

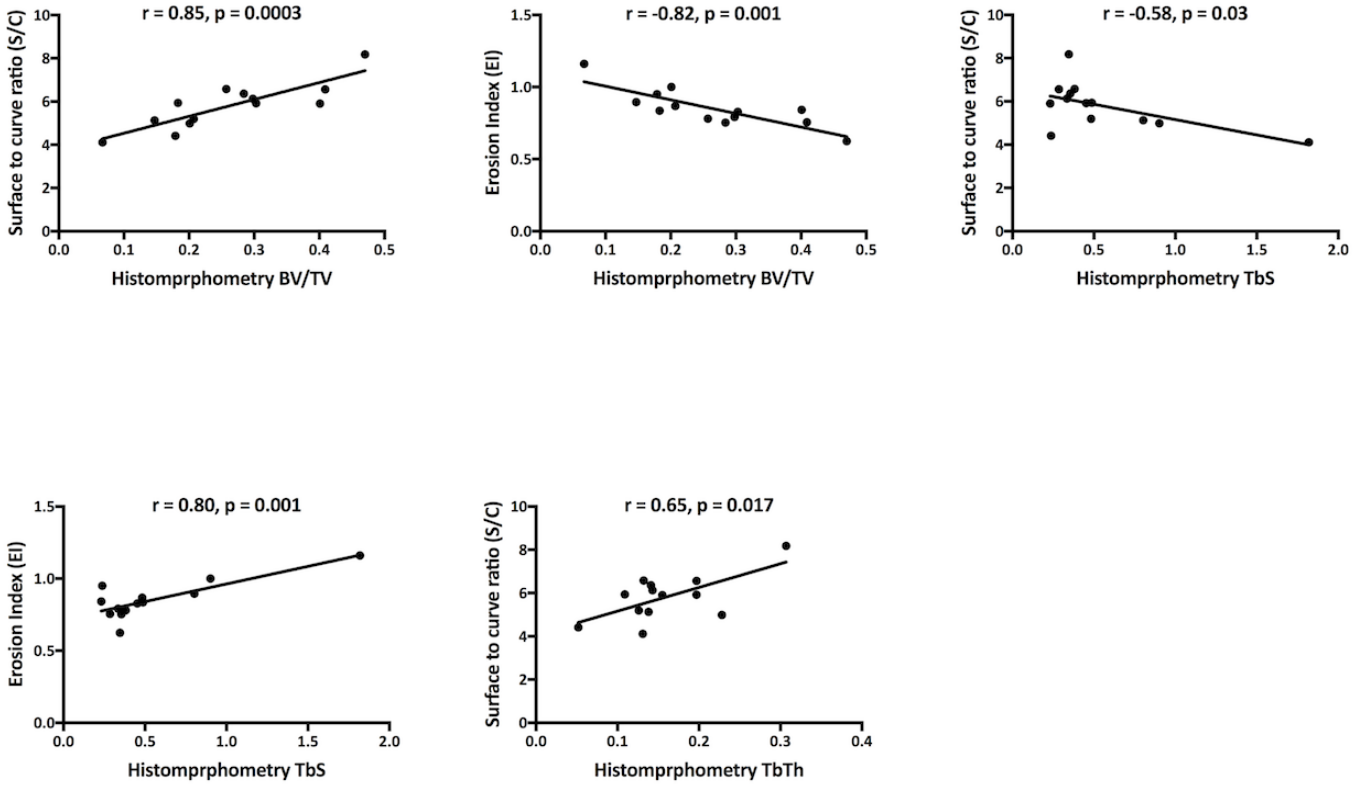

Abbreviations: Surface to curve ratio (S/C), erosion index (EI), trabecular bone volume (BV/TV), trabecular thickness (TbTh, μm), trabecular separation (TbS, μm)

Supplementary Table 1 - Mean values of lumbar spine, femoral neck and total hip bone mineral density (BMD) determined by DXA

Site	Variable	Mean±SD
Lumbar spine	Absolute BMD (g/cm^2)	1.0 ± 11.3
	T-score	-0.65 ± 0.92
Femoral neck	Absolute BMD (g/cm^2)	0.71 +/- 0.13
	T-score	-1.56 ± 1.01
Total proximal femur	Absolute BMD (g/cm^2)	0.88 ± 0.13
	T-score	- 0.88 ± 0.82

Supplementary Table 2 – Correlations, Pearson's or Spearman's (r), between trabecular and cortical microarchitecture parameters measured by MRI with bone mineral density (BMD) by DXA

Modalities		**MRI (Tibia)**						
	Parameters	**BV/TV**	**TbTh**	**TbN**	**TbS**	**CtTh**	**S/C**	**EI**
DXA	**LS BMD**	-0.26	-0.28	-0.26	0.18	0.14	0.13	-0.10
	LS T Score	-0.30	-0.32	-0.30	0.22	0.02	0.07	-0.02
	FN BMD	0.46	0.50	0.45	-0.53*	0.09	0.71**	0.61*
	FN T Score	0.42	0.47	0.41	-0.50	-0.00	0.69**	-0.59*
	TH BMD	0.62*	0.65*	0.62*	-0.72**	0.27	0.67**	0.56*
	TH T Score	0.57*	0.65*	0.54*	-0.55*	0.26	0.68**	0.75**

Abbreviations: Surface to curve ratio (S/C) and erosion index (EI) by MRI, trabecular bone volume (BV/TV %), trabecular thickness (TbTh), trabecular separation (TbSp), cortical thickness (CtTh), lumbar spine (LS), total hip (TH), femoral neck (FN)

*p≤0.05**;** **p≤0.01

CHAPTER 4: CHANGES IN BONE MICROARCHITECTURE FOLLOWING KIDNEY TRANSPLANTATION – BEYOND BONE MINERAL DENSITY

The research presented in this chapter has been published in the following article.

AK Sharma, ND Toussaint, GJ Elder, CS Rajapakse, SG Holt, P Baldock, PL Robertson, PR Ebeling, OR Sorci and R Masterson. Changes in bone microarchitecture following kidney transplantation – beyond bone mineral density. *Clinical Transplantation* 2018; **32**(9):e13347.

Author affiliations

Ashish K SHARMA[1,2], Nigel D TOUSSAINT[1,2], Grahame J ELDER[3,4], Chamith S RAJAPAKSE[5], Stephen G HOLT[1,2], Paul BALDOCK[4], Patricia L ROBERTSON[2,6], Peter R EBELING[7], Olivia R SORCI[5], Rosemary MASTERSON[1,2]

[1]*Department of Nephrology, The Royal Melbourne Hospital, Parkville, Australia*

[2]*Department of Medicine (RMH), University of Melbourne, Parkville, Australia*

[3]*Department of Renal Medicine, Westmead Hospital, Westmead, Australia*

[4]*Osteoporosis and Bone Biology Division, Garvan Institute of Medical Research, Darlinghurst, Australia*

[5]*Departments of Radiology and Orthopaedic Surgery, University of Pennsylvania, PA, USA*

[6]*Department of Radiology, The Royal Melbourne Hospital, Parkville, Australia,* [7]*Monash University, Clayton, Australia*

Summary

Bone disease in kidney transplant recipients (KTRs) is characterised by bone mineral density (BMD) loss but bone microarchitecture changes are poorly defined. In this prospective cohort study, we evaluated bone microarchitecture using non-invasive imaging modalities; high-resolution magnetic resonance imaging (MRI), peripheral quantitative computed tomography (pQCT), dual energy X-ray absorptiometry (DXA) and the trabecular bone score (TBS) following kidney transplantation. Eleven KTRs (48.3±11.2 years) underwent MRI (tibia), pQCT (radius) and DXA at baseline and 12 months post-transplantation. Transiliac bone biopsies, performed at transplantation, showed 70% of patients with high/normal bone turnover. Compared with baseline, 12-month MRI showed deterioration in indices of trabecular network integrity - surface to curve ratio (S/C;-15%,p=0.03) and erosion index (EI;+19%,p=0.01). However, cortical area increased (+10.3%,p=0.04), with a non-significant increase in cortical thickness (+7.8%,p=0.06). At 12 months, parathyroid hormone values (median 10.7 pmol/L) correlated with improved S/C (r=0.75,p=009) and EI (r=-0.71,p=0.01) while osteocalcin correlated with cortical thickness (r=0.72,p=0.02) and area (r=0.70,p=0.02). TBS decreased from baseline (-5.1%,p=0.01) with no significant changes in BMD or pQCT. These findings highlight a post-transplant deterioration in trabecular bone quality detected by MRI and TBS, independent of changes in BMD, underlining the potential utility of these modalities in evaluating bone microarchitecture in KTRs.

Keywords: post-transplant bone disease, fracture, magnetic resonance imaging, bone mineral density, trabecular bone score, kidney transplantation

Introduction

Fractures are a common and serious clinical complication of the mineral and bone disorder (MBD) that is almost ubiquitous in patients with chronic kidney disease (CKD). A number of epidemiological studies have highlighted that CKD predisposes to a dramatic increase in fracture risk and resultant morbidity and mortality when compared to an age and gender-matched population without CKD [1-4]. Kidney transplantation is the optimal treatment for end-stage kidney disease (ESKD) but does not attenuate the susceptibility to fracture. Indeed, fracture risk has been reported up to 34% higher in the first two years post transplantation compared to the preceding period on dialysis [5], with a fracture incidence up to 22.5% over the first five years post transplantation [6]. In addition, kidney transplant recipients (KTRs) have higher rates of hospitalization and mortality after fracture than do people in the general population [7]. Although reductions in bone mineral density (BMD) after transplantation have been extensively reported, there is a paucity of post-transplant data regarding modifiable risk factors for fracture [8]. Improved graft and patient survival has further emphasized the importance of optimising long-term clinical outcomes including risk of fracture and cardiovascular disease in KTRs.

Post-transplant bone disease is multifactorial, and includes effects of immunosuppressive therapy, persisting hyperparathyroidism, 'hyperphosphatoninism' and the consequences of post-transplant impairment of renal function (CKD-T) superimposed on pre-existing renal bone abnormalities [9]. The diagnosis and management of post-transplant bone disease is therefore difficult, with limited validation of available diagnostic tools to evaluate changes in bone structure or predict fracture risk. Although accelerated loss of BMD in the first year after transplantation has been described as the hallmark of post-transplant bone disease [10-12],

recent studies have demonstrated a more conservative estimate of early BMD loss with long term values nearer to average for age and gender [13]. The focus of contemporary research has been on change in bone microarchitecture post kidney transplantation and its potential relationship to bone fragility and biomarkers [14-18]. A few studies based on histomorphometry have addressed this issue [18-21] and, more recently, studies involving non-invasive imaging, such as high-resolution peripheral quantitative computed tomography (HR-pQCT) [15], high-resolution magnetic resonance imaging (MRI) [14, 22] and the Trabecular Bone Score (TBS) [23-26] have focused on defining changes in bone microarchitecture.

In this prospective, observational study over the first 12 months following transplantation, we report changes in bone microarchitecture and bone mass that were assessed using non-invasive techniques: high-resolution MRI (tibia), dual-energy X-ray absorptiometry (DXA) to assess BMD and the TBS, peripheral quantitative computed tomography (pQCT, radius) and changes in biochemical markers.

Materials and Methods

Study participants

All patients referred for a living donor kidney transplant at The Royal Melbourne Hospital between December 2014 and January 2016 were eligible for this study, providing they had no contraindication to MRI, and were not participating in another trial. The protocol was approved by the local ethics committee and all patients provided informed consent. A total of 27 patients planned for living donor kidney transplantation were approached for this study. Five transplant surgeries were rescheduled or cancelled for clinical or logistical reasons.

Fourteen of the remaining 22 patients were recruited and underwent kidney transplantation. Eleven of these patients completed follow up at 12 months. Among the exclusions, two patients moved to a different state for post-transplant care and one patient had to undergo nephrectomy after transplantation and was not included in analysis.

Immunosuppressive therapy

Patients received induction with basiliximab and methylprednisolone (500mg) and subsequently maintenance immunosuppression comprising tacrolimus, mycophenolate mofetil and prednisolone. Initial prednisolone dose was 25mg daily, tapered over 3-months to a maintenance dose of 5 mg/day. Beyond three months, triple immunosuppression was continued in the absence of any abnormal findings on protocol transplant biopsies (at 3 and 12 months post-transplant) or a clinical indication to the contrary determined by the treating team.

Bone histomorphometry

Transiliac biopsies were performed using a modified Bordier trephine (Landanger) in 10 of 11 participants at the time of transplantation. The transiliac cores measuring 7mm in diameter were analyzed by histomorphometry and micro computed tomography (micro-CT) and were classified by Turnover (T), Mineralisation (M) and Volume (V) using the Kidney Disease Improving Global Outcomes (KDIGO) recommended classification [27]. Methodology relating to bone biopsies has been described previously [28].

Noninvasive Assessment of Bone

MRI

MRI images were obtained within 2 weeks preceding transplantation (baseline) with a commercial 3.0-Tesla whole-body imager (Siemens Trio, Germany) and at 12 months after kidney transplantation. Participants were imaged in a feet-first prone position. MRI acquisitions were performed at the left tibial metaphysis using a three dimensional (3D) 'fast spin echo' pulse sequence readily available on any clinical MRI system requiring a scan time of 12 minutes. This was undertaken utilizing a commercially available eight-channel radiofrequency (RF) extremity coil used in clinical practice. MRI parameters include 0.273 mm x 0.273 mm x 0.6 mm voxel size, 70 mm x 70 mm x 19.2 mm field-of-view, 53ms repetition time, 16ms echo time, 12 averages, and echo train length of two. Raw MRI data was pre-processed via bone volume fraction (BVF) mapping and segmentation of the bone into trabecular and cortical compartments for structural measurements and topological analysis using published algorithms [29]. Topological analysis of the trabecular network was performed and two composite parameters, reported to be sensitive to microstructure of bone [30, 31], were calculated. The first of these, surface/curve ratio (S/C) is the ratio of all surface voxels to all curve voxels with the former representing plate-like elements and the latter being a marker of rod-like elements of the trabecular network. Age and disease related deterioration of trabecular bone involves conversion of plate (surface) like trabeculae to rod (curve) like trabeculae. A higher S/C therefore indicates improved trabecular structure and strength. Trabecular deterioration also involves erosion of trabecular elements, which is measured by the Erosion Index (EI), defined as the ratio of all topological parameters (image voxel parameters representing various trabecular elements) expected to increase, to those parameters likely to decrease with network erosion caused by osteoclastic resorption. A

higher ratio is consistent with greater deterioration. Both S/C and EI are derived parameters which have been validated and used in previous studies [30, 31].

DXA-derived BMD and TBS

Participants underwent baseline and 12-month BMD measurements by DXA (QDR-4500 Discovery, Hologic, Waltham, MA), at the lumbar spine, femoral neck and total proximal femur. BMD values were expressed in g/cm^2 and as T -scores. TBS is a novel indirect index of trabecular microarchitecture derived from pixel greyscale texture variations in the lumbar spine images acquired by DXA [32]. TBS iNsight Software (version 3.0.2.0; Medimaps) was used to calculate TBS values for the lumbar spine (L1-L4). A higher TBS score is consistent with better trabecular connectivity and a reduced risk for microarchitectural damage, while a lower TBS is consistent with increased risk for microarchitectural damage. Based on results of two recent studies [23, 24], a TBS cut point of 1.37 was used to stratify patients to reduced or increased fracture risk.

Peripheral quantitative computed tomography (pQCT)

Three dimensional pQCT tomographic images can be used to assess cross-sectional structure and volumetric density. We used pQCT (Stratec XCT-300, Germany) at the distal radius to derive total, cortical and trabecular volumetric BMD (vBMD), cortical thickness (CtTh) and cortical area (CtA) at baseline and 12 months. All DXA and pQCT scans and TBS measurements were performed at one center by a single operator not involved in the care of study participants and blinded to other study measurements.

Laboratory measurements

Blood samples for routine biomarkers were obtained before transplantation and at 3, 6 and 12 months post transplantation. Serum concentrations of intact parathyroid hormone (iPTH) were determined using Architect Intact PTH (Abbott Laboratories, USA) chemiluminescent microparticle immunoassay (CMIA). Bone turnover markers and serum 1,25-dihydroxyvitamin D ($1,25[OH]_2D$) were also measured at baseline, 6 and 12 months. Osteocalcin (OC) and procollagen type 1 N-terminal propeptide (P1NP), markers of osteoblast activity, and the osteoclastic resorption marker beta-cross linked telopeptide (β-CTx) were assayed by an electrochemiluminescence immunoassay (Elecsys®, Roche, Switzerland). Serum $1,25[OH]_2D$ was measured by radioimmunoassay (Immunodiagnostic Systems Ltd).

Statistical methods

Results are presented as mean (+/- standard deviation) for normally distributed continuous variables and as median (and interquartile range) for continuous variables with skewed distributions. Wilcoxon signed-rank test was used to assess changes in parameters between baseline and at 12 months post transplantation. Correlation analyses using Spearman correlation coefficient were conducted to investigate associations between longitudinal changes in parameters obtained by various modalities. A two-tailed p value <0.05 was considered statistically significant. Stata statistical software package (version 11.0, Stata Corporation, College Station, TX) was used for analysis.

Results

Participant characteristics

Baseline demographic characteristics and potential bone modulating medications prior to and after transplantation are shown in Table 1 and Table 2 respectively. The mean age of participants was 48 ± 11 years, 72.7% were male and mean body mass index of the cohort was 26.4 ± 4.1 kg/m^2. Glomerulonephritis (36.3%) was the most common cause of ESKD followed by reflux nephropathy (27.2%) and diabetes mellitus (18.1%). Seven (63.6%) participants were on dialysis (mean duration 19.4 ± 16.7 months) and 4 underwent pre-emptive kidney transplantation. None of the participants received anti-resorptive therapy prior to or after transplantation. There was one episode of biopsy proven acute cellular rejection treated with methylprednisolone and increased tacrolimus and mycophenolate. The remainder of participants continued on maintenance immunosuppression, including prednisolone 5 mg daily, after their respective 3-month protocol biopsies. The mean cumulative dose of prednisolone over 12 months per patient was 3244 +/- 68.6 mg.

Bone histomorphometry

Ten patients had baseline bone histomorphometry with 4 (40%) having evidence of high bone turnover, 3 normal and 3 low turnover. Mineralisation was abnormal in 4 and trabecular bone volume was normal in 7 and low in 3. By micro-CT mean cortical thickness was reduced and cortical porosity was increased in all patients [28].

Longitudinal changes in bone microarchitecture by MRI

At 12 months there was deterioration in MRI-derived parameters of integrity of the trabecular network. S/C, indicating the plate to rod ratio of trabeculae, decreased by 15% (p=0.03) from

baseline. EI, which increases with trabecular deterioration, increased by 19% (p=0.01) (Table 4, Figure 2). There were no statistically significant differences between pre and post transplantation trabecular bone volume, trabecular number and trabecular separation. Post transplantation cortical area increased significantly by 10.3% (p=0.04) while there was a non-statistically significant 7.8% increase in cortical thickness (p=0.06).

Longitudinal changes in pQCT

By pQCT at the radius there was a non-significant increase in cortical thickness. There were no longitudinal changes in pQCT derived cortical or trabecular area or in total, cortical or trabecular volumetric BMD.

Longitudinal changes in DXA-derived BMD and the TBS

At the time of transplantation, 80% of the study participants met BMD criteria for osteopenia or osteoporosis at the femoral neck. The median T-score at the femoral neck was -1.6 (-2.4 to -0.6), whereas T-scores at the total proximal femur and lumbar spine were in the normal range (Table 3). At 12 months, there was a 2.2% decrease in lumbar spine BMD (mean change -0.22 g/cm2 [-0.56, 0.12], a 2.7% decrease in femoral neck BMD (mean change -0.10 g/cm2 [-0.39, 0.19]) and a 1.1% increase in BMD at the total hip (mean change 0.1 g/cm2 [-0.14, 0.34]), with none of these changes reaching statistical significance.

Prior to transplantation the mean TBS was 1.27 ± 0.11, with 9 of 11 (81.8%) patients having a TBS below 1.37. The mean TBS decreased at 12 months to 1.21 ± 0.12 (p = 0.02) with 10 out of 11 (90.9%) patients having a TBS lower than 1.37. The TBS at baseline and follow-up, was not significantly related to BMD or any structural parameter derived by MRI.

Changes in biochemical markers

Baseline and 12-month follow up biochemical parameters and bone turnover markers are presented in Table 3. Immediately before transplantation, the median serum iPTH was 43.6 (16.5 – 57.5) pmol/L, which is within the target range recommended by the KDIGO Chronic Kidney Disease-Mineral and Bone Disorder (CKD-MBD) guidelines. At 12 months, 54.5% of patients had mild persistent hyperparathyroidism with median PTH 10.7 (7.4 – 17.0) pmol/L. With return of renal function, values of $1,25[OH]_2D$ rose by 78% from baseline to 6 months and remained stable within the normal reference range to 12 months. Values of bone turnover markers affected by renal function (OC, β-CTx and P1NP) fell from the pre-transplant period to 12 months as expected. On the other hand, alkaline phosphatase (ALP), which reflects osteoblast activity and is not influenced by renal function, did not change significantly from pre-transplant to 12 months. As indicated in Figure 1, mean values of serum P1NP, β-CTX and OC had all fallen towards the upper normal range by 6 months, with no statistically significant change from 6 to 12 months.

Associations of laboratory variables to structural parameters

Pre-transplant values of serum PTH, P1NP, β-CTx and OC were not significantly associated with any structural MRI parameters. However, at 12-months, levels of PTH correlated to S/C (r = 0.75; *p* = 0.009) and EI = (r -0.71; *p* = 0.01) but not to other structural parameters (Figure 3). OC levels at 12 months correlated to MRI derived cortical thickness (r=0.72; *p*=0.02) and area (r=0.70; *p*=0.02) at the tibia. OC also correlated to pQCT parameters of cortical thickness (r=0.70; *p*=0.03) and area (r=0.67; *p*=0.05) at the radius. On the other hand, values of serum PTH and the assayed bone turnover markers were not correlated to any BMD value or the TBS at baseline or 12 months.

Clinical outcomes

One patient (with type 2 diabetes mellitus and PTH 65 pmol/L at baseline) was diagnosed with avascular necrosis of both hips after the study period completed, and subsequently sustained a spontaneous trochanteric fracture requiring total hip replacement. There were no clinically detected incident fractures during the 12-month study period.

Discussion

After kidney transplantation, factors contributing to deterioration in bone quality include immunosuppressive therapy, abnormalities in mineral homeostasis and remodelling superimposed upon pre-existing renal osteodystrophy. Although post transplantation loss of bone mass or BMD has been well documented, changes in bone microarchitecture are not well described. In this study, we aimed to define changes in bone microarchitecture over the first post-transplant year using a combination of high-resolution imaging techniques and biochemical markers of bone turnover.

In this cohort study of 11 KTRs with predominantly high or normal turnover at baseline, changes in some MRI parameters and the TBS were consistent with deterioration in trabecular network and connectivity, while MRI suggested an improvement in cortical microarchitecture over 12 months post transplantation. Notably, there were no statistically significant changes in BMD by DXA, despite a significant decline in the TBS to values associated with an increased fracture risk [24]. These changes in bone were accompanied by changes in biomarkers of mineral metabolism, which were concordant with published data [33, 34].

Progressive deterioration in trabecular connectivity and microarchitecture after transplantation is clinically relevant because it may increase bone fragility without quantifiable changes in bone volume. It has previously been reported that the conversion of trabecular structure from plate-like to rod-like and disruption of network connectivity adversely impacts mechanical strength of bone [35], is associated with aging and osteoporosis [36-38] and discriminates between participants with or without fractures in imaging studies [30, 39]. The observed relationship of post-transplantation PTH values to improvements in the S/C and EI measurements, likely reflects an anabolic effect of mild hyperparathyroidism on trabecular bone [40].

The MRI-derived longitudinal improvement in cortical microarchitecture in our study is contrary to changes reported by contemporary imaging studies in kidney transplantation [14, 15]. The only other MRI study to longitudinally evaluate cortical and trabecular microarchitecture in KTRs reported a decline in cortical, trabecular, and whole-bone stiffness at 6 months after transplantation in the absence of any significant corresponding changes in microarchitecture or BMD [14]. However, Iyer *et al*. investigated bone structure changes in KTRs on an early corticosteroid withdrawal regimen and demonstrated a decrease in HR-pQCT-derived cortical area (-3.9%, radius; -2.7% tibia) and thickness (-3.1%, radius; -1.9% tibia) and an increase in cortical porosity at one-year post transplantation [15]. This decrease in cortical thickness and area was related to higher PTH levels. In comparison to the study by Iyer *et al*, the participants in our study had higher baseline PTH (43.7 pmol/L vs 27 pmol/L), were generally more osteopenic (mean T-score -1.5 vs -0.8) and were on traditional corticosteroid regimen. The overall results should be interpreted in the context of these differences. Participants in the present study were also significantly younger with only two

(of 11) over 55 years of age compared to 27 (of 47, 57%) patients above 55 years of age in the study by *Iyer et al*. Notably cortical deterioration occurs with advancing age and is more common in people above 60 years of age. Few other studies have described longitudinal changes in cortical bone post kidney transplantation.

In contrast to previously published data about the predominance of low bone turnover in ESKD patients [41, 42], 70% of our participants had features of high or normal bone turnover at the time of transplantation, accompanied by universally thin cortices on micro-CT but with relatively preserved trabecular bone volume – an overall picture suggestive of moderate to severe secondary hyperparathyroidism. We postulate that the improvement in MRI-assessed cortical microarchitecture in our study is likely a result of suppression of excessive bone resorption and unmasking of bone modelling due to a decline in PTH levels and represents a partial correction of hyperparathyroidism-related bone changes after kidney transplantation. This release from excess remodelling and endocortical resorption may lead to net adaptive periosteal apposition and a stabilisation or increase in cortical surface area and thickness [43, 44]. In our study, the relationship between post transplantation osteocalcin levels and cortical thickness and area at both the tibia (MRI) and the radius (pQCT) are suggestive of net bone formation. Similar to these conclusions, a recent study of paired bone biopsies at baseline and one-year post transplant reported significant declines in parameters of bone resorption at one year, with no changes in other static parameters [18]. Trabecular bone volume was also normal in most patients at baseline and only decreased minimally after transplantation. Julian *et al,* in an early prospective histomorphometry study, also reported similar normalisation of osteoclast resorption markers and resolution of hyperparathyroidism at 6 months post transplantation [10].

Currently, there is no reference range for TBS for individuals with CKD because of the relative lack of studies investigating its utility in CKD [26, 45] and renal transplantation [24, 25]. Two studies have proposed values of the TBS to discriminate between subjects with and without fracture in CKD stages 3-4 (TBS less than 1.27) [45] and in KTRs shortly after kidney transplantation (TBS less than 1.37) [24]. In the current study we observed a significant decline in mean TBS at 12 months post transplantation from a baseline score already consistent with an increased fracture risk. It is possible that the TBS is reduced early after transplantation with recovery over the longer term [25]. The longitudinal decline in TBS paralleled the MRI-derived deterioration in trabecular architecture and was unrelated to areal or volumetric BMD changes. By comparison, we observed no significant decline in BMD over 12 months. This is consistent with contemporary data showing more stable BMD long term after transplantation [13, 18] and may represent a recovery after loss of bone mass early after transplant [10].

Our study has several limitations. The small sample size limits its statistical robustness and restricts the ability to apply regression analysis to evaluate predictors of changes in bone microarchitecture. This includes the effects of bone-modifying treatments on changes in bone structure. Also, being a single-center study, the relevance of our findings to other centers is limited. Despite these limitations, our study is one of very few to explore longitudinal changes in bone structure after transplantation using high-resolution imaging.

In summary, using MRI and DXA-derived TBS in a small sample of relatively young living donor KTRs, we identified changes consistent with a progressive deterioration in trabecular bone quality and an increased fracture risk. The lack of significant interval changes in BMD or pQCT

parameters accentuates the potential importance of assessing bone health post transplantation by alternate means. The preservation of cortical structure in our cohort, although different to available data, may represent a partial correction of bone abnormalities related to secondary hyperparathyroidism. Overall, our study highlights the heterogeneous nature of bone microarchitecture changes in post-transplant bone disease and supports further investigation of non-invasive imaging modalities in larger prospective trials to assess the evolution of histologic and structural changes in bone after transplantation. Changes in MRI parameters and the TBS may be of particular interest for detecting changes that may increase post-transplant fracture risk.

References

1. Alem, A.M., et al., *Increased risk of hip fracture among patients with end-stage renal disease*. Kidney Int, 2000. 58(1): p. 396-9.
2. Naylor, K.L., et al., *The three-year incidence of fracture in chronic kidney disease.* Kidney Int, 2014. 86(4): p. 810-8.
3. Hansen, D., et al., *Risk of fracture in adults on renal replacement therapy: a Danish national cohort study.* Nephrol Dial Transplant, 2016. 31(10): p. 1654-62.
4. Tentori, F., et al., *High rates of death and hospitalization follow bone fracture among hemodialysis patients.* Kidney Int, 2014. 85(1): p. 166-73.
5. Ball, A.M., *Risk of Hip Fracture Among Dialysis and Renal Transplant Recipients.* JAMA, 2002. 288(23): p. 3014-3018.
6. Nikkel, L.E., et al., *Risk of fractures after renal transplantation in the United States.* Transplantation, 2009. 87(12): p. 1846-51.
7. Abbott, K.C., et al., *Hospitalizations for fractures after renal transplantation in the United States.* Ann Epidemiol, 2001. 11(7): p. 450-7.
8. Naylor, K.L., et al., *Fracture risk in kidney transplant recipients: a systematic review.* Transplantation, 2013. 95(12): p. 1461-70.
9. Malluche, H.H., M.C. Monier-Faugere, and J. Herberth, *Bone disease after renal transplantation.* Nat Rev Nephrol, 2010. 6(1): p. 32-40.
10. Julian, B.A., et al., *Rapid loss of vertebral mineral density after renal transplantation.* N Engl J Med, 1991. 325(8): p. 544-50.
11. Almond, M.K., et al., *Loss of regional bone mineral density in the first 12 months following renal transplantation.* Nephron, 1994. 66(1): p. 52-7.
12. Brandenburg, V.M., et al., *Early rapid loss followed by long-term consolidation characterizes the development of lumbar bone mineral density after kidney transplantation.* Transplantation, 2004. 77(10): p. 1566-71.
13. Naylor, K.L., et al., *Long-term changes in bone mineral density in kidney transplant recipients.* Transplantation, 2014. 98(12): p. 1279-85.
14. Rajapakse, C.S., et al., *Micro-MR imaging-based computational biomechanics demonstrates reduction in cortical and trabecular bone strength after renal transplantation.* Radiology, 2012. 262(3): p. 912-20.

15. Iyer, S.P., et al., *Kidney transplantation with early corticosteroid withdrawal: paradoxical effects at the central and peripheral skeleton.* J Am Soc Nephrol, 2014. 25(6): p. 1331-41.
16. Nishiyama, K.K., et al., *Longitudinal HR-pQCT and image registration detects endocortical bone loss in kidney transplantation patients*. J Bone Miner Res, 2015. 30(3): p. 554-61.
17. Bonani, M., et al., *Effect of Twice-Yearly Denosumab on Prevention of Bone Mineral Density Loss in De Novo Kidney Transplant Recipients: A Randomized Controlled Trial.* Am J Transplant, 2016. 16(6): p. 1882-91.
18. Evenepoel, P., et al., *Bone histomorphometry in de novo renal transplant recipients indicates a further decline in bone resorption 1 year posttransplantation.* Kidney Int, 2017. 91(2): p. 469-476.
19. Monier-Faugere, M.C., et al., *High prevalence of low bone turnover and occurrence of osteomalacia after kidney transplantation.* J Am Soc Nephrol, 2000. 11(6): p. 1093-9.
20. Cruz, E.A., et al., *Histologic evolution of bone disease 6 months after successful kidney transplantation.* Am J Kidney Dis, 2004. 44(4): p. 747-56.
21. Kodras, K. and M. Haas, *Effect of kidney transplantation on bone.* Eur J Clin Invest, 2006. 36 Suppl 2: p. 63-75.
22. Link, T.M., et al., *Changes in calcaneal trabecular bone structure assessed with high-resolution MR imaging in patients with kidney transplantation.* Osteoporos Int, 2002. 13(2): p. 119-29.
23. Luckman, M., et al., *Spine Trabecular Bone Score as an Indicator of Bone Microarchitecture at the Peripheral Skeleton in Kidney Transplant Recipients.* Clin J Am Soc Nephrol, 2017. 12(4): p. 644-652.
24. Naylor, K.L., et al., *Trabecular bone score in kidney transplant recipients.* Osteoporos Int, 2016. 27(3): p. 1115-1121.
25. Perez-Saez, M.J., et al., *Bone Density, Microarchitecture, and Tissue Quality Long-term After Kidney Transplant.* Transplantation, 2017. 101(6): p. 1290-1294.
26. Perez-Saez, M.J., et al., *Bone density, microarchitecture, and material strength in chronic kidney disease patients at the time of kidney transplantation.* Osteoporos Int, 2017. 28(9): p. 2723-2727.

27. Moe, S., et al., *Definition, evaluation, and classification of renal osteodystrophy: a position statement from Kidney Disease: Improving Global Outcomes (KDIGO).* Kidney Int, 2006. 69(11): p. 1945-53.
28. Sharma, A.K., *Deterioration of Cortical Bone Microarchitecture: Critical Component of Renal Osteodystrophy Evaluation.* American Journal of Nephrology, 2018.
29. Rajapakse, C., et al., *Vertebral deformities and fractures are associated with MRI and pQCT measures obtained at the distal tibia and radius of postmenopausal women.* Osteoporosis International, 2014. 25(3): p. 973-982.
30. Wehrli, F.W., et al., *Digital topological analysis of in vivo magnetic resonance microimages of trabecular bone reveals structural implications of osteoporosis.* J Bone Miner Res, 2001. 16(8): p. 1520-31.
31. Benito, M., et al., *Deterioration of trabecular architecture in hypogonadal men.* J Clin Endocrinol Metab, 2003. 88(4): p. 1497-502.
32. Silva, B.C., et al., *Trabecular bone score: a noninvasive analytical method based upon the DXA image.* J Bone Miner Res, 2014. 29(3): p. 518-30.
33. Evenepoel, P., et al., *Natural history of parathyroid function and calcium metabolism after kidney transplantation: a single-centre study.* Nephrol Dial Transplant, 2004. 19(5): p. 1281-7.
34. Wolf, M., et al., *A Prospective Cohort Study of Mineral Metabolism After Kidney Transplantation.* Transplantation, 2016. 100(1): p. 184-93.
35. Van der Linden, J.C., et al., *Mechanical consequences of bone loss in cancellous bone.* J Bone Miner Res, 2001. 16(3): p. 457-65.
36. Seeman, E. and P.D. Delmas, *Bone quality--the material and structural basis of bone strength and fragility.* N Engl J Med, 2006. 354(21): p. 2250-61.
37. Kimmel, D.B., et al., *A comparison of iliac bone histomorphometric data in post-menopausal osteoporotic and normal subjects.* Bone Miner, 1990. 11(2): p. 217-35.
38. Akhter, M.P., et al., *Transmenopausal changes in the trabecular bone structure.* Bone, 2007. 41(1): p. 111-6.
39. Boutroy, S., et al., *Comparison of 2D and 3D bone microarchitecture evaluation at the femoral neck, among postmenopausal women with hip fracture or hip osteoarthritis.* Bone, 2011. 49(5): p. 1055-61.

40. Leonard, M.B., *A structural approach to skeletal fragility in chronic kidney disease.* Semin Nephrol, 2009. 29(2): p. 133-43.
41. Graciolli, F.G., et al., *The complexity of chronic kidney disease-mineral and bone disorder across stages of chronic kidney disease.* Kidney Int, 2017. 91(6): p. 1436-1446.
42. Drueke, T.B. and Z.A. Massy, *Changing bone patterns with progression of chronic kidney disease.* Kidney Int, 2016. 89(2): p. 289-302.
43. Seeman, E., *Periosteal Bone Formation — A Neglected Determinant of Bone Strength.* N Engl J Med, 2003. 349(4): p. 320-323.
44. Ahlborg, H.G., et al., *Bone loss and bone size after menopause.* N Engl J Med, 2003. 349(4): p. 327-34.
45. Naylor, K.L., et al., *Trabecular Bone Score and Incident Fragility Fracture Risk in Adults with Reduced Kidney Function.* Clin J Am Soc Nephrol, 2016. 11(11): p. 2032-2040.

Tables

Table 1. Demographic parameters at the time of transplantation (n = 11)

Variable	Values
Age at surgery (years)	48.3 ± 11.2
Gender (n of males)	8
Body mass index (kg/m^2)	26.4 ± 4.1
Cause of ESKD (n)	
- Glomerulonephritis	4
- Reflux nephropathy	3
- Diabetes mellitus	2
- Hypertension	1
- Polycystic kidney disease	1
Dialysis: HD / PD / None (n)	3/4/4
Parathyroidectomy (n)	1

Abbreviations: ESKD, end-stage kidney disease; HD, hemodialysis; PD, peritoneal dialysis

Table 2. Bone modulating therapy prior to and after transplantation (n = 11)

Bone Modulating Therapy	At transplantation (n)	Post-transplantation (n)
Cinacalcet	1	1
Phosphate binder (CCB/NCCB)	3/5	0
Calcitriol	4	3
Cholecalciferol	3	5
Prednisolone	3	11

Abbreviations: CBB, calcium containing binders; NCBB, non-calcium containing binders

Table 3. Biochemical parameters at the time of transplantation and at 12 months follow-up

Biomarker	Baseline	12 months	P value
Creatinine (mmol/L)*	501 ± 54.3	106.2 ± 21.5	0.003
eGFR*	10.4 ± 2.0	67.1 ± 11.2	0.003
Calcium (mmol/L)	2.45 ± 0.13	2.47 ± 0.11	0.82
Phosphate (mmol/L)	1.98 ± 0.39	1.00 ± 0.16	0.003
iPTH (pmol/L)	43.6 (16.5 – 57.5)	10.7 (7.4 – 17.0)	0.01
ALP (IU/L)	79.0 (66.0 – 111.0)	84.0 (68.0 – 109.0)	0.79
25[OH]D (nmol/L)	63.7 ± 24.0	86.0 ± 29.4	0.14
1,25$[OH]_2$D (nmol/L)	38.5 (20.0 – 72.5)	144.5 (97.0 – 173.7)	0.01
OC (ng/ml)	125.8 (30.8 – 161.7)	24.3 (20.3 – 38.1)	0.01
β-CTx (ng/ml)	1.08 (0.81 – 2.3)	0.69 (0.41 – 1.24)	0.02
P1NP (μg/L)	134.2 (43.0 – 269.2)	66.0 (42.8 – 117.0)	0.20

Abbreviations: eGFR, estimated glomerular filtration rate; iPTH, intact parathyroid hormone; ALP, alkaline phosphatase; 25[OH]D, 25-hydroxyvitamin D; 1,25$[OH]_2$D, serum 1,25-dihydroxyvitamin D; OC, osteocalcin; β-CTx, beta-cross linked telopeptides; P1NP, procollagen type 1 N-terminal propeptide

*Values at baseline for pre-dialysis patients receiving pre-emptive transplants only (n=4)

Table 4. Bone microarchitecture parameters measured by magnetic resonance imaging (MRI), bone mineral density (BMD) determined by dual energy x-ray absorptiometry (DXA) and peripheral quantitative computed tomography (pQCT) and Trabecular Bone Score (TBS) at the time of transplantation and at 12 months follow up

Modality	Parameter	Baseline	12 months	P value
MRI (tibia)	S/C	5.5 ± 1.50	4.6 ± 1.66	**0.03**
	EI	0.9 ± 0.29	1.11 ± 0.34	**0.01**
	BV/TV (%)	10.0 ± 2.1	9.9 ± 2.4	0.76
	TbTh (µm)	125.0 ± 5.3	125.7 ± 5.0	0.33
	TbN	0.80 ± 0.14	0.77 ± 0.14	0.54
	TbS (µm)	1161.6 ± 246.3	1187.1 ± 241.1	0.72
	CtTh (mm)	2.68 ± 0.55	2.89 ± 0.64	**0.06**
	Total area (mm^2)	9788.8 ± 1996.3	9931.0 ± 2712.6	0.59
	Trabecular area (mm^2)	6692.2 ± 1742.4	6443.0 ± 2552.3	0.65
	Cortical area (mm^2)	3107.8 ± 692.5	3428.5 ± 811.5	**0.04**
DXA	LS BMD (g/cm^2)	1.02 ± 0.09	0.99 ± 0.10	0.20
	LS T-score	-0.85 (-1.2 – 0.37)	-0.9 (-1.5 – 0.15)	0.17
	FN BMD (g/cm^2)	0.70 ± 0.14	0.69 ± 0.12	0.50
	FN T-score	-1.5 (-2.4 - -0.6)	-1.6 (-2.5 - -0.9)	0.47
	TH BMD (g/cm^2)	0.86 ± 0.14	0.86 ± 0.11	0.50
	TH T-score	-0.9 (-1.7 - -0.25)	-0.6 (-1.6 - -0.25)	0.30
TBS	TBS	1.27 ± 0.11	1.21 ± 0.12	**0.02**
pQCT (radius)	Tb vBMD (g/cm^3)	186.8 ± 48.7	174 ± 43.5	0.07
	Ct vBMD (g/cm^3)	1164.2 ± 50.9	1161.4 ± 39.7	0.65
	Total vBMD (g/cm^3)	319.6 ± 76.4	302 ± 69.2	0.20
	CtTh (mm)	2.62 ± 0.50	2.72 ± 0.45	0.20
	Trabecular area (mm^2)	176.6 ± 29.8	175.6 ± 34.02	0.81
	Cortical area (mm^2)	92.0 ± 19.8	92.1 ± 21.3	0.72

Abbreviations: S/C, Surface to curve ratio; EI, Erosion index; BV/TV, trabecular bone volume; TbTh, trabecular thickness; TbN, trabecular number; TbS, Trabecular separation; CtTh, cortical thickness; LS, Lumbar spine; FN, femoral neck; TH, total hip; vBMD, trabecular and cortical volumetric bone mineral density (Tb vBMD and Ct vBMD

Figures

Figure 1. Longitudinal changes in levels (mean±SD) of parathyroid hormone (PTH) and bone turnover markers after transplantation.

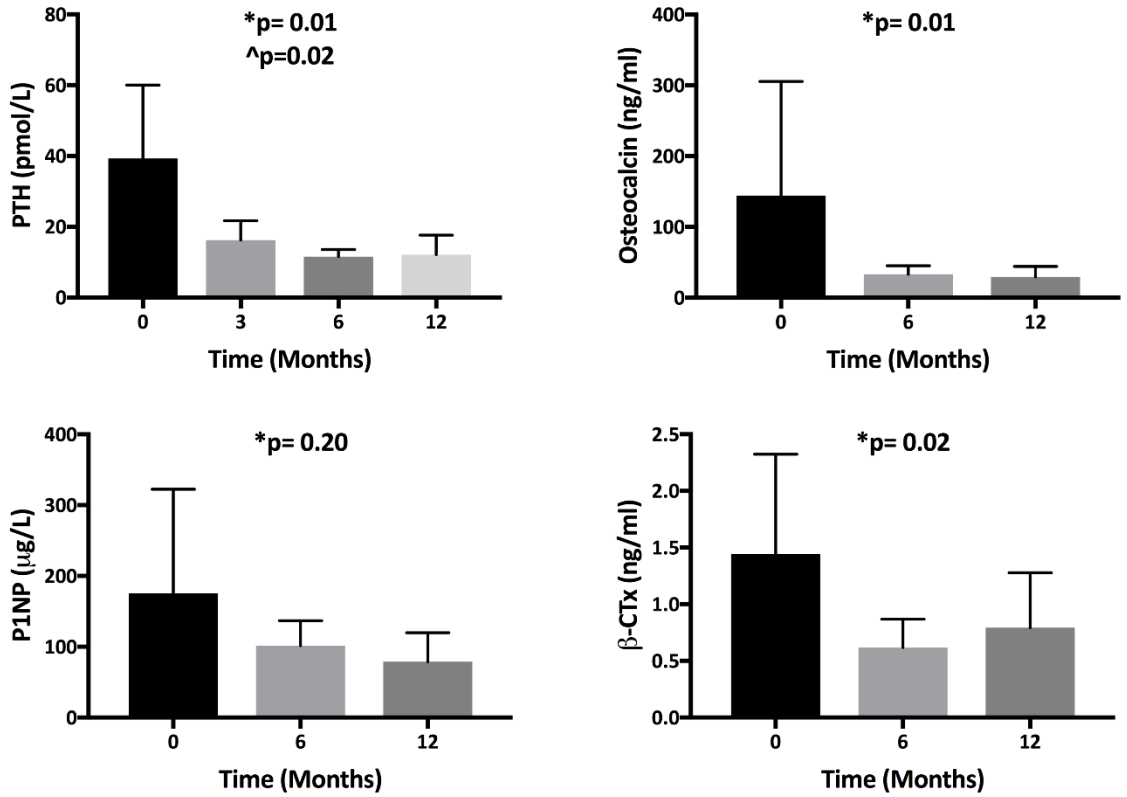

*Comparison between values at baseline (0 months) and 12 months.

There were no statistically significant changes in 6-month and 12-month levels of bone turnover markers.

^ Comparison of PTH values between 3 months and 12 months.

Abbreviations: PTH, intact parathyroid hormone; β-CTx, beta-cross linked telopeptides; P1NP, procollagen type 1 N-terminal propeptide

Figure 2. Longitudinal changes in MRI-derived parameters of bone microarchitecture

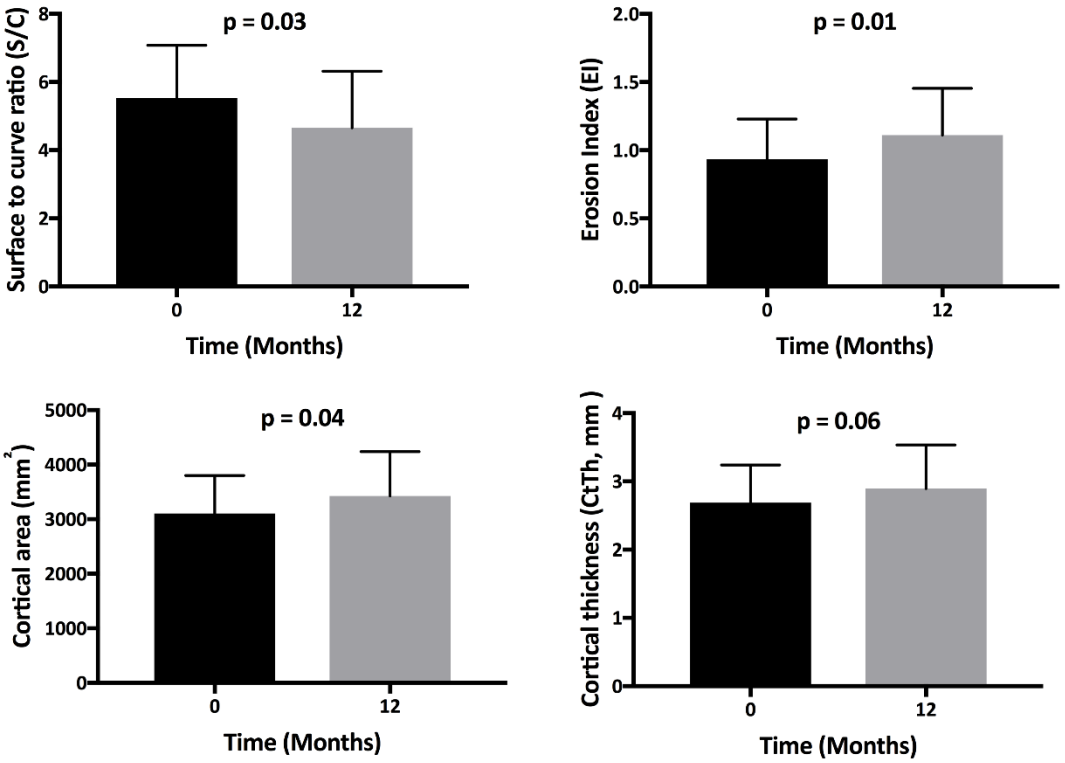

Figure 3. Relationship between parathyroid hormone (PTH) levels and parameters of trabecular connectivity derived by MRI at 12 months post kidney transplantation

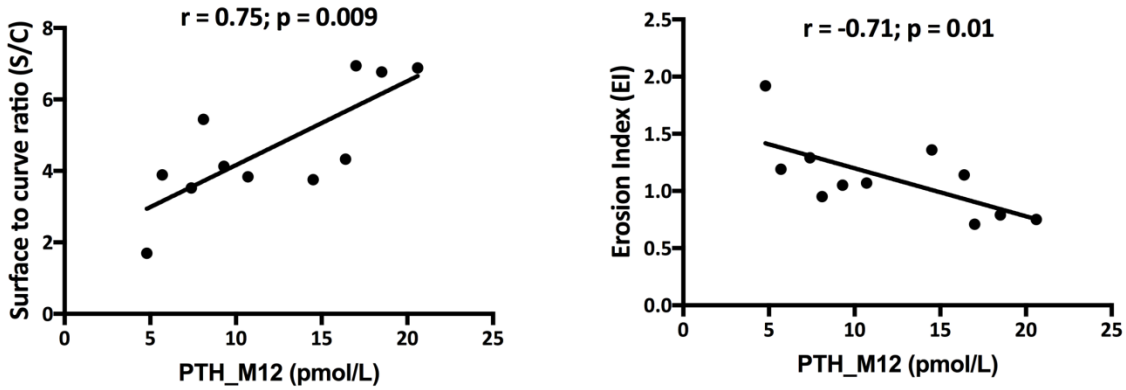

CHAPTER 5: IMPACT OF CINACALCET PRE-TRANSPLANTATION ON MINERAL METABOLISM IN RENAL TRANSPLANT RECIPIENTS

The research presented in this chapter has been published in the following article.

AK Sharma, R Masterson, SG Holt, SJ Tan, PD Hughes, M Chu, P Jayadeva and ND Toussaint. Impact of cinacalcet pre-transplantation on mineral metabolism in renal transplant recipients. *Nephrology* 2016; 21(1):46-54.

Author affiliations

Ashish K SHARMA[1,2], Rosemary MASTERSON[1], Stephen G HOLT[1,2], Sven-Jean TAN[1,2], Peter D HUGHES[1], Melissa CHU[1], Pavithra JAYADEVA[1], Nigel D TOUSSAINT[1,2]

[1]*The Royal Melbourne Hospital, Parkville, Victoria, Australia*

[2]*Department of Medicine (RMH), The University of Melbourne, Melbourne, Australia*

Summary

Background: Cinacalcet is effective in reducing parathyroid hormone (PTH) in patients on dialysis. Reports of biochemical profiles and other clinical outcomes in patients discontinuing cinacalcet at time of renal transplantation are limited.

Methods: A retrospective study assessing markers of mineral metabolism, graft and patient outcomes in renal transplant recipients to determine differences in patients discontinuing cinacalcet (C+) compared with patients not treated with cinacalcet (C-) at time of transplantation. To allow for differences between groups in pre-transplant biochemical parameters, we also analysed a matched cohort of C- with C+ recipients (2:1), matched for age, calcium and PTH levels at transplantation.

Results: 532 recipients (460 C-, 72 C+), transplanted Jan 2006- Dec 2012, were analysed, mean age 48.0+/-12.7 years and 64.3% male. Median 42.9 months follow-up there were 10 deaths (1.9%), 56 allograft loss (10.6%) and 5 parathyroidectomies post-transplant (0.8%). Median PTH immediately pre-transplant was higher in C+ vs C- (50.7[25.4–75.2] vs 28.3[13.9–49.7]pmol/L, p<0.001). Twelve-month post-transplant PTH was reduced but higher in C+ (11.7[6.9–21.2] vs 7.2[4.6–11.2]pmol/L, p<0.001). Mean calcium was higher for C+ vs C- at 12 months (2.50+/-0.19 vs 2.43+/-0.17mmol/L, p<0.001), with differences to 4 years post-transplant. No difference was seen in renal function, graft loss, post-transplant parathyroidectomy rate and mortality. In the matched cohort (144 C- vs 72 C+), similar findings were also seen.

Conclusion: Differences in mineral metabolism post-transplant are seen with cinacalcet pre-transplant compared to no cinacalcet. Transplant recipients discontinuing cinacalcet had higher post-transplant PTH and calcium although the clinical significance is unclear.

Keywords: secondary hyperparathyroidism, calcimimetic, cinacalcet, renal transplantation, hypercalcemia, mineral metabolism

Introduction

Secondary hyperparathyroidism (SHPT) is associated with abnormalities in mineral metabolism and is a progressive disease which affects a substantial proportion of patients with chronic kidney disease (CKD).[1] Mineral and bone disorder in CKD (CKD-MBD), particularly elevated levels of calcium, phosphate and parathyroid hormone (PTH), has been associated with increased morbidity and mortality in numerous studies of patients with CKD and end-stage kidney disease (ESKD) on dialysis.[2,3] At the time of renal transplantation the majority of patients with ESKD have SHPT.[4] Successful renal transplantation improves calcitriol synthesis and appears to reduce PTH levels in most cases. However resolution of SHPT is incomplete in up to 50% of renal transplant recipients at one year after transplantation even in the presence of good renal allograft function.[4,5] Hyperparathyroidism and hypercalcemia post-transplantation have been associated with poorer graft outcomes,[6,7] soft tissue and vascular calcification,[8,9] and increased incidence of fractures.[10]

Calcimimetic agents increase the sensitivity of the calcium sensing receptor (CaSR) to extracellular calcium and have been an important therapeutic option in patients with persistent SHPT despite use of standard therapies including phosphate binders and vitamin D analogues. Cinacalcet, an allosteric modulator of the CaSR, has been approved for treatment of SHPT in dialysis patients since 2004 in the United States (US), 2005 in Europe and 2007 in Australia. Studies have reported efficacy in suppressing PTH secretion, reducing serum calcium and phosphate levels, reducing the need for parathyroidectomy, and potentially lowering fracture rate and reducing cardiovascular hospitalisation in dialysis patients.[11-13] In a large randomised placebo-controlled trial evaluating the effect of cinacalcet on clinical outcomes in dialysis participants however, there was no statistically significant difference,

according to intention-to-treat analysis, for the primary outcome which was a composite end-point of mortality and cardiovascular end-points, perhaps related to methodological problems including drop-in and drop-out of the treatment arm and a predictably low event rate in patients aged less than 65 years.[14] In Australia, cinacalcet was approved in late 2007 for treatment of SHPT in patients with ESKD on dialysis, but not for use in renal transplant recipients and has therefore been discontinued in most patients at the time of transplantation. This potentially results in marked hyperparathyroidism and associated metabolic consequences post-transplant leading to adverse biochemical and clinical outcomes.

Few studies have attempted to evaluate the effects of discontinuing cinacalcet at the time of transplantation on mineral metabolism (Table 1).[15-19, 38] Studies are limited by low patient numbers or lack of data concerning clinical outcomes. Most studies have found that a proportion of patients receiving cinacalcet before transplantation develop hypercalcaemia with persistent hyperparathyroidism and, in some cases hypophosphataemia, after renal transplantation. We report a retrospective study of renal transplant recipients, transplanted over a 7-year period, assessing markers of mineral metabolism and other patient outcomes for up to 5-year follow-up. We aimed to determine differences in post-transplant biochemical parameters and long-term clinical outcomes of graft function, parathyroidectomy rates and survival in transplant recipients administered cinacalcet on dialysis prior to transplantation compared to those who were not treated with cinacalcet.

Methods

Study design and setting

We performed a single-centre retrospective study at The Royal Melbourne Hospital (RMH), Parkville, Australia, which included all patients who received a renal transplant between 1st January 2006 and 31st December 2012. We obtained information regarding patient demographics, aetiology of ESKD, dialysis details, transplantation details (including date of engraftment, graft number, mode, immunosuppressive therapy), comorbidities (including parathyroidectomy pre-transplant), and patient outcomes such as graft loss, post-transplant parathyroidectomy and mortality from our computerized nephrology database developed in-house (Nephworks 6). Nephworks contains prospectively documented patient history, medications, comorbid events and outcomes for all dialysis and transplant patients at RMH. Blood results related to biochemical profile, namely serum levels of 25-hydroxy vitamin D (25(OH)D), calcium, phosphate, PTH, alkaline phosphatase (ALP) and creatinine, were also obtained. Patients administered cinacalcet therapy at the time of transplantation were identified and classified as cinacalcet-treated patients (C+) whereas patients not administered cinacalcet were designated cinacalcet non-treated (C-). Cinacalcet doses were retrieved and included in the analysis. Patients who received cinacalcet after renal transplantation were excluded from analysis and patients without at least 12-month follow-up data were also excluded (those who moved interstate).

Biochemical parameters

Laboratory data relating to serum PTH, calcium, phosphate, ALP and creatinine included pre-transplant levels and levels at 3, 6, 9 and 12 months post-transplantation as well as yearly thereafter to 5 years post-transplant. Serum 25(OH)D levels were available for patients at 12

months post-transplantation but unfortunately not at the time of transplantation on all patients. All biochemistry was performed at Melbourne Health Pathology at RMH. Serum concentrations of intact PTH were determined using a solid-phase, two-site chemiluminescent enzyme-labelled immunometric assay on the IMMULITE® 2000 Analyzer (Siemens Healthcare Global, Erlangen, Germany). All other biochemical markers were measured using standard assays and analyses were performed according to the manufacturer's instructions. The estimated glomerular filtration rate (eGFR) was calculated according to the Modification of Diet in Renal Disease (MDRD) formula.[20] Hypercalcemia was defined as serum calcium level >2.60mmol/L and hyperparathyroidism a PTH level greater than the upper range of normal for the assay (>7.0pmol/L).

Statistical methods

Results are presented as mean (+/- standard deviation) for normally distributed continuous variables and as median (interquartile range) for continuous variables with skewed distributions. The Kolmogorov-Smirnov test was performed to determine the distribution of variables. For differences between groups, Student's *t* test or the Mann-Whitney U-test was used. For differences between periods, the paired Student's *t* test or Wilcoxon's test for paired values was used. Given differences in demographic characteristics and baseline biochemical data between C- and C+ groups (Table 2), we performed analysis of a matched cohort of C- recipients (matching 2:1 with the C+ cohort) primarily to adjust for the differences in age, duration of dialysis and severity of SHPT at time of transplantation. Similar statistical analyses were performed to assess for biochemical changes post-transplantation as well as other clinical outcomes. For associations among variables, linear regression was used, considering variables with a P value <0.05 in the univariate analysis. A P value <0.05 was

considered statistically significant. Stata statistical software package (version 11.0, Stata Corporation, College Station, TX) was used for analysis.

Results

Study population and baseline results

A total of 543 renal transplants were performed over the 7-year period. 11 patients were excluded from analysis; 2 received cinacalcet following transplantation and 9 were enrolled in a randomised controlled clinical trial comparing cinacalcet and placebo in transplant recipients.[21] Demographic and baseline characteristics of our study population (n=532) are shown in Table 2. Mean age of patients at the time of transplant was 48.0+/-12.7 years and 64.3% were male. Glomerulonephritis was the predominant cause of ESKD in the cohort (29.5%) and 82.2% were undertaking dialysis at the time of transplantation (compared to 17.8% of transplants which were pre-emptive).

72 patients, 13.5% of the total cohort (Jan 2006-Dec 2012) were taking cinacalcet at the time of transplantation. When considering only the time period after November 2007 when cinacalcet was approved for use in Australia, these 72 patients accounted for 16.8% of the cohort. The median daily dose of cinacalcet in C+ patients at time of transplantation was 60 mg (range 30-180mg). C+ patients were older than C- patients (50.2+/-12.4 *vs* 47.6+/-12.7 years. p=0.01).

The median PTH levels at the time of transplantation were higher in C+ *vs* C- patients (50.7[25.4-75.2] *vs* 28.3[13.9-49.7]pmol/L, p<0.001). Mean serum calcium levels were statistically lower in C+ *vs* C- (2.22+/-0.20 vs 2.31+/-0.23mmol/L, p=0.001) although

phosphate levels were not significantly different between groups at the time of transplantation. Mean ALP levels were greater in C+ *vs* C- patients pre-transplantation (164.5+/-128.3 *vs* 95.0+/-48.5IU, p<0.001).

Post-transplant biochemical parameters

Twelve months post-transplant median PTH was significantly higher in those administered cinacalcet prior to transplant (11.7[6.9-21.2] *vs* 7.2[4.6-11.2]pmol/L, p<0.001) indicating persisting hyperparathyroidism but showing marked improvement in both groups (Table 3). Mean serum calcium was also significantly higher in C+ patients at 12 months (2.50+/-0.19 *vs* 2.43+/-0.17mmol/L, p<0.001). Mean ALP levels were not different between groups (103.6+/-43.9 *vs* 97.0+/-41.6IU, p=0.23). Serum 25(OH)D levels at 12 months following transplantation did not differ between groups (57.8+/-26.0 *vs* 51.9+/-24.7 for C- vs C+ respectively, p=0.10).

The proportion of all patients at 12 months post-transplant with hypercalcemia was 17.1%, with a greater proportion in the C+ group compared to C- (25.0% *vs* 16.2%, p=0.06) (Table 4). Only 31 patients had severe hypercalcaemia (serum calcium >2.80mmol/L) at 12 months with no difference between groups (p=0.23). Of all recipients at 12 months, 60.7% had high PTH levels (>7.0pmol/L), with a significant difference between C+ and C- (76.4% *vs* 58.3%, p=0.003). Differences in biochemical markers persisted post-transplant between groups, with higher post-transplant serum calcium levels in C+ patients compared to C- present to 4 years following the transplant and PTH levels significantly higher in C+ vs C- until 2 years post-transplant.

In relation to number of previous allografts, most transplant recipients in this study were first graft recipients (83.2%) and the proportion of these patients with high PTH and high calcium at 12 months post-transplant was 60.0% and 17.2% respectively. For recipients with a second and third graft, 63.2% and 63.6% had high PTH and 18.4% and 10% had high calcium levels at 12 months following transplantation respectively (not statistically different to those with a first graft).

Multivariate regression analyses with serum PTH at 12 months as the dependent variable showed independent associations with PTH level at the time of transplantation, renal function at 12 months post-transplant, and cinacalcet use pre-transplant. Serum calcium at 12 months post-transplant was independently associated with age, pre-transplant calcium, PTH and ALP levels, renal function 12 months post-transplant, and cinacalcet use at the time of transplantation.

Cinacalcet dose

Most patients (n=52, 72.2%) were administered a dose of 60mg or less prior to transplantation. Comparing the higher vs lower cinacalcet doses (>=60mg vs <60mg daily) the mean PTH levels were 16.4+/-16.1 *vs* 16.0+/-11.4pmol/L (p=0.92) and mean calcium levels were 2.57+/-0.17 *vs* 2.47+/-0.20mmol/L (p=0.06) respectively. Thus for those taking more than 60mg daily there were no statistically significant differences in serum PTH or calcium levels at 12 months compared to those prescribed lower doses.

Other clinical outcomes

At a median of 42.9 months follow up there were 10 deaths (1.9%), 56 recipients with failed grafts (10.6%) and 5 parathyroidectomies performed in recipients post-transplant (0.8%)

(Table 5). There were no differences in any of these clinical outcomes between the C+ and C- groups, although the numbers of deaths and parathyroidectomies following transplantation were low.

There was no difference in renal function between the two groups, at any stage out to 5 years post-transplant, and no difference in graft failure rates in those who had received cinacalcet compared to the C- group (Table 6).

Matched cohort

As there were significant differences in the severity of SHPT between groups at the time of transplantation (and differences in some demographic parameters including age and duration of dialysis), we matched 144 C- recipients for age and biochemical markers at the time of transplantation (serum calcium and PTH) with the 72 C+ transplant recipients (matching 2:1) for assessment of outcomes (Table 7). We found similar findings as with the total transplant cohort in that post-transplant serum calcium levels were significantly higher up to 4 years and PTH levels were higher to 12 months following transplantation in those who had previously been administered cinacalcet (Table 8). Similar to the total cohort, there was no difference in serum phosphate levels following transplantation between the matched C- cohort and the C+ group. Estimated GFR was also similar in matched C- recipients compared to C+, with mean eGFR of 52.8+/-21.6 *vs* 54.4+/-24.1ml/min/1.73m^2 at 12 months and 50.9+/-25.6 *vs* 48.8+/-22.7ml/min/1.73m^2 at 3 years post-transplant for C- and C+ groups respectively. Clinical outcomes were also similar with no difference between matched C- and C+ in rates of graft failure (9.2% *vs* 8.3%), post-transplant diabetes (15.1% *vs* 14.5%), post-transplant parathyroidectomy (1.0% *vs* 1.4%) and overall mortality (1.4% *vs* 1.4%).

Discussion

In this single-centre retrospective study, which has larger patient numbers and longer duration of follow-up than previous reported studies,[15-19] we compared the post-transplantation mineral profiles of renal transplant recipients treated with cinacalcet to those who were cinacalcet-naïve. We report differences between the two groups, mainly of higher post-transplant serum PTH and calcium in those administered cinacalcet until time of transplantation, up to 12 months and 4 years post-transplantation respectively.

Traditional treatment for SHPT consists of dietary phosphate restriction, vitamin D analogues, and phosphate binding agents. The international Kidney Disease: Improving Global Outcomes (KDIGO) CKD-MBD guidelines recommend parathyroidectomy in patients with severe SHPT associated with hypercalcaemia and/or hyperphosphataemia that is refractory to medical therapy.[22] Calcimimetics are relatively new therapeutic agents introduced for the treatment of SHPT over the last decade. Calcimimetics act by allosteric modification of CaSR on the parathyroid gland, increasing its sensitivity to extracellular levels by decreasing PTH gene expression [23,24] Cinacalcet hydrochloride remains the first and only commercially available calcimimetic approved for clinical use to date. Over the last decade a number of studies have demonstrated efficacy in lowering serum levels of PTH, calcium and phosphate with benefits including reducing the risk of parathyroidectomy, fracture, cardiovascular hospitalisation, and cardiovascular death in patients over 65 years in patients on dialysis with SHPT.[11-14,25]

Persistent hyperparathyroidism is common post renal transplantation. High PTH levels, hypercalcaemia and duration on dialysis at the time of transplantation are risk factors for persistent SHPT, especially in transplant recipients with subsequent suboptimal renal function.[4] High PTH is noted in 17-60% of patients at 12 months following transplantation,[4,5]

and is a major determinant of post-transplant hypercalcaemia[26] which occurs in 11-66% with casemix and differences in diagnostic criteria accounting for the wide variation.[16,27-29] Post-transplant hyperparathyroidism can result in complications of worse graft outcome,[6,7] soft tissue and vascular calcification[8,9] and increased incidence of fracture.[10] In our cohort, ~60% of transplant recipients had high PTH and ~17% had hypercalcaemia at 12 months post-transplant.

Cinacalcet, is efficacious in treating SHPT not responding to standard therapy in patients on dialysis and has resulted in a decline in rates of parathyroidectomy. Parathyroidectomy is an operation with appreciable mortality and morbidity in this cohort, and not analogous to single gland parathyroidectomy in patients with primary hyperparathyroidism. A recent paper by Ishani *et al* describes the problems associated with parathyroidectomy in the setting of haemodialysis demonstrating the significant healthcare costs and burden of this procedure in a US ESKD cohort.[30] There is evidence however that cinacalcet is ineffective in promoting the regression of parathyroid hyperplasia particularly where the gland volume is greater than 500mm^3 although this is controversial.[31,32]

Cinacalcet is not currently approved for use in transplant recipients and so is often discontinued at the time of transplantation or very shortly thereafter. Our retrospective cohort study determined the impact of discontinuation of this calcimimetic at the time of transplantation on the biochemical profile and other clinical outcomes of patients after transplantation and reports higher serum PTH and serum calcium levels, in the first 12 months and 4 years post-transplant respectively, in patients prescribed cinacalcet prior to transplantation compared with the cinacalcet naïve cohort. Ongoing SHPT post-transplant

leads to persisting abnormalities in metabolic bone parameters but by 5 years the difference is small. Our results, in larger numbers than previous studies,[15-19] show that biochemical profiles after transplantation are relatively slow to correct although a trend in the right direction. Nevertheless, use of cinacalcet prior to transplantation, and lower parathyroidectomy rates, does not seem to have any significant impact on clinical outcomes in this study.

There is limited data available regarding the effect of persistent SHPT and hypercalcaemia on long-term renal graft and patient outcomes. It has been reported that hyperparathyroidism particularly in combination with hypercalcaemia is associated with increased fracture risk[10] and progression of coronary artery calcification.[9] One study by Evenepeol *et al* looking at protocol allograft biopsies demonstrated calcium and phosphate deposition was highly prevalent in the early post-transplant period and was related to the severity of disturbance in mineral metabolism.[33] Despite the high prevalence of calcium phosphate deposition, the clinical significance was unclear as no difference in renal function was evident at 36 months between recipients with deposition and those without. In another study from the same group, a higher incidence of nephrocalcinosis was demonstrated in recipients who had been treated with cinacalcet prior to transplantation compared with cinacalcet-naïve patients, over a median follow-up of 35 months, although there was no difference in renal allograft function between groups.[15] Our study supports these findings with no difference in eGFR at a median of 43 months post-transplant between groups despite higher PTH and calcium levels in those prescribed cinacalcet prior to transplantation.

There are several studies evaluating biochemical and clinical consequences of discontinuing cinacalcet at the time of transplantation (summarised in Table 1).[15-19] Discontinuing cinacalcet may potentially result in a rebound of PTH levels in the early post-transplant period in renal transplant recipients. Similar to our study findings, two prospective studies reported higher PTH and calcium levels post-transplant consistent with persistent hyperparathyroidism.[15,16] One of these looked at differences in the dose of cinacalcet whilst on dialysis and reported that ongoing or rebound hyperparathyroidism was only relevant for those receiving 60mg daily or more.[18] Evenepoel *et al* also showed a significantly higher parathyroidectomy rate in cinacalcet-treated patients, particularly with increasing doses, whereas graft nephrocalcinosis, although higher in cinacalcet-treated patients, did not reach statistical significance.[15] Barros *et al*, in a recently published prospective study, also reported higher PTH and calcium levels at 6 months post transplantation, with 75% of patients taking a median daily dose of 30 mg of cinacalcet pre-transplant.[16] This study also evaluated the impact of the phosphatonin fibroblast growth factor-23 (FGF23) post-transplant, reporting higher levels in those administered cinacalcet prior to transplantation (although not statistically significantly different compared to cinacalcet-naïve patients). We found no difference in post-transplant PTH or calcium levels in recipients on higher doses of cinacalcet (>60mg daily) compared to lower (≤60mg daily), although the percentage of patients on higher doses was small making it difficult to draw conclusions from our data regarding the impact of cinacalcet dose.

Although cinacalcet is not currently approved for use post transplantation there have been a number of studies of renal transplant recipients evaluating the impact of administration of this medication in this population. A recent meta-analysis including 21 studies, 15 prospective and six retrospective predominantly small observational studies with no randomized

controlled trials, concluded that cinacalcet was a safe and effective treatment for post-transplant hyperparathyroidism and suggested a role for cinacalcet as an alternative to parathyroidectomy.[34] One large retrospective study reported sustained control of serum PTH, calcium and phosphate levels over three years in renal transplant recipients administered cinacalcet for persistent SHPT.[35] A more recent randomised placebo-controlled trial reported a benefit of cinacalcet in transplantation to improve post-transplant hypercalcaemia, with a 75.4[63.8-87.1]% difference in achieving a serum calcium less than 2.55mmol/L compared to placebo.[21] It is interesting to note that despite the effectiveness in reducing PTH levels and hypercalcemia in this study, there was no difference in renal function between the cinacalcet and placebo arms.

Like previous retrospective studies we observed higher post-transplantation serum calcium and PTH levels along with a higher proportion of hypercalcaemia in patients receiving cinacalcet before transplantation compared with patients not on cinacalcet. Rebound or persisting hyperparathyroidism and hypercalcaemia may be a significant clinical problem as it may result in bone loss and may impair graft function either acutely, by inducing vasoconstriction, or chronically, by mediating calcification of the tubulointerstitium (nephrocalcinosis).[6,36,37] The main factors related to post-transplant hypercalcaemia are likely PTH-mediated bone resorption and recovery of calcitriol levels. Recent clinical data also support the theory that increased PTH-mediated calcium release from the skeleton is the major pathophysiological mechanism underlying post-transplant hypercalcaemia, rather than an increased renal tubular calcium reabsorption.[27] Although analysis of our data suggested no association between cincacalcet-treated patients and mortality or the need for parathyroidectomy post-transplant, the numbers of these events were too low to determine

a clinically significant difference. There was also no association with allograft loss between groups, although other studies have suggested that hypercalcaemia may potentially be related to increased nephrocalcinosis and poorer graft outcomes. One previous study reported a tendency for higher eGFR in cinacalcet-treated patients,[17] however in our cohort there was no significant difference in renal function between groups at any stage up to 5 years post-transplant.

Recent literature has suggested that the use of cinacalcet at the time of transplantation may exacerbate kidney injury and contribute to delayed graft function following transplantation.[38] One recent retrospective study reported on 36 transplant recipients who were administered cinacalcet at the time of transplantation and, after matching with 61 recipients not on cinacalcet, found an association between cinacalcet use and delayed graft function (42% vs 23% for cinacalcet group vs controls respectively). Unfortunately we did not have information on delayed graft function in our transplant cohort to assess for this association.

There are several limitations of our study including the retrospective nature. We have included all renal transplant patients over the study period (who had not been administered cinacalcet post-transplant), however this cohort is likely representative of the transplant population at our centre without selection bias. Our study is also the largest reported of renal transplant recipients to date assessing the impact of cessation of cinacalcet at the time of transplantation. Indication bias is a potential limitation given the retrospective nature of this study as patients administered cinacalcet likely had more severe SHPT, compared to cinacalcet-naïve patients, which justified cinacalcet initiation during dialysis to avoid severe complications of SHPT. We could not establish the duration of cinacalcet use in the cinacalcet-

treated patients from our records and therefore the duration and degree of SHPT before transplantation. However, we performed analysis of a matched cohort of transplant recipients who had not been administered cinacalcet prior to transplantation, matching 2:1 with the cinacalcet recipients for age, duration of dialysis and degree of SHPT (serum calcium and PTH) at the time of transplantation. This analysis revealed similar findings to comparison between cinacalcet patients and cinacalcet naïve patients in the total study group. Other limitations of our study include the lack of 25(OH)D levels at the time of transplantation, and no FGF23 and calcitriol levels at any time point, as well as no available data on fractures, bone mineral density, indications for parathyroidectomy, nor medications that may have influenced bone and mineral metabolism including bisphosphonates, phosphate binders and vitamin D analogues or vitamin D supplements.

In summary, biochemical profiles are suggestive of persisting hyperparathyroidism upon cessation of cinacalcet in patients at the time of transplantation and reinforce the need for ongoing monitoring and management of this patient subgroup. However, no significant adverse clinical outcome was noted in our cohort with the use of cinacalcet prior to transplantation and this strategy likely avoids a significant number of parathyroidectomy operations and consequent morbidity and mortality associated with this procedure. There is conflicting evidence regarding the dose response relationship between pre-transplant cinacalcet use and SHPT on its withdrawal which needs to be investigated and might provide a guide to risk stratification of these patients. These findings provide impetus to the need for not only larger interventional studies in this cohort but also further exploring the role of calcimimetics in transplant recipients. More studies involving continuation of cinacalcet post-

transplantation are required to determine the optimal treatment of SHPT in patients listed for transplantation.

References

1. Levin A, Bakris G, Molitch M, et al. *Prevalence of abnormal serum vitamin D, PTH, calcium, and phosphorus in patients with chronic kidney disease: results of the study to evaluate early kidney disease.* Kidney Int. 2006;71(1):31-38.
2. Block GA, Klassen PS, Lazarus JM, Ofsthun N, Lowrie EG, Chertow GM. *Mineral metabolism, mortality, and morbidity in maintenance hemodialysis.* J Am Soc Nephrol. 2004;15(8):2208-2218.
3. Ganesh SK, Stack AG, Levin NW, Hulbert-Shearon T, Port FK. *Association of elevated serum PO4, Ca× PO4 product, and parathyroid hormone with cardiac mortality risk in chronic hemodialysis patients.* J Am Soc Nephrol. 2001;12(10):2131-2138.
4. Evenepoel P, Claes K, Kuypers D, Maes B, Bammens B, Vanrenterghem Y. *Natural history of parathyroid function and calcium metabolism after kidney transplantation: a single-centre study.* Nephrol Dial Transplant. 2004;19(5):1281-1287.
5. Torres A, Lorenzo V, Salido E. *Calcium metabolism and skeletal problems after transplantation.* J Am Soc Nephrol. 2002;13(2):551-558.
6. Gwinner W, Suppa S, Mengel M, et al. *Early calcification of renal allografts detected by protocol biopsies: causes and clinical implications.* Am J Transplant. 2005;5(8):1934-1941.
7. Schwarz A, Mengel M, Gwinner W, et al. *Risk factors for chronic allograft nephropathy after renal transplantation: a protocol biopsy study.* Kidney Int. 2005;67(1):341-348.
8. Reynolds JL, Joannides AJ, Skepper JN, et al. *Human vascular smooth muscle cells undergo vesicle-mediated calcification in response to changes in extracellular calcium and phosphate concentrations: a potential mechanism for accelerated vascular calcification in ESRD.* J Am Soc Nephrol. 2004;15(11):2857-2867.
9. Mazzaferro S, Pasquali M, Taggi F, et al. *Progression of coronary artery calcification in renal transplantation and the role of secondary hyperparathyroidism and inflammation.* Clin J Am Soc Nephrol. 2009;4(3):685-690.
10. Perrin P, Caillard S, Javier RM, et al. *Persistent hyperparathyroidism is a major risk factor for fractures in the five years after kidney transplantation.* Am J Transplant.. 2013;13(10):2653-2663.

11. Block GA, Martin KJ, de Francisco AL, et al. *Cinacalcet for secondary hyperparathyroidism in patients receiving hemodialysis.* N Engl J Med. 2004; 350(15):1516-1525.
12. Cunningham J, Danese M, Olson K, Klassen P, Chertow GM. *Effects of the calcimimetic cinacalcet HCl on cardiovascular disease, fracture, and health-related quality of life in secondary hyperparathyroidism.* Kidney Int. 2005;68(4):1793-1800.
13. Lindberg JS, Culleton B, Wong G, et al. *Cinacalcet HCl, an oral calcimimetic agent for the treatment of secondary hyperparathyroidism in hemodialysis and peritoneal dialysis: a randomized, double-blind, multicenter study.* J Am Soc Nephrol. 2005;16(3):800-807.
14. Chertow GM, Block GA, Correa-Rotter R, et al. *Effect of cinacalcet on cardiovascular disease in patients undergoing dialysis.* N Engl J Med. 2012;367(26):2482-2494.
15. Evenepoel P, Sprangers B, Lerut E, et al. *Mineral metabolism in renal transplant recipients discontinuing cinacalcet at the time of transplantation: a prospective observational study.* Clin Transplant. 2012;26(3):393-402.
16. Barros X, Fuster D, Paschoalin R, et al. *Changes in bone mineral metabolism parameters, including FGF23, after discontinuing cinacalcet at kidney transplantation.* Endocrine. 2014:1-7.
17. Jadoul M, Banos A, Zani VJ, Hercz G. *The effects of discontinuing cinacalcet at the time of kidney transplantation.* NDT plus. 2010;3(1):37-41.
18. Torregrosa JV, Bergua C, Martinez de Osaba MJ, Oppenheimer F, Campistol JM. *Evolution of secondary hyperparathyroidism after kidney transplantation in patients receiving cinacalcet on dialysis.* Transplant Proc. 2009;41(6):2396-2398.
19. Paschoalin RP, Torregrosa JV, Barros X, Duran CE, Soler M, Campistol JM. *Withdrawal of cinacalcet at the time of renal transplantation is not a risk factor for allograft calcifications in the early posttransplantation period.* Transplant Proc. 2012;44(8):2379-2380.
20. Levey AS, Bosch JP, Lewis JB, Greene T, Rogers N, Roth D. *A more accurate method to estimate glomerular filtration rate from serum creatinine: a new prediction equation.* Annals of Internal Medicine. 1999;130(6):461-470.
21. Evenepoel P, Cooper K, Holdaas H, et al. *A Randomized Study Evaluating Cinacalcet to Treat Hypercalcemia in Renal Transplant Recipients With Persistent Hyperparathyroidism.* Am J Transplant. 2014.

22. *KDIGO clinical practice guideline for the diagnosis, evaluation, prevention, and treatment of Chronic Kidney Disease-Mineral and Bone Disorder (CKD-MBD).* Kidney Int Suppl. 2009(113):S1-130.
23. Levi R, Ben-Dov IZ, Lavi-Moshayoff V, et al. *Increased parathyroid hormone gene expression in secondary hyperparathyroidism of experimental uremia is reversed by calcimimetics: correlation with posttranslational modification of the trans acting factor AUF1.* J Am Soc Nephrol. 2006;17(1):107-112.
24. Nagano N. *Pharmacological and clinical properties of calcimimetics: calcium receptor activators that afford an innovative approach to controlling hyperparathyroidism.* Pharmacol Ther. 2006;109(3):339-365.
25. Moe SM, Chertow GM, Coburn JW, et al. *Achieving NKF-K/DOQI™ bone metabolism and disease treatment goals with cinacalcet HCl.* Kidney Int. 2005;67(2):760-771.
26. David DS, Sakai S, Brennan BL, et al. *Hypercalcemia after renal transplantation: Long-term follow-up data.* N Engl J Med. 1973;289(8):398-401.
27. Evenepoel P, Van Den Bergh B, Naesens M, et al. *Calcium metabolism in the early posttransplantation period.* Clin J Am Soc Nephrol. 2009;4(3):665-672.
28. Ramezani M, Einollahi B, Asl MA, et al. *Calcium and phosphorus metabolism disturbances after renal transplantation.* Transplant Proc. 2007;39(4):1033-1035.
29. Reinhardt W, Bartelworth H, Jockenhövel F, et al. *Sequential changes of biochemical bone parameters after kidney transplantation*. Nephrol Dial Transplant. 1998;13(2):436-442.
30. Ishani A, Liu J, Wetmore JB, et al. *Clinical Outcomes after Parathyroidectomy in a Nationwide Cohort of Patients on Hemodialysis.* Clin J Am Soc Nephrol. 2015;10(1):90-97.
31. Meola M, Petrucci I, Barsotti G. *Long-term treatment with cinacalcet and conventional therapy reduces parathyroid hyperplasia in severe secondary hyperparathyroidism.* Nephrol Dial Transplant. 2009; 24(3):982-989.
32. Komaba H, Nakanishi S, Fujimori A, et al. *Cinacalcet effectively reduces parathyroid hormone secretion and gland volume regardless of pretreatment gland size in patients with secondary hyperparathyroidism.* Clin J Am Soc Nephrol. 2010;5(12):2305-2314.
33. Evenepoel P, Lerut E, Naesens M, et al. *Localization, etiology and impact of calcium phosphate deposits in renal allografts.* Am J Transplant. 2009;9(11):2470-2478.

34. Cohen JB, Gordon CE, Balk EM, Francis JM. *Cinacalcet for the treatment of hyperparathyroidism in kidney transplant recipients: a systematic review and meta-analysis.* Transplantation. 2012;94(10):1041-1048.
35. Torregrosa JV, Morales E, Diaz JM, et al. *Cinacalcet for hypercalcaemic secondary hyperparathyroidism after renal transplantation: a multicentre, retrospective, 3-year study.* Nephrology. 2014;19(2):84-93.
36. Boom H, Mallat MJ, de Fijter JW, Paul LC, Bruijn JA, van Es LA. *Calcium levels as a risk factor for delayed graft function.* Transplantation. 2004;77(6):868-873.
37. Heaf J, Tvedegaard E, Kanstrup IL, Fogh-Andersen N. *Hyperparathyroidism and long-term bone loss after renal transplantation.* Clin Transplant. 2003;17(3):268-274.
38. Weekers L, de Tullio P, Bovy C, et al. *Activation of the calcium-sensing receptor before renal ischemia/reperfusion excerbates kidney injury.* Am J Transl Res 2015;7(1):128-138.

Tables

Table 1. Studies evaluating post-transplant biochemical profiles in patients discontinuing cinacalcet at the time of transplantation

Study	Year	Study design	Sample size 'n' (on cinacalcet)	Follow up – mean (months)	Results
Torregrosa *et al*[18]	2009	Prospective	19 (19)	6	• PTH and Ca higher in 6/19* • PTH and Ca unchanged in 13/19^
Jadoul *et al*[17]	2010	Retrospective	38 (28)	12	• No change in PTH, Ca and P
Evenepoel *et al*.[15]	2012	Prospective	303 (21)	35.6 ± 15.8	• PTH and Ca higher in cinacalcet-treated • Higher rate of parathyroidectomy and nephrocalcinosis in cinacalcet-treated
Paschoalin *et al*.[19]	2012	Retrospective	46 (46)	12	• Cinacalcet pre-transplant not associated with allograft calcification
Barros *et al*.[16]	2014	Prospective	48 (20)	6	• PTH and Ca higher in cinacalcet-treated
Weekers *et al*.[38]	2015	Retrospective	97 (36)	1	• Delayed graft function higher in cinacalcet-treated

Abbreviations: Ca, calcium; P, phosphate; PTH, parathyroid hormone;

*cinacalcet dose ≥ 60 mg/day; ^ cinacalcet dose = 30 mg/day

Table 2. Patient characteristics of all transplant recipients, divided according to those who were not taking cinacalcet (C-) or administered cinacalcet (C+) at the time of transplantation.

Characteristics	**All (n=532)**	**C- (n=460)**	**C+ (n=72)**	**P value**
Age at transplantation (yrs)	48.0 +/- 12.7	47.6 +/- 12.7	50.2 +/- 12.4	0.01
Gender (%M)	64.3	65.9	54.2	0.05
Cause of ESKD				NS
- DM	8.0	7.8	8.7	
- GN	29.5	30.1	28.2	
- HT	3.8	3.7	4.3	
- PCKD	15.9	15.3	20.3	
- Reflux	16.5	16.3	17.4	
- Other	26.3	26.8	21.1	
Dialysis modality (HD/PD/pre-emptive, %)	53.8/28.4/17.8	50.1/30.3/19.6	71.5/21.1/7.4	0.03
Duration on dialysis (yrs)	3.41 +/- 2.53	3.53 +/- 2.58	2.59 +/- 2.08	0.009
DM (%)	24.6	23.8	29.6	NS
IHD (%)	10.6	9.4	13.9	NS
HT (%)	71.9	71.2	76.1	NS
Parathyroidectomy (%)	13.9	14.3	11.1	NS
Donor age (yrs)	52.8 +/- 13.4	53.2 +/- 12.8	50.3 +/- 16.5	0.05
Living (%)	49.4	54.1	19.4	<0.001
First graft (%)	83.2	83.2	83.3	NS
Duration of transplant (mths)	45.0 +/- 22.9	46.9 +/- 23.1	32.3 +/- 17.0	<0.001

Abbreviations: DM, diabetes mellitus; ESKD, end-stage kidney disease; GN, glomerulonephritis; HD, haemodialysis; HT, hypertension; IHD, ischaemic heart disease; PCKD, polycystic kidney disease; PD, peritoneal dialysis

Table 3. Biochemical parameters of mineral metabolism at time of transplantation and post-transplant in recipients who were either not taking cinacalcet (C-) or previously administered cinacalcet until the time of transplantation (C+).

Time post	Ca (mmol/l)			Phos (mmol/L)			PTH (pmol/L)		
	C-	C+	P value	C-	C+	P value	C-	C+	P value
Pre-transplant	2.31 +/-0.23	2.22 +/- 0.20	0.001	1.73 +/- 0.59	1.64 +/- 0.53	0.21	28.3 (13.9-49.7)	50.7 (25.4-75.2)	<0.001
3 mths	2.43 +/- 0.17	2.51 +/- 0.17	<0.001	0.95 +/- 0.29	0.92 +/- 0.29	0.50	8.8 (5.0-14)	13.2 (8.6-24.6)	<0.001
6 mths	2.44 +/- 0.16	2.54 +/- 0.17	<0.001	1.02 +/- 0.51	0.93 +/- 0.28	0.19	7.4 (4.8-11.7)	12.0 (7.5-20.1)	<0.001
9 mths	2.44 +/- 0.17	2.53 +/- 0.15	<0.001	1.03 +/- 0.35	0.97 +/- 0.32	0.20	7.9 (4.6-10.8)	13.1 (7.8-21.6)	<0.001
12 mths (n=532)	2.43 +/- 0.17	2.50 +/- 0.19	0.001	1.02 +/- 0.28	0.95 +/- 0.41	0.07	7.2 (4.6-11.2)	11.7 (6.9-21.2)	0.005
2 yrs (n=398)	2.43 +/- 0.18	2.50 +/- 0.18	0.007	1.06 +/- 0.32	0.94 +/- 0.28	0.02	8 (5.4-14.3)	10.7 (6.4-22.1)	0.43
3 yrs (n=296)	2.42 +/- 0.21	2.53 +/- 0.17	0.006	1.07 +/- 0.35	0.97 +/- 0.26	0.15	6.9 (4.4-12.7)	14.4 (11.3-28.7)	0.11
4 yrs (n=155)	2.44 +/- 0.18	2.52 +/- 018	0.09	1.11 +/- 0.35	1.16 +/- 0.54	0.59	8.2 (5.5-13.6)	16.7 (8.4-52.3)	0.16
5 yrs (n=98)	2.35 +/- 0.23	2.50 +/- 0.20	0.16	1.26 +/- 0.56	1.21 +/- 0.41	0.23	10.5 (6.0-15.9)	21.4 (10.2-50.1)	0.21

*Serum calcium and phosphate levels are shown as mean+/-SD, and PTH levels are median (IQR)

Abbreviations: Ca, calcium; Phos, phosphate; PTH, parathyroid hormone

Table 4. Proportion of patients (%) with abnormal biochemical parameters following transplantation (6 months, 12 months and 2 years)

Biochemical parameter	**All**	**C -**	**C +**	**P value**
PTH (>7.0pmol/L)				
- 6 mths	69.0	66.5	84.7	0.002
- 12 mths	60.7	58.3	76.4	0.003
- 2 yrs	86.3	85.7	90.3	0.29
Calcium (>2.60mmol/L)				
- 6 mths	17.7	14.6	37.5	<0.001
- 12 mths	17.1	16.1	25.0	0.06
- 2 yrs	36.5	34.6	48.6	0.02
Phosphate (<0.80mmol/L)				
- 6 mths	20.5	19.3	27.8	0.10
- 12 mths	19.5	17.6	32.0	0.004
- 2 yrs	10.2	9.1	16.7	0.05

Table 5. Outcomes of transplant recipients who were either not taking cinacalcet (C-) or previously administered cinacalcet until the time of transplantation (C+).

Outcomes	**All**	**C -**	**C +**	**P value**
Graft failure (%)	10.6	10.9	8.3	0.51
Post-transplant DM (%)	12.7	12.4	14.5	0.66
Post-transplant parathyroidectomy (%)	0.8	0.7	1.4	0.50
Mortality (%)	1.9	2.0	1.4	0.74

Abbreviations: DM, diabetes mellitus

Table 6. Renal function (measured by MDRD eGFR) at time of transplantation and post-transplant in recipients who were either not taking cinacalcet (C-) or previously administered cinacalcet until the time of transplantation (C+).

eGFR (ml/min/1.73m^2)	**C -**	**C +**	**P value**
Pre-transplant	7.7 +/- 5.0	6.5 +/- 2.8	0.1
1 yr	50.7 +/- 18.7	54.4 +/- 24.1	0.14
2 yrs	50.9 +/- 24.1	53.2 +/- 21.1	0.56
3 yrs	50.5 +/- 22.2	48.8 +/- 22.7	0.78
5 yrs	41.8 +/- 22.2	47.3 +/- 18.8	0.73

Table 7. Patient characteristics of the matched cohort of transplant recipients (n=216), divided according to those who were either not taking cinacalcet (C-) or administered cinacalcet (C+) at the time of transplantation.

Characteristics	**C- (n=144)**	**C+ (n=72)**	**P value**
Age at transplantation (yrs)	49.3 +/- 13.1	50.2 +/- 12.4	0.52
Gender (%M)	60.7	54.2	0.36
Dialysis vs pre-emptive (%)	90.1/9.9	92.6/7.4	0.55
Duration on dialysis (yrs)	3.51 +/- 2.69	2.59 +/- 2.08	0.64
DM (%)	31.6	29.6	0.76
Donor age (yrs)	53.1 +/- 13.0	50.3 +/- 16.5	0.21
Duration of transplant (mths)	32.6 +/- 12.1	32.3 +/- 17.0	0.54

Abbreviations: DM, diabetes mellitus

Table 8. Biochemical parameters of mineral metabolism at time of transplantation and post-transplant in matched transplant recipients (n=216) who were either not taking cinacalcet (C-, n=144) or previously administered cinacalcet until the time of transplantation (C+, n=72).

Time post	Ca (mmol/l)			PTH (pmol/L)		
	C-	C+	P value	C-	C+	P value
Pre-transplant	2.24 +/- 0.21	2.22 +/- 0.20	0.32	40.9 (20.8-63.6)	50.7 (25.4-75.2)	0.29
3 mths	2.41 +/- 0.19	2.51 +/- 0.17	<0.001	10.6 (5.2-15.4)	13.2 (8.6-24.6)	0.001
6 mths	2.44 +/- 0.16	2.54 +/- 0.17	<0.001	7.8 (5.2-14.1)	12.0 (7.5-20.1)	<0.001
9 mths	2.46 +/- 0.16	2.53 +/- 0.15	0.005	8.0 (4.2-11.0)	13.1 (7.8-21.6)	<0.001
12 mths (n=532)	2.43 +/- 0.18	2.50 +/- 0.19	0.01	7.3 (4.5-12.3)	11.7 (6.9-21.2)	<0.001
2 yrs (n=398)	2.42 +/- 0.15	2.50 +/- 0.18	0.002	7.7 (5.0-14.5)	10.7 (6.4-22.1)	0.37
3 yrs (n=296)	2.42 +/- 0.21	2.53 +/- 0.17	0.009	7.3 (4.4-12.7)	14.4 (11.3-28.7)	0.43
4 yrs (n=155)	2.43 +/- 0.18	2.52 +/- 018	0.13	8.1 (4.4-17.4)	16.7 (8.4-52.3)	0.08

*Serum calcium levels are shown as mean+/-SD, and PTH levels are median (IQR)

Abbreviations: Ca, calcium; PTH, parathyroid hormone

CHAPTER 6: ASSESSING THE UTILITY OF TESTING ALUMINIUM LEVELS IN DIALYSIS PATIENTS

The research presented in this chapter has been published in the following article.

Sharma AK, ND Toussaint, J Pickering, T Beeston, ER Smith, SG Holt. Assessing the utility of testing aluminum levels in dialysis patients. *Hemodialysis International* 2015; **19**(2):256-262.

Author affiliations

Ashish K SHARMA[1,2], Nigel D TOUSSAINT[1,2], Janice PICKERING[1], Tony BEESTON[1], Edward R SMITH[1], Stephen G HOLT[1,2]

[1]*The Royal Melbourne Hospital, Parkville, Victoria, Australia;*

[2]*Department of Medicine (RMH), The University of Melbourne, Melbourne, Australia*

Summary

Background: Plasma aluminium (Al) is routinely tested in many dialysis patients. Al exposure may lead to acute toxicity and levels in excess of ~2.2µmol/L (60µg/L) should be avoided. Historically toxicity has been caused by excessive dialysate Al but modern reverse osmosis (RO) water should be Al-free. Nevertheless many units continued to perform routine Al levels on dialysis patients.

Methods: This single-centre study retrospectively analysed Al levels in plasma, raw water feed and RO product between 2010 and 2013 using our database (Nephworks 6) with the aim of determining the utility of these measurements.

Results: 2058 plasma Al tests in 755 patients (61.9% male, mean age 64.7 years) were reviewed showing mean +/-SD of 0.41 +/-0.30µmol/L. 111 (5.4%) tests from 61 patients had Al levels >0.74µmol/L and 45 (73.8%) of these patients were or had been prescribed Al hydroxide ($Al(OH)_3$) as a phosphate binder. Seven patients had Al concentrations >2.2µmol/L with no source of Al identified in one patient. 166 patients taking $Al(OH)_3$ (78.7% of all patients on $Al(OH)_3$) had levels ≤0.74µmol/L, the odds ratio of plasma Al >0.74µmol/L on $Al(OH)_3$ was 9. The cost of plasma Al assay is AU$30.60, thus costs were AU$62,974.80 over the study period. Despite RO feed water Al levels as high as 48µmol/L, Al output from the RO was almost always undetectable (<0.1µmol/L) with dialysate Al levels >2.2µmo/L only 3 times since 2010, and never in last 3 years.

Conclusions: Routine unselected testing of plasma Al appears unnecessary and expensive and more selective testing in dialysis patients should be considered.

Keywords: aluminium, chronic kidney disease, contamination, dialysis, haemodialysis, phosphate binders

Introduction

Aluminium (Al) is cleared from the blood exclusively by glomerular filtration. Thus, patients with renal failure accumulate Al and are the only routine patient group likely to be at risk of Al toxicity. Al overload results in accumulation principally in the skeleton and the brain and manifests with osteomalacia (resistant to vitamin D therapy), bone and muscle pain, iron-resistant microcytic anaemia, and neurologic abnormalities including speech disorders, encephalopathy and dementia [1]

Acute Al toxicity is rare, and mostly related to Al phosphide (AlP), which is used as a pesticide. Exposure to water or ingestion of AlP causes the release of the highly toxic phosphine (PH_3) leading to rapid free radical injury, circulatory collapse and death [2]. The Al *per se* only seems to be an issue if given concurrently with sodium citrate which dramatically increases Al uptake, and in dialysis patients this leads to very high plasma levels ~2000µg/L (~75µmol/L) which can result in potentially fatal neurological toxicity. [3]

Most of the early occurrence of chronic Al toxicity was reported between 1965 and mid 1980s and primarily caused by excessive Al in dialysate water in patients undergoing chronic haemodialysis (HD) therapy [4] but it has also been reported after contaminated peritoneal dialysis (PD) fluid [5]. In the early days of dialysis, the preparation of dialysate water was unsophisticated and subject to contamination from a number of sources, including the addition of Al as a flocculant to remove colloidal matter. Moreover, water purification often involved using stainless steel boilers, sometimes fitted with Al-based cathodic corrosion protection systems, leading to high Al levels in the dialysate. Modern water preparation using reverse osmosis (RO) membrane systems, reduction in the use of Al-based phosphate binders

and the avoidance of calcium citrate means that acute or chronic Al toxicity is rarely (if ever) encountered in modern practice [6]. Al-based phosphate binders are now infrequently prescribed across the world, but apparently more in Australia/New-Zealand [6]. Thus Al-based binders [6] and Al containing antacids now represent the major source of Al exposure in patients with end-stage kidney disease (ESKD). Al can also be a contaminant present in oral and injectable medications as part of the manufacturing process [7, 8] in particular albumin products. Albumin binds Al during the purification process when passed through Al silicate filters, and thus long-term use of intravenous (IV)/blood products is another potential source of excess Al [9]. There have also been reports of sepsis causing release of Al from tissue stores [10].

The National Kidney Foundation's Kidney Disease Outcomes Quality Initiative (KDOQI) guidelines for the care of patients with ESKD recommended screening for Al toxicity with Al concentrations at least yearly, and quarterly in those receiving Al-containing medications, however these were outlined in the guidelines as opinion-based recommendations [11]. The more recent international Kidney Disease: Improving Global Outcomes (KDIGO) Chronic Kidney Disease – Mineral and Bone Disorder (CKD-MBD) guidelines recommend avoiding long-term use of Al-containing phosphate binders and, in patients with ESKD on dialysis, dialysate Al decontamination to prevent Al intoxication [12]. However there are no KDIGO recommendations regarding measurement of plasma Al levels. There appears to be a low incidence of high Al levels among current dialysis patients [13] with no reported outbreaks of Al toxicity in recent literature except sporadic clusters of cases of elevated Al levels [14].

There have only been a few retrospective studies published evaluating the frequency of abnormal plasma Al levels, the predictive value of Al testing, cut-off levels for toxicity and the utility of routine screening in an era of Al-free dialysate water and decreased Al-based binder administration [13, 15-17]. Some investigators have advocated re-evaluating the safety of Al-based phosphate binders given low demonstrated risk of toxicity and a cost benefit over contemporary first line phosphate binders although prospective trials are lacking [6, 18].

In light of the reduction in exposure of dialysis patients to Al, an audit at our institution was undertaken to assess the requirements for continued monitoring of patients and the water quality of dialysate. We report a single-centre study assessing the frequency of abnormal Al levels in a cohort of dialysis patients over a period of 4 years with the aim of evaluating the clinical benefit of routine Al measurement.

Methods

We performed a retrospective cohort study of dialysis patients at The Royal Melbourne Hospital (RMH), Parkville, Australia. All dialysis patients undergo routine annual surveillance of plasma Al concentrations at RMH, with bi-annual measurements for patients prescribed Al-based phosphate binders. We retrospectively retrieved all plasma Al levels tested for the dialysis population from January 2010 to December 2013 using our computerized nephrology database (Nephworks 6), as well as RO and water feed Al levels on all HD patients. Nephworks contains prospectively documented patient history, medications, comorbid events and outcomes for all dialysis patients at RMH. Medical records of patients with abnormal plasma Al levels were reviewed to determine Al exposure.

Laboratory methods

5 mL of blood was collected into K_2-EDTA anticoagulated BD Vacutainer® Blood Collection Tubes for Trace Element Testing, this avoids significant contamination (20-60ug/L) by the rubber stoppers made from Al silicate that are commonly used in standard evacuated blood tubes [19]. The sampling needle is not usually a problem for Al.

Plasma Al levels were measured using dual beam graphite furnace atomic absorption spectrophotometry with an AAnalyst 800 spectrophotometer (Perkin Elmer, MA) throughout the study period. The lab cut-off value for plasma Al was <0.8µmol/L with a local range of between 1.5µmol/L and 2.0µmol/L for patients with ESKD on Al-based binders. There is no well-defined threshold level of plasma Al concentration indicating toxicity in dialysis patients [20]. Previous studies have used different cutoff levels including 0.74µmol/L (20µg/L), 1.48µmol/L (40µg/L), 2.22µmol/L (60µg/L) and 3.0µmol/L based on varying evidence and local lab parameters [13, 16-18]. KDOQI guidelines recommend Al levels to be tested quarterly and be less than 0.74µmol/L with the use of the desferoxamine (DFO) mobilisation test [21] for elevated levels between 2.22 to 7.42µmol/L (60 to 200µg/L respectively) [11]. In our study we used a cutoff value of > 0.74µmol/L to indicate abnormal levels and ≥2.2µmol/L to indicate risk of toxicity for analysis.

We routinely undertake trace element analysis in dialysate water collected from various sites across multiple dialysis centres. Mains water and RO output is regularly tested for Al by our service [22]. There are suggested limits of <100µg/L (3.71µmol/L) for large processing plants and <200µg/L (7.42µmol/L) for smaller plants serving 10,000 people or less [23]. We reference American National Standard ANSI/AAMI RD62:2006, which indicates maximum

allowable concentration of Al in 'water used to prepare dialysate' as <10ug/L (<0.37µmol) for our dialysis network. We also reviewed Al levels in the dialysate water source over this period as there are guidelines for drinking water Al content suggested by the World Health Organization (WHO).

Statistics

This is predominantly a descriptive study. Descriptive statistics are presented as mean (+/- standard deviation) or percentages. Data analyses were performed on individual plasma Al concentrations and not based on the mean plasma Al level per patient. Therefore both the number of Al determinations and the number of patients are given. Mann-Whitney U test was used to determine differences between patients taking and not taking Al-based phosphate binders according to Al levels. Logistic regression was used to compare differences in Al levels and $Al(OH)_3$ use over time. Stata statistical software package (version 11.0, Stata Corporation, College Station, TX) was used for analysis.

Results

We retrieved a total of 2058 plasma Al measurements for 755 patients over the 4-year period. The dialysis cohort had a mean age of 64 years and 62% were male (Table 1). The mean plasma Al level was 0.41+/-0.30µmol/L (11+/-8.08ug/L). A total of 211 of these patients were or had been prescribed Al hydroxide ($Al(OH)_3$) as an oral phosphate binder. Of 2058 measurements, 111 (5.4%) tests from 61 patients had Al levels greater than 0.74µmol/L with 45 (73.8%) being on $Al(OH)_3$. These 61 patients included 47 on HD, 6 on PD and 8 on home HD. Ten results (0.49%) were equal to or greater than 2.2µmol/L in 7 patients out of which 6 patients had been prescribed $Al(OH)_3$ with no source of Al identified in 1 patient who was undergoing

dialysis at home at the time and returned normal Al level on repeat testing. There was no evidence of clinical toxicity due to elevated Al levels on review of the available medical records for these patients. 166 patients taking $Al(OH)_3$ (78.7% of all patients on $Al(OH)_3$) had levels ≤0.74μmol/L. The odds ratio (OR) of plasma Al >0.74μmol/L on $Al(OH)_3$ was 9.

$Al(OH)_3$ as a potential source of abnormal levels was identified in 45 out of 61 patients, (Table 2) although the cumulative Al load in patients on $Al(OH)_3$ could not be calculated given inconsistent information available regarding the dose of binders administered. In the remaining 16 patients the abnormal results were presumed to be erroneous or a result of inadvertent exposure to Al through equipment or medications based on the lack of repeated elevated levels, levels in the non-toxic range (93.7%) and a tendency to revert to normal on repeat testing. On follow up tests the levels reverted to or trended towards normal in 47 out of 61 patients (77%, including 12 patients not on $Al(OH)_3$) with Al levels >0.74μmol/L. Out of 7 patients with Al >2.2μmol/L only one patient had multiple elevated levels, with maximum of 3.64μmol/L, which reverted back to normal on cessation of $Al(OH)_3$. None of the patients had Al level >7.4μmol/L.

Al levels measured in the dialysate water precluded any risk of exposure from that source. Despite RO feed water Al levels as high as 48μmol/L (1300ng/mL), Al output from the RO was almost always undetectable (<0.1μmol/L). We have detected dialysate Al levels >2.2μmol/L only 3 times since January 2010, and never in last 3 years.

The frequency of elevated plasma Al levels (>0.74 μmol/L) in patients on dialysis declined each year from 8.72% in 2010 to 2.35% in 2013, perhaps related to declining use of Al-based phosphate binders. Administration of $Al(OH)_3$ in subjects in this study declined from 31.7% to 4.75% over the same period (Table 3). The cost of single plasma Al assay is AU$30.60 resulting

in the total cost over the study period of AU$62,974.80, or amounting to over AU$1300 per month.

Discussion

Al toxicity has been known to cause serious complications although the incidence of cases in the current dialysis population is very low given the elimination of Al from dialysate water and the decreased use of Al-based phosphate binders. As we have continued to routinely measure plasma Al levels on all dialysis patients at our local centre we performed a retrospective observational study to determine the frequency of abnormal Al concentrations and assess for associations with any clinical history of toxicity, use of Al-based binders and cost of routine measurements. We report a very low number of elevated Al levels in 755 patients over a 4 year period.

Al is ubiquitous in nature with only a tiny fraction of ingested Al absorbed and normally excreted by the kidneys. Previously when Al was added to the dialysate for patients undertaking HD, it would enter the body directly leading to syndromes from toxicity. However, there has been complete absence of reports of the 'dialysis dementia' syndromes formerly attributed to Al toxicity in ESKD, and a substantial reduction in the prevalence of Al-related bone disease, with improvements in the quality of dialysate water.

Plasma Al levels reflect relatively recent exposure to Al [24, 25]. Monitoring Al levels might identify excessive Al intake or absorption in individual patients, aid in the recognition of accidental contamination of dialysate with Al and screening may potentially allow earlier

recognition of Al loading with greater ability to prevent toxicity. Plasma Al levels however, are not reliable predictors of chronic Al exposure and there is lack of consensus on threshold cutoff values indicating toxic levels. Historically routine measurements of plasma Al concentrations have been recommended based on prevalent significant risk of toxicity [15, 26] but later studies have questioned the utility and cost effectiveness of routine plasma Al measurements in all dialysis patients [13, 16-18]. Many dialysis units however continue to measure Al levels routinely.

One study reported the incidence of abnormal Al levels in dialysis patients to be as low as 2.1% [13] while another reported an incidence of 4.2%, although the cutoff value of abnormal results in this study was 0.74µmol/L compared to 1.48µmol/L in the former [16]. The frequency of abnormal results in our study was 5.4% and 0.49% for results signifying risk of toxicity using the cutoffs of 0.74µmol/L and 2.2µmol/L respectively. This is consistent with previous studies reflecting an extremely low incidence of abnormal Al levels and greatly reduced risk of toxicity compared to the era of significant Al exposure via dialysate water and regular use of Al-based phosphate binders.

One study from the United Kingdom argued that measuring Al levels routinely in the current era was unnecessary, although the dialysis patients in that study were not taking any Al-based phosphate binders and Al testing of the dialysis water supply achieved an acceptable minimum safety requirement [8]. Another study reported on the impact of double RO system and continued use of Al phosphate binders in a cohort of dialysis patients between 1998 and 2007 [27]. This study reported a reduction in serum Al levels in patients after the new RO with no plasma Al level more than 40µg/L (1.48µmol/L), even with Al-based binders.

Plasma Al levels of >3.0µmol/L have been associated with toxicity, however defining a baseline plasma Al concentration threshold to diagnose toxic Al accumulation is difficult [20]. There is not a single report in the literature of significant Al toxicity occurring in the presence of Al levels less than 1.5µmol/L. Elevated Al levels above 1.5µmol/L in one Australian report occurred in less than 2% of patients [6]. Most elevated Al concentrations are one-off isolated levels with sustained abnormal concentrations being uncommon [16]. Therefore consistent with our study, the literature also supports that the number of elevated Al levels are exceedingly low and often transient. There is no published data to determine whether an increase in plasma levels over time leads to tissue accumulation of Al.

Al replaces calcium at the mineralization front in bone, disturbing osteoid formation and causing low turnover bone problems. There is evidence that single measurements of serum Al show correlation with Al bone disease, with one study demonstrating a level greater than 100µg/L (3.7µmol/L) as a reliable indicator of Al deposits in bone [28]. Another reported a 3-fold higher risk for this complication in patients in the highest quartile of serum Al, although there was no threshold level of Al that discriminated between patients with Al bone disease and those without [15]. Another reported that a serum Al level of 60µg/L (2.22µmol/L) in combination with an intact PTH <16pmol/L provided a relatively sensitive and specific index for the detection of Al-related bone disease [26].

The diagnosis of Al bone disease is important and some dialysis units continue to monitor Al levels regularly because of concerns that exposure may continue from medications used without knowledge such as over-the-counter antacids. Many other prescribed medications

also contain hidden Al in smaller amounts [6-8, 16]. One report suggested regular attention should be paid to reviewing medications known to contain significant amounts of Al that patients may be taking without knowledge of their physicians [16]. Al levels have been shown to be higher in patients receiving injectable drugs such as iron, insulin or erythropoietin compared to those who did not receive these medications [8].

With the move towards haemodiafiltration (HDF) and the exposure to even more dialysate water there is the potential for increased exposure to Al from poorly maintained or failing RO membranes, so it would be important to maintain review of dialysate Al and raw water Al levels. The problems associated with Al toxicity are not just confined to HD patients but patients undertaking PD are also at risk. Al-based phosphate binders have been reported to contribute to toxicity in the latter population as well as non-dialysed uremic individuals [29, 30].

The possibility of sample contamination due to extraneous sources of Al in samples needs to be considered. Al is a ubiquitous metal and contamination of plasma can occur from sources including environmental dust on the blood tubes or gloves. Considerable care is required in the storage of tubes, phlebotomy procedure and sample preparation for the determination of Al levels to prevent contamination.

With a very low frequency of elevated total Al levels signifying risk of toxicity (0.49%) at our centre and at a significant monetary cost, routine plasma Al determinations in patients at low risk are unlikely to be cost-effective. One report from the United States highlighted that the cost of Al levels may range from $40-$100 (Spectra Laboratories) and therefore yearly costs

of $32,000-$80,000 could be incurred with routine measurement for an average dialysis unit[16].

Studies have reported that patients on dialysis taking Al-based phosphate binders with RO-treated water had no evidence of Al toxicity and therefore arguing that the use of Al binders in the era of RO-treated dialysis water may be safe. The vast majority of dialysis patients in our cohort with abnormal plasma Al levels were taking $Al(OH)_3$ as a binder. Although only 21% of all patients on $Al(OH)_3$ had transiently elevated Al levels, this compares to only 3% of subjects not taking Al-based binders. We also report the reduction in use of $Al(OH)_3$ over time with a significantly decreased exposure to these binders being associated with a decreased proportion of patients having elevated Al levels in the more recent period.

Limitations of our study include lack of information on residual renal function, inability to accurately determine the cumulative dose of Al-based binders in individuals and absence of DFO testing to assess total body Al load. Our study does not address the predictive value of abnormal plasma Al levels and when the frequency of abnormal levels in a population is extremely low, the utility of that test as a screening tool becomes negligible. The other consideration of Al measurement should be of cost effectiveness, which could not be demonstrated in our study.

Plasma Al as a suitable measure of the body burden to this metal is questionable. Although there is a correlation between plasma levels and Al bone disease, the predictive value of Al concentrations for bone disease is poor. The evidence that Al is absorbed from $Al(OH)_3$ and other Al-containing compounds is indirect, and the methodology for measuring Al levels using

stable isotope and mass spectroscopy is very expensive, has limited availability and should only be performed on a small number of patients. In summary, we feel that regular unselected testing of all dialysis patients is probably unnecessary given the frequency of plasma results indicative of Al overload. The costs of such a testing strategy make it unlikely to be cost effective. From a patient safety point of view it makes more sense to monitor RO water levels periodically to ensure the RO is working efficiently. There is some logic in assessing Al levels in patients in whom the risk of overload is high and there is clinical suspicion of toxicity, for example those exposed to long-term therapy with Al-containing medications like $Al(OH)_3$, antacids, and concomitant use of any drug that augments gut absorption. Furthermore, guidelines and recommendations should be updated to reflect the reduced risk of exposure from Al-containing dialysate. Isolated high levels are likely to be caused by contamination at the time of testing and not true Al overload. On the basis of our review we have now moved to only perform selected testing of plasma Al on the basis of assessment of clinical risk, whilst routine testing of dialysate Al is continuing.

References

1. Erasmus, R.T., et al., *Aluminum neurotoxicity in experimental animals.* Ther Drug Monit, 1993. **15**(6): p. 588-92.
2. Perry, L., et al., *National toxicovigilance for pesticide exposures resulting in health care contact-An example from the UK's National Poisons Information Service.* Clinical toxicology, 2014(0): p. 1-7.
3. Kirschbaum, B.B. and A.C. Schoolwerth, *Acute aluminum toxicity associated with oral citrate and aluminum-containing antacids.* Am J Med Sci, 1989. **297**(1): p. 9-11.
4. Dunea, G., et al., *Role of aluminum in dialysis dementia.* Ann Intern Med, 1978. **88**(4): p. 502-4.
5. Gumming, A., et al., *Acute Aluminium Intoxication in Patients on Continuous Ambulatory Peritoneal Dialysis.* The Lancet, 1982. **319**(8263): p. 103-104.
6. Mudge, D.W., et al., *Do aluminium-based phosphate binders continue to have a role in contemporary nephrology practice?* BMC Nephrol, 2011. **12**: p. 20.
7. Bohrer, D., et al., *Drugs as a hidden source of aluminium for chronic renal patients.* Nephrol Dial Transplant, 2007. **22**(2): p. 605-11.
8. Bohrer, D., et al., *Role of medication in the level of aluminium in the blood of chronic haemodialysis patients.* Nephrol Dial Transplant, 2009. **24**(4): p. 1277-81.
9. Bohrer, D., et al., *Influence of the glass packing on the contamination of pharmaceutical products by aluminum. Part I: Salts, glucose, heparin and albumin.* Journal of trace elements in medicine and biology, 2001. **15**(2): p. 95-101.
10. Davenport, A., et al., *Sepsis: a cause of aluminum release from tissue stores associated with acute neurological dysfunction and mortality.* Clin Nephrol, 1988. **30**(1): p. 48-51.
11. National Kidney Foundation. *K/DOQI clinical practice guidelines for bone metabolism and disease in chronic kidney disease.* Am J Kidney Dis, 2003. **42**(4 Suppl 3): p. S1-201.
12. *KDIGO clinical practice guideline for the diagnosis, evaluation, prevention, and treatment of Chronic Kidney Disease-Mineral and Bone Disorder (CKD-MBD).* Kidney Int Suppl, 2009(113): p. S1-130.
13. Jaffe, J.A., C. Liftman, and J.D. Glickman, *Frequency of elevated serum aluminum levels in adult dialysis patients.* Am J Kidney Dis, 2005. **46**(2): p. 316-9.

14. Centers for Disease Control and Prevention (CDC), *Elevated serum aluminum levels in hemodialysis patients associated with use of electric pumps--Wyoming, 2007.* MMWR Morb Mortal Wkly Rep, 2008. **57**(25): p. 689-91.
15. Kausz, A.T., et al., *Screening plasma aluminum levels in relation to aluminum bone disease among asymptomatic dialysis patients.* Am J Kidney Dis, 1999. **34**(4): p. 688-93.
16. Sandhu, G., et al., *Serum concentrations of aluminum in hemodialysis patients.* Am J Kidney Dis, 2011. **57**(3): p. 523-5.
17. Gault, P.M., K.R. Allen, and K.E. Newton, *Plasma aluminium: a redundant test for patients on dialysis?* Ann Clin Biochem, 2005. **42**(Pt 1): p. 51-4.
18. Pepper, R., et al., *Do oral aluminium phosphate binders cause accumulation of aluminium to toxic levels?* BMC Nephrol, 2011. **12**: p. 55.
19. Moyer, T.P., G.V. Mussmann, and D.E. Nixon, *Blood-collection device for trace and ultra-trace metal specimens evaluated.* Clin Chem, 1991. **37**(5): p. 709-14.
20. Altmann, P., *Aluminium toxicity in dialysis patients: no evidence for a threshold serum aluminium concentration.* Nephrol Dial Transplant, 1993. **8 Suppl 1**: p. 25-34.
21. Milliner, D.S., et al., *Use of the deferoxamine infusion test in the diagnosis of aluminum-related osteodystrophy.* Annals of Internal Medicine, 1984. **101**(6): p. 775-780.
22. CEC. *Resolution of the council and the representatives of the governments of the member states, meeting within the council, of 16 june 1986, concerning the protection of dialysis patients by minimizing the exposure to aluminium*. 1986; Available from: http://policy.mofcom.gov.cn/english/flaw!fetch.action?libcode=flaw&id=f3558ede-4604-439a-be3a-484f1c1226ba&classcode=293;330.
23. WHO, *Guidelines for Drinking-Water quality*. 4th ed. 2011: World Health Organization. 564.
24. Alfrey, A., *Aluminum metabolism in uremia.* Neurotoxicology, 1980. **1**(4): p. 43-53.
25. Salusky, I.B., et al., *Role of aluminum hydroxide in raising serum aluminum levels in children undergoing continuous ambulatory peritoneal dialysis.* J Pediatr, 1984. **105**(5): p. 717-20.
26. D'Haese, P.C., et al., *Value of serum aluminium monitoring in dialysis patients: a multicentre study.* Nephrol Dial Transplant, 1990. **5**(1): p. 45-53.

27. Arenas, M.D., et al., *[Use of the aluminum phosphate-binders in hemodialysis in the ultrapure water era].* Nefrologia, 2008. **28**(2): p. 168-73.
28. Charhon, S.A., et al., *Serum aluminium concentration and aluminium deposits in bone in patients receiving haemodialysis.* Br Med J (Clin Res Ed), 1985. **290**(6482): p. 1613-4.
29. Smith, D.B., et al., *Dialysis encephalopathy in peritoneal dialysis.* JAMA, 1980. **244**(4): p. 365-6.
30. Hewitt, C.D., J. Savory, and M.R. Wills, *Aspects of aluminum toxicity.* Clin Lab Med, 1990. **10**(2): p. 403-22.

Tables

Table 1. Patient characteristics for all dialysis patients

Characteristics	N=755 (%)
Age (years) [1]	63.2 +/- 14.9
Gender	
- Male	467 (61.9)
- Female	288 (38.2)
Cause of ESKD	
- DM	197 (26.1)
- GN	200 (26.5)
- HT	59 (7.8)
- PCKD	55 (7.3)
- Reflux	39 (5.2)
- Other (and unknown)	205 (27.1)
Dialysis modality	
- HD	582 (77.0)
- PD	119 (15.8)
- HHD	54 (7.2)
Duration on dialysis (mths, median (IQR)) [1]	32 (61.5-9.9)

[1]at the time of the last Al level

Abbreviations: DM, diabetes mellitus; GN, glomerulonephritis, HT, hypertension; PCKD, polycystic kidney disease, Reflux, reflux nephropathy; HD, hemodialysis; PD, peritoneal dialysis; HHD, home hemodialysis,

Table 2. Number of patients with normal and abnormal plasma aluminium levels in relation to administration of aluminium-based phosphate binders

Al level (µmol/L)	**N=755**	**No $Al(OH)_3$ N= 544 (%)**	**$Al(OH)_3$ N= 211 (%)**	**P-Value***
<0.74	694 (91.9%)	528 (97.1%)	166 (78.7%)	<0.01
0.74 – 2.1	54 (7.2%)	15 (2.8%)	39 (18.5%)	<0.01
≥2.2	7 (0.9%)	1 (0.2%)	6 (2.8%)	0.01

Abbreviations: Al, aluminium; $Al(OH)_3$, aluminium hydroxide

* P-value for significance between subjects taking vs not taking $Al(OH)_3$ for various Al concentrations

Table 3. Percentage of abnormal plasma aluminium levels with relationship to patients on aluminium hydroxide according to each year

Year	Patients, N	Patients on $Al(OH)_3$, N (%)*	Plasma Al levels, N	Al>0.74 µmol/L, N (%)#	Al>2.2 µmol/L, N (%)
2010	451	143 (31.7%)	562	49 (8.7%)	5 (0.9%)
2011	401	46 (11.5%)	524	32 (6.1%)	3 (0.6%)
2012	420	26 (6.2%)	547	20 (3.7%)	2 (0.4%)
2013	363	18 (4.9%)	425	10 (2.4%)	0 (0.00%)

Abbreviations: Al, aluminium; $Al(OH)_3$, aluminium hydroxide

* P-value <0.01 for relationship between $Al(OH)_3$ administration over time.

P-value <0.01 for relationship between Al>0.74µmol/L over time.

CHAPTER 7: GENERAL DISCUSSION, CONCLUSIONS AND FUTURE DIRECTIONS

In people with CKD, altered biochemical milieu due to disordered mineral metabolism, deterioration in bone quality and extra-skeletal calcification constitute the clinical syndrome known as CKD-MBD [1], which is associated with poor cardiovascular outcomes, increased fracture risk and increased mortality [2-4]. ROD, as currently defined, is the skeletal component of CKD-MBD and refers to abnormalities of bone turnover, mineralisation, volume, linear growth, or strength encountered in CKD [5]. Disruption of bone and mineral metabolism and altered biochemical milieu invariably cause erosion in bone quality in patients with CKD. Renal bone disease is complex and multidimensional and confers an excess fracture risk in patients with CKD, in addition to traditional risk factors for fracture such as older age and postmenopausal status. This is reflected in numerous epidemiological studies describing an increased prevalence of fractures in patients with CKD compared to age- and gender-matched individuals in the general population [4, 6-10], and is also associated with increased hospitalisation and mortality [11]. This higher susceptibility to fracture is not attenuated by kidney transplantation and is, in fact, higher during the early post-transplant period [12, 13]. Moreover, abnormalities of mineral metabolism, particularly persistent SHPT, may occur after kidney transplantation [14], with unclear clinical sequalae and management strategies. Traditionally, bone disease after transplantation has been synonymous with changes in BMD and osteoporosis, but more recent research has demonstrated a less significant change in BMD in the early post-transplantation period with a trend towards stability in later years [15]. Currently, there is a paucity of data about changes in bone

structure and histomorphometry and their relationship with markers of mineral metabolism after kidney transplantation, with mechanisms of underlying bone loss poorly understood.

More than a century after the initial descriptions of renal bone disease [16-20], and despite significant advances in this field during this time, major gaps still exist in our knowledge about management of ROD in the clinical setting. Inability to accurately identify the type of ROD by non-invasive means, lack of CKD-specific screening tools for assessing fracture risk, and limited supportive evidence for appropriate therapy has hampered our ability to institute preventative treatment in this high-risk group of patients. Currently available diagnostic tools in routine clinical practice have limited utility in assisting with management of ROD and therefore add to diagnostic and therapeutic uncertainty in this area. Bone biopsy captures a comprehensive snapshot of bone microarchitecture, turnover and mineralisation, but the procedure and its subsequent analysis have their own caveats and limitations. Hence, it is rarely performed routinely in clinical practice.

Over the last two decades, there has been a significant increase in research interest in CKD-MBD and ROD. During this period, notable advances in high-resolution imaging have occurred and novel biomarkers specific to CKD-MBD have been identified. This has enhanced our knowledge of bone microarchitecture in patients with CKD and provided new insights into the pathophysiology and progression of CKD-MBD. Increased understanding of bone abnormalities in CKD has highlighted the important contribution of cortical bone structure to overall bone strength and the association of cortical bone fragility with bone loss and SHPT in CKD and in kidney transplant recipients [21-25].

High-resolution MRI, using customised processing techniques, has proven to be an excellent non-invasive tool for studying bone microarchitecture in the non-CKD population [26-33]. The research described in this thesis concentrated on the potential role of MRI as a non-invasive tool to evaluate ROD, including comparing its utility with other contemporary and novel diagnostic tools within the overall umbrella of CKD-MBD. The studies presented here also highlight severe cortical bone abnormalities prevalent in patients with CKD, explore abnormalities of bone structure and mineral metabolism after kidney transplantation, and question the utility of routine screening of aluminium levels in the era of non-aluminium phosphate binders. The major findings of this thesis and their potential impact are summarised and discussed below.

Summary of results

Bone histomorphometry in CKD – highlighting the role of cortical bone

Bone biopsy and histomorphometry is the gold standard for evaluating bone quality in CKD but is used very infrequently in clinical practice due to associated limitations. Traditionally described histological patterns of renal bone disease have given way to a newer classification according to the KDIGO TMV system [5] in a major, and advantageous, shift in approach towards defining ROD. The TMV classification provides clinically relevant descriptors but fails to emphasise the importance of assessment of cortical microarchitecture, which is described as an adjunct to trabecular bone measurements. Common findings of cortical thinning and increased cortical porosity in recent studies of patients with CKD [22, 23, 34, 35] and their potential contribution to bone fragility suggest a need to emphasise the evaluation of cortical microarchitecture as a key parameter in addition to trabecular changes within the TMV classification.

In the cross-sectional study described in **Chapter 2**, I studied histological abnormalities of bone, particularly cortical bone structure, in a relatively young cohort of patients with ESKD at the time of kidney transplantation. I demonstrated severe thinning of cortical bone and increased cortical porosity, the latter associated with PTH levels, despite predominantly normal trabecular parameters. These findings, consistent with more recent studies in CKD describing deterioration in cortical microarchitecture, reinforce the importance of comprehensive cortical bone evaluation in patients with CKD and incorporating it as a central parameter in the TMV classification. The fact that severe cortical porosity is correlated to PTH levels is only a reminder of the perils of SHPT in CKD. Notably, this study is also the first to report the role of micro-CT in assessing cortical porosity in patients with CKD. Micro-CT is an *ex vivo* ultra-high resolution, non-destructive method to acquire direct 3D measurements of bone microarchitecture and images in a much larger volume of interest than 2D histology. These benefits, combined with a shorter turnaround time for processing and results, make micro-CT a desirable tool for studying bone structure and worthy of consideration in larger studies. This study also provides a snapshot of the severity of ROD, even in a relatively young and healthy, fit-for-surgery cohort of patients with ESKD. Whilst this is a small study and may not be representative of the larger study population of older and more unwell dialysis patients, it raises awareness of severe bone abnormalities on a histological level which can manifest in serious clinical outcomes. These results also serve as a reminder of the importance of the ongoing quest to find optimal treatments for SHPT and its related mineral abnormalities.

Bone microarchitecture – comparing MRI to bone histomorphometry

High-resolution imaging modalities, mainly HR-pQCT and MRI, have demonstrated potential in evaluating bone microarchitecture over the last 15 years, but this research success has not been embraced in the case of MRI in the field of renal bone disease [36]. Moreover, these modalities, at the time of commencement of this project, remained untested against the quintessential gold standard of a bone biopsy. In the work described in **Chapter 3**, I aimed to highlight advantages of MRI as a diagnostic tool in renal bone disease. In this proof of concept study, I evaluated bone microarchitecture in patients with CKD using MRI and correlated findings to those obtained by bone biopsy and other contemporary bone imaging techniques (DXA, pQCT, TBS). MRI demonstrated significant and relevant associations to important bone biopsy and DXA parameters. Significant correlations were also observed between histomorphometric mineralisation and turnover indices and various MRI parameters, but no such associations of MRI parameters could be elicited in relation to bone turnover markers. This study also underlined the inherent heterogeneity of bone microarchitecture at differing skeletal sites and the pitfalls of assessing and interpreting bone structure parameters obtained by imaging modalities with vast technical and analytic differences. Although I was able to demonstrate the utility of MRI in evaluating bone microarchitecture in patients with ESKD, it did not provide reliable information about bone turnover – the other important component of assessing ROD. Lastly, this study was the first to use commercially available hardware (coils) for MRI, which is a small but important step towards increasing the generalisability of these scans.

Bone changes after kidney transplantation – looking beyond BMD

In **Chapter 4**, I described an evaluation and comparison of longitudinal changes in bone density and microarchitecture over the first year after kidney transplantation. MRI, DXA, pQCT and TBS were used for evaluation, in association with changes in bone turnover markers, during this period. Study results confirmed the lack of significant change in BMD after kidney transplantation and highlighted deterioration in trabecular bone structure and connectivity independent of changes in BMD but associated with PTH levels. These findings were also complemented by a significant deterioration in TBS during this period. Unlike other contemporary studies, which are few in number, I found no deterioration in cortical bone at one year after transplantation. This is an important finding which highlights the lack of data about changes in bone microarchitecture and their relationship to PTH status after kidney transplantation. I also studied the impact of discontinuation of cinacalcet at the time of kidney transplantation on mineral metabolism in a retrospective audit of biochemical parameters and clinical outcomes in a large cohort of kidney transplant recipients (**Chapter 5**). Whilst I demonstrated persistent hyperparathyroidism and hypercalcaemia after transplantation in a large proportion of patients, worse in patients on cinacalcet prior to transplant, the clinical significance of these mineral metabolism markers was unclear.

Monitoring aluminium levels in the contemporary era

Historically, aluminium deposition in bone was recognised as a major cause of adynamic bone disease [37] and added an important dimension to the pathophysiology of ROD. This is less relevant in the current era due to the overall higher prevalence of low-turnover bone disease, unrelated to aluminium, in patients with ESKD. This may be related to reduction in prescription, and phasing out, of aluminium-containing phosphate binders in current clinical

practice. However, many centres continue to routinely screen dialysis patients for aluminium levels. In **Chapter 6**, I described an assessment of the utility of routine testing of serum aluminium levels in the haemodialysis population in my centre via a retrospective audit of aluminium levels tested in 755 patients over four years. Only 0.5% of 2058 test results matched criteria for toxic aluminium levels, and there was no evidence of clinical toxicity. There was progressive reduction in the proportion of elevated aluminium levels over the years, correlating with decreasing use of aluminium-based binders during this period. I concluded that routine unselected testing of serum aluminium was unnecessary and expensive and more selective testing in dialysis patients should be considered.

Significance

Overall, my research highlights the utility and potential of MRI for non-invasive evaluation of bone microarchitecture in patients with CKD. My studies underline the severity and the spectrum of bone abnormalities prevalent in patients with ESKD and raise awareness about the potential novel use of micro-CT for evaluating 3D microstructure of bone in biopsy cores. The clinical studies presented here describe bone structural abnormalities detected by MRI in patients with ESKD and highlight subsequent changes after kidney transplantation. The finding that MRI results were consistent with those obtained by the gold standard – bone histomorphometry – partially fulfils the premise of this proof-of-concept study. Notably, structural parameters obtained by MRI did not correlate with bone turnover, which remains a big gap in meeting the criteria of a “virtual bone biopsy” and is an objective to be pursued in future studies. Another significant outcome of this study is the identification of bone abnormalities which may not be detectable or explained by BMD measurements acquired by DXA, which is the current standard of care. This adds to the increasing literature advocating

for a broader approach towards assessment of ROD beyond BMD as a marker of bone health. Bone structure changes observed after transplantation in my studies differ from those in several other studies and likely represent the multifaceted effects of PTH. My assessment of changes in mineral metabolism, particularly persistent SHPT after transplantation in a large cohort of KTRs, did not demonstrate any clinical correlations, within the limitations of study design.

Limitations

The findings of the studies included in this thesis, though significant, need to be viewed in the context of several limitations. While limitations specific to each study are discussed in detail in their respective chapters, some common issues provide a wider perspective on the results. A small study cohort **(Chapters 2–4)**, without a non-CKD control group, limited our ability to apply regression analyses to determine the ability of a combination of imaging and biomarkers to predict TMV parameters. The small cohort of relatively young and healthy patients from a single centre may not be representative of the wider population with ESKD and restricts the generalisability of the results. Also, the small study size may not lend itself to robust statistical conclusions, and results need validation in larger studies. Another limitation of these studies is the lack of data demonstrating the trend of biochemical parameters reflective of CKD-MBD and its management in the months leading up to kidney transplantation. This would have provided a boarder perspective into the evolution of changes in bone structure after transplantation. The interpretation of results obtained by multiple novel imaging techniques used in these studies (micro-CT, MRI, TBS, pQCT) is difficult given the lack of normative data for these modalities in the CKD population. The studies described in **Chapters 5 and 6** each had a robust sample size but were limited by retrospective

design. Elimination of some missing data, particularly related to bone modulating medication use and associated clinical outcomes, would have added to the clinical significance of these studies. Overall, future larger multi-centre studies with prospective design are needed to validate these data and to determine their utility in guiding clinical decision-making and improving outcomes in the CKD population. For now, this thesis represents a small but useful step in the right direction.

Future directions

In 2017, the global prevalence of CKD was 9.1%, equating to roughly 700 million cases. CKD was associated with 4.6% of global deaths and was the 12th leading cause of death, an increase from 17th in 1990 [38, 39]. Between 1990 and 2017, there was also a significant rise in age-standardised incidence of ESKD and subsequent renal replacement therapy (dialysis or transplantation), a concerning increase when extrapolated to the potential increased burden of ROD and fractures. Over the last few years, during the timeline of this project, international studies have continued to report fracture risk associated with the spectrum of CKD and longer hospitalisation and high mortality associated with these episodes [40-42]. Meanwhile, there has been progress in the field of HR imaging. A metanalysis of 40 studies, including several involving the CKD population, demonstrated the predictive value for fracture of HRpQCT for obtaining bone structural parameters [43]. There also have been more studies in patients with CKD utilising various imaging techniques to study ROD [44-49] and more insights into the pathophysiology of CKD-MBD and ROD [50-53]. A more detailed description of these studies is beyond the scope of this section.

Renal bone disease and the associated consequence of fracture have been the proverbial elephant in the room for many decades, but over the last 15 years there has been increasing awareness of these issues amongst the nephrology community and calls to action from many experts [54-59]. The common thread has been a need for a paradigm shift in how the nephrology community should approach, manage and research renal bone disease, and this thesis adds to this view. We can start by developing algorithms to help utilise available diagnostic tools and therapeutic options based on currently available data. Some authors have already proposed approaches for management of bone disease and fracture risk, which may serve as a starting point [4, 57, 60]. Fracture screening tools, like FRAX, which are currently an important part of the management of fracture risk in the non-CKD population, can be used judiciously to determine fracture risk in patients with mild to moderate CKD [61]. Several other authors have reported adequate fracture discrimination results with FRAX in CKD, including dialysis patients, but there has been both an overestimation and underestimation of fracture risk in these studies, indicating a calibration issue [62-64]. Another newer modality to consider is the TBS, which has limitations in assessing bone microarchitecture, but is more easily accessible and has proven useful in the non-CKD population with encouraging data in CKD cohorts [65-67]. This can be potentially utilised in the clinical setting, pending more studies in the CKD population.

Despite advances to date, there remains a critical need for non-invasive means to assess bone quality in CKD to obviate the requirement for bone biopsy. Ideal non-invasive assessment of bone quality would constitute evaluation of bone microarchitecture, turnover and mineralisation by a single modality or a combination of modalities, which would provide similar information to bone histomorphometry. Overall, there is growing data establishing

credentials of high-resolution imaging in accurately defining bone structure, but these modalities are currently inadequate in determining bone turnover. Bone structure parameters, even if correlated with turnover indices obtained by histomorphometry, as shown in my study, cannot be used to determine turnover, which is a dynamic event. In 2018, Salam *et al.* [48] explored the utility of HRpQCT and circulating bone turnover markers in discriminating turnover and compared these to the gold standard bone turnover by tetracycline-labelled bone biopsies. Among the biomarkers, PTH and bALP provided the best discrimination for low and high turnover, with AUCs of 0.82 and 0.76 respectively. This is similar to the performance of PTH and bALP in large histomorphometry studies performed previously [68], and does not advance the quest for better markers for bone turnover [69].

High-resolution imaging modalities, at present, are confined to research settings and their transition to clinical setting is currently not on the horizon. HR-MRI, although performed on commercially performed scanners and potentially with un-customised hardware (as in my study), requires specialist expertise and equipment for processing which are limited to only a few institutions worldwide. Currently used HR imaging modalities are also limited to imaging peripheral sites due to technical limitations. More recent studies in MRI have, however, added to the feasibility of imaging of the femur, a site of high fracture incidence in CKD, and subjecting the scans to FEA to assess strength parameters [70-74]. This is an important development because, if translated into clinical practice, it would be a major breakthrough in the assessment of the vulnerability of the femur to fracture. Overall, more frequent and larger clinical trials with hard clinical endpoints are needed to enable formation of normative database, dissemination of expertise and to render these modalities more cost-effective and accessible. Patients with CKD have traditionally been excluded from large clinical trials of

fracture prevention or treatment in the general population. Future studies should target patients with various stages of CKD and should be designed in the context of the uniqueness of ROD. Studies are also needed to develop and trial accurate turnover markers to complement imaging studies.

Conclusion

This thesis is the culmination of several highly enjoyable years of clinical research, during which I developed greater insight into the area of ROD and its associated conditions. Clinical studies presented in this thesis contribute to the increasing body of literature about bone abnormalities prevalent in CKD and the potential utility of HR imaging techniques in assessing bone quality in CKD and in KTRs. This thesis also puts into perspective the many challenges we continue to face in managing ROD and ways forward in addressing them. Overall, I believe my research has shown that non-invasive HR imaging has the potential to fill, at least partially, the vast gap between screening of BMD using DXA and comprehensive diagnosis by bone biopsy. MRI, in conjunction with accurate and appropriate bone turnover markers, can potentially be used to screen for bone fragility, predict fracture, and help in developing therapeutic interventions and monitoring treatment effect in the CKD population and in KTRs. The utility of MRI (and other such imaging) would be enhanced by availability of more accurate and reliable non-invasive markers of bone turnover and mineralisation, validated against bone histology. These challenges are significant but not insurmountable. A coordinated, structured, multidisciplinary, patient-focused effort is needed from the nephrology research community to address the unmet needs of patients with ROD and CKD-MBD.

References

1. *KDIGO clinical practice guideline for the diagnosis, evaluation, prevention, and treatment of Chronic Kidney Disease-Mineral and Bone Disorder (CKD-MBD).* Kidney Int Suppl, 2009. **76**(113): p. S1-130.
2. Go, A.S., et al., *Chronic kidney disease and the risks of death, cardiovascular events, and hospitalization.* N Engl J Med, 2004. **351**(13): p. 1296-305.
3. Consortium, C.P., *Association of estimated glomerular filtration rate and albuminuria with all-cause and cardiovascular mortality in general population cohorts: a collaborative meta-analysis.* Lancet, 2010. **375**(9731): p. 2073-81.
4. Pimentel, A., et al., *Fractures in patients with CKD-diagnosis, treatment, and prevention: a review by members of the European Calcified Tissue Society and the European Renal Association of Nephrology Dialysis and Transplantation.* Kidney Int, 2017. **92**(6): p. 1343-1355.
5. Moe, S., et al., *Definition, evaluation, and classification of renal osteodystrophy: a position statement from Kidney Disease: Improving Global Outcomes (KDIGO).* Kidney Int, 2006. **69**(11): p. 1945-53.
6. Naylor, K.L., et al., *The three-year incidence of fracture in chronic kidney disease.* Kidney Int, 2014. **86**(4): p. 810-8.
7. Kim, S.M., et al., *Hip Fracture in Patients With Non-Dialysis-Requiring Chronic Kidney Disease.* J Bone Miner Res, 2016. **31**(10): p. 1803-1809.
8. Alem, A.M., et al., *Increased risk of hip fracture among patients with end-stage renal disease.* Kidney Int, 2000. **58**(1): p. 396-9.
9. Coco, M. and H. Rush, *Increased incidence of hip fractures in dialysis patients with low serum parathyroid hormone.* Am J Kidney Dis, 2000. **36**(6): p. 1115-21.
10. Hansen, D., et al., *Risk of fracture in adults on renal replacement therapy: a Danish national cohort study.* Nephrol Dial Transplant, 2016. **31**(10): p. 1654-62.
11. Tentori, F., et al., *High rates of death and hospitalization follow bone fracture among hemodialysis patients.* Kidney Int, 2014. **85**(1): p. 166-73.
12. Ball, A.M., *Risk of Hip Fracture Among Dialysis and Renal Transplant Recipients.* Jama, 2002. **288**(23): p. 3014-3018.
13. Nikkel, L.E., et al., *Risk of fractures after renal transplantation in the United States.* Transplantation, 2009. **87**(12): p. 1846-51.

14. Evenepoel, P., et al., *Natural history of parathyroid function and calcium metabolism after kidney transplantation: a single-centre study.* Nephrol Dial Transplant, 2004. **19**(5): p. 1281-7.
15. Naylor, K.L., et al., *Long-term changes in bone mineral density in kidney transplant recipients.* Transplantation, 2014. **98**(12): p. 1279-85.
16. Barber, H., *The bone deformities of renal dwarfism.* The Lancet, 1920. **195**(5027): p. 18-19.
17. Barber, H., *Renal dwarfism.* QJM: Quarterly Journal of Medicine, 1921(55): p. 205-213.
18. Brockman, E., *Some observations on the bone changes in renal rickets.* British Journal of Surgery, 1927. **14**(56): p. 634-645.
19. Malluche, H.H. and M.C. Monier-Faugere, *Renal osteodystrophy: what's in a name? Presentation of a clinically useful new model to interpret bone histologic findings.* Clin Nephrol, 2006. **65**(4): p. 235-42.
20. Ott, S.M., *Renal Osteodystrophy-Time for Common Nomenclature.* Curr Osteoporos Rep, 2017. **15**(3): p. 187-193.
21. Iyer, S.P., et al., *Kidney transplantation with early corticosteroid withdrawal: paradoxical effects at the central and peripheral skeleton.* J Am Soc Nephrol, 2014. **25**(6): p. 1331-41.
22. Nickolas, T.L., et al., *Rapid cortical bone loss in patients with chronic kidney disease.* J Bone Miner Res, 2013. **28**(8): p. 1811-20.
23. Nishiyama, K.K., et al., *Longitudinal HR-pQCT and image registration detects endocortical bone loss in kidney transplantation patients.* J Bone Miner Res, 2015. **30**(3): p. 554-61.
24. Rajapakse, C.S., et al., *Micro-MR imaging-based computational biomechanics demonstrates reduction in cortical and trabecular bone strength after renal transplantation.* Radiology, 2012. **262**(3): p. 912-20.
25. Wehrli, F.W., et al., *Quantitative high-resolution magnetic resonance imaging reveals structural implications of renal osteodystrophy on trabecular and cortical bone.* J Magn Reson Imaging, 2004. **20**(1): p. 83-9.
26. Majumdar, S., et al., *Trabecular bone architecture in the distal radius using magnetic resonance imaging in subjects with fractures of the proximal femur. Magnetic*

Resonance Science Center and Osteoporosis and Arthritis Research Group. Osteoporos Int, 1999. **10**(3): p. 231-9.

27. Wehrli, F.W., et al., *Digital topological analysis of in vivo magnetic resonance microimages of trabecular bone reveals structural implications of osteoporosis.* J Bone Miner Res, 2001. **16**(8): p. 1520-31.
28. Benito, M., et al., *Deterioration of trabecular architecture in hypogonadal men.* J Clin Endocrinol Metab, 2003. **88**(4): p. 1497-502.
29. Benito, M., et al., *Effect of testosterone replacement on trabecular architecture in hypogonadal men.* J Bone Miner Res, 2005. **20**(10): p. 1785-91.
30. Chesnut, C.H., 3rd, et al., *Effects of salmon calcitonin on trabecular microarchitecture as determined by magnetic resonance imaging: results from the QUEST study.* J Bone Miner Res, 2005. **20**(9): p. 1548-61.
31. Zhang, X.H., et al., *In Vivo μMRI-Based Finite Element and Morphological Analyses of Tibial Trabecular Bone in Eugonadal and Hypogonadal Men Before and After Testosterone Treatment.* Journal of Bone and Mineral Research, 2008. **23**(9): p. 1426-1434.
32. Folkesson, J., et al., *Longitudinal evaluation of the effects of alendronate on MRI bone microarchitecture in postmenopausal osteopenic women.* Bone, 2011. **48**(3): p. 611-21.
33. Al Mukaddam, M., et al., *Effects of testosterone and growth hormone on the structural and mechanical properties of bone by micro-MRI in the distal tibia of men with hypopituitarism.* J Clin Endocrinol Metab, 2014. **99**(4): p. 1236-44.
34. Malluche, H.H., H.W. Mawad, and M.C. Monier-Faugere, *Renal osteodystrophy in the first decade of the new millennium: analysis of 630 bone biopsies in black and white patients.* J Bone Miner Res, 2011. **26**(6): p. 1368-76.
35. Adragao, T., et al., *Femoral bone mineral density reflects histologically determined cortical bone volume in hemodialysis patients.* Osteoporosis Int 2010. **21**(4): p. 619-625.
36. Sharma, A.K., et al., *Emerging role of high-resolution imaging in the detection of renal osteodystrophy.* Nephrology (Carlton), 2016. **21**(10): p. 801-11.
37. Ott, S.M., et al., *The prevalence of bone aluminum deposition in renal osteodystrophy and its relation to the response to calcitriol therapy.* N Engl J Med, 1982. **307**(12): p. 709-13.

38. Bikbov, B., et al., *Global, regional, and national burden of chronic kidney disease, 1990–2017: a systematic analysis for the Global Burden of Disease Study 2017.* The Lancet, 2020. **395**(10225): p. 709-733.
39. Cockwell, P. and L.-A. Fisher, *The global burden of chronic kidney disease.* The Lancet, 2020. **395**(10225): p. 662-664.
40. Lin, R., et al., *Hospitalized fracture rates amongst patients with chronic kidney disease in Australia using data linkage.* Nephrology (Carlton), 2019. **n/a**(n/a).
41. Kim, S.H., et al., *Chronic Kidney Disease Increases the Risk of Hip Fracture: A Prospective Cohort Study in Korean Adults.* J Bone Miner Res, 2020. **n/a**(n/a).
42. Iseri, K., et al., *Major fractures after initiation of dialysis: Incidence, predictors and association with mortality.* Bone, 2020. **133**: p. 115242.
43. Mikolajewicz, N., et al., *HR-pQCT Measures of Bone Microarchitecture Predict Fracture: Systematic Review and Meta-Analysis.* J Bone Miner Res, 2020. **35**(3): p. 446-459.
44. Araujo, M.J., et al., *The pitfall of treating low bone turnover: Effects on cortical porosity.* Bone, 2016. **91**: p. 75-80.
45. Bonani, M., et al., *Effect of denosumab on trabecular bone score in de novo kidney transplant recipients.* Nephrol Dial Transplant, 2019. **34**(10): p. 1773-1780.
46. Chandran, M., et al., *Addressing bone quality and bone density after renal transplantation: A prospective evaluation of the evolution of trabecular bone score and bone mineral density over the first 5 years following renal transplantation in Asian patients.* Clin Transplant, 2019. **33**(10): p. e13671.
47. Marques, I.D., et al., *Biopsy vs. peripheral computed tomography to assess bone disease in CKD patients on dialysis: differences and similarities.* Osteoporos Int, 2017. **28**(5): p. 1675-1683.
48. Salam, S., et al., *Diagnostic Accuracy of Biomarkers and Imaging for Bone Turnover in Renal Osteodystrophy.* J Am Soc Nephrol, 2018. **29**(5): p. 1557-1565.
49. Aleksova, J., et al., *Patients with end-stage kidney disease have markedly abnormal cortical hip parameters by dual-energy X-ray absorptiometry.* Nephrol Dial Transplant, 2019.
50. Elias, R.M., et al., *CKD-MBD: from the Pathogenesis to the Identification and Development of Potential Novel Therapeutic Targets.* Curr Osteoporos Rep, 2018. **16**(6): p. 693-702.

51. Graciolli, F.G., et al., *The complexity of chronic kidney disease-mineral and bone disorder across stages of chronic kidney disease.* Kidney Int, 2017. **91**(6): p. 1436-1446.
52. Hruska, K.A., et al., *The chronic kidney disease - Mineral bone disorder (CKD-MBD): Advances in pathophysiology.* Bone, 2017. **100**: p. 80-86.
53. Araujo, M., et al., *Comparison of serum levels with bone content and gene expression indicate a contradictory effect of kidney transplantation on sclerostin.* Kidney Int, 2019. **96**(5): p. 1100-1104.
54. Nickolas, T.L., M.B. Leonard, and E. Shane, *Chronic kidney disease and bone fracture: a growing concern.* Kidney Int, 2008. **74**(6): p. 721-31.
55. Fusaro, M., M. Gallieni, and S.A. Jamal, *Fractures in chronic kidney disease: neglected, common, and associated with sickness and death.* Kidney Int, 2014. **85**(1): p. 20-22.
56. Moe, S.M. and T.L. Nickolas, *Fractures in Patients with CKD: Time for Action.* Clin J Am Soc Nephrol, 2016. **11**(11): p. 1929-1931.
57. Damasiewicz, M.J. and T.L. Nickolas, *Rethinking Bone Disease in Kidney Disease.* JBMR Plus, 2018. **2**(6): p. 309-322.
58. Denburg, M. and T.L. Nickolas, *Declining Hip Fracture Rates in Dialysis Patients: Is This Winning the War?* Am J Kidney Dis, 2018. **71**(2): p. 154-156.
59. Messa, P., *Skeletal fractures in patients on renal replacement therapy: how large still is the knowledge gap?* Nephrology Dialysis Transplantation, 2016. **31**(10): p. 1554-1556.
60. Khairallah, P. and T.L. Nickolas, *Management of Osteoporosis in CKD.* Clin J Am Soc Nephrol, 2018. **13**(6): p. 962-969.
61. Desbiens, L.C., et al., *Comparison of Fracture Prediction Tools in Individuals Without and With Early Chronic Kidney Disease: A Population-Based Analysis of CARTaGENE.* J Bone Miner Res, 2020. **n/a**(n/a).
62. Naylor, K.L., et al., *Comparison of fracture risk prediction among individuals with reduced and normal kidney function.* Clin J Am Soc Nephrol, 2015. **10**(4): p. 646-653.
63. Whitlock, R.H., et al., *The Fracture Risk Assessment Tool (FRAX(R)) predicts fracture risk in patients with chronic kidney disease.* Kidney Int, 2019. **95**(2): p. 447-454.
64. Przedlacki, J., et al., *The utility of FRAX(R) in predicting bone fractures in patients with chronic kidney disease on hemodialysis: a two-year prospective multicenter cohort study.* Osteoporos Int, 2018. **29**(5): p. 1105-1115.

65. Ramalho, J., et al., *The trabecular bone score: Relationships with trabecular and cortical microarchitecture measured by HR-pQCT and histomorphometry in patients with chronic kidney disease.* Bone, 2018. **116**: p. 215-220.
66. Naylor, K.L., et al., *Trabecular bone score in kidney transplant recipients.* Osteoporos Int, 2016. **27**(3): p. 1115-1121.
67. Luckman, M., et al., *Spine Trabecular Bone Score as an Indicator of Bone Microarchitecture at the Peripheral Skeleton in Kidney Transplant Recipients.* Clin J Am Soc Nephrol, 2017. **12**(4): p. 644-652.
68. Sprague, S.M., et al., *Diagnostic Accuracy of Bone Turnover Markers and Bone Histology in Patients With CKD Treated by Dialysis.* Am J Kidney Dis, 2016. **67**(4): p. 559-66.
69. Nickolas, T.L., *The Quest for Better Biomarkers of Bone Turnover in CKD.* J Am Soc Nephrol, 2018. **29**(5): p. 1353-1355.
70. Chang, G., et al., *Feasibility of three-dimensional MRI of proximal femur microarchitecture at 3 tesla using 26 receive elements without and with parallel imaging.* J Magn Reson Imaging, 2014. **40**(1): p. 229-38.
71. Chang, G., et al., *3-T MR Imaging of Proximal Femur Microarchitecture in Subjects with and without Fragility Fracture and Nonosteoporotic Proximal Femur Bone Mineral Density.* Radiology, 2018. **287**(2): p. 608-619.
72. Hotca, A., et al., *In vivo measurement reproducibility of femoral neck microarchitectural parameters derived from 3T MR images.* J Magn Reson Imaging, 2015. **42**(5): p. 1339-45.
73. Rajapakse, C.S., et al., *MRI-based assessment of proximal femur strength compared to mechanical testing.* Bone, 2020. **133**: p. 115227.
74. Rajapakse, C.S., et al., *Patient-specific Hip Fracture Strength Assessment with Microstructural MR Imaging-based Finite Element Modeling.* Radiology, 2017. **283**(3): p. 854-861.

APPENDIX: Publications included in this thesis

AK Sharma, R Masterson, SG Holt, ND Toussaint. Emerging role of high-resolution imaging in the detection of renal osteodystrophy. *Nephrology* 2016; **21**(10): 801-11.

AK Sharma and ND Toussaint. Is there a practical role for a virtual bone biopsy using high-resolution imaging of bone in patients with chronic kidney disease? *Nephrology* 2017; **22**: 27-30. 1

AK Sharma, ND Toussaint, R Masterson, SG Holt, CS Rajapakse, PR Ebeling, ST Mohanty, P Baldock and GJ Elder. Deterioration of cortical bone microarchitecture: critical component of renal osteodystrophy evaluation. *American Journal of Nephrology*, 2018; **47**(6): 376-384.

AK Sharma, ND Toussaint, GJ Elder, R Masterson, SG Holt, PL Robertson, PR Ebeling, P Baldock, RC Miller and CS Rajapakse. Magnetic resonance imaging based assessment of bone microstructure as a non-invasive alternative to histomorphometry in patients with chronic kidney disease. *Bone* 2018; **114**: 14-21.

AK Sharma, ND Toussaint, GJ Elder, CS Rajapakse, SG Holt, P Baldock, PL Robertson, PR Ebeling, OR Sorci and R Masterson. Changes in bone

microarchitecture following kidney transplantation – beyond bone mineral density. *Clinical Transplantation* 2018; **32**(9): e13347.

AK Sharma, R Masterson, SG Holt, SJ Tan, PD Hughes, M Chu, P Jayadeva and ND Toussaint. Impact of cinacalcet pre-transplantation on mineral metabolism in renal transplant recipients. *Nephrology*. 2016; **21**(1):46-54.

AK Sharma, ND Toussaint, J Pickering, T Beeston, ER Smith and SG Holt. Assessing the utility of testing aluminum levels in dialysis patients. *Hemodialysis International*. 2015; **19**(2):256-62.

NEPHROLOGY

Nephrology **21** (2016) 801–811

Review Article

Emerging role of high-resolution imaging in the detection of renal osteodystrophy

ASHISH K SHARMA,[1,2] ROSEMARY MASTERSON,[1,2] STEPHEN G HOLT[1,2] and NIGEL D TOUSSAINT[1,2]

[1]Department of Nephrology, The Royal Melbourne Hospital, Parkville, Victoria, Australia, and [2]Department of Medicine (RMH), The University of Melbourne, Melbourne, Victoria, Australia

KEY WORDS:
bone mineral density, chronic kidney disease – mineral and bone disorder (CKD-MBD), fracture, high-resolution magnetic resonance imaging, peripheral quantitative computed tomography, renal osteodystrophy.

Correspondence:
Nigel Toussaint, Department of Nephrology, The Royal Melbourne Hospital, Grattan Street, Parkville, Vic. 3052, Australia. Email: Nigel.Toussaint@mh.org.au

Accepted for publication 25 March 2016.
Accepted manuscript online 4 April 2016.

doi: 10.1111/nep.12790

ABSTRACT:

The term renal osteodystrophy refers to changes in bone morphology induced by chronic kidney disease (CKD) and represents the skeletal component of the entity 'chronic kidney disease – mineral and bone disorder'. Changes in turnover, mineralization, mass and microarchitecture impair bone quality, compromising strength and increasing susceptibility to fractures. Fractures are more common in CKD compared with the general population and result in increased morbidity and mortality. Screening for fracture risk and management of renal osteodystrophy are hindered by the complex, and still only partially understood, pathophysiology and the inadequacy of currently available diagnostic methods. Bone densitometry and bone turnover markers, although potentially helpful, have significant limitations in patients with CKD, and the 'gold standard' test of bone biopsy is infrequently performed in routine clinical practice. However, recent advances in high-resolution bone microarchitecture imaging may offer greater potential for quantification and assessment of bone structure and strength and, when used in conjunction with serum biomarkers, may allow non-invasive testing for a diagnostic virtual bone biopsy.

SUMMARY AT A GLANCE

This is a review of the dilemmas and pitfalls of investigative modalities in their prediction of bone morphology in renal osteodystrophy and fracture risk in patients and an update on the emerging role of high resolution imagining in patients with chronic kidney disease.

INTRODUCTION

Renal osteodystrophy (ROD) is a disorder of bone due to metabolic and hormonal abnormalities resulting in high fracture risk across the spectrum of chronic kidney disease (CKD) and associated with hospitalization, excess morbidity and mortality.[1–3] Even after kidney transplantation, patients have increased fracture risk, although the aetiology and pathophysiology of bone disease differs.[4,5] Accurate identification of bone pathology is difficult owing to lack of homogenous bone changes combined with the reduced ability of routine tests (e.g. dual-energy X-ray absorptiometry (DXA)) to predict fracture risk and the poor reliability of serum biomarkers. Thus, bone biopsy is currently the only dependable method of defining the bone abnormalities present in patients with CKD; however, limitations of bone biopsies for ROD restrict their use in guiding treatment and are often unhelpful or impractical for monitoring response to therapy.

More recently, studies in both the general and CKD populations have used novel, non-invasive, high-resolution (HR) imaging techniques to elucidate bone microarchitecture and estimate bone strength. HR imaging may have the potential to more accurately predict bone changes and fracture risk without the need for bone biopsy, with the potential to better shape and monitor novel treatment strategies. We review these new imaging modalities, including HR peripheral quantitative computed tomography (HR-pQCT) and HR magnetic resonance imaging (HR-MRI, or micro-MRI), in the diagnosis and risk stratification in ROD.

RENAL OSTEODYSTROPHY AND FRACTURE RISK

Kidney Disease: Improving Global Outcomes (KDIGO) state that the term chronic kidney disease – mineral and bone

disorder (CKD-MBD) should be used to describe a clinical entity involving the disruption of mineral and bone metabolism in patients with CKD. This terminology encompasses a constellation of biochemical abnormalities, bone disturbances and extra-skeletal calcification in soft tissue and arteries.[6] ROD refers to alteration of bone morphology, forming the skeletal component of CKD-MBD, and is quantifiable by histomorphometric parameters of turnover, mineralization and volume (TMV).[7] The TMV classification determined from bone biopsy provides a clinically relevant and standardized description of bone pathology, which can help define the pathophysiology, although the traditional classification of ROD, based on the degree of bone turnover (adynamic bone disease, osteitis fibrosa or mixed osteodystrophy) and mineralization (osteomalacia), is still commonly used in clinical practice.[8]

Progressive deterioration in kidney function is accompanied by characteristic metabolic and hormonal abnormalities including reduced renal synthesis of 1,25-dihydroxyvitamin D (1,25(OH)2D), elevated fibroblast growth factor-23 (FGF23), hyperphosphataemia, hypocalcaemia, increased parathyroid hormone (PTH) and chronic metabolic acidosis. These abnormalities adversely affect bone remodelling resulting in alterations of turnover and mineralization and changes in microarchitecture of the bone akin to normal ageing.[9,10] Loss of bone mass, cortical thinning, increased cortical porosity, trabecular thinning, perforation and disintegration are some of the microstructural consequences of impaired remodelling. ROD adversely affects bone quantity and quality at all hierarchical levels of bone structure. Bone strength, a composite of bone quantity and quality,[11] is compromised in patients with CKD, increasing the susceptibility to fragility fractures.

The risk of fractures is reported to be 4–14 times higher in dialysis patients compared with individuals without kidney disease, and fracture incidence is similar to individuals 10–15 years older in the general population.[12–14] This excess risk also extends to earlier stages of CKD where estimated glomerular filtration rate (eGFR) of 15–60 ml/min per 1.73 m^2 confers a 1.5–3 times greater risk of fracture compared with that of the non-CKD population.[15–17] The increased susceptibility to fractures in the CKD population is not, at least initially, attenuated by kidney transplantation, with the relative risk of hip fracture in renal transplant recipients up to 1.34-fold greater compared with that of patients on dialysis over the first 2 years after transplantation.[4] Several studies have recently explored contemporary fracture epidemiology and highlighted the persistence of this risk in the CKD population.[1–3,18–20] Mortality from fractures in patients with CKD also remains significantly high, despite competing risk analysis taking excess mortality in CKD into account and adjusting for other likely confounders.[21] The potential for improvement and development of novel screening tools for assessment of fracture risk in patients with CKD assumes considerable importance given the global burden of CKD and increasing incidence and prevalence of end-stage kidney disease.[22,23]

DIAGNOSTIC TOOLS FOR RENAL OSTEODYSTROPHY IN CLINICAL PRACTICE

Measurement of bone mineral density (BMD) with DXA, or using serum markers like PTH, alkaline phosphatase (ALP) and bone-specific ALP (bALP) to determine bone turnover, are current diagnostic aids for the determination of ROD in clinical practice, with bone biopsy infrequently used in most parts of the world.

Dual-energy X-ray absorptiometry

Bone mineral density measured by DXA is calculated by averaging X-ray absorption over a two-dimensional area and therefore represents areal BMD (aBMD, in grams per square centimetre), compared with volumetric BMD (vBMD, grams per cubic centimetre), and thus may not be an accurate measurement of true BMD (which is mass/volume). However, DXA is the most widely used, inexpensive, non-invasive screening technique for evaluating bone mass with low radiation exposure. In patients without kidney disease, a low aBMD measurement by DXA is a predictor of fracture risk[24] and a useful guide to the efficacy of anti-resorptive treatments in conditions of low BMD such as osteoporosis. However, fracture risk assessment using DXA in the CKD population remains controversial. The KDIGO CKD-MBD international clinical guidelines,[6] published in 2009, recommended the use of DXA to assess fracture risk in patients with CKD stages 1–3 but not in CKD stages 4–5 given the lack of definitive data demonstrating predictive validity in the latter group. More recent prospective studies have reported that low DXA-measured BMD was predictive of future fracture risk in patients with CKD stages 3–5 and on dialysis,[25–27] although the pharmacological or other response to such a finding in this group is unclear. KDIGO have recommended reassessment of the 2009 guideline statements regarding DXA and CKD at a CKD-MBD Controversies Conference in 2013,[28] and a guideline revision is currently in progress. DXA has technical limitations when used in the CKD cohort as aBMD measurement is unable to distinguish individual trabecular or cortical BMD. This is a significant potential confounder in ROD given the differential effects of secondary hyperparathyroidism with greater bone resorption resulting in cortical thinning.[10] Additionally, although BMD is an estimate of bone mass or 'quantity', it provides no information regarding bone quality or turnover, and measurements may be skewed by degenerative bone changes in the spine and extra-skeletal calcification, especially in the aorta, which can contribute to the density score.

Bone turnover markers

Parathyroid hormone, as a hormone influencing bone, and total ALP or bALP are biomarkers commonly used in clinical practice as surrogate markers of bone turnover despite assay limitations and inconsistent results when assessing risk stratification.

Osteocalcin and procollagen type 1 N-terminal propeptide are other markers of osteoblast function and bone formation. Bone resorption markers include tartrate-resistant acid phosphatase 5b and C-terminal telopeptide of type I collagen (CTX) for monitoring osteoclast number and function respectively. However, these serum markers are not widely used clinically because of analytical and biological variability, and in patients with CKD, variable renal clearances and undefined reference ranges (e.g. osteocalcin, CTX and procollagen type 1 N-terminal propeptide) make these markers difficult to interpret.

Both very low and very high PTH levels predict bone turnover consistent with bone histomorphometry[29]; however, the predictive value between these extremes is poor. The relationship between PTH levels and fracture is also inconsistent in observational studies.[13,14,30] Additionally, racial differences influence the predictive ability of PTH to define bone turnover status using the TMV classification.[31] There is also significant biologic variation of PTH in patients with CKD with one study reporting a high intra-individual coefficient of variance (CV) for PTH of 25.6% (i.e. requiring measurement of 26 specimens to estimate intact PTH of an individual undergoing dialysis), which undermines the value of PTH as a reliable biomarker in ROD.[32]

More recent cross-sectional and prospective imaging studies in CKD and kidney transplant patients have noted strong associations between levels of certain bone turnover markers and changes in bone mass and architecture, which are potentially useful in determining prevalent fractures, predicting bone loss and fracture risk.[25,33–37] In a prospective study involving 485 HD patients, Iimori *et al.*[25] reported a higher fracture risk with higher bALP, and both low and high PTH levels, as well as low hip BMD. In another study including 143 consecutive kidney transplant recipients, PTH levels >130 pg/ml at 3 months after transplantation were an independent predictor of new fractures in the 5 years post-transplantation.[38] In contrast, other imaging studies have shown inconsistent, absent or only weak correlation between biomarkers and bone microarchitecture.[39–41]

Novel circulating biomarkers of bone function include FGF23 and the Wnt inhibitors (sclerostin and dickkopf-1). In a recent prospective trial of HD patients, baseline levels of FGF23 predicted changes in aBMD at the spine, and baseline tartrate-resistant acid phosphatase 5b, with sclerostin predicting loss of total vBMD at the hip as measured by QCT.[37] In a cross-sectional study that evaluated bone histomorphometry in 60 dialysis patients, low sclerostin levels were found to predict high bone turnover better than PTH in adjusted analyses.[42] Low PTH levels, however, were more predictive of low bone turnover. Serum levels of dickkopf-1 did not correlate with PTH or any histomorphometric parameter.

Bone biopsy

Bone biopsy is typically performed at the iliac crest after double tetracycline labelling to allow assessment of bone formation rate over time.[43,44] The procedure is invasive; requires expertise to perform, process and interpret; and is rarely performed in most clinical nephrological practice. Moreover, histomorphometry only depicts bone microstructure at that single point in time and place, and biopsies performed at one site may not reflect concurrent changes in another. Despite these limitations, bone biopsy provides the best 'snapshot' of bone microarchitecture, turnover and mineralization and continues to be the gold standard for the diagnosis of ROD. However, use of bone biopsy for monitoring response to treatment of ROD is limited because of its invasive nature.

HIGH-RESOLUTION IMAGING

High-resolution imaging techniques enable imaging of the bone at the micro-level. Bone trabeculae measure 50–200 μm in thickness; therefore, any imaging system applied to *in vivo* non-invasive micro-imaging of bone structure requires a high enough spatial resolution in this range. Currently used *in vivo* HR imaging modalities, HR-pQCT and HR-MRI, measure and quantify cortical and trabecular geometry, microarchitecture and strength.[45–47] The structural parameters are similar to those obtained using classical histomorphometry, for example, trabecular measurements like bone fraction, thickness, separation and number. In addition, topological analysis of trabeculae (rod and plates) can be performed, and cortical measures like thickness and porosity can also be estimated. HR-pQCT also provides an accurate estimate of vBMD (Table 1).

Morphometric analysis performed by HR imaging techniques has been validated with measurement by micro-CT in *ex vivo* and *in vivo* studies,[48–51] and HR imaging has been referred to as a 'virtual bone biopsy'[52,53] by some authors. Finite element analysis (FEA), a computer-based simulation of stresses and forces induced by the mechanical loading of a structure, can be applied to three-dimensional HR-pQCT or HR-MRI data to measure strength of whole bone or various compartments. The apparent biomechanical properties of a complex structure like bone (stiffness and elastic modulus) may be computed by analysing small cubic elements (voxels) with each voxel corresponding to a hexahedral finite element of the bone structure. Micro-FEA (μFEA) may be a valuable tool that may provide additional discriminatory power to predict fracture, independent of bone structural measures by HR imaging and aBMD.[54]

Quantitative computed tomography and high-resolution peripheral quantitative computed tomography

Quantitative computed tomography has a resolution of approximately 300 μm and can be applied to central skeletal sites (hip and spine) on whole-body CT scanners and peripheral sites (e.g. radius or tibia) using dedicated smaller scanners manufactured for this purpose. The effective radiation doses differ and are in the range of 1.5–3 and <0.003 mSv respectively for imaging at central and peripheral sites[55] (Table 2).

Table 1 Comparison of HR-MRI and HR-pQCT

	HR-MRI	HR-pQCT
Imaging sites	Distal tibia, radius,† femur[76,77]	Distal tibia, radius
Spatial resolution	$137 \times 137 \times 410\ \mu m^3$ anisotropic	$82\ \mu m^3$ isotropic
Scan time	~12 min	~3 min
Radiation	No	$<4\ \mu Sv$
Measures	Microarchitecture	vBMD, microarchitecture
Reproducibility (% root mean square CV)	3–8%[45,75]	<1% for vBMD, 0.9–5% for morphometric parameters[46,64,65]
Validation	μCT[49–51]	μCT[48,50]
Evidence for clinical applications	• Microstructural changes in osteoporosis,[82] hypogonadism[83] • Fracture discrimination[81]• Longitudinal monitoring of treatment effect[74,84–87] • Transplant bone disease[88,89] • CKD and kidney transplant (Table 4) • No prospective studies for predicting fracture risk yet	• Age-, gender-, development- and ethnicity-related microstructural changes, osteoporosis, with treatment interventions, fracture discrimination have been studied in non-CKD cohorts[46,47] • CKD and kidney transplant including evaluating prediction for fracture risk (Tables 2 and 3)
μFEA applications	• Converts voxel to finite element model • Mechanical competence and strength • Monitoring longitudinal changes with treatment • Fracture discrimination	• Converts voxel to finite element model • Mechanical competence and strength • Fracture discrimination
Advantages	• Performed on widely available clinical MRI scanners • No ionizing radiation • Potential to asses femur microarchitecture† – most common site of fractures	• Automated protocol once periosteal contouring defined by the operator • Assess all parameters of bone architecture including vBMD and cortical porosity •Low radiation
Limitations	• Customized radio-frequency sequences and peripheral hardware • Sophisticated and complicated post-processing techniques • Lack of standardized reference data and heterogeneity of processing techniques • Specialized techniques to measure cortical porosity • Very few studies in CKD and lack of robust validation against histomorphometry	• Dedicated scanner – not available in clinical settings • Scans limited to peripheral sites by bore size and potential radiation exposure • Problems with segmentation and image registration techniques • Lack of standardized reference data • Few but increasing number of studies in CKD and lack of robust validation against histomorphometry

†Feasibility studies only. μCT, micro-computed tomography – a 'gold' standard *ex vivo* imaging method with a resolution of ~10 μm; μFEA, micro-finite element analysis; CKD, chronic kidney disease; CV, coefficient of variance; HR-MRI, high-resolution magnetic resonance imaging; HR-pQCT, HR peripheral quantitative computed tomography; vBMD, volumetric bone mineral density.

Table 2 Comparison of effective radiation exposure[91,92]

Imaging technique/radiation exposure	Effective dose (μSv)
DXA	5–15
QCT 2D spine (2 vertebrae – scout)	60–300
QCT 3D spine	1500
pQCT	5–10
HR-pQCT	<5
CXR	20
Abdominal CT	8000
Background exposure (per year)	1500–2400
Public exposure limits (per year)	1000

CT, computed tomography; CXR, chest X-ray; DXA, dual-energy X-ray absorptiometry; HR-pQCT, high-resolution peripheral quantitative CT; Sv, sieverts.

QCT can discriminate cortical and trabecular compartments providing separate measurements of total and compartmental vBMD and cortical thickness and area. This is of particular relevance in CKD where the aBMD measurements by DXA can potentially be confounded by the opposing affects of hyperparathyroidism on cortical and trabecular compartments. Central QCT studies have demonstrated strong association between spinal cortical vBMD and prevalent fractures[56] and outperformed DXA in identifying bone loss at the hip.[37] pQCT, on the other hand, has lower radiation exposure and has been used in several studies in the CKD population. Most of these studies have been cross-sectional and highlight the predominant loss of cortical vBMD and cortical thickness in patients on HD,[57–59] peritoneal dialysis[60] and with kidney transplants.[61] Two prospective studies, involving pre-dialysis[62] and HD[63] patients, reported yearly loss in cortical vBMD up to 2 years with pre-dialysis patients also showing decreased trabecular vBMD. In a cross-sectional study of 52 HD patients, Jamal *et al.*[59] reported an association between fracture and decreased radial cortical parameters of vBMD, thickness and area determined by pQCT. Fractures were not associated with trabecular vBMD and DXA measurements at central sites in this study. Despite the advantages of pQCT however, HR-pQCT, with its higher resolution and increased versatility, has become the preferred tool to quantify bone microarchitecture in research studies over the last decade.

High-resolution pQCT uses a dedicated extremity scanner to measure total, cortical or trabecular vBMD and bone structure parameters from the distal radius or distal tibia, using the endplate as the reference. The region of interest spans 9 mm of tissue, giving a special resolution ~80 μm with a 3 min scan time and radiation exposure of ≤5 μSv (Table 2). Image analysis and post-processing are carried out using a standard protocol built into the system and include semiautomatic contouring of the periosteal perimeter and automated segmentation into cortical and trabecular compartments by a 'thresholding' technique with subsequent morphometric and densitometric analysis. A hydroxyapatite calibration phantom provided is used to independently determine compartment-specific vBMD by converting attenuation values of tomographic images to hydroxyapatite mineral densities.[46] HR-pQCT is an accurate method for bone image acquisition and analysis with high reproducibly[46,64,65] for measuring vBMD (CV <1%) and morphometric parameters (CV 5%), but motion artefacts are frequent and the technique has limitations in delineating the transitional or cortico-trabecular zone of the bone which may lead to erroneous measurements. Other potential problems associated with this method include difficulties in growing children or when comparing individuals of different races, ages or genders.[47] Currently, HR-pQCT scans are not readily accessible, being used as research tools in a small number of centres, and are also limited to peripheral sites, although second-generation scanners potentially allow for *in vivo* measurements of the knee.

High-resolution peripheral quantitative computed tomography in chronic kidney disease

A number of cross-sectional studies in CKD patients have underlined the efficacy of HR-pQCT in detection of disrupted cortical and trabecular microarchitecture[34,35,40,41,66–68] and discrimination of fracture status[35,39,67,68] by demonstrating lower cortical and trabecular vBMD, thinner cortices and abnormal trabecular microarchitecture of the distal radius and tibia (Table 3). Such studies have also provided evidence of an association between hyperparathyroidism and increased levels of bone turnover markers with abnormal bone microarchitecture and fracture.[34,35] Some studies have highlighted an association between bone microstructure parameters derived with HR-pQCT and vascular calcification in dialysis patients.[69,70] A few studies have demonstrated the ability of DXA to discriminate and predict fracture risk as equivalent to HR-pQCT,[35,67,71] while others have reported limitations. Jamal *et al.*[67] compared the ability for fracture discrimination of HR-pQCT with DXA in 211 participants with stage 3–5 CKD, 74 of whom had prevalent fractures. HR-pQCT did not improve upon BMD measured by DXA at the ultradistal radius (area under the curve = 0.80) to discriminate between patients with and without fractures. After a 2-year follow-up of this cohort, aBMD by DXA at the ultradistal radius emerged as the strongest predictor of incident fractures (area under the curve = 0.74, 95% CI 0.65–0.83), with HR-pQCT parameters exhibiting similar prognostic ability.[71]

There has been a relative paucity of studies evaluating longitudinal assessment of bone microarchitecture by HR-pQCT in patients with CKD and in renal transplant recipients[33,36,71,72] (Table 4). In one longitudinal study involving 53 patients with CKD stages 2 to 5D (9 on HD), Nickolas *et al.*[36] reported deterioration in the cortical microarchitecture after a median follow-up of 1.5 years. There was reduced cortical area (−2.9%), density (−1.3%), thickness (−2.8%) and significant increases in cortical porosity (+4.2%) complemented by a decline in DXA-derived aBMD at the ultradistal radius and total hip but no significant change at the femoral neck or spine. Elevated PTH and bone turnover markers predicted cortical changes. Iyer *et al.*[33] measured BMD by DXA and bone microarchitecture by HR-pQCT at baseline, and 3, 6, and 12 months in 47 renal transplant recipients on early corticosteroid withdrawal immunosuppressive protocol and demonstrated significant

Table 3 Cross-sectional studies involving use of HR-pQCT in CKD

Author	Year	Sample size *n* (controls)	CKD stage	Site of imaging	Results
Bacchetta *et al.*[66]	2010	70†	2–4	Radius, tibia	• Decreased total and Tb vBMD and impaired trabecular microarchitecture • Decreased CtTh in men • Parameters similar to or better than those of osteopenic controls • Patients with fractures ($n = 13$) had decreased total vBMD, TbN and CtTh status
Nickolas *et al.*[68]	2010	91	Pre-dialysis	Radius, tibia	• Lower aBMD, vBMD decreased CtTh and trabecular losses modestly discriminated for fracture status • Longer duration of CKD in patients with fracture associated with AUC > 0.75 for aBMD by DXA at hip and ultradistal radius and decreased vBMD and cortical microarchitecture by HR-pQCT
Nickolas *et al.*[35]	2011	82	3–5	Radius, tibia	• Highest tertile of P1NP and TRAP5b independently associated with prevalent fracture • Femoral neck *T*-score of −2.0 BMD by DXA combined with highest tertile of P1NP and TRAP5b provided best discrimination of fracture prevalence • HR-pQCT strongly associated with fractures with strongest performance by tibial CtTh (AUC = 0.78)
Cejka *et al.*[39]	2011	74 (40)	5D	Radius, tibia	• Non-statistically significant differences in aBMD between dialysis patients with and without fracture • All HR-pQCT parameters at the tibia (except TbTh), but only TbN and trabecular heterogeneity at the radius were significantly different between those with and without fracture • ALP and PTH only weakly correlated with some HR-pQCT indices
Cejka *et al.*[93]	2012	76 (45)	5D	Radius, tibia	• $n = 37$ for HR-pQCT and DXA • Sclerostin levels were 3 times higher in dialysis patients • Modest positive correlation of sclerostin with aBMD by DXA and mainly trabecular parameters by HR-pQCT • Bone measures were not related to dickkopf-1
Negri *et al.*[34]	2012	50 (50)	5D	Radius, tibia	• Lower aBMD in HD patients compared with controls • All HR-pQCT parameters at the radius and tibia (except TbTh) were significantly different between dialysis group and healthy controls. Cortical parameters affected more than trabecular • Differences more marked in women compared with men • PTH and ALP had modest correlation with cortical parameters only in women
Jamal *et al.*[67]	2012	211	3–5	Radius	• Decreased BMD at ultradistal radius by DXA (OR 1.56, 95% CI 1.41–1.71) and cortical area by HR-pQCT (OR 1.24, 95% CI 1.2–1.36) associated with fracture risk • Best fracture discrimination measure was aBMD by DXA at ultradistal radius (AUC = 0.80) • HR-pQCT measures had strong fracture discrimination ability but did not improve overall performance when added to aBMD by DXA
Pelletier *et al.*[40]	2012	79 (79)	5D (56 HD + 23 PD)	Radius, tibia	• Hip aBMD by DXA was lower compared with controls with no difference in lumbar spine aBMD • HD patients had both Ct and Tb bone impairment and decreased total vBMD compared with controls at the tibia with less marked differences at the radius • PD patients had similar trend (not statistically significant except for CtTh at distal tibia) • bALP showed weak negative correlation ($r = -0.28$) with CtTh, but PTH did not correlate with DXA or HR-pQCT
Trombetti *et al.*[41]	2012	33 (33)	5D	Radius, tibia	• Hip and spine aBMD lower in women on dialysis compared with controls (but not men) • Women had higher radial CtPo and more disturbances of trabecular microarchitecture compared with controls. Men had lower cortical vBMD • Stiffness and predicted failure load by FEA were lower in women but not in men with ESKD
Cejka *et al.*[69]	2014	66	5D	Tibia	• Total tibial vBMD and bone volume/total volume (BV/TV) were lower in patients with CAC scores > 100
Pelletier *et al.*[70]	2015	53	5D	Tibia	CtTh and elevated sclerostin level associated with severe abdominal aortic calcification

†Controls drawn from population-based epidemiological cohorts. aBMD, areal bone mineral density; AUC, area under the curve; ALP, total alkaline phosphate; bALP, bone-specific alkaline phosphatase; BV/TV, bone volume/total volume; CAC, coronary artery calcification; CKD, chronic kidney disease; CtPo, cortical porosity; CtTh, cortical thickness; DXA, dual-energy X-ray absorptiometry; ESKD, end-stage kidney disease; FEA, finite element analysis; HD, haemodialysis; HR-pQCT, high-resolution peripheral quantitative computed tomography; P1NP, procollagen type 1 N-terminal propeptide; PD, peritoneal dialysis; PTH, parathyroid hormone; TbN, Tb number; TRAP, tartrate-resistant acid phosphatase 5b; vBMD, volumetric bone mineral density.

Table 4 Longitudinal studies involving use of HR-pQCT in CKD

Author	Year	Duration (months)	Sample size, *n*	CKD stage	Site of imaging	Results
Nickolas *et al.*[36]	2013	18	53	2–5D	Radius, tibia	• aBMD by DXA decreased at ultradistal radius and total hip • Decreased cortical area, vBMD, and CtTh and increased CtPo by HR-pQCT at the radius • Higher PTH and BTM levels predicted cortical deterioration by HR-pQCT
Iyer *et al.*[33]	2014	12	47	KT	Radius, tibia	• aBMD by DXA decreased at ultradistal radius but no change at hip and spine • Decreased cortical and trabecular vBMD • Deterioration of cortical architecture at distal radius and tibia • Cortical bone loss directly related with higher PTH levels • Decreased whole bone stiffness and failure load at the radius by FEA
Nishiyama *et al.*[72]	2015	12	31	KT	Radius, tibia	• 3 image registration methods to best define cortical ROI to asses endocortical bone loss • CtPo increased 63.4% at radius by baseline indexed ROI
West *et al.*[71]	2015	24	131	3–5	Radius	• aBMD by DXA; AUC† = 0.74 at ultradistal radius biggest predictor of incident fracture • HR-pQCT; AUC† = 0.70–0.72 for cortical parameters and AUC† = 0.59–0.65 for trabecular parameters to predict incident fractures

†Fully adjusted model. aBMD, areal bone mineral density; AUC, area under the curve; BTM, bone turnover markers; CKD, chronic kidney disease; CtPo, cortical porosity; CtTh, cortical thickness; DXA, dual-energy X-ray absorptiometry; FEA, finite element analysis; HR-pQCT, high-resolution peripheral quantitative computed tomography; KT, kidney transplant; PTH, parathyroid hormone; ROI, region of interest; vBMD, volumetric bone mineral density.

decline in cortical area, thickness, total density and trabecular density and increases in trabecular area over the first post-transplant year. Cortical decreases related directly to PTH levels, whereas the relationship between PTH and trabecular bone decrease was bimodal. Moreover, these changes were linked to significant reductions in estimated bone strength. Nishiyama *et al.*[72] explored the changes in cortical porosity following renal transplantation in 31 recipients over 1 year using three different fully automated methods to best detect endocortical bone loss. The 'baseline-index' method, in which exactly the same region was sequentially analysed, showed an increase in porosity, and these changes had the strongest relationship with changes in PTH and bone turnover markers. There was a significant deterioration in cortical and trabecular parameters and vBMD with a reduction in bone strength using FEA.

High-resolution magnetic resonance imaging

High-resolution MRI is an evolving, non-ionizing method for quantification of bone microarchitecture *in vivo* analogous to HR-pQCT. MRI uses the energy released by relaxation of the magnetic spin of the hydrogen atoms (in water) in the tissues induced by strong magnetic fields and radio-frequency energy for image generation. In conventional T2 weighted MRI, cortical bone appears dark (low signal) owing to its relatively low water content compared with the bone marrow and surrounding soft tissues. HR-MRI is performed using clinical scanners and customized pulse sequences, coils and post-processing software, achieving a spatial resolution of 150–300 μm. This involves a complex cascade of steps (Fig. 1) generally including customized radio-frequency sequences, region of interest selection, image acquisition, correction of motion artefacts and image processing, which includes bone/marrow segmentation and structural analysis yielding measurements corresponding to parameters studied by bone histomorphometry.[45,46] Like HR-pQCT, the three-dimensional MRI data can also be subjected to μFEA to estimate mechanical competence of the bone and its interrelationship with structural measurements.[73,74] In contrast to HR-pQCT, HR-MRI can be performed on routine MRI scanners, with the appropriate software, and therefore may potentially have greater accessibility for future clinical use. Most of the studies in MRI have reproducible results,[75] albeit with significant heterogeneity in the techniques used.

High-resolution MRI of bone architecture has proven to be technically challenging to optimize and standardize despite the wide availability of MRI scanners in clinical practice. Marrow heterogeneity, propensity for off-resonance effects to generate artefacts, achievable signal to noise ratio and limited spatial resolution, which depend upon sophisticated post-processing techniques, have limited the use of HR-MRI largely to peripheral sites (distal radius, distal tibia and calcaneus). These issues have been addressed by researchers developing innovative image acquisition, processing and analysis

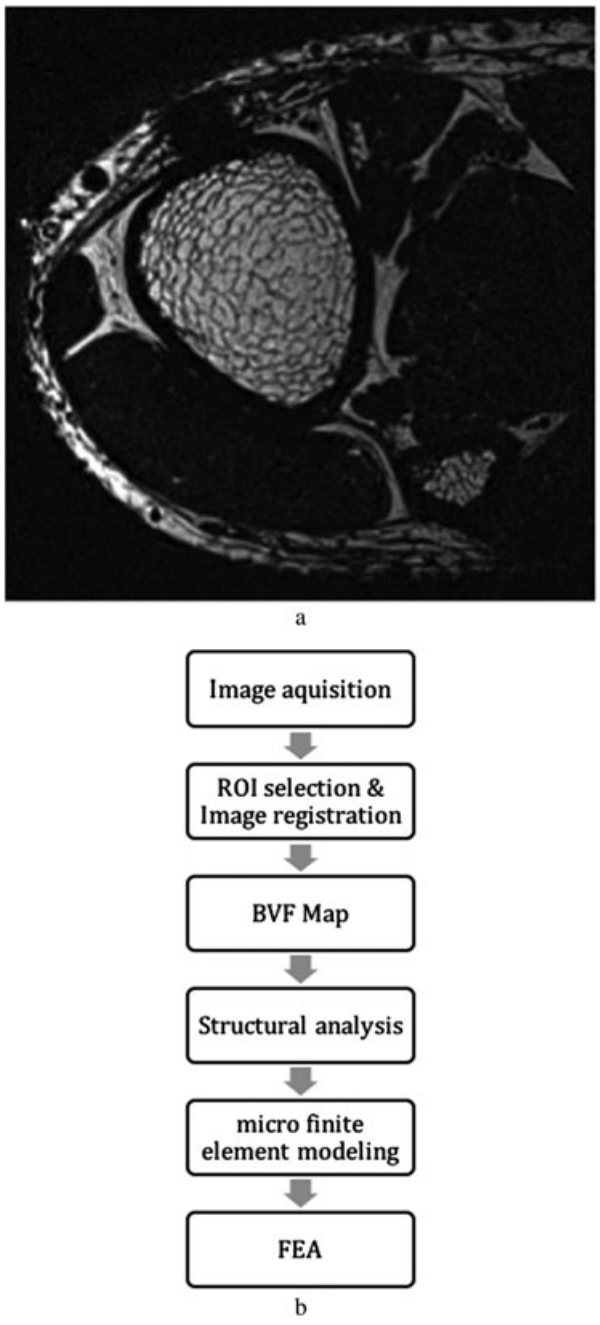

Fig. 1 (a) Representative high-resolution magnetic resonance imaging (HR-MRI) image of distal tibia of a 34 year old man 12 months after renal transplantation. (b) An illustration of HR-MRI image acquisition and processing steps.[45,73] Images are acquired using custom-designed radio-frequency pulse sequences and coils. The region of interest (ROI) for analysis is selected, and image is 'registered' to ascertain imaging of the same region during subsequent scans motion artefacts are screened for and corrected. The gray-scale values of the images are scaled to range from 0% to 100%, with pure marrow and pure bone having minimum and maximum values, respectively. This is known as bone volume fraction (BVF or BV/TV = bone volume/tissue volume) mapping, with individual voxel values representing the fraction of the voxel occupied by bone. Three-dimensional renditions of cortical and trabecular compartments can then be extracted from these images for structural and micro-finite element analysis (FEA) (please note that there may be relative heterogeneity in processing techniques used by different MRI labs).

Table 5 Studies involving use of HR-MRI in CKD

Author	Year	Study design	Sample size *n* (controls)	CKD stage	Site of imaging	Results
Link *et al.*[89]	2002	Cross-sectional	60 (20)	12 HD, 48 KT	Calcaneus	• Non-significant difference in aBMD in the 3 groups • BV/TV, TbSp, TbTh and TbN were significantly different between groups and discriminated for fracture status with spine BMD by QCT • Best diagnostic performance by combination of BMD and structural measures (AUC = 0.85)
Werhli *et al.*[90]	2004	Cross-sectional	17 (17)	5D	Tibia	• Decreased CtTh and cortical cross-sectional area in dialysis patients • Trabecular disruption but not statistically significant
Techawiboonwong *et al.*[79]		Cross-sectional	6 (10)	5D	Tibia	• Feasibility study to quantify bone water *in vivo* as a surrogate for CtPo • HD patients had 135% and 43% higher bone water than pre-menopausal and post-menopausal controls, respectively
Rajapakse *et al.*[73]	2012	Prospective (6 months)	49	KT	Tibia	• Decreased aBMD at spine but not hip • No correlation between % change in spine or hip BMD with % change in failure strengths by FEA • Significant decrease in cortical, trabecular and whole bone stiffness and failure strength • No change in conventional microstructural parameters

aBMD, areal bone mineral density; AUC, area under the curve; BV/TV, bone volume/total volume; CKD, chronic kidney disease; CtPo, cortical porosity; CtTh, cortical thickness; FEA, finite element analysis; HD, haemodialysis; HR-MRI, high-resolution magnetic resonance imaging; KT, kidney transplant; QCT, quantitative computed tomography; TbN, trabecular number; TbSp, trabecular separation; TbTh, trabecular thickness.

techniques, which have been subjected to calibration and validation studies over the last 15 years.[49–51] However, in recent years, the feasibility of assessing cortical microarchitecture of the proximal femur[76,77] and bone strength has been demonstrated.[78] In addition, ultrashort echo time imaging techniques have been applied to quantify the water content of cortical bone[79] as a potential surrogate measure of cortical porosity, which is an important determinant of bone strength.[80] Techawiboonwong *et al*.[79] validated ultrashort echo time imaging in bone specimens and demonstrated increased cortical porosity by showing the bone water content to be 135% higher in patients undergoing maintenance HD compared with premenopausal women, with no significant differences in tibial vBMD of the respective groups.

Multiple *in vivo* clinical studies performed in non-CKD cohorts have reported the utility of HR-MRI in demonstrating the association between bone structure and fracture discrimination,[81,82] structural and mechanical implications of therapeutic interventions longitudinally on bone microarchitecture[74,83–87] and differential diagnosis in metabolic bone disease.[88–90] However, there have been no prospective studies evaluating the role of HR-MRI in fracture prediction, and the technique has not been validated against bone histomorphometry. Moreover, despite the advances in MRI techniques over the last decade, there have been very few studies examining its role in ROD.

High-resolution magnetic resonance imaging in chronic kidney disease

To date, there have been few studies assessing the use of HR-MRI in the CKD population (Table 5). In a cross-sectional study involving 60 patients and 20 controls, Link *et al*. reported that MRI measures of trabecular structure of the calcaneus and BMD of the spine (by QCT) could discriminate between patients with and without fractures.[89] The highest diagnostic performance was achieved by combining the techniques. In addition, MRI trabecular parameters were significantly lower in pre-renal and post-renal transplant patients compared with those in healthy controls, yet no changes were observed in DXA-derived hip BMD in the groups. Wehrli *et al*.[90] evaluated the role of micro-MRI in assessing bone microstructure in 17 young adults on maintenance HD, compared with that in age-, gender- and BMI-matched healthy controls, and reported significantly lower cortical thickness and cross-sectional area in dialysis patients compared with those in controls. There was a non-significant trend suggesting trabecular disruption with reduced trabecular numbers and an increased erosion index. More recently, Rajapakse *et al*.[73] applied μFEA to HR-MRI images to assess cortical and trabecular bone strength in addition to structural parameters prospectively in 49 renal transplant recipients. They demonstrated a decrease in stiffness and failure strength in the distal tibia over 6 months after transplantation without corresponding changes in the conventional structural parameters.

CONCLUSION

Chronic kidney disease results in changes in bone structure associated with increased fracture risk leading to enhanced morbidity, mortality and healthcare costs. Bone biopsy, the current gold standard to assess ROD, is invasive and suboptimal for determination of renal bone disease and management in routine clinical practice. HR-pQCT and HR-MRI provide accurate non-invasive quantification of bone microarchitecture and facilitate assessment of its mechanical competence, which correlates well with skeletal fragility. Although emerging imaging techniques show promise, such studies need to be interpreted in the context of the technical caveats, relative lack of standardization and the limitations of imaging only peripheral sites. HR techniques need validation against bone histology, and trials are required to determine their utility to predict fracture risk and as substitutes for bone biopsy in intervention studies in the CKD population. More accurate methods of imaging at proximal skeletal sites and validated non-invasive markers of bone turnover and mineralization are also required before the 'virtual bone biopsy' becomes a reality.

REFERENCES

1. Nair SS, Mitani AA, Goldstein BA *et al.* Temporal trends in the incidence, treatment, and outcomes of hip fracture in older patients initiating dialysis in the United States. *Clin. J. Am. Soc. Nephrol.* 2013; **8** (8): 1336–42.
2. Naylor KL, McArthur E, Leslie WD *et al.* The three-year incidence of fracture in chronic kidney disease. *Kidney Int.* 2014; **86** (4): 810–8.
3. Tentori F, McCullough K, Kilpatrick RD *et al.* High rates of death and hospitalization follow bone fracture among hemodialysis patients. *Kidney Int.* 2014; **85** (1): 166–73.
4. Ball AM, Gillen DL, Sherrard D *et al.* Risk of hip fracture among dialysis and renal transplant recipients. *JAMA* 2002; **288** (23): 3014–3018.
5. Nikkel LE, Hollenbeak CS, Fox EJ, Uemura T, Ghahramani N. Risk of fractures after renal transplantation in the United States. *Translat* 2009; **87** (12): 1846–51.
6. Group, K.D.I.G.O.K.C.-M.W. KDIGO clinical practice guideline for the diagnosis, evaluation, prevention, and treatment of chronic kidney disease – mineral and bone disorder (CKD-MBD). *Kidney Int. Suppl.* 2009; (113): S1–130.
7. Moe S, Drueke T, Cunningham J *et al.* Definition, evaluation, and classification of renal osteodystrophy: a position statement from Kidney Disease: Improving Global Outcomes (KDIGO). *Kidney Int.* 2006; **69** (11): 1945–53.
8. Sherrard DJ, Hercz G, Pei Y *et al.* The spectrum of bone-disease in end-stage renal-failure – an evolving disorder. *Kidney Int.* 1993; **43** (2): 436–442.
9. Epstein FH, Hruska KA, Teitelbaum SL. Renal osteodystrophy. *New Engl J Med* 1995; **333** (3): 166–175.
10. Parfitt AM. A structural approach to renal bone disease. *J. Bone Miner. Res.* 1998; **13** (8): 1213–20.
11. Seeman E, Delmas PD. Bone quality – the material and structural basis of bone strength and fragility. *N. Engl. J. Med.* 2006; **354** (21): 2250–61.
12. Alem AM, Sherrard DJ, Gillen DL *et al.* Increased risk of hip fracture among patients with end-stage renal disease. *Kidney Int.* 2000; **58** (1): 396–399.
13. Coco M, Rush H. Increased incidence of hip fractures in dialysis patients with low serum parathyroid hormone. *Am. J. Kidney Dis.* 2000; **36** (6): 1115–21.

14. Jadoul M, Albert JM, Akiba T *et al.* Incidence and risk factors for hip or other bone fractures among hemodialysis patients in the Dialysis Outcomes and Practice Patterns Study. *Kidney Int.* 2006; **70** (7): 1358–1366.
15. Nickolas TL, McMahon DJ, Shane E. Relationship between moderate to severe kidney disease and hip fracture in the United States. *J. Am. Soc. Nephrol.* 2006; **17** (11): 3223–3232.
16. Ensrud KE, Lui L-Y, Taylor BC *et al.* Renal function and risk of hip and vertebral fractures in older women. *Arch. Intern. Med.* 2007; **167** (2): 133–139.
17. Dooley AC, Weiss NS, Kestenbaum B. Increased risk of hip fracture among men with CKD. *Am. J. Kidney Dis.* 2008; **51** (1): 38–44.
18. Wagner J, Jhaveri KD, Rosen L *et al.* Increased bone fractures among elderly United States hemodialysis patients. *Nephrol. Dial. Transplant.* 2014; **29** (1): 146–51.
19. Mathew AT, Hazzan A, Jhaveri KD *et al.* Increasing hip fractures in patients receiving hemodialysis and peritoneal dialysis. *Am. J. Nephrol.* 2014; **40** (5): 451–7.
20. Arneson TJ, Li S, Liu J *et al.* Trends in hip fracture rates in US hemodialysis patients, 1993–2010. *Am. J. Kidney Dis.* 2013; **62** (4): 747–754.
21. Perez-Saez MJ, Prieto-Alhambra D, Barrios C *et al.* Increased hip fracture and mortality in chronic kidney disease individuals: the importance of competing risks. *Bone* 2015; **73**: 154–9.
22. Mills KT, Xu Y, Zhang W *et al.* A systematic analysis of worldwide population-based data on the global burden of chronic kidney disease in 2010. *Kidney Int.* 2015; **88** (5): 950–7.
23. Thomas B, Wulf S, Bikbov B *et al.* Maintenance dialysis throughout the world in years 1990 and 2010. *J. Am. Soc. Nephrol.* 2015; **26** (11): 2621–33.
24. Johnell O, Kanis JA, Oden A *et al.* Predictive value of BMD for hip and other fractures. *J. Bone Miner. Res.* 2005; **20** (7): 1185–94.
25. Iimori S, Mori Y, Akita W *et al.* Diagnostic usefulness of bone mineral density and biochemical markers of bone turnover in predicting fracture in CKD stage 5D patients – a single-center cohort study. *Nephrol. Dial. Transplant.* 2012; **27** (1): 345–51.
26. Yenchek RH, Ix JH, Shlipak MG *et al.* Bone mineral density and fracture risk in older individuals with CKD. *Clin. J. Am. Soc. Nephrol.* 2012; **7** (7): 1130–6.
27. West SL, Lok CE, Langsetmo L *et al.* Bone mineral density predicts fractures in chronic kidney disease. *J. Bone Miner. Res.* 2015; **30** (5): 913–9.
28. Ketteler M, Elder GJ, Evenepoel P *et al.* Revisiting KDIGO clinical practice guideline on chronic kidney disease – mineral and bone disorder: a commentary from a Kidney Disease: Improving Global Outcomes controversies conference. *Kidney Int.* 2015; **87** (3): p. 502–28.
29. Sprague SM, Bellorin-Font E, Jorgetti V *et al.* Diagnostic accuracy of bone turnover markers and bone histology in patients with CKD treated by dialysis. *Am. J. Kidney Dis.* 2016; **67** (4): p. 559–66.
30. Danese MD, Kim J, Doan QV, Dylan M, Griffiths R, Chertow GM. PTH and the risks for hip, vertebral, and pelvic fractures among patients on dialysis. *Am. J. Kidney Dis.* 2006; **47** (1): 149–156.
31. Malluche HH, Mawad HW, Monier-Faugere MC. Renal osteodystrophy in the first decade of the new millennium: analysis of 630 bone biopsies in black and white patients. *J. Bone Miner. Res.* 2011; **26** (6): 1368–76.
32. Gardham C, Stevens PE, Delaney MP, LeRoux M, Coleman A, Lamb EJ. Variability of parathyroid hormone and other markers of bone mineral metabolism in patients receiving hemodialysis. *Clin. J. Am. Soc. Nephrol.* 2010; **5** (7): 1261–1267.
33. Iyer SP, Nikkel LE, Nishiyama KK *et al.* Kidney transplantation with early corticosteroid withdrawal: paradoxical effects at the central and peripheral skeleton. *J. Am. Soc. Nephrol.* 2014; **25** (6): 1331–41.
34. Negri AL, Del Valle EE, Zanchetta MB *et al.* Evaluation of bone microarchitecture by high-resolution peripheral quantitative computed tomography (HR-pQCT) in hemodialysis patients. *Osteoporos. Int.* 2012; **23** (10): 2543–50.
35. Nickolas TL, Cremers S, Zhang A *et al.* Discriminants of prevalent fractures in chronic kidney disease. *J. Am. Soc. Nephrol.* 2011; **22** (8): 1560–72.
36. Nickolas TL, Stein EM, Dworakowski E *et al.* Rapid cortical bone loss in patients with chronic kidney disease. *J. Bone Miner. Res.* 2013; **28** (8): 1811–20.
37. Malluche HH, Davenport DL, Cantor T, Monier-Faugere MC *et al.* Bone mineral density and serum biochemical predictors of bone loss in patients with CKD on dialysis. *Clin. J. Am. Soc. Nephrol.* 2014; **9** (7): 1254–62.
38. Perrin P, Caillard S, Javier RM *et al.* Persistent hyperparathyroidism is a major risk factor for fractures in the five years after kidney transplantation. *Am. J. Transplant.* 2013; **13** (10): 2653–63.
39. Cejka D, Patsch JM, Weber M *et al.* Bone microarchitecture in hemodialysis patients assessed by HR-pQCT. *Clin. J. Am. Soc. Nephrol.* 2011; **6** (9): 2264–71.
40. Pelletier S, Vilayphiou N, Boutroy S *et al.* Bone microarchitecture is more severely affected in patients on hemodialysis than in those receiving peritoneal dialysis. *Kidney Int.* 2012; **82** (5): 581–588.
41. Trombetti A, Stoermann C, Chevalley T *et al.* Alterations of bone microstructure and strength in end-stage renal failure. *Osteoporos. Int.* 2013; **24** (5): 1721–32.
42. Cejka D, Herberth J, Branscum AJ *et al.* Sclerostin and Dickkopf-1 in renal osteodystrophy. *Clin. J. Am. Soc. Nephrol.* 2011; **6** (4): 877–82.
43. Malluche HH, Monier-Faugere MC. The role of bone biopsy in the management of patients with renal osteodystrophy. *J. Am. Soc. Nephrol.* 1994; **4** (9): 1631–42.
44. Torres PU, Bover J, Mazzaferro S, de Vernejoul MC, Cohen-Solal M. When, how, and why a bone biopsy should be performed in patients with chronic kidney disease. In: *Seminars in Nephrology*. Elsevier, 2014; **34** (6): p. 612–25.
45. Wehrli FW. Structural and functional assessment of trabecular and cortical bone by micro magnetic resonance imaging. *J. Magn. Reson. Imaging* 2007; **25** (2): 390–409.
46. Krug R, Burghardt AJ, Majumdar S, Link TM. High-resolution imaging techniques for the assessment of osteoporosis. *Radiol. Clin. North Am.* 2010; **48** (3): 601–21.
47. Geusens P, Chapurlat R, Schett G *et al.* High-resolution in vivo imaging of bone and joints: a window to microarchitecture. *Nat. Rev. Rheumatol.* 2014; **10** (5): 304–13.
48. Liu XS, Zhang XH, Sekhon KK *et al.* High-resolution peripheral quantitative computed tomography can assess microstructural and mechanical properties of human distal tibial bone. *J. Bone Miner. Res.* 2010; **25** (4): 746–756.
49. Phan CM, Matsuura M, Bauer JS *et al.* Trabecular bone structure of the calcaneus: comparison of MR imaging at 3.0 and 1.5 T with micro-CT as the standard of reference. *Radiol* 2006; **239** (2): 488–496.
50. Krug R, Carballido-Gamio J, Burghardt AJ *et al.* Assessment of trabecular bone structure comparing magnetic resonance imaging at 3 Tesla with high-resolution peripheral quantitative computed tomography *ex vivo* and *in vivo*. *Osteoporos. Int.* 2008; **19** (5): 653–661.
51. Liu XS, Zhang XH, Rajapakse CS *et al.* Accuracy of high-resolution *in vivo* micro magnetic resonance imaging for measurements of microstructural and mechanical properties of human distal tibial bone. *J. Bone Miner. Res.* 2010; **25** (9): 2039–50.
52. Wehrli FW, Saha PK, Gomberg BR *et al.* Role of magnetic resonance for assessing structure and function of trabecular bone. *Top. Magn. Reson. Imaging* 2002; **13** (5): 335–55.
53. Nickolas TL, Shirazian S, Shane E. High-resolution computed tomography imaging: a virtual bone biopsy. *Kidney Int.* 2010; **77** (11): 1046.
54. Boutroy S, Van Rietbergen B, Sornay-Rendu E, Munoz F, Bouxsein ML, Delmas PD. Finite element analysis based on *in vivo* HR-pQCT images of the distal radius is associated with wrist fracture in postmenopausal women. *J. Bone Miner. Res.* 2008; **23** (3): 392–399.
55. Adams JE. Quantitative computed tomography. *Eur. J. Radiol.* 2009; **71** (3): 415–24.
56. Mares J, Ohlidalova K, Opatrna S, Ferda J. Determinants of prevalent vertebral fractures and progressive bone loss in long-term hemodialysis patients. *J. Bone Miner. Metab.* 2009; **27** (2): 217–23.

57. Russo CR, Taccetti G, Caneva P, Mannarino A, Maranghi P, Ricca M. Volumetric bone density and geometry assessed by peripheral quantitative computed tomography in uremic patients on maintenance hemodialysis. *Osteoporos. Int.* 1998; **8** (5): 443–8.
58. Hasegawa K, Hasegawa Y, Nagano A. Estimation of bone mineral density and architectural parameters of the distal radius in hemodialysis patients using peripheral quantitative computed tomography. *J. Biomech.* 2004; **37** (5): 751–756.
59. Jamal SA, Gilbert J, Gordon C, Bauer DC. Cortical pQCT measures are associated with fractures in dialysis patients. *J. Bone Miner. Res.* 2006; **21** (4): 543–8.
60. Negri AL, Barone R, Lombas C, Bogado CE, Zanchetta JR. Evaluation of cortical bone by peripheral quantitative computed tomography in continuous ambulatory peritoneal dialysis patients. *Hemodial. Int.* 2006; **10** (4): 351–5.
61. Negri A, Lombas C, Cuevas C, Schiavelli R, Bogado C, Zanchetta J. Evaluation of cortical bone by peripheral quantitative computed tomography in renal transplant recipients. In: *Transplantation Proceedings*. Elsevier, 2005; **37** (2): p. 1020–2.
62. Obatake N, Ishimura E, Tsuchida T *et al.* Annual change in bone mineral density in predialysis patients with chronic renal failure: significance of a decrease in serum 1,25-dihydroxy-vitamin D. *J. Bone Miner. Metab.* 2007; **25** (1): 74–9.
63. Fujimori A, Okada S, Sakai M, Tome K, Fukagawa M. Relationship between biochemical markers and radial cortical bone changes in hemodialysis patients. *Nephron Clin. Pract.* 2011; **118** (4): C375–C379.
64. Boutroy S, Bouxsein ML, Munoz F, Delmas PD. In vivo assessment of trabecular bone microarchitecture by high-resolution peripheral quantitative computed tomography. *J. Clin. Endocrinol. Metab.* 2005; **90** (12): 6508–15.
65. Khosla S, Riggs BL, Atkinson EJ *et al.* Effects of sex and age on bone microstructure at the ultradistal radius: a population-based noninvasive *in vivo* assessment. *J. Bone Miner. Res.* 2006; **21** (1): 124–131.
66. Bacchetta J, Boutroy S, Vilayphiou N *et al.*. Early impairment of trabecular microarchitecture assessed with HR-pQCT in patients with stage II–IV chronic kidney disease. *J. Bone Miner. Res.* 2010; **25** (4): 849–57.
67. Jamal S, Cheung A, West S, Lok C. Bone mineral density by DXA and HR pQCT can discriminate fracture status in men and women with stages 3 to 5 chronic kidney disease. *Osteoporos. Int.* 2012; **23** (12): 2805–2813.
68. Nickolas TL, Stein E, Cohen A *et al*. Bone mass and microarchitecture in CKD patients with fracture. *J. Am. Soc. Nephrol.* 2010; **21** (8): 1371–80.
69. Cejka D, Weber M, Diarra D, Reiter T, Kainberger F, Haas M. Inverse association between bone microarchitecture assessed by HR-pQCT and coronary artery calcification in patients with end-stage renal disease. *Bone* 2014; **64**: 33–38.
70. Pelletier S, Confavreux CB, Haesebaert J *et al*. Serum sclerostin: the missing link in the bone-vessel cross-talk in hemodialysis patients? *Osteoporos. Int.* 2015; **26** (8): 2165–74.
71. West SL, Lok CE, Langsetmo L *et al*. Bone mineral density predicts fractures in chronic kidney disease. *J. Bone Miner. Res.* 2015; **30** (5): 913–9.
72. Nishiyama KK, Pauchard Y, Nikkel LE *et al*. Longitudinal HR-pQCT and image registration detects endocortical bone loss in kidney transplantation patients. *J. Bone Miner. Res.* 2015; **30** (3): 554–61.
73. Rajapakse CS, Leonard MB, Bhagat YA, Sun W, Magland JF, Wehrli FW. Micro-MR imaging-based computational biomechanics demonstrates reduction in cortical and trabecular bone strength after renal transplantation. *Radiology* 2012; **262** (3): 912–20.
74. Al Mukaddam M, Rajapakse CS, Bhagat YA *et al*. Effects of testosterone and growth hormone on the structural and mechanical properties of bone by micro-MRI in the distal tibia of men with hypopituitarism. *J. Clin. Endocrinol. Metab.* 2014; **99** (4): 1236–44.
75. Gomberg B, Wehrli F, Vasilić B *et al*. Reproducibility and error sources of μ-MRI-based trabecular bone structural parameters of the distal radius and tibia. *Bone* 2004; **35** (1): 266–276.
76. Krug R, Banerjee S, Han ET, Newitt DC, Link TM, Majumdar S. Feasibility of in vivo structural analysis of high-resolution magnetic resonance images of the proximal femur. *Osteoporos. Int.* 2005; **16** (11): 1307–14.
77. Chang G, Deniz CM, Honig S *et al*. Feasibility of three-dimensional MRI of proximal femur microarchitecture at 3 Tesla using 26 receive elements without and with parallel imaging. *J. Magn. Reson. Imaging* 2014; **40** (1): 229–38.
78. Chang G, Honig S, Brown R *et al*. Finite element analysis applied to 3-T MR imaging of proximal femur microarchitecture: lower bone strength in patients with fragility fractures compared with control subjects. *Radiology* 2014; **272** (2): 464–74.
79. Techawiboonwong A, Song HK, Leonard MB, Wehrli FW. Cortical bone water: in vivo quantification with ultrashort echo-time MR imaging. *Radiology* 2008; **248** (3): 824–33.
80. Bala Y, Zebaze R, Seeman E. Role of cortical bone in bone fragility. *Curr. Opin. Rheumatol.* 2015; **27** (4): 406–13.
81. Majumdar S, Link TM, Augat P *et al*.. Trabecular bone architecture in the distal radius using magnetic resonance imaging in subjects with fractures of the proximal femur. *Osteoporosis Int* 1999; **10** (3): 231–239.
82. Wehrli FW, Gomberg BR, Saha PK, Song HK, Hwang SN, Snyder PJ. Digital topological analysis of in vivo magnetic resonance microimages of trabecular bone reveals structural implications of osteoporosis. *J. Bone Miner. Res.* 2001; **16** (8): 1520–31.
83. Benito M, Gomberg B, Wehrli FW *et al*. Deterioration of trabecular architecture in hypogonadal men. *J. Clin. Endocrinol. Metab.* 2003; **88** (4): 1497–502.
84. Benito M, Vasilic B, Wehrli FW *et al*. Effect of testosterone replacement on trabecular architecture in hypogonadal men. *J. Bone Miner. Res.* 2005; **20** (10): 1785–91.
85. Zhang XH, Liu XS, Vasilic B *et al*. In vivo μMRI-based finite element and morphological analyses of tibial trabecular bone in eugonadal and hypogonadal men before and after testosterone treatment. *J. Bone Miner. Res.* 2008; **23** (9): 1426–1434.
86. Chesnut CH, Majumdar S, Newitt DC *et al*. Effects of salmon calcitonin on trabecular microarchitecture as determined by magnetic resonance imaging: results from the QUEST study. *J. Bone Miner. Res.* 2005; **20** (9): 1548–1561.
87. Folkesson J, Goldenstein J, Carballido-Gamio J *et al*. Longitudinal evaluation of the effects of alendronate on MRI bone microarchitecture in postmenopausal osteopenic women. *Bone* 2011; **48** (3): 611–21.
88. Link TM, Lotter A, Beyer F *et al*. Changes in calcaneal trabecular bone structure after heart transplantation: an MR imaging study. *Radiology* 2000; **217** (3): 855–62.
89. Link TM, Saborowski, Kisters K *et al*. Changes in calcaneal trabecular bone structure assessed with high-resolution MR imaging in patients with kidney transplantation. *Osteoporos. Int.* 2002; **13** (2): 119–29.
90. Wehrli FW, Leonard MB, Saha PK, Gomberg BR. Quantitative high-resolution magnetic resonance imaging reveals structural implications of renal osteodystrophy on trabecular and cortical bone. *J. Magn. Reson. Imaging* 2004; **20** (1): 83–9.
91. Damilakis J, Adams JE, Guglielmi G *et al*. Radiation exposure in X-ray-based imaging techniques used in osteoporosis. *Eur. Radiol.* 2010; **20** (11): 2707–14.
92. The 2007 Recommendations of the International Commission on Radiological Protection. ICRP publication 103. *Ann. ICRP* 2007; **37** (2–4): 1–332.
93. Cejka D, Jager-Lansky A, Kieweg H *et al*. Sclerostin serum levels correlate positively with bone mineral density and microarchitecture in haemodialysis patients. *Nephrol. Dial. Transplant.* 2012; **27** (1): 226–30.

NEPHROLOGY

Nephrology **22**, Suppl. 2 (2017) 27–30

Supplement Article

Is there a practical role for a virtual bone biopsy using high-resolution imaging of bone in patients with chronic kidney disease?

ASHISH K SHARMA[1,2] and NIGEL D TOUSSAINT[1,2]

[1]Department of Nephrology, The Royal Melbourne Hospital, Parkville, Victoria and [2]Department of Medicine (RMH), The University of Melbourne, Melbourne, Australia

KEY WORDS:
bone mineral density, chronic kidney disease, fracture, high-resolution magnetic resonance imaging, peripheral quantitative high-resolution computed tomography, renal osteodystrophy.

Correspondence:
Dr Ashish Sharma, Department of Nephrology, The Royal Melbourne Hospital, Grattan Street, Parkville, Victoria 3052, Australia. Email: ashish.sharma@mh.org.au

doi: 10.1111/nep.13018

ABSTRACT:

Renal osteodystrophy (ROD) refers to alterations in bone turnover, mineralisation, mass and microarchitecture in patients with chronic kidney disease (CKD) and represents the skeletal component of 'CKD–mineral and bone disorder'. Changes in bone structure lead to impaired bone quality, compromised bone strength and increased susceptibility to fractures with associated significant morbidity, mortality and financial cost. Diagnosis and management of ROD is hindered by the inadequacy of currently available diagnostic methods to interpret the complex pathophysiology. Bone biopsy, the perceived gold standard test to assess ROD, is invasive and suboptimal for disease screening and management in routine clinical practice. High-resolution imaging, such as high-resolution peripheral quantitative computed tomography and high-resolution magnetic resonance imaging provide accurate non-invasive quantification of bone microarchitecture and facilitate assessment of mechanical competence of bone, correlating with skeletal fragility. We discuss the potential for these imaging techniques in patients with CKD to provide quantification and assessment of bone structure and strength. When used in conjunction with serum biomarkers, these investigative tools may provide a non-invasive diagnostic virtual bone biopsy.

INTRODUCTION

Renal osteodystrophy (ROD) is a complex disorder of bone resulting from the metabolic and hormonal abnormalities that arise in chronic kidney disease (CKD). ROD is manifested as disruption of bone architecture and abnormal remodeling and affects all levels of bone structure hierarchy, leading to impaired bone quality and compromised bone strength with an increased susceptibility to fracture. Studies in patients across the spectrum of CKD, ranging from CKD stage 3 to end-stage kidney disease including dialysis and especially renal transplantation, have overwhelmingly highlighted the greater risk of fracture in the CKD population when compared with age-matched and gender-matched populations.[1–5] Higher rates of hospitalization and mortality occur in patients with advanced CKD who develop fractures.[4,6] Early and accurate diagnosis of ROD is therefore crucial, but current diagnostic methods are inadequate for the need. Lack of robust screening tools for ROD has also limited our ability to develop therapeutic options and conduct appropriate interventional trials. Routinely used validated therapeutics, such as bisphosphonates and other anti-resorptive agents, remain underused in advanced CKD due to the paucity of evidence and the dynamic nature of ROD.

The complex pathophysiology of ROD, combined with the limited efficacy of dual-energy X-ray absorptiometry (DXA) and the unreliability of currently used serum and urinary biomarkers to act as stand-alone screening tools for fracture risk in patients with CKD, puts the onus of a definitive diagnosis on bone biopsy. However, this procedure is invasive, requires specialist expertise to perform and interpret the results and is rarely performed in current clinical practice. Moreover, bone histomorphometry only depicts microstructure at a single point in time and bone biopsies performed at one site may not reflect concurrent changes at another. The non-invasive assessment of bone microstructure, by high-resolution imaging techniques such as high-resolution peripheral quantitative computed tomography (HR-pQCT) and high-resolution magnetic resonance imaging (HR-MRI or micro-MRI), has therefore attracted increased attention. To date, most research in high-resolution imaging of bone has focused on populations without CKD; however, a few imaging studies have targeted the added

complexities of bone pathology unique to the CKD population. We discuss the importance of these to the future diagnosis and management of ROD.

High-resolution imaging – nuts and bolts

Bone mineral density (BMD) explains around 70–75% of the variance in bone strength, while the remaining variance is due to the cumulative and synergistic effect of factors such as bone microarchitecture, tissue composition and accumulated microdamage.[7] Assessment of the microarchitecture, in addition to BMD, is important in the context of ROD, although the high spatial resolution required to resolve bone microstructure in a clinically feasible scan time is challenging. Currently, the best modalities reported to achieve these requirements are HR-pQCT and micro-MRI.

High-resolution peripheral quantitative computed tomography uses a low radiation dedicated extremity scanner (XtremeCT; Scanco Medical AG, Brüttisellen, Switzerland) to measure cortical and trabecular bone structural parameters and volumetric BMD (vBMD) from the distal radius or tibia.[8] Micro-MRI, a non-ionizing method for *in vivo* quantification of bone microarchitecture, is performed using readily available clinical scanners but with customized pulse sequences, coils and sophisticated post-processing and analysis.[9] HR-pQCT is limited to peripheral skeletal regions like the wrist and ankle, whereas micro-MRI can image other sites, such as the proximal femur though, usually with lower spatial resolution.[10] The structural parameters measured by both these modalities have been validated against the 'gold standard' measurements of bone structure obtained by micro-computed tomography of bone from a biopsy.[11,12] The description of these parameters follows the same nomenclature as classical bone histomorphometry, leading some clinicians to refer to the process as a 'virtual bone biopsy'.[13,14]

Traditionally, vertebral fractures have been the clinical endpoints assessed in research studies, which has led to a focus on deterioration in trabecular bone structure as a marker of bone fragility. In recent years, research has seen the emergence of cortical bone as a determinant of bone strength and cortical porosity as a surrogate marker of bone loss and fragility,[15] helping to explain the vast preponderance of non-vertebral and hip fractures. HR-pQCT measures cortical thickness and porosity *via* a semi-automated protocol, which segments the bone into cortical and trabecular compartments. This process is susceptible to the confounding effect of 'trabecularisation' of the cortex, and can lead to errors in quantifying changes in trabecular and cortical morphology with advancing age or drug therapy.[8] While newer image analysis programs are being developed for HR-pQCT to negate this confounding, feasibility studies using micro-MRI and ultrashort-echo-time imaging technique to quantify water content of cortical bone as a surrogate measure of cortical porosity have been encouraging.[16] Techawiboonwong *et al.*[16] validated ultrashort-echo-time imaging in bone specimens and demonstrated increased cortical porosity with bone water content 135% higher in patients undergoing maintenance haemodialysis compared to pre-menopausal women with normal renal function, despite no significant differences in tibial vBMD of the respective groups.

Finite element analysis (FEA), a computational method that provides estimates of bone stiffness and failure load in response to simulated mechanical loading scenarios, can be applied to 3-D HR-pQCT and micro-MRI data to measure strength, either of whole bone or its compartments.[17,18] In addition to correlating bone strength with its microarchitecture, bone mechanical properties assessed by FEA may provide information about skeletal fragility and fracture risk, independent of BMD or architecture measurements, and add another potential method of assessing bone vulnerability.[19] Recently Rajapakse *et al.*[20] described a reproducible FEA method by using MRI to estimate mechanical parameters that relate to hip fracture resistance. This method is an attractive future proposition, and particularly relevant to a population with advanced CKD and high rates of hip fractures[3,21]

Role of high-resolution imaging in patients with CKD

Cross-sectional studies utilizing HR-pQCT have demonstrated lower cortical and trabecular vBMD, thinner cortices, and abnormal trabecular microarchitecture of the distal radius and tibia in CKD patients with prevalent fractures.[22–24] Similar investigations have also linked hyperparathyroidism and increased levels of bone turnover markers with low vBMD, abnormal bone microarchitecture and fracture.[25,26] These findings have been highlighted by prospective studies that have reported progressive deterioration of cortical microarchitecture and increased cortical porosity at peripheral sites in patients with CKD stages 2 to 5D[27] and post renal transplantation[18,28] and have demonstrated associations with elevated parathyroid hormone levels and bone turnover markers.

In one prospective study of 131 patients with pre-dialysis CKD (stages 3–5), West *et al.*[29] assessed the use of both DXA and HR-pQCT to predict fractures, and after 2 year follow-up demonstrated an association between low baseline BMD using either method, incident morphometric spine fractures and low-trauma clinical fractures. Bone loss occurred in all subjects in this study, but was significantly greater among those with incident fractures. The potential role of high resolution imaging and FEA in therapeutic interventional trials has been illustrated by Bonani *et al.*[30] in a small randomised controlled trial of the effect of denosumab on bone microarchitecture and mechanical competence, assessed by HR-pQCT, in kidney transplant recipients. Participants in the treatment group showed increased total and cortical vBMD, cortical thickness and bone stiffness compared to control group.

Multiple *in vivo* clinical studies using micro-MRI in non-CKD cohorts have associated bone structure with fracture discrimination and demonstrated structural and mechanical implications of therapeutic interventions longitudinally on bone

Table 1 Comparison between HR-pQCT and micro-MRI imaging techniques

	Micro-MRI	HR-pQCT
Imaging sites	Distal tibia, radius, femur	Distal tibia, radius
Scan time	~12 min	~3 min
Spatial resolution	137 × 137 × 410 μm^3 anisotropic	82μm^3 isotropic
Radiation	No	<4 μSv
Measures	Microarchitecture	vBMD, microarchitecture
Evidence for clinical applications	• Microstructural changes in osteoporosis, hypogonadism • Fracture discrimination • Longitudinal monitoring of treatment effect • CKD and kidney transplant • No prospective studies for predicting fracture risk yet	• Microstructural changes in osteoporosis, with associated treatment interventions and fracture discrimination, have been studied in non-CKD cohorts • CKD and kidney transplant including evaluating prediction for fracture risk
Advantages	• Performed on widely available clinical MRI scanners • No ionizing radiation • Potential to assess femur microarchitecture	• Automated protocol once periosteal contouring defined by the operator • Assess all parameters of bone architecture including vBMD and cortical porosity •Low radiation
Limitations	• Customized radio-frequency sequences and peripheral hardware • Sophisticated and complicated post-processing techniques • Lack of standardized reference data and heterogeneity of processing techniques • Specialized techniques to measure cortical porosity • Very few studies in CKD and lack of robust validation against histomorphometry	• Dedicated scanner – not available in clinical settings • Scans limited to peripheral sites by bore size and potential radiation exposure • Problems with segmentation and image registration techniques • Lack of standardized reference data • Few but increasing number of studies in CKD and lack of robust validation against histomorphometry

CKD, chronic kidney disease; HR-pQCT, high-resolution peripheral quantitative computed tomography; micro MRI, high-resolution magnetic resonance imaging; vBMD, volumetric bone mineral density.

microarchitecture[31–33] Unfortunately, despite advances in MRI techniques over the last decade, there have been few studies examining its role in ROD. Micro-MRI derived bone structural parameters in patients with CKD and renal transplant recipients have been reported to discriminate between patients with and without fractures.[34] Wehrli *et al.*[35] evaluated the role of micro-MRI in assessing bone microstructure in 17 young adults on maintenance haemodialysis, demonstrating significantly lower cortical thickness and cross-sectional area and evidence of trabecular disruption in the dialysis patients compared to controls. Rajapakse *et al.*[17] applied finite element modeling to micro-MRI images to assess cortical and trabecular structure and bone strength in renal transplant recipients, and demonstrated a decrease in stiffness and failure strength in distal tibia over 6 months post renal transplantation without corresponding changes in the conventional structural parameters.

The future of high-resolution imaging in CKD – more research needed

Bone abnormalities in CKD are inadequately understood and poorly managed, mainly owing to the unique and complex pathophysiology of ROD and the lack of diagnostic tools. Non-invasive high-resolution imaging has the potential to fill, at least partially, the significant gap between screening of BMD using DXA and the comprehensive diagnosis by bone biopsy. HR-pQCT and micro-MRI, in conjunction with accurate and appropriate bone turnover markers, can potentially be used to screen for bone fragility, predict fracture and help in developing therapeutic interventions and monitoring treatment effect in the CKD population.

While the euphoria surrounding the potential of high-resolution imaging is not unfounded, it has to be viewed in the context of technical caveats, relative lack of standardization of reference and technical parameters, limitation of imaging to peripheral sites and high costs (Table 1). These are potential hurdles in the projected implementation of high-resolution imaging into mainstream clinical practice, and currently these modalities are confined to the research setting. Moreover, both techniques need validation in large multi-centre prospective trials to determine their utility in guiding clinical decision-making and improving outcomes in the CKD population. Requirements for further study before implementation include developing and validating fracture prediction tools incorporating the uniqueness of ROD and techniques to image bone microstructure at proximal sites. These challenges are significant but not insurmountable, and once met, may fulfill the vision of a 'virtual bone biopsy'.

REFERENCES

1. Alem AM *et al.* Increased risk of hip fracture among patients with end-stage renal disease. *Kidney Int.* 2000; **58** (1): 396–399.
2. Ball AM *et al.* RIsk of hip fracture among dialysis and renal transplant recipients. *JAMA* 2002; **288** (23): 3014–3018.

3. Naylor KL *et al.* The three-year incidence of fracture in chronic kidney disease. *Kidney Int.* 2014; **86** (4): 810–818.
4. Tentori F *et al.* High rates of death and hospitalization follow bone fracture among hemodialysis patients. *Kidney Int.* 2014; **85** (1): 166–173.
5. Hansen D *et al.* Risk of fracture in adults on renal replacement therapy: a Danish national cohort study. *Nephrol. Dial. Transplant.* 2016; **31** (10): 1654–1662.
6. Perez-Saez MJ *et al.* Increased hip fracture and mortality in chronic kidney disease individuals: the importance of competing risks. *Bone* 2015; **73**: 154–159.
7. Krug R *et al.* High-resolution imaging techniques for the assessment of osteoporosis. *Radiol. Clin. North Am.* 2010; **48** (3): 601–621.
8. Geusens P *et al.* High-resolution in vivo imaging of bone and joints: a window to microarchitecture. *Nat. Rev. Rheumatol.* 2014; **10** (5): 304–313.
9. Wehrli FW. Structural and functional assessment of trabecular and cortical bone by micro magnetic resonance imaging. *J. Magn. Reson. Imaging* 2007; **25** (2): 390–409.
10. Krug R *et al.* Feasibility of in vivo structural analysis of high-resolution magnetic resonance images of the proximal femur. *Osteoporos. Int.* 2005; **16** (11): 1307–1314.
11. Liu XS *et al.* High-resolution peripheral quantitative computed tomography can assess microstructural and mechanical properties of human distal tibial bone. *J. Bone Miner. Res.* 2010; **25** (4): 746–756.
12. Krug R *et al.* Assessment of trabecular bone structure comparing magnetic resonance imaging at 3 Tesla with high-resolution peripheral quantitative computed tomography ex vivo and in vivo. *Osteoporos. Int.* 2008; **19** (5): 653–661.
13. Wehrli FW *et al.* Role of magnetic resonance for assessing structure and function of trabecular bone. *Top. Magn. Reson. Imaging* 2002; **13** (5): 335–355.
14. Nickolas TL, Shirazian S, Shane E. High-resolution computed tomography imaging: a virtual bone biopsy. *Kidney Int.* 2010; **77** (11): 1046.
15. Bala Y, Zebaze R, Seeman E. Role of cortical bone in bone fragility. *Curr. Opin. Rheumatol.* 2015; **27** (4): 406–413.
16. Techawiboonwong A *et al.* Cortical bone water: in vivo quantification with ultrashort echo-time MR imaging. *Radiology* 2008; **248** (3): 824–833.
17. Rajapakse CS *et al.* Micro–MR imaging–based computational biomechanics demonstrates reduction in cortical and trabecular bone strength after renal transplantation. *Radiology* 2012; **262** (3): 912–920.
18. Nishiyama KK *et al.* Longitudinal HR-pQCT and image registration detects endocortical bone loss in kidney transplantation patients. *J. Bone Miner. Res.* 2015; **30** (3): 554–561.
19. Boutroy S *et al.* Finite element analysis based on in vivo HR-pQCT images of the distal radius is associated with wrist fracture in postmenopausal women. *J. Bone Miner. Res.* 2008; **23** (3): 392–399.
20. Rajapakse CS *et al.* Patient-specific hip fracture strength assessment with microstructural MR imaging-based finite element modeling. *Radiology* 2016; **0** (0): 160874.
21. Coco M, Rush H. Increased incidence of hip fractures in dialysis patients with low serum parathyroid hormone. *Am. J. Kidney Dis.* 2000; **36** (6): 1115–1121.
22. Jamal S *et al.* Bone mineral density by DXA and HR pQCT can discriminate fracture status in men and women with stages 3 to 5 chronic kidney disease. *Osteoporos. Int.* 2012; **23** (12): 2805–2813.
23. Cejka D *et al.* Bone microarchitecture in hemodialysis patients assessed by HR-pQCT. *Clin. J. Am. Soc. Nephrol.* 2011; **6** (9): 2264–2271.
24. Nickolas TL *et al.* Bone mass and microarchitecture in CKD patients with fracture. *J. Am. Soc. Nephrol.* 2010; **21** (8): 1371–1380.
25. Negri AL *et al.* Evaluation of bone microarchitecture by high-resolution peripheral quantitative computed tomography (HR-pQCT) in hemodialysis patients. *Osteoporos. Int.* 2012; **23** (10): 2543–2550.
26. Nickolas TL *et al.* Discriminants of prevalent fractures in chronic kidney disease. *J. Am. Soc. Nephrol.* 2011; **22** (8): 1560–1572.
27. Nickolas TL *et al.* Rapid cortical bone loss in patients with chronic kidney disease. *J. Bone Miner. Res.* 2013; **28** (8): 1811–1820.
28. Iyer SP *et al.* Kidney transplantation with early corticosteroid withdrawal: paradoxical effects at the central and peripheral skeleton. *J. Am. Soc. Nephrol.* 2014; **25** (6): 1331–1341.
29. West SL *et al.* Bone mineral density predicts fractures in chronic kidney disease. *J. Bone Miner. Res.* 2015; **30** (5): 913–919.
30. Bonani M *et al.* Effect of denosumab on peripheral compartmental bone density, microarchitecture and estimated bone strength in **de novo** kidney transplant recipients. *Kidney Blood Press. Res.* 2016; **41** (5): 614–622.
31. Wehrli FW *et al.* Digital topological analysis of in vivo magnetic resonance microimages of trabecular bone reveals structural implications of osteoporosis. *J. Bone Miner. Res.* 2001; **16** (8): 1520–1531.
32. Folkesson J *et al.* Longitudinal evaluation of the effects of alendronate on MRI bone microarchitecture in postmenopausal osteopenic women. *Bone* 2011; **48** (3): 611–621.
33. Zhang XH *et al.* In vivo μMRI-based finite element and morphological analyses of tibial trabecular bone in eugonadal and hypogonadal men before and after testosterone treatment. *J. Bone Miner. Res.* 2008; **23** (9): 1426–1434.
34. Link TM *et al.* Changes in calcaneal trabecular bone structure assessed with high-resolution MR imaging in patients with kidney transplantation. *Osteoporos. Int.* 2002; **13** (2): 119–129.
35. Wehrli FW *et al.* Quantitative high-resolution magnetic resonance imaging reveals structural implications of renal osteodystrophy on trabecular and cortical bone. *J. Magn. Reson. Imaging* 2004; **20** (1): 83–89.

Original Report: Patient-Oriented, Translational Research

American Journal of Nephrology

Am J Nephrol 2018;47:376–384
DOI: 10.1159/000489671

Received: November 22, 2017
Accepted: March 27, 2018
Published online: May 23, 2018

Deterioration of Cortical Bone Microarchitecture: Critical Component of Renal Osteodystrophy Evaluation

Ashish K. Sharma[a, b] Nigel D. Toussaint[a, b] Rosemary Masterson[a, b]
Stephen G. Holt[a, b] Chamith S. Rajapakse[c] Peter R. Ebeling[d]
Sindhu T. Mohanty[e] Paul Baldock[e] Grahame J. Elder[e, f]

[a]Department of Nephrology, The Royal Melbourne Hospital, Parkville, VIC, Australia; [b]Department of Medicine (RMH), University of Melbourne, Parkville, VIC, Australia; [c]Departments of Radiology and Orthopaedic Surgery, University of Pennsylvania, Philadelphia, PA, USA; [d]Monash University, Clayton, VIC, Australia; [e]Osteoporosis and Bone Biology Division, Garvan Institute of Medical Research, Darlinghurst, NSW, Australia; [f]Department of Renal Medicine, Westmead Hospital, Westmead, NSW, Australia

Keywords
Renal osteodystrophy · Bone biopsy · Micro-computed tomography · Cortical thickness · Cortical porosity

Abstract
Background: Cortical bone is a significant determinant of bone strength and its deterioration contributes to bone fragility. Thin cortices and increased cortical porosity have been noted in patients with chronic kidney disease (CKD), but the "Turnover Mineralization Volume" classification of renal osteodystrophy does not emphasize cortical bone as a key parameter. We aimed to assess trabecular and cortical bone microarchitecture by histomorphometry and micro-CT in patients with CKD G5 and 5D (dialysis). ***Methods:*** Transiliac bone biopsies were performed in 14 patients undergoing kidney transplantation (n = 12) and parathyroidectomy (n = 2). Structural parameters were analysed by histomorphometry and micro-CT including trabecular bone volume, thickness (TbTh), number (TbN) and separation and cortical thickness (CtTh) and porosity (CtPo). Indices of bone remodelling and mineralisation were obtained and relationships to bone biomarkers examined. Associations were determined by Spearman's or Pearson's rank correlation coefficients. ***Results:*** By micro-CT, trabecular parameters were within normal ranges in most patients, but all patients showed very low CtTh (127 ± 44 μm) and high CtPo (60.3 ± 22.5%). CtPo was inversely related to TbN (r = –0.56; p = 0.03) by micro-CT and to TbTh (r = –0.60; p = 0.024) by histomorphometry and correlated to parathyroid hormone values (r = 0.62; p = 0.021). By histomorphometry, bone turnover was high in 50%, low in 21% and normal in 29%, while 36% showed abnormal patterns of mineralization. Significant positive associations were observed between osteoblast surface, osteoclast surface, mineralization surface and bone turnover markers. ***Conclusions:*** Deterioration of cortical microarchitecture despite predominantly normal trabecular parameters reinforces the importance of comprehensive cortical evaluation in patients with CKD.

KARGER

E-Mail karger@karger.com
www.karger.com/ajn

Dr. Ashish K. Sharma
Department of Nephrology
The Royal Melbourne Hospital, Grattan Street
Parkville, VIC 3052 (Australia)
E-Mail a.k.sharma@hotmail.com

Introduction

Bone structure can be divided into cortical and cancellous tissue compartments with approximately 80% of the adult skeleton comprised of cortical bone and trabecular bone in the cancellous compartment comprising the remainder. The ratio of cortical to trabecular bone varies widely for bones at different anatomic locations and within the same bone at different sites. The 2 types of bones also differ in arrangement of microstructure, which is responsible for the difference in their functional attributes. Cortical bone is compact and dense and provides bulk and strength, whereas the more "metabolically active" trabecular bone is a honeycomb-like network of plates and rods [1]. Trabecular bone provides larger surface area per matrix volume for remodelling to occur and is the site of earlier and more rapid bone loss. With ageing, the cortical bone undergoes increased remodelling leading to the widening of long bones, thinner cortices and increased remodelling spaces that are visualized as "pores" [2, 3]. When these changes are in great numbers, they can potentially result in a marked increase in bone fragility and heightened fracture risk.

The current concept of "bone quality" includes all levels of bone structure and material composition as determinants of bone strength [4, 5]. Although lower values of bone mineral density measured by dual-energy X-ray absorptiometry (DXA) and trabecular bone loss have been traditionally associated with increased fracture risk, newer high-resolution imaging techniques have highlighted the important and independent contribution of the cortical bone to overall bone strength and fragility [6–9]. Studies in people with chronic kidney disease (CKD), including after renal transplantation, have highlighted their enhanced susceptibility to fracture compared with age- and gender-matched controls [10–13] with consequent increases in hospitalization and mortality [14]. For the classification of bone structural abnormalities in patients with CKD, the development of the Kidney Disease Improving Global Outcomes "Turnover Mineralization Volume" (TMV) system [15] has been the most notable advancement because it provides clinically relevant descriptors. However, the assessment of cortical microarchitecture is described as an adjunct to the trabecular bone measurements. The common findings of cortical thinning and increased cortical porosity in recent studies of patients with CKD [16, 17] and their potential contribution to bone fragility suggest a need to emphasize the evaluation of cortical microarchitecture as a key parameter in addition to trabecular changes within the TMV classification.

In this cross-sectional study, we describe trabecular and cortical microarchitecture obtained by classical histomorphometry and micro-CT of iliac crest biopsies in participants with CKD G5 and 5D (dialysis). Micro-CT is an ex-vivo ultra-high resolution, non-destructive method to acquire direct three-dimensional (3D) measurements of cortical and cancellous bone microarchitecture and images a much larger volume of interest than two-dimensional (2D) histology.

Materials and Methods

Study Participants

Between December 2014 and January 2016, 14 participants, planned for living donor kidney transplantation ($n = 12$) and parathyroidectomy ($n = 2$), underwent transiliac bone biopsies at the completion of their surgical procedure. Inclusion criteria were CKD G.5 and 5D and non-participation in another trial at the time of recruitment. The protocol was approved by the local Ethics Committee and all patients provided informed consent.

Biochemical Measurements

Blood samples were obtained prior to surgery and analysed at the Royal Melbourne Hospital using standard laboratory analysis on an Elecsys Cobas autoanalyser system. Serum concentrations of intact parathyroid hormone (iPTH) were determined using Architect iPTH (Abbott Laboratories, USA) chemiluminescent microparticle immunoassay. Osteocalcin (OC) and procollagen type 1 N-terminal propeptide (P1NP), markers of osteoblast activity, and beta-cross linked telopeptides (β-CTx), a marker of osteoclastic resorption, were assayed by an electrochemiluminescence immunoassay (Elecsys®, Roche, Switzerland). Serum 1,25-dihydroxyvitamin D ($1,25[OH]_2D$) was measured by radioimmunoassay (Immunodiagnostic Systems Ltd.).

Bone Histomorphometry

Participants underwent double tetracycline labelling for bone histomorphometry, consisting of 3 days of doxycycline hydrochloride (100 mg twice daily), followed by a tetracycline-free interval of 10 days and then tetracycline hydrochloride (500 mg twice daily) for 3 days. Anterior iliac crest bone biopsies were obtained under general anaesthesia using a modified 7.5 mm Bordier trephine (Landanger) via a horizontal approach as described elsewhere [18]. The specimens were fixed in cold, neutral, buffered 10% formalin for up to 48 h and then dehydrated in 70% ethanol. The static and dynamic parameters were examined and reported as measurements in 2D using nomenclature established by the American Society for Bone and Mineral Research [19]. Normal ranges of bone histomorphometry [20, 21] and micro-CT [22, 23] derived parameters were defined from previously reported data and local experience. Final histomorphometry results were categorized according to the TMV classification [15].

Micro-CT

Micro-CT was performed by an experienced operator blinded to patient characteristics. Bone debris was first eliminated from the biopsy core (Fig. 1a), and the complete biopsy core was

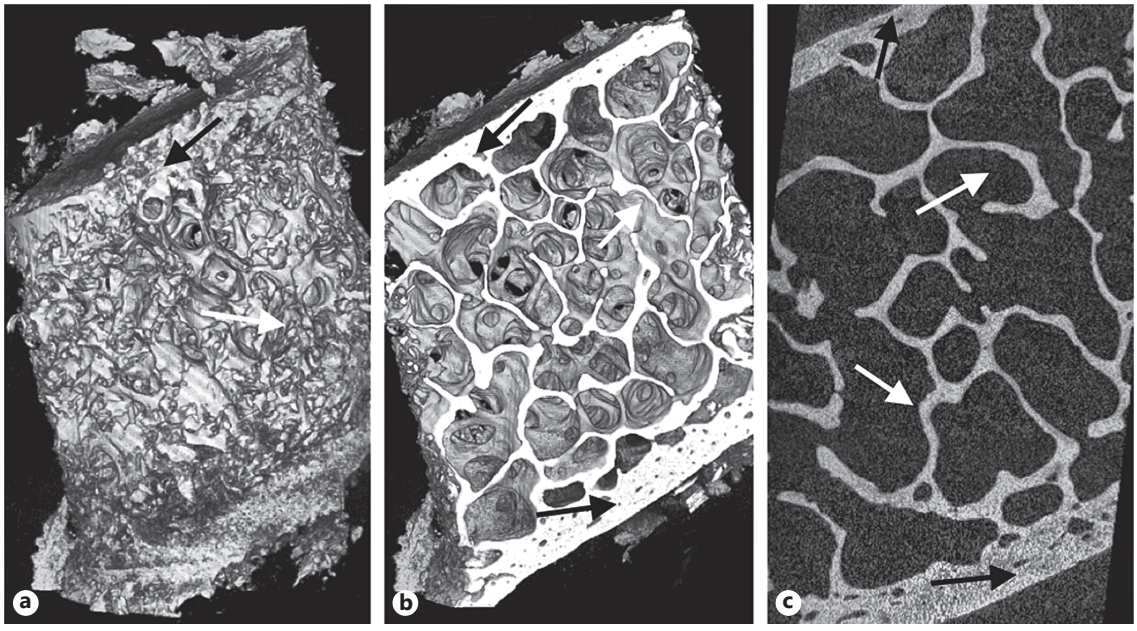

Fig. 1. Representative micro-CT images of a biopsy obtained from a study subject showing stages in processing (**a**) biopsy core with debris, (**b**) three-dimensional longitudinal slice, and (**c**) two-dimensional longitudinal slice. Trabecular bone, white arrows; Cortical bone, black arrows.

scanned using a Skyscan Model 1172 Micro-CT scanner (Bruker, Aartselar, Belgium) at 50 kV, 200 mA with a 0.5-mm aluminium filter using a isotropic voxel size of 4.3 microns. Images were captured every 0.4° through 180° and then reconstructed and analyzed using NRecon software (version 1.6.10.5; Bruker, Belgium). The average scan time was 60 min per sample. CTAnalyser software (version 1.16.1.0; Bruker, Belgium) was applied to quantify bone volume (BV) and architecture. Boundaries of the cortical and cancellous compartments, indicated in Figure 1b and c, were determined by X-ray attenuation of voxels on a grey scale from 1 – black, indicating empty space and no bone – to 255 – white, indicating most dense bone. A range from 1 to 59 for the cancellous compartment and 60–255 for the cortical compartment produced the best binary images for analysis of each compartment in the bone biopsy samples and these threshold values were maintained across all samples to ensure integrity of the study.

Three-dimensional analysis was applied to calculate morphometric parameters within the total cancellous compartment of each biopsy core, including trabecular BV to tissue volume (BV/TV), trabecular number (TbN) and trabecular thickness (TbTh). Using the binary images created by thresholding at 60–255 to exclude denser (cortical) areas of the biopsy, the cancellous region of interest (ROI) was then inverted to measure cortical BV (C.BV) and cortical bone thickness (CTh). Within the cortical ROI, total cortical porosity was calculated as the volume of all open and closed pores as a percentage of the total C.BV. The cortical thickness and porosity represent the mean of the 2 cortices for 10 biopsy samples, while in the remaining 4 samples, only the intact outer cortex was available for measurements. Analysis of the structure model index, which corresponds to the trabecular plate- or rod-like geometry, and the degree of anisotropy, for which higher values indicate disruption of trabecular network connectivity, was performed according to manufacturer's specifications.

Statistical Methods

Results are presented as mean (±SD) for normally distributed continuous variables and as median (and interquartile range [IQR]) for continuous variables with skewed distributions. Correlation analyses were conducted to investigate associations between parameters obtained by classical histomorphometry and those obtained by micro-CT as well as biomarkers. Pearson correlation coefficients were used to express the relationship between variables if both parameters were normally distributed. Spearman correlation coefficients were used if results of one or both parameters were not normally distributed. We compared the cortical structural parameters measured by micro-CT in subjects with or without high turnover and in subjects with or without normal mineralisation. A 2-tailed p value <0.05 was considered statistically significant. Stata statistical software package (version 11.0, Stata Corporation, College Station, TX, USA) was used for conducting the analysis.

Results

Participant Characteristics

Demographic and biochemical parameters of the study cohort are shown in Tables 1 and 2 respectively. The mean age of participants was 44.4 ± 10.3 years and

Table 1. Baseline demographic parameters (n = 14)

Variable	Values
Age at surgery, years	44.4±10.3
Gender, male, %	64.2
BMI, kg/m^2	27.1±4.8
Cause of CKD, %	
Glomerulonephritis	42.8
Diabetes mellitus	14.2
Polycystic kidney disease	14.2
Reflux nephropathy	21.4
Other	7.14
Dialysis: HD/PD/none, %	42.8/21.4/35.7
Parathyroidectomy, %	7.14
Bone modulating therapy, %	
Cinacalcet	7.14
Phosphate binder	57.1
Calcitriol	42.8
Cholecalciferol	21.4
Prednisolone	28.5

HD, haemodialysis; PD, peritoneal dialysis; BMI, body mass index; CKD, chronic kidney disease.

64.3% were male. Glomerulonephritis (42.8%) was the most common cause of CKD. Nine (64.2%) participants were on renal replacement therapy (hemodialysis n = 6; peritoneal dialysis n = 3) for a median duration of 8.5 (IQR 0–32.75) months, and 5 underwent preemptive living donor renal transplantation. Potential bone-modulating medications prescribed to participants are listed in Table 1. Median serum iPTH was 45.3 (24–66.5) pmol/L. Serum iPTH values were above the Kidney Disease Improving Global Outcomes CKD – Mineral and Bone Disorder Guidelines [24] target range of up to 9 times the normal upper reference range of the assay in 3 patients, 2 of whom were undergoing parathyroidectomy. Median values of bone turnover markers were elevated as expected for these markers in patients with CKD G5 and 5D. P1NP and β-CTx were approximately 2 times and OC was 4 times the normal upper reference value.

Bone Trephine Histomorphometry and Micro-CT Measures

On histomorphometry of the cancellous compartment, features of hyperparathyroidism and increased bone turnover were present in 50% (n = 7) of participants, while 21.4% (n = 3) had low or absent bone turnover and little or no evidence of bone resorption based on static indices of cellular activity; osteoblast, osteoclast and eroded surface to bone surface (Table 3). Features of osteomalacia, based on osteoid thickness, surface, volume and smeared or absent tetracycline label were present in 35.7% (n = 5). The mean trabecular BV was within the normal range (Table 4) and was low or low normal only in 28.6% of participants. The mean cortical thickness was 868 ± 410 μm (normal range 800–1,400 μm) and cortical porosity was 10.8 ± 8.2% (high >10%).

Quantitative histomorphometry by micro-CT was characterised by deterioration in cortical bone, with thin cortices (mean thickness 127 ± 44 μm) and high cortical porosity (60.3 ± 22.5%) in all participants. Trabecular parameters were relatively preserved (Table 4), with reduced trabecular BV in only 21.4% of participants.

Comparing results from micro-CT and histomorphometry, measures of cortical thickness showed no significant correlation but cortical porosity correlated significantly (0.56; p = 0.036). Cortical porosity by micro-CT correlated to values of iPTH (r = 0.62; p = 0.02) and was negatively correlated to TbN by micro-CT (r = –0.56; p = 0.03) and TbTh (r = –0.60; p = 0.02) by histomorphometry. Cortical thickness and porosity by micro-CT showed no significant variation with histomorphometric parmeters of mineralisation or with contemporaneous high or low turnover status. The median trabecular structure model index value was negative at –0.8 (–7.7 to 0.7; normal range 1.15 ± 0.61), indicative of cavities, and anisotropy was increased with the mean degree of anisotropy 2.04 ± 0.8 (normal range 1.49 ± 0.18), indicating fewer trabeculae in directions of lower load and disruption of trabecular network connectivity. Histomorphometry parameters arranged by the TMV classification are presented in Table 3 and structural parameters by both techniques are listed in Table 4.

Bone Biomarkers and Histomorphometry

Bone turnover markers correlated significantly with all histomorphometric remodelling indices. P1NP was positively correlated to osteoblast surface (r = 0.54; p = 0.04), osteoclast surface (r = 0.65; p = 0.01) and mineralization surface (r = 0.74; p = 0.002). Similarly, β-CTx was positively correlated to osteoblast surface (r = 0.61; p = 0.02), osteoclast surface (r = 0.66; p = 0.009) and mineralization surface (r = 0.77; p = 0.001). There was also a positive correlation of OC to both osteoblast surface (r = 0.65; p = 0.01) and mineralization surface (r = 0.75; p = 0.003). Serum 25(OH)D values were associ-

Table 2. Baseline biochemical parameters for KTRs and patients undergoing PTHx. Data presented as mean ± SD or median (IQR)

Biomarker	KTR (n = 12)	PTHx (n = 2)	Normal range
Calcium	2.44±0.1	2.46±0.3	2.10–2.60 mmol/L
Phosphate	2.07±0.3	2.83±0.2	0.75–1.50 mmol/L
Parathyroid hormone	38.4 (19–55)	246±101.6	1.7–10.0 pmol/L
Alkaline phosphatase	78 (63–121.5)	290±168.2	30–120 IU/L
25-hydroxyvitamin D	65.1±21.6	77.5±20.5	55–108 nmol/L
1,25-dihydroxyvitamin D	29 (20–70)	N/A[#]	50–190 nmol/L
Osteocalcin	149.2 (30.9–203.6)	895±841.4	14–46 ng/mL
Beta-cross linked telopeptide	1.26 (0.82–2.48)	6.0±0.0	Males 0.1–0.6 ng/mL Females* 0.05–0.8 ng/mL
Procollagen type 1 N-propeptide	123.6 (47.3–262.1)	1,665±657.6	Males 15–80 μg/L Females* 15–90 μg/L

* Premenopausal reference range.

[#] Patients undergoing parathyroidectomy were pre-loaded with calcitriol, which would influence these results. Values of serum osteocalcin, beta-cross linked telopeptide and procollagen type 1 N-propeptide increase above the normal range in patients with reduced renal function.

KTRs, kidney transplant recipients; PTHx, parathyroidectomy; IQR, interquartile range.

Table 3. Parameters measured by histomorphometry arranged by the TMV classification (n = 14). Data presented as mean ± SD or median (IQR)

TMV	Variable	Value	Normal range
Turnover*	Ob.S/BS, %	6.5 (2.9–16.6)	5.3±2.7
	ES/BS, %	2.8 (0.4–5.2)	0.4–3.4
	Oc.S/BS, %	3.4 (0.4–6.5)	0.5–2.5
	sLS/BS, %	16.4 (4.9–37.2)	0.5–10.5
Mineralization	OV/BV, %	2.1 (0.8–9.2)	1.3–3.1
	OS/BS, %	11.6 (8.4–32.6)	7.1–13.9
	O.Th, μm	14.1±9.1	9.2–14.9
Volume	BV/TV, %	27±1.1	21–29

* In patients with features of hyperparathyroidism, the mineral apposition rate varied from 0.77 to 1.08 μm/day (normal range 0.6–0.8 μm/day) and bone formation rate from 0.09 to 0.62 mm^3/mm^2/day (normal range 0.03–0.09 mm^3/mm^2/day). No label was detected for patients with adynamic bone and patients with normal bone surfaces had indices in the intermediate range or smeared label for mixed uraemic osteodystrophy. Due to difficulty reading the doxycycline label in some biopsies, sLS/BS is provided.

Ob.S/BS, osteoblast surface/bone surface; ES/BS, eroded surface; Oc.S/BS, osteoclast surface; sLS/BS, single-labelled surface (mineralising surface); OV/BV, osteoid volume/bone volume; OS/BS, osteoid surface; O.Th, osteoid thickness; BV/TV, cancellous bone volume/total volume; IQR, interquartile range.

ated with indices of resorption – osteoclast surface (r = 0.62; p = 0.02) and osteoclast number (r = 0.62; p = 0.01) – and mineralization surface (r = 0.64; p = 0.01). Serum $1,25(OH)_2D$ values were associated with osteoid width (r = –0.86; p = 0.001). There were no significant relationships of bone biomarkers to other structural parameters derived by histomorphometry or micro-CT.

Discussion

Cortical bone constitutes approximately 80% of the adult skeleton and its contribution to fracture resistance is well recognised. However, relatively few studies have endeavoured to use histomorphometry [25, 26] or micro-CT of bone trephine samples, or utilised non-invasive techniques [16, 17, 27] to assess cortical microarchi-

Table 4. Microarchitectural parameters measured by 2D histomorphometry and micro-CT (n = 14). Data presented as mean ± SD or median (IQR)

	Variable	Mean ± SD	Normal range
Histomorphometry	BV/TV, %	27.1±11.5	21–29
	TbTh, μm	157.6±60.1	90–175
	TbN, 1/mm	1.83±0.75	1.1–2.2
	TbSp, μm	368.5 (273.3–566.4)	770
Micro-CT	BV/TV, %	20.3±7.0	15.6±5.4
	TbTh, μm	110±37.0	151±27
	TbN, 1/mm	2.20±1.44	1.4±0.27
	TbSp, μm	593±203	747±150
	Mean cortical thickness, μm	127±44	381±120*
	Cortical porosity, %	60.31±22.53	4–10*

* Average values only; cortical thickness and porosity vary by gender and age.

BV/TV, trabecular bone volume; TbTh, trabecular thickness; TbN, trabecular number; TbSp, trabecular separation; IQR, interquartile range.

tecture and porosity in patients with CKD G5, 5D or after kidney transplantation. In the current study, 50% of patients had changes consistent with high bone turnover on histomorphometry, accompanied by elevated PTH values, but all participants had markedly abnormal cortical microarchitecture assessed by micro-CT with relatively preserved trabecular structural parameters. This severe cortical bone loss is remarkable, given that patients in this study were relatively young (mean 44.4 ± 10.3 years) and healthy, with the majority undergoing transplantation, compared with older and non-transplantable patients with CKD G5 and 5D. However, these characteristics also limit the extrapolation of our results to a general dialysis population. Of note, the cortical abnormalities were not as prominent by histomorphometry and values for cortical thickness by micro-CT and histomorphometry were not significantly correlated. Differences in cortical thickness are unlikely to be due to the segmentation threshold used for delineation of cortex from the cancellous compartments by micro-CT, since the thresholding value was consistent throughout the samples. More likely, differences in thickness and porosity relate to the limited portion of cortex assessed in 2D by histomorphometry versus the entire cortex assessed in 3D by micro-CT.

Physiological remodelling of bone with aging, or rapid unbalanced remodelling associated with metabolic disease plays a key role in the pathogenesis of cortical bone loss. Trabecular bone has a high surface-to-matrix-volume ratio and provides a larger surface for initiation of remodelling compared with cortical bone. Interestingly, the bone turnover markers P1NP, β-CTx and OC correlated to histomorphometric remodelling indices in this study, despite the recognised difficulty of interpreting these markers due to rises that accompany deteriorating renal function. Serum 25(OH)D values also correlated to indices of resorption and mineralization. While vitamin D and its metabolites may have local actions in the bone environment that include the facilitation of mineral deposition and the enhancement of bone resorption [28], the basis of these associations is unclear.

Cortical bone, although traditionally described as being compact, is traversed by Haversian and Volkmann canals, which provide the intracortical surface for remodelling. Over time, with fewer trabecular sites available for remodelling, there is increased bone loss from the cortical compartment. Increased remodelling at intracortical and endocortical surfaces, and uncoupling of bone formation from resorption, lead to incomplete refilling of cavities and widening of canals, and increases the available cortical surface area for the initiation of remodelling events. This results in the "trabecularisation" of the cortex and increased cortical porosity [3]. A small increase in cortical porosity disproportionately affects bone strength and may potentially contribute to bone fragility [9, 29]. This is significant, given that more than 70% of all fractures occur at non-vertebral sites [30, 31] that are rich in both cortical and trabecular bone. A number of studies have demonstrated a relationship of fracture to the deterioration of cortical architecture with aging and metabolic disease [3, 6–8].

To our knowledge, this study is the first to report the role of micro-CT in assessing cortical porosity in patients with CKD. Data on cortical porosity in the CKD population is derived mainly from studies using HR-pQCT, an imaging modality prone to certain limitations in quantifying cortical bone structure [32]. For example, trabecularisation of cortical bone may cause potential measurement errors in segmentation between cortical and trabecular bone compartments, leading to the overestimation of trabecular density or underestimation of cortical porosity [3, 33]. HR-pQCT does not have the requisite resolution to measure cortical pores smaller than 100 μm, which constitute about 60% of total pores, and this leads to significant underestimation of total cortical porosity [29]. The average cortical porosity defined by HR-pQCT is approximately 3–7% [34] compared with a cortical void volume of 15–40% derived by direct measurements of cortical bone water identified in MRI studies [35, 36]. However, the very high mean cortical porosity in our study (mean 60.3 ± 22.5%), representing a higher number of larger "pores" is likely to reflect uncoupled, largely PTH-mediated cortical remodelling, and can only be partly attributed to identification of larger numbers of pores by micro-CT due to its higher resolution. In such a scenario, the relatively normal trabecular structure observed in our study may represent a differential action of PTH on trabecular and cortical bone compartments.

This study supports recent histomorphometric [25, 26, 37, 38] and imaging studies [16, 17, 27, 39, 40] that have reported changes in cortical bone microarchitecture in individuals with CKD. In a cross-sectional study involving 38 dialysis patients, Adragao et al. [25] reported high cortical porosity in 57% and reported a significant inverse relationship between femoral bone mineral density and cortical porosity. The presence of high cortical porosity and reduced cortical thickness in dialysis patients was also reported by Malluche et al. [26] in a large histomorphometry study of 630 bone biopsies. Cortical porosity was related to hyper-resorption and high turnover, and varied with race, being present in 50% of white and 75% of black patients, while reduced cortical thickness was reported in 50% of white patients and 10% of black patients. In a recent post hoc analysis of histomorphometry data from a randomized controlled trial [41], Araujo et al. [38] reported high cortical porosity in 85% of 52 hemodialysis patients at baseline and a subsequent increase in both PTH levels and cortical porosity in patients who were treated for low bone turnover. Similarly, imaging studies have described abnormal cortical bone microarchitecture [39], progressive cortical loss and increased cortical porosity to be associated with hyperparathyroidism in patients with CKD [16] including kidney transplant recipients [40]. In the TMV classification, the measurement of cortical BV and thickness is described as additional information to that provided by the trabecular BV [15]. However, the current and aforementioned studies emphasize the importance of describing cortical microarchitecture as a central parameter of the TMV classification, together with the trabecular parameters.

Our study has some limitations including its cross-sectional nature and small sample size without a non-CKD control group. The sample size limits statistical robustness, and as a single-center study with 13 of 14 patients being Caucasian, the generalisability of our findings to other centers and racial groups may be limited. Four patients in our cohort were on maintenance prednisolone therapy at the time of transplantation and this might have contributed to the overall finding of abnormal bone structure in our patients. It is, however, hard to delineate these manifestations from those due to ESKD in a small cohort. The thresholding method of segmentation between cortical and cancellous compartments used in our micro-CT analysis has known limitations. Inaccuracy in differentiating cortical and trabecular bone by thresholding can potentially result in overestimation of trabecular parameters, which may be reflected in our finding of relatively normal trabecular indices [33]. Some voxels being evaluated for cortical porosity may contain varying proportions of void volume and mineralized bone matrix. In such voxels, the photo-attenuation caused by mineralized bone may lead to the underestimation of the void volume and cortical porosity [42]. These potential measurement errors, if applied to our study, may present a more severe picture of both cortical and trabecular architecture in our cohort. Despite these limitations, this study is one of relatively few to report cortical microstructure and the first to utilize micro-CT to measure cortical porosity and thickness from 3D sections in a CKD-G5 and 5D cohort.

In summary, this study highlights a marked deterioration of cortical bone microarchitecture in CKD. Cortical porosity has an established role in bone fragility, and a focus on cortical changes represents a significant shift in the assessment of renal osteodystrophy that may have diagnostic and treatment implications. In addition to the TMV classification of trabecular bone, the assessment of the cortex ("C") requires emphasis, but to establish an association of cortical porosity and thickness to fractures in

people with CKD, prospective studies are required. Such studies, using newer non-invasive means to assess the cortical and cancellous compartments that can be readily repeated over time, might lead to interventions using cortical bone as a therapeutic target.

Acknowledgement

We acknowledge and thank Dr. Emma Tully, Department of Nephrology Surgery, RMH, for performing iliac crest biopsies.

Disclosure Statement

S.G.H. has received funding and honoraria from Amgen, Baxter and Sanofi, and honoraria from Astra-Zeneca. RM has received funding from Amgen.

The results presented in this paper have not been published previously in whole or part, except in the abstract format.

Funding Source

We acknowledge and thank Amgen Australia for providing an unrestricted educational grant that partly funded this study.

References

1 Clarke B: Normal bone anatomy and physiology. Clin J Am Soc Nephrol 2008;3(suppl 3): S131–S139.
2 Seeman E: Pathogenesis of bone fragility in women and men. Lancet 2002;359:1841–1850.
3 Zebaze RM, et al: Intracortical remodelling and porosity in the distal radius and postmortem femurs of women: a cross-sectional study. Lancet 2010;375:1729–1736.
4 Seeman E, Delmas PD: Bone quality – the material and structural basis of bone strength and fragility. N Engl J Med 2006;354:2250–2261.
5 Malluche HH, Porter DS, Pienkowski D: Evaluating bone quality in patients with chronic kidney disease. Nat Rev Nephrol 2013;9:671–680.
6 Nishiyama KK, et al: Postmenopausal women with osteopenia have higher cortical porosity and thinner cortices at the distal radius and tibia than women with normal aBMD: an in vivo HR-pQCT study. J Bone Miner Res 2010; 25:882–890.
7 Patsch JM, et al: Increased cortical porosity in type 2 diabetic postmenopausal women with fragility fractures. J Bone Miner Res 2013;28: 313–324.
8 Bala Y, et al: Cortical porosity identifies women with osteopenia at increased risk for forearm fractures. J Bone Miner Res 2014;29: 1356–1362.
9 Bala Y, Zebaze R, Seeman E: Role of cortical bone in bone fragility. Curr Opin Rheumatol 2015;27:406–413.
10 Alem AM, et al: Increased risk of hip fracture among patients with end-stage renal disease. Kidney Int 2000;58:396–399.
11 Ball AM: Risk of hip fracture among dialysis and renal transplant recipients. JAMA 2002; 288:3014–3018.
12 Naylor KL, et al: The three-year incidence of fracture in chronic kidney disease. Kidney Int 2014;86:810–818.
13 Hansen D: et al: Risk of fracture in adults on renal replacement therapy: a Danish national cohort study. Nephrol Dial Transplant 2016; 31:1654–1662.
14 Tentori F, et al: High rates of death and hospitalization follow bone fracture among hemodialysis patients. Kidney Int 2014;85:166–173.
15 Moe S, et al: Definition, evaluation, and classification of renal osteodystrophy: a position statement from Kidney Disease: Improving Global Outcomes (KDIGO). Kidney Int 2006; 69:1945–1953.
16 Nickolas TL, et al: Rapid cortical bone loss in patients with chronic kidney disease. J Bone Miner Res 2013;28:1811–1820.
17 Nishiyama KK, et al: Longitudinal HR-pQCT and image registration detects endocortical bone loss in kidney transplantation patients. J Bone Miner Res 2015;30:554–561.
18 Hernandez JD, et al: Technical approach to iliac crest biopsy. Clin J Am Soc Nephrol 2008;3(suppl 3):S164–S169.
19 Dempster DW, et al: Standardized nomenclature, symbols, and units for bone histomorphometry: a 2012 update of the report of the ASBMR Histomorphometry Nomenclature Committee. J Bone Miner Res 2013;28: 2–17.
20 Malluche HH, Faugere MC: Atlas of Mineralized Bone Histology. 1986. Karger, New York.
21 Malluche HH, et al: Quantitative bone histology in 84 normal American subjects. Calcif Tissue Int 1982;34:449–455.
22 Hildebrand T, et al: Direct three-dimensional morphometric analysis of human cancellous bone: microstructural data from spine, femur, iliac crest, and calcaneus. J Bone Miner Res 1999;14:1167–1174.
23 Kulak CA, et al: Skeletal microstructural abnormalities in postmenopausal women with chronic obstructive pulmonary disease. J Bone Miner Res 2010;25:1931–1940.
24 Kidney Disease: Improving Global Outcomes (KDIGO) CKD-MBD Work Group: KDIGO clinical practice guideline for the diagnosis, evaluation, prevention, and treatment of Chronic Kidney Disease-Mineral and Bone Disorder (CKD-MBD). Kidney Int Suppl 2009;113:S1–S130.
25 Adragao T, et al: Femoral bone mineral density reflects histologically determined cortical bone volume in hemodialysis patients. Osteoporos Int 2010;21:619–625.
26 Malluche HH, Mawad HW, Monier-Faugere MC: Renal osteodystrophy in the first decade of the new millennium: analysis of 630 bone biopsies in black and white patients. J Bone Miner Res 2011;26:1368–1376.
27 Rajapakse CS, et al: Micro-MR imaging-based computational biomechanics demonstrates reduction in cortical and trabecular bone strength after renal transplantation. Radiology 2012;262:912–920.
28 Eisman JA, Bouillon R: Vitamin D: direct effects of vitamin D metabolites on bone: lessons from genetically modified mice. Bonekey Rep 2014;3:499.
29 Cooper DM, et al: Cortical bone porosity: what is it, why is it important, and how can we detect it? Curr Osteoporos Rep 2016;14:187–198.
30 Roux C, et al: Burden of non-hip, non-vertebral fractures on quality of life in postmenopausal women: the Global Longitudinal study of Osteoporosis in Women (GLOW). Osteoporos Int 2012;23:2863–2871.
31 Rosengren BE, et al: The 21st-century landscape of adult fractures: cohort study of a complete adult regional population. J Bone Miner Res 2015;30:535–542.
32 Geusens P, et al: High-resolution in vivo imaging of bone and joints: a window to microarchitecture. Nat Rev Rheumatol 2014;10: 304–313.
33 Zebaze R, Seeman E, Cortical bone: a challenging geography. J Bone Miner Res 2015;30: 24–29.
34 Burghardt AJ, et al: Reproducibility of direct quantitative measures of cortical bone microarchitecture of the distal radius and tibia by HR-pQCT. Bone 2010;47:519–528.

35 Techawiboonwong A, et al: Cortical bone water: in vivo quantification with ultrashort echo-time MR imaging. Radiology 2008;248: 824–833.
36 Rajapakse CS, et al: Volumetric cortical bone porosity assessment with MR imaging: validation and clinical feasibility. Radiology 2015; 276:526–535.
37 Carvalho C, et al: Cortical bone analysis in a predialysis population: a comparison with a dialysis population. J Bone Miner Metab 2016.
38 Araujo MJ, et al: The pitfall of treating low bone turnover: effects on cortical porosity. Bone 2016;91:75–80.
39 Wehrli FW, et al: Quantitative high-resolution magnetic resonance imaging reveals structural implications of renal osteodystrophy on trabecular and cortical bone. J Magn Reson Imaging 2004;20:83–89.
40 Iyer SP, et al: Kidney transplantation with early corticosteroid withdrawal: paradoxical effects at the central and peripheral skeleton. J Am Soc Nephrol 2014;25:1331–1341.
41 Barreto DV, et al: Phosphate binder impact on bone remodeling and coronary calcification–results from the BRiC study. Nephron Clin Pract 2008;110:c273–c283.
42 Zebaze R, et al: A new method of segmentation of compact-appearing, transitional and trabecular compartments and quantification of cortical porosity from high resolution peripheral quantitative computed tomographic images. Bone 2013;54:8–20.

Bone 114 (2018) 14–21

Contents lists available at ScienceDirect

Bone

journal homepage: www.elsevier.com/locate/bone

Full Length Article

Magnetic resonance imaging based assessment of bone microstructure as a non-invasive alternative to histomorphometry in patients with chronic kidney disease

Ashish K. Sharma[a,b,*], Nigel D. Toussaint[a,b], Grahame J. Elder[c,d], Rosemary Masterson[a,b], Stephen G. Holt[a,b], Patricia L. Robertson[b,e], Peter R. Ebeling[f], Paul Baldock[d], Rhiannon C. Miller[g], Chamith S. Rajapakse[g]

[a] Department of Nephrology, The Royal Melbourne Hospital, Parkville, Australia
[b] Department of Medicine (RMH), University of Melbourne, Parkville, Australia
[c] Department of Renal Medicine, Westmead Hospital, Westmead, Australia
[d] Osteoporosis and Bone Biology Division, Garvan Institute of Medical Research, Darlinghurst, Australia
[e] Department of Radiology, The Royal Melbourne Hospital, Parkville, Australia
[f] Monash University, Clayton, Australia
[g] Departments of Radiology and Orthopaedic Surgery, University of Pennsylvania, PA, USA

ARTICLE INFO

Keywords:
Renal osteodystrophy
Bone biopsy
Magnetic resonance imaging
Micro computed tomography
Bone mineral density
Bone turnover

ABSTRACT

Background: Chronic kidney disease (CKD) adversely affects bone microarchitecture and increases fracture risk. Historically, bone biopsy has been the 'gold standard' for evaluating renal bone disease but is invasive and infrequently performed. High-resolution magnetic resonance imaging (MRI) quantifies bone microarchitecture noninvasively. In patients with CKD, it has not been compared with results derived from bone biopsy or with imaging using dual energy X-ray absorptiometry (DXA).

Methods: Fourteen patients with end-stage kidney disease (ESKD) underwent MRI at the distal tibia, bone mineral density (BMD) by dual energy X-ray absorptiometry (DXA; hip and spine) and transiliac bone biopsies with histomorphometry and microcomputed tomography (micro-CT). All patients had biomarkers of mineral metabolism. Associations were determined by Spearman's or Pearson's rank correlation coefficients.

Results: MRI indices of trabecular network integrity, surface to curve ratio (S/C) and erosion index (EI), correlated to histomorphometric trabecular bone volume (S/C $r = 0.85$, $p = 0.0003$; EI $r = -0.82$, $p = 0.001$), separation (S/C $r = -0.58$, $p = 0.039$; EI $r = 0.79$, $p = 0.0012$) and thickness (S/C, $r = 0.65$, $p = 0.017$). MRI EI and trabecular thickness (TbTh) also correlated to micro-CT trabecular separation (EI $r = 0.63$, $p = 0.02$; TbTh $r = -0.60$, $p = 0.02$). Significant correlations were observed between histomorphometric mineralization and turnover indices and various MRI parameters. MRI-derived trabecular parameters were also significantly related to femoral neck BMD.

Conclusions: This study highlights the heterogeneity of bone microarchitecture at differing skeletal sites. MRI demonstrates significant, relevant associations to important bone biopsy and DXA indices and warrants further investigation to assess its potential to non-invasively evaluate changes in bone structure and quality over time.

1. Introduction

Renal osteodystrophy (ROD) refers to changes in bone quality associated with chronic kidney disease (CKD), and has been defined by changes to histomorphometric parameters of turnover, mineralization, and volume (TMV) [1]. Progressive decline in renal function adversely affects bone microarchitecture, mineralization, collagen structure and marrow composition. This may result in deterioration in both cancellous and cortical bone architecture to varying degrees. Structural changes in ROD include alterations in thickness, number and spacing of trabecular bone and disruption to its orientation, connectivity, and the ratio of its plate-like to rod-like structure. Similarly, abnormal bone remodelling and turnover results in thinned cortices and increased cortical porosity. These trabecular and cortical changes may lead to a loss of overall bone volume and increased bone fragility [2, 3].

Patients with CKD have significantly more fractures than age- and

* Corresponding author at: Department of Nephrology, The Royal Melbourne Hospital, Grattan Street, Parkville, Victoria 3052, Australia.
E-mail address: a.k.sharma@hotmail.com (A.K. Sharma).

https://doi.org/10.1016/j.bone.2018.05.029
Received 2 November 2017; Received in revised form 22 May 2018; Accepted 29 May 2018
Available online 31 May 2018

gender-matched individuals without CKD [4]. The risk of sustaining a fracture increases progressively as the glomerular filtration rate (GFR) falls [5] and persists in the early years after transplantation [6]. Moreover, fractures in patients with CKD are associated with increased morbidity and mortality compared to the general population [7]. Whilst recent epidemiological studies have emphasized the increased fracture risks of CKD [8, 9], tools used in clinical practice to evaluate ROD, including dual-energy X-ray absorptiometry (DXA) to assess bone mineral density (BMD) and biochemical bone turnover markers, have more diagnostic limitations in patients with CKD than in the general population. Bone biopsy and quantitative histomorphometry, the 'gold standard' for diagnosis and classification of ROD, is invasive, expensive, requires expertise to perform, process and interpret and is rarely used in clinical practice. Furthermore, the microstructure of the non-weight bearing iliac crest may differ in strength and structure from the peripheral skeleton, where clinically relevant fractures often occur. This has led to a search for reliable biomarkers and non-invasive high-resolution imaging modalities such as high-resolution peripheral computed tomography (HR-pQCT) [10, 11], to determine bone microarchitecture and to estimate bone strength in-vivo.

High-resolution magnetic resonance imaging (MRI) is a non-ionising and non-invasive method for quantification of bone microstructure in-vivo [12]. Clinical studies using MRI scans at peripheral anatomical sites have reported associations between bone structure and fracture in non-CKD cohorts [13]. Additionally, the long-term impact of therapeutic interventions on the structural and mechanical components of bone microarchitecture [14–16] can be evaluated using MRI. Despite these putative advantages, few studies have examined its role in ROD [17–20] or its utility in evaluating changes in cortical and trabecular microarchitecture in patients with CKD. Moreover, in patients with CKD, the relationship of structural parameters obtained by in-vivo MRI to those derived from bone biopsy has not been explored. If validated, MRI has the potential to assess bone microstructure and estimate structural manifestations of strength at any anatomical site, including common sites of fracture such as the hip, a site at which feasibility studies have proven encouraging [21, 22].

The aim of this study was to compare information on bone structure obtained from non-invasive MRI at the distal tibia, to parameters obtained from transiliac bone biopsies submitted to standard histomorphometry and microcomputed tomography (micro-CT). Micro-CT analyses a much larger volume of interest compared with two-dimensional (2D) histology and is a non-destructive method to acquire direct three-dimensional (3D) measurements of cortical and cancellous bone microarchitecture, providing greater structural detail. In addition to comparing bone structure parameters, we also assessed the relationship of MRI to BMD obtained by DXA, the current standard of care in clinical practice, and to laboratory indices. For this study, we recruited patients with CKD stage 5 or 5D (on dialysis), who were likely on clinical grounds to have ROD, with a range of structural bone abnormalities.

2. Materials and methods

2.1. Study participants

A total of 31 patients were approached, including 27 patients planned for living donor kidney transplantation and four patients on hemodialysis awaiting parathyroidectomy. Five transplant surgeries were rescheduled or cancelled for clinical or logistical reasons. Sixteen of the remaining 26 patients consented and were recruited between December 2014 and January 2016, with 14 undergoing living donor kidney transplantation and two undergoing parathyroidectomies. Fourteen of the patients underwent transiliac bone biopsies at completion of the surgical procedure whilst under general anesthesia (12 after renal transplantation and 2 after parathyroidectomy). Inclusion criteria were end-stage kidney disease (ESKD), no contraindications to MRI, and non-participation in another trial. The protocol was approved by the local ethics committee and all patients provided informed consent.

2.2. MRI

MRI images were obtained within a 2-week period preceding the surgery with a commercial 3.0-Tesla whole-body imager (Siemens Trio, Germany). Participants were imaged in a feet-first prone position. MRI acquisitions were performed at the left distal tibial metaphysis using a 3D 'fast spin echo' pulse sequence readily available on any clinical MRI system requiring a scan time of 12 min. This was undertaken utilizing a commercially available eight-channel radiofrequency (RF) extremity coil used in clinical practice. MRI parameters include 0.273 mm × 0.273 mm × 0.6 mm voxel size, 70 mm × 70 mm × 19.2 mm field-of-view, 53 ms repetition time, 16 ms echo time, 12 averages, and echo train length of two. Raw MRI data was pre-processed via bone volume fraction (BVF) mapping and segmentation of the bone into trabecular and cortical compartments for structural measurements and topological analysis using published algorithms [12, 19]. In brief, segmentation was determined by delineating the periosteal and endosteal boundaries of the bone using an operator-guided semi-automatic algorithm using a custom-built software [19] and standard microarchitecture parameters were derived for trabecular and cortical bone (Table 1). Topological analysis of the trabecular network was performed as previously described and two composite parameters, reported to be sensitive to microstructural change were also calculated [23, 24]. The surface/

Table 1
Bone microarchitecture parameters measured by MRI, micro-CT and histomorphometry.

	Variable	Mean ± SD	Normal range [28–31]
MRI (tibia)[#]			
	BV/TV (%)	10.4 ± 2.2	
	TbTh (μm)	126 ± 5.6	
	TbN (1/mm)	0.82 ± 0.14	
	TbS (μm)	1120 ± 23	
	Cortical thickness (μm)	2632 ± 545	
	S/C	5.51 ± 1.36	
	EI	0.91 ± 0.25	
Transiliac biopsies			
Micro-CT	BV/TV (%)	20.3 ± 7.1	15.6 ± 5.4%
	TbTh (μm)	110 ± 37.0	150 ± 30 μm
	TbN (1/mm)	2.20 ± 1.44	1.4 ± 0.27/mm
	TbS (μm)	593 ± 203	770 ± 350
	Mean single cortical thickness (μm)	127 ± 44	381 ± 120[*]
	Cortical porosity (%)	60.3 ± 22.5	4–10%[*]
	Structure model index	−0.8 (−7.7 to 0.7)[^]	1.15 ± 0.61
	Degree of anisotropy	2.04 ± 0.8	1.49 ± 0.18
	Connectivity density ($1/\mu m^3$)	31 (−59 to 101)	–
Histomorphometry	BV/TV (%)	27.1 ± 11.6	21–29%
	TbTh (μm)	157.7 ± 60.2	90–175 μm
	TbN (1/mm)	1.83 ± 0.75	1.1–2.2/mm
	TbS (μm)	368.5 (273.3–566.4)	280–658 μm

Abbreviations: Trabecular bone volume (BV/TV %), trabecular thickness (TbTh), trabecular number (TbN), trabecular separation (TbS), surface to curve ratio (S/C), erosion index (EI).

[*] Cortical thickness and porosity vary by age and sex. Thresholding and voxel size may differ from current study.

[^] Median (Range).

[#] No validated normative data is currently available for structural parameters derived by MRI.

curve ratio (S/C) is the ratio of all surface voxels to all curve voxels with the former representing plate like elements and the latter being a marker of rod like elements of the trabecular network. A higher S/C ratio indicates a higher ratio of trabecular plates to rods, which is a hallmark of trabecular network integrity. The other parameter is the erosion index (EI), the ratio of topological parameters expected to increase to those parameters likely to decrease with network erosion caused by osteoclastic resorption. A higher ratio is consistent with greater deterioration.

2.3. Micro-computed tomography

Transiliac bone biopsies were performed under general anesthesia at the end of the renal transplant or parathyroidectomy using a modified Bordier trephine [25]. Specimens were fixed in cold neutral buffered formalin 10% for up to 48 h and then dehydrated in 70% ethanol. The intact iliac crest cores were analysed using a Skyscan Model 1172 Micro-CT scanner (Bruker, Aartselar, Belgium) at 50 kV, 200 mA with a 0.5-mm aluminium filter using a pixel size of 4.3 μm. Scanned images were captured every 0.4° through 180°, reconstructed and analysed by NRecon (software version 1.6.10.5; Bruker, Belgium). CTAnalyser software (version 1.16.1.0; Bruker, Belgium) to quantify bone volume and architecture. Boundaries of the cortical and cancellous compartments were determined by X-ray attenuation of voxels on a grey scale from 1; black, indicating empty space and no bone, to 255; white, indicating most dense bone. A range from 1 to 59 for the cancellous compartment and 60–255 for the cortical compartment produced the best binary images for analysis of each compartment in the samples and these threshold values were maintained across all samples. Three-dimensional analysis was applied to calculate standard morphometric parameters within the total cancellous and cortical compartments of each biopsy core (Table 1). The cortical porosity was calculated as the volume of all open and closed 'pores' as a percentage of the total cortical bone volume, and cortical thickness represented the mean of two cortices for 10 biopsy samples, while in the remaining four samples only the intact outer cortex was available for measurements. Other derived parameters included structure model index (SMI), indicating trabecular plate or rod-like geometry, degree of anisotropy (DA) and connectivity density, which are surrogates for trabecular connectivity. Micro-CT nomenclature and units accord with published guidelines [26].

2.4. Bone histomorphometry

Histomorphometry was performed on the non-decalcified iliac crest biopsies following completion of the micro-CT examination. Prior to biopsy, participants had three days of doxycycline hydrochloride (100 mg twice daily), followed by a tetracycline-free interval of 10–14 days and then tetracycline hydrochloride (500 mg twice daily) for three days, with the biopsy performed three to five days later. Static parameters were reported as measurements in two dimensions using established nomenclature [27]. Bone turnover activity was assessed from static indices including osteoblast surface and number and osteoclast surface, number and perimeter/eroded fraction, in addition to tetracycline labeled perimeter/bone perimeter, mineral apposition rate and bone formation rate derived from the tetracycline labels. Normal ranges of bone histomorphometry, and micro-CT derived parameters were defined from previously reported data [28–31] and local experience. Final histomorphometry results were categorized according to the TMV classification [1].

2.5. DXA

Participants scheduled for kidney transplantation ($n = 14$) underwent BMD measurements by DXA (QDR-4500 Discovery, Hologic, Waltham, MA), at the lumbar spine, femoral neck and total proximal femur. BMD values were expressed in g/cm^2 and as T- and *Z*-scores. All DXA scans were performed at one center by a single operator not involved in the care of study participants and blinded to other study measurements.

2.6. Biochemical measurements

All biochemical measurements were performed at The Royal Melbourne Hospital prior to surgery. These included serum levels of creatinine, calcium, phosphate, 25-hydroxyvitamin D (25(OH)D), intact parathyroid hormone (iPTH) and alkaline phosphatase (ALP). The estimated GFR (eGFR) was calculated according to the Chronic Kidney Disease Epidemiology Collaboration (CKD-EPI) formula for non-dialysis patients. All biochemical markers were measured using standard assays and analyses were performed according to the manufacturer's instructions. Serum concentrations of iPTH were determined using Architect Intact PTH (Abbott Laboratories, USA) chemiluminescent microparticle immunoassay (CMIA).

2.7. Statistical methods

Results are presented as mean (± standard deviation [SD]) for normally distributed continuous variables and as median (and interquartile range) for continuous variables with skewed distributions. Correlation analyses were conducted to investigate associations between BMD and bone structural parameters, obtained at different anatomical locations using the different imaging techniques and histomorphometry, as well as biomarkers. Pearson correlation coefficients were used to express the relationship between variables if both parameters were normally distributed. Spearman correlation coefficients were used if results of one or both parameters were not normally distributed. Independent sample *t*-test or Mann-Whitney tests were used to explore associations between MRI parameters and TMV parameters. A two-tailed p value < 0.05 was considered statistically significant. Stata statistical software package (version 11.0, Stata Corporation, College Station, TX) was used for analysis.

3. Results

3.1. Patient characteristics

The mean age of patients at the time of surgery was 46.0 ± 11.3 years with 62.5% being male. Glomerulonephritis was the predominant cause of ESKD in the cohort (37.5%) followed by reflux nephropathy (18.8%) and diabetes (18.8%). At the time of surgery 11 of 16 patients were on renal replacement therapy (hemodialysis [HD] $n = 7$; peritoneal dialysis [PD] $n = 4$) for a median duration of 20.5 months (5–34.2 months), whilst 5 of 16 were scheduled for preemptive living donor renal transplantation. One patient, a 30-year-old female undergoing parathyroidectomy, had a history of a low trauma fracture. Another, 50-year female recipient of a kidney transplant had a prior history of parathyroidectomy. Potential bone modulating treatment used by participants in our cohort involved phosphate binders ($n = 8$, 50%), prednisolone ($n = 4$, 25%), calcimimetics ($n = 1$, 6.3%) and calcitriol ($n = 5$, 31.3%). Median serum iPTH was 45.3 (26.8–64.8) pmol/L, and in four patients, iPTH values were above the Kidney Disease Improving Global Outcomes (KDIGO) recommended target range of up to nine times the normal upper reference range of the iPTH assay.

Representative images illustrating trabecular and cortical compartments of study participants are shown for MRI in Fig. 1 and micro-CT in Fig. 2. Mean values of trabecular and cortical structural parameters assessed at the distal tibia by MRI and at the iliac crest by micro-CT and histomorphometry are presented in Table 1. Biochemical parameters of patients are outlined in Table 2.

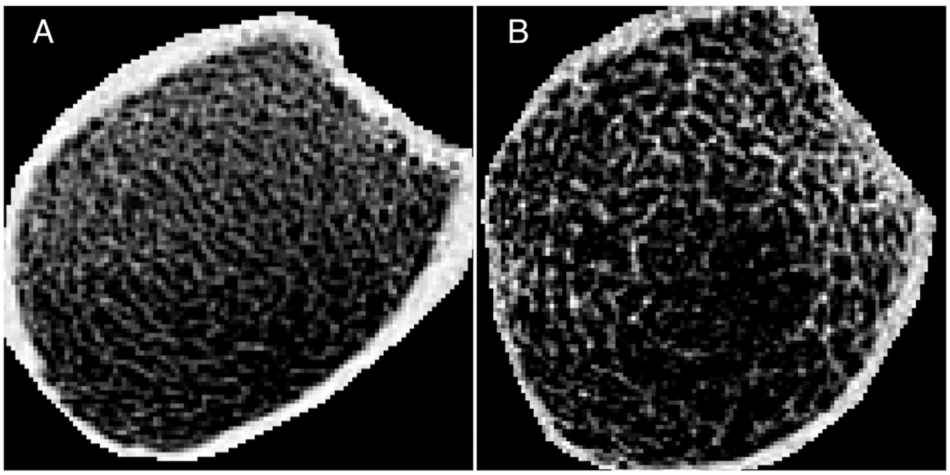

Fig. 1. Intensity-inverted magnetic resonance images (MRI) of distal tibia of two study participants respectively showing (A) compact cortical bone and well connected trabecular bone compartment; and (B) thinned and porous cortical bone and disconnected trabecular bone regions.

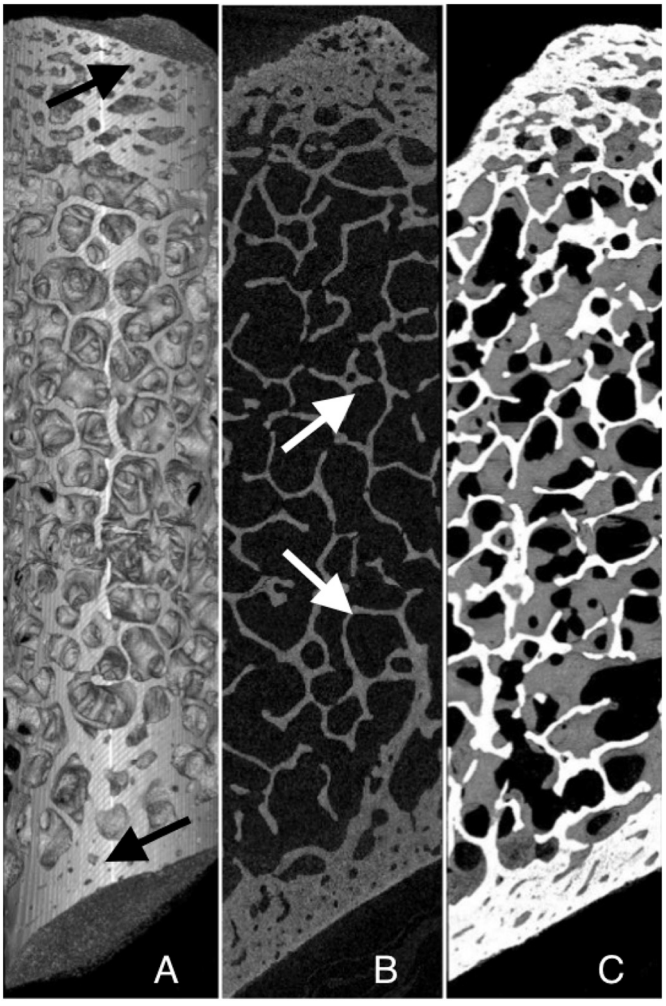

Fig. 2. Representative micro-CT images of a biopsy obtained from a study subject showing trabecular (white arrow) and cortical bone (black arrow) compartments in (A) biopsy core, (B) two-dimensional section, and (C) three-dimensional section.

3.2. Bone histomorphometry and micro-CT

Bone turnover (T) activity was assessed as low in 21%, normal in 29%, and high in 50% of participants. For patients with histomorphometry findings suggestive of hyperparathyroidism, the mineral apposition rate (MAR) varied from 0.77 to 1.08 μm/day (normal 0.6–0.8 μm/day) and bone formation rate (BFR) from 0.09–0.62 mm^3/mm^2/day (normal 0.03–0.09 mm^3/mm^2/day). Mineralization (M) was abnormal in 35.7%, based on histological features of increased osteoid surface, volume and seam width. Trabecular bone volume (V) was relatively preserved. By micro-CT, only 28.5% % of patients had BV/TV values > 1 SD below the mean, and mean trabecular thickness, number and separation were also within the normal range. However, cortical bone was characterised by thin cortices and increased cortical porosity (Table 1). Cortical porosity by 2D histomorphometry correlated to porosity by 3D micro-CT ($r = 0.56$; $p = 0.03$), but there was no significant relationship between cortical thickness measured by 2D histomorphometry and 3D micro-CT.

Table 2
Biochemical parameters of the study cohort ($n = 16$), median ± SD or median (IQR).

Biomarker	Values	Normal range
Calcium	2.45 ± 0.11	2.10–2.60 mmol/L
Phosphate	2.1 ± 0.46	0.75–1.50 mmol/L
Parathyroid hormone	45.3 (26.8–64.8)	1.7–10.0 pmol/L
Alkaline phosphatase	89.5 (67.5–131.8)	30–120 IU/L
25-Hydroxyvitamin D	65.2 ± 21.2	55–108 nmol/L

3.3. Associations of MRI and bone histology

3.3.1. Turnover

MRI parameters are static, and like static histomorphometric indices, are likely to reflect the cumulative impact on bone structure of changes in bone turnover over time. Significant negative associations were present between eroded surface (ES/BS) by histomorphometry and MRI-derived total bone area ($r = -0.85$, $p = 0.004$), trabecular bone area ($r = -0.71$, $p = 0.03$) and cortical bone area ($r = -0.83$, $p = 0.005$), Osteoclast surface (Oc.S/BS %) by histomorphometry was negatively correlated to MRI-derived cortical area ($r = -0.67$, $p = 0.01$). Unlike these static parameters, tetracycline labelling represents current bone turnover. Nevertheless, a significant positive association was detected between BFR and MRI derived trabecular volume ($r = 0.56$, $p = 0.04$), and negative associations were present between BFR and MRI derived trabecular number ($r = -0.59$, $p = 0.03$) and trabecular spacing ($r = -0.58$, $p = 0.03$). MAR correlated significantly with S/C (r = 0.56, $p = 0.04$) with a negative trend for EI ($r = -0.53$, $p = 0.06$). However, BFR and MAR were not reliably determined on all samples due to inconsistent uptake of the first

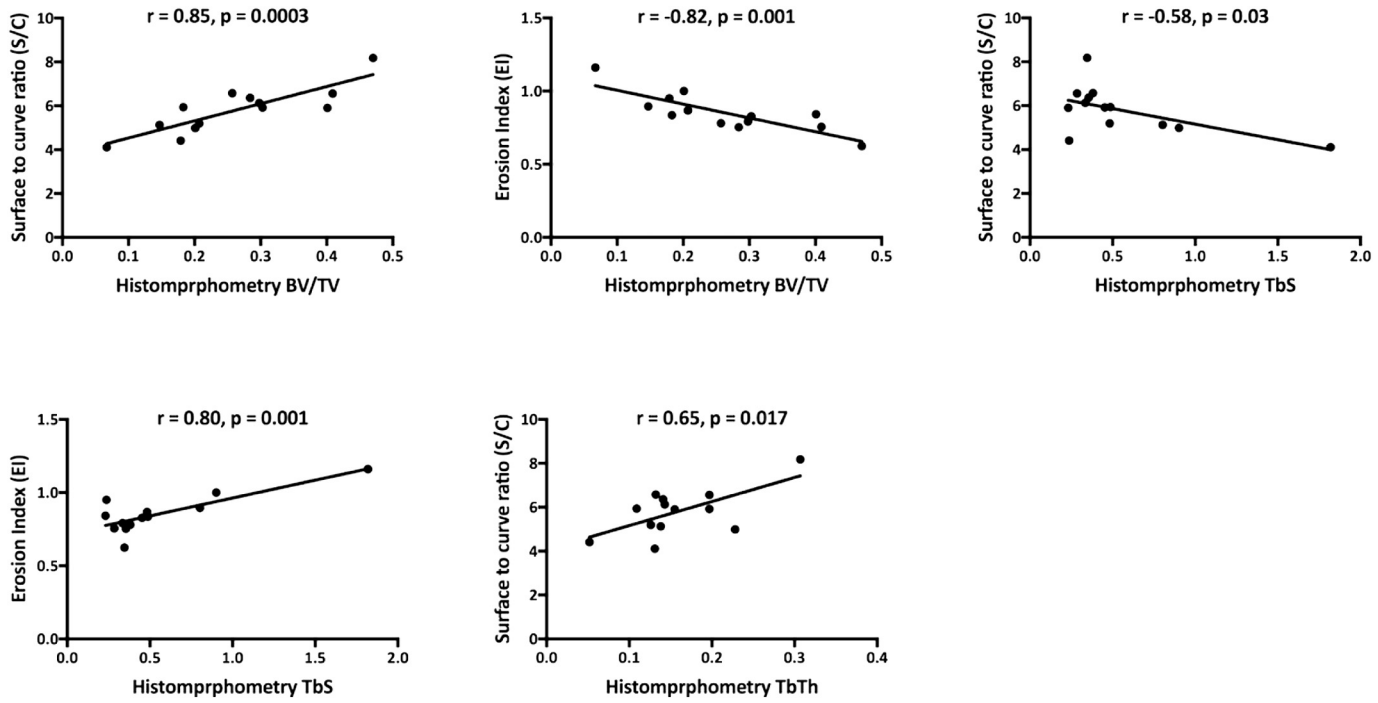

Fig. 3. Correlations, Pearson's (*r*), between trabecular topological parameters derived by MRI of distal tibia (MRI) with those at the iliac crest by 2D-histomorphometry.
Abbreviations: Surface to curve ratio (S/C), erosion index (EI), trabecular bone volume (BV/TV), trabecular thickness (TbTh, μm), trabecular separation (TbS, μm).

doxycycline label, so these correlations should be interpreted with caution.

3.3.2. Mineralization

There were no significant associations between MRI derived trabecular or cortical bone structure and osteoid thickness or volume used to assess mineralization. However, total bone area measured by MRI correlated to osteoid thickness ($r = 0.71$, $p = 0.006$) and osteoid volume ($r = 0.59$, $p = 0.03$). Positive correlations were observed between tetracycline labeled mineralizing surface to bone surface and MRI-derived BV/TV ($r = 0.61$, $p = 0.02$) and TbN ($r = 0.64$, $p = 0.04$), with a negative association to TbS ($r = -0.63$, $p = 0.02$).

3.3.3. Volume

When assessing volume, 3D techniques are superior to the 2D structural parameters provided by histological sections. Nevertheless, MRI derived S/C, indicating the plate to rod ratio of trabeculae at the distal tibia, correlated positively to histomorphometry at the iliac crest for trabecular bone volume (BV/TV, $r = 0.85$, $p = 0.0003$), trabecular thickness (TbTh, $r = 0.65$, $p = 0.017$) and negatively to trabecular separation (TbS, $r = -0.58$, $p = 0.039$) (Fig. 3). MRI-derived EI, which increases with trabecular deterioration, correlated negatively to histomorphometric BV/TV ($r = -0.82$, $p = 0.0006$) and positively to TbS ($r = 0.80$, $p = 0.001$) at the iliac crest.

MRI parameters and micro-CT-derived bone trephine indices are listed in Table 1 and compared in Table 3. There were no significant correlations between micro-CT-derived BV/TV, trabecular parameters (TbTh, TbN, TbS) or cortical thickness (CtTh) with the same MRI parameter, possibly due to differences in microarchitecture between the different skeletal sites. However, lower micro-CT-derived cortical and trabecular thickness and increased micro-CT-derived trabecular number were inversely related to the MRI-derived S/C ratio, and there was a positive association of increased trabecular separation by micro-CT and the MRI-derived erosion index (EI) ($r = 0.63$, $p = 0.02$), which increases with trabecular deterioration, (Table 3).

3.4. MRI, BMD and biomarkers

Mean values of lumbar spine, femoral neck and total hip BMD determined by DXA are presented in Supplementary Table 1, and the correlations of these parameters with MRI indices are presented in Supplementary Table 2.

Seven out of 14 (50%) patients, aged 33 to 63 years, met the World Health Organization (WHO) criteria for osteopenia (T-Score -1.0 to -2.5) and two for osteoporosis (T-Score < -2.5) respectively at the femoral neck. Significant correlations were observed between BMD at the hip and trabecular microarchitecture at the distal tibia by MRI and iliac crest histomorphometry. All MRI-derived trabecular parameters differed significantly for the participants with femoral neck T-scores ≤ -2.5 versus those with T-scores > -2.5 whereas total bone area and trabecular area differed significantly for those with T-scores within versus above the osteopenic range (Table 4). Similar relationships were not observed between MRI and T-scores at the total proximal femur or lumbar spine.

MRI-derived trabecular area correlated to values of ALP ($r = 0.55$, $p = 0.03$) and TbS correlated to values of 25(OH)D ($r = -0.57$, $p = 0.03$). There were no other significant associations between MRI indices and biomarkers.

4. Discussion

To our knowledge, this study is the first to explore relationships between non-invasive assessment of bone microarchitecture using MRI at a peripheral skeletal site and quantitative histomorphometry at the iliac crest in patients with CKD. The results of this study confirm the complex skeletal phenotype of ROD and provide some encouraging data for the potential utility of MRI. Our results are congruent with previous studies showing widespread bone loss and deranged bone microarchitecture in relatively young patients with CKD. We observed significant cortical bone loss with increased cortical porosity and trabecular network deterioration but preserved trabecular volume at the iliac crest; and demonstrated correlations between some structural

Table 3
Correlations, Pearson's (r), between trabecular and cortical microarchitecture parameters measured by MRI and bone histomorphometry measured by micro-CT.

Modalities	MRI (tibia)						
	Parameters	BV/TV	TbTh	TbN	TbS	CtTh	S/C	EI
Micro-CT (iliac crest)	BV/TV	0.25	0.30	0.24	−0.28	−0.43	0.30	−0.34
	TbTh	0.05	−0.09	−0.03	−0.06	0.06	−0.61*	0.43
	TbN	0.21	0.25	0.20	0.22	−0.24	0.60*	−0.47
	TbS	−0.52	−0.60*	−0.48	0.45	0.06	−0.51	0.63*
	CtTh	0.01	−0.01	0.01	−0.04	0.20	−0.62*	0.41
	SMI	0.25	0.18	0.23	−0.24	–	−0.11	0.11
	DA	0.28	0.35	0.30	−0.29	–	0.39	−0.53
	Conn.D ($1/\mu m^3$)	0.46	0.51	0.46	−0.45	–	0.49	−0.53

Abbreviations: surface to curve ratio (S/C), erosion index (EI), trabecular bone volume (BV/TV %), trabecular thickness (TbTh), trabecular separation (TbS), cortical thickness (CtTh), structural model index (SMI) — relative index of rods and plates or cavities if negative), degree of anisotropy (DA), connectivity density (Conn.D).
* $p \leq 0.05$.

Table 4
Associations of trabecular and cortical microarchitecture parameters measured by MRI (mean ± SD) with bone mineral density findings at the femoral neck (according to the WHO classification).

MRI parameter	Value in patients with osteopenia	Value in patients with osteoporosis
Surface to curve ratio	5.5 ± 0.85	3.6 ± 2.1*
Erosion index	0.90 ± 0.1	1.3 ± 0.6
Bone volume (%)	11.0 ± 2.2	7.2 ± 0.8*
Trabecular thickness (mm)	0.13 ± 0.006	0.12 ± 0.0*
Trabecular number (1/mm)	0.86 ± 0.14	0.62 ± 0.1*
Trabecular separation (mm)	1.05 ± 0.2	1.5 ± 0.25**
Cortical thickness (mm)	2.7 ± 0.51	2.4 ± 0.46

* $p \leq 0.05$ compared to subjects without osteopenia or osteoporosis respectively.
** $p \leq 0.01$ compared to subjects without osteopenia or osteoporosis respectively.

parameters assessed by different imaging modalities at skeletal sites with varying load bearing profiles.

The relationships between parameters of trabecular network integrity at the tibia (S/C and EI with MRI), trabecular microarchitecture at the iliac crest and BMD at the hip, demonstrate the widespread and serious nature of bone deficits in CKD. This is clinically relevant because disruption of trabecular network connectivity, increased trabecular separation and decreased trabecular number are associated with aging and osteoporosis [32, 33] and have assisted in discriminating between participants with or without fractures in histomorphometric [34, 35] and HR-pQCT studies [36, 37]. Other structural measurements derived from tibial MRI correlated weakly with corresponding parameters evaluated by histomorphometry. On the other hand, MRI-derived trabecular measurements were predictive of BMD at the femoral neck. The inverse relationships observed between MRI derived cortical thickness and trabecular structural parameters by micro-CT are likely representative of 'trabecularisation' of endocortical bone. This can lead to inaccuracies in distinguishing the cancellous from the cortical compartments in this 'transitional zone' [38] causing potential overestimation of trabecular parameters.

This study demonstrates that MRI may have utility beyond quantification of bone microarchitecture, especially if combined with BMD measurement and reliable markers of bone turnover. While we demonstrated significant correlations between MRI and histomorphometric bone turnover parameters, these should be viewed with caution given our small cohort and inconsistent uptake of doxycycline labels. It is also important to recognize that MRI or micro-CT parameters are static and represent a legacy of changes to bone accumulated over time, which may not be indicative of current, dynamic bone turnover.

There are few other studies that can be compared or contrasted with our results. Cohen et al. [39] compared HR-pQCT to classical bone histomorphometry and micro-CT of iliac crest biopsies in 54 participants without secondary osteoporosis or metabolic bone disease. They demonstrated weak to modest but statistically significant correlations between structural parameters obtained by these modalities. In a recent study, Marques et al. [40] compared HR-pQCT (radius and tibia) and bone histomorphometry in 31 CKD patients. They reported modest, statistically significant correlations between structural parameters at the two sites. Similar to those studies, our results suggest that structural parameters measured by MRI are weakly to modestly associated to their direct counterparts measured by histomorphometry. It is important that these relationships are interpreted in the context of technical and analytic differences in the measurement of similarly named parameters by MRI, micro-CT and histomorphometry, three modalities with very different image resolutions and processing algorithms.

This study highlights the variation in indices of bone structure by anatomical site. While iliac crest biopsy has an established role as the 'gold standard' for ROD diagnosis, other skeletal sites also need consideration as targets for systemic treatments that affect the whole skeleton. In fact, even at the iliac crest, contiguous bone biopsies in the same patient with ROD have been reported to show up to 24% variability in trabecular bone parameters [41]. Similar variation has also been demonstrated in measurements by micro-CT of biopsies obtained from the cadavers of postmenopausal women [42]. Recent studies have also reported variability in cortical bone architecture at various sites [43]. The current study also demonstrates poor within-patient correlation of cortical thickness and porosity measured by micro-CT and histomorphometry. These differences are likely due to the larger 3D sample size and higher resolution of micro-CT, versus the smaller, 2D sample assessed by classical histomorphometry. Although histomorphometry studies in patients with CKD have described skeletal microstructural and mechanical abnormalities [44], the few studies designed to examine links between bone histology and fracture have provided mixed results [45, 46]. By contrast, several studies using MRI have reported associations between microstructural parameters at peripheral sites and spinal [13] and hip fracture [47], although only one such study has been conducted in patients with CKD [17].

Our study has several limitations including its cross-sectional nature and small sample size without a normal control group. The sample size limits our ability to apply regression analyses to determine the ability of a combination of imaging and biomarkers to predict TMV parameters. Also, being a single-center study, the generalisability of our findings is limited. Despite these limitations, this is the first study to compare MRI measurements to histomorphometry plus micro-CT in patients with CKD and provides a 'proof of concept' for larger studies. Notably, for MRI, this was achieved using a commercially available, routinely used RF coil, which is a significant step towards wider availability. It also compares multiple standards of care and experimental imaging modalities (DXA, micro-CT, MRI) at different skeletal sites with histomorphometry. Although this approach gives us a comprehensive

comparison of modalities, the technical and analytic differences in the techniques and the inherent variations between structural and adaptive characteristics of different skeletal sites make interpretation challenging.

There is a heightened awareness of the increased fracture risk in the CKD population, with a knowledge gap related to the pathologic mechanisms leading to fractures and the unmet need for adequate screening tools to identify and stratify this risk [48, 49]. This has resulted in an increased number of studies evaluating the utility of non-invasive imaging techniques and biomarkers in renal bone disease. There is also declining expertise in bone biopsy handling and analysis, patients may be reluctant to undergo the procedure, and processing is time consuming [50]. Whilst MRI is expensive, it is a technique widely researched in the non-CKD population, and scanners and commercial hardware are readily available. MRI may be able to quantify bone microarchitecture, improve fracture risk stratification and monitor intervention in ROD.

5. Conclusion

In summary, our study compared new HR imaging technology to traditional bone histomorphometry. Despite technical and analytical differences and skeletal heterogeneity, we observed statistically significant correlations between parameters assessed by histomorphometry and MRI at different anatomical sites, while demonstrating associations of MRI parameters to BMD and indices of bone remodelling. Validation of the role of MRI in CKD will require prospective trials, designed to assess its potential for fracture prediction and monitoring therapeutic intervention.

Acknowledgements

We acknowledge and thank Emma Tully for performing biopsies, Susan Harvey for conducting densitometry scans, Sindhu Mohanty for performing micro-CT scans and Chris Kokkinos and RMH radiology team for setting up and conducting the MRI scans for their respective contributions and support during the study.

Funding

We acknowledge Amgen Australia for an unrestricted educational grant for part funding of this study.

Appendix A. Supplementary data

Supplementary data to this article can be found online at https://doi.org/10.1016/j.bone.2018.05.029.

References

[1] S. Moe, et al., Definition, evaluation, and classification of renal osteodystrophy: a position statement from kidney disease: improving global outcomes (KDIGO), Kidney Int. 69 (11) (2006) 1945–1953.
[2] F.H. Epstein, K.A. Hruska, S.L. Teitelbaum, Renal osteodystrophy, N. Engl. J. Med. 333 (3) (1995) 166–175.
[3] A.M. Parfitt, Renal bone disease: a new conceptual framework for the interpretation of bone histomorphometry, Curr. Opin. Nephrol. Hypertens. 12 (4) (2003) 387–403.
[4] A.M. Alem, et al., Increased risk of hip fracture among patients with end-stage renal disease, Kidney Int. 58 (1) (2000) 396–399.
[5] K.L. Naylor, et al., The three-year incidence of fracture in chronic kidney disease, Kidney Int. 86 (4) (2014) 810–818.
[6] A.M. Ball, Risk of hip fracture among dialysis and renal transplant recipients, JAMA 288 (23) (2002) 3014–3018.
[7] F. Tentori, et al., High rates of death and hospitalization follow bone fracture among hemodialysis patients, Kidney Int. 85 (1) (2014) 166–173.
[8] S.S. Nair, et al., Temporal trends in the incidence, treatment, and outcomes of hip fracture in older patients initiating dialysis in the United States, Clin. J. Am. Soc. Nephrol. 8 (8) (2013) 1336–1342.
[9] D. Hansen, et al., Risk of fracture in adults on renal replacement therapy: a Danish national cohort study, Nephrol. Dial. Transplant. 31 (10) (2016) 1654–1662.
[10] S.P. Iyer, et al., Kidney transplantation with early corticosteroid withdrawal: paradoxical effects at the central and peripheral skeleton, J. Am. Soc. Nephrol. 25 (6) (2014) 1331–1341.
[11] T.L. Nickolas, et al., Rapid cortical bone loss in patients with chronic kidney disease, J. Bone Miner. Res. 28 (8) (2013) 1811–1820.
[12] F.W. Wehrli, Structural and functional assessment of trabecular and cortical bone by micro magnetic resonance imaging, J. Magn. Reson. Imaging 25 (2) (2007) 390–409.
[13] R. Kijowski, et al., Evaluation of trabecular microarchitecture in nonosteoporotic postmenopausal women with and without fracture, J. Bone Miner. Res. 27 (7) (2012) 1494–1500.
[14] M. Benito, et al., Effect of testosterone replacement on trabecular architecture in hypogonadal men, J. Bone Miner. Res. 20 (10) (2005) 1785–1791.
[15] J. Folkesson, et al., Longitudinal evaluation of the effects of alendronate on MRI bone microarchitecture in postmenopausal osteopenic women, Bone 48 (3) (2011) 611–621.
[16] X.H. Zhang, et al., In vivo μMRI-based finite element and morphological analyses of tibial trabecular bone in eugonadal and hypogonadal men before and after testosterone treatment, J. Bone Miner. Res. 23 (9) (2008) 1426–1434.
[17] T.M. Link, et al., Changes in calcaneal trabecular bone structure assessed with high-resolution MR imaging in patients with kidney transplantation, Osteoporos. Int. 13 (2) (2002) 119–129.
[18] F.W. Wehrli, et al., Quantitative high-resolution magnetic resonance imaging reveals structural implications of renal osteodystrophy on trabecular and cortical bone, J. Magn. Reson. Imaging 20 (1) (2004) 83–89.
[19] C.S. Rajapakse, et al., Micro-MR imaging-based computational biomechanics demonstrates reduction in cortical and trabecular bone strength after renal transplantation, Radiology 262 (3) (2012) 912–920.
[20] C.S. Rajapakse, et al., The efficacy of low-intensity vibration to improve bone health in patients with end-stage renal disease is highly dependent on compliance and muscle response, Acad. Radiol. 24 (2017) 1332–1342.
[21] M. Han, et al., Variable flip angle three-dimensional fast spin-echo sequence combined with outer volume suppression for imaging trabecular bone structure of the proximal femur, J. Magn. Reson. Imaging 41 (5) (2015) 1300–1310.
[22] C.S. Rajapakse, et al., Patient-specific hip fracture strength assessment with microstructural MR imaging-based finite element modeling, Radiology 283 (3) (2017) 854–861.
[23] F.W. Wehrli, et al., Digital topological analysis of in vivo magnetic resonance microimages of trabecular bone reveals structural implications of osteoporosis, J. Bone Miner. Res. 16 (8) (2001) 1520–1531.
[24] M. Benito, et al., Deterioration of trabecular architecture in hypogonadal men, J. Clin. Endocrinol. Metab. 88 (4) (2003) 1497–1502.
[25] J.D. Hernandez, et al., Technical approach to iliac crest biopsy, Clin. J. Am. Soc. Nephrol. 3 (Suppl 3) (2008) S164–S169.
[26] M.L. Bouxsein, et al., Guidelines for assessment of bone microstructure in rodents using micro–computed tomography, J. Bone Miner. Res. 25 (7) (2010) 1468–1486.
[27] D.W. Dempster, et al., Standardized nomenclature, symbols, and units for bone histomorphometry: a 2012 update of the report of the ASBMR Histomorphometry Nomenclature Committee, J. Bone Miner. Res. 28 (1) (2013) 2–17.
[28] H.H. Malluche, et al., Quantitative bone histology in 84 normal American subjects, Calcif. Tissue Int. 34 (1) (1982) 449–455.
[29] H.H. Malluche, M.-C. Faugere, Atlas of Mineralized Bone Histology, Karger, New York, 1986.
[30] T. Hildebrand, et al., Direct three-dimensional morphometric analysis of human cancellous bone: microstructural data from spine, femur, iliac crest, and calcaneus, J. Bone Miner. Res. 14 (7) (1999) 1167–1174.
[31] C.A.M. Kulak, et al., Skeletal microstructural abnormalities in postmenopausal women with chronic obstructive pulmonary disease, J. Bone Miner. Res. 25 (9) (2010) 1931–1940.
[32] E. Seeman, P.D. Delmas, Bone quality—the material and structural basis of bone strength and fragility, N. Engl. J. Med. 354 (21) (2006) 2250–2261.
[33] M.P. Akhter, et al., Transmenopausal changes in the trabecular bone structure, Bone 41 (1) (2007) 111–116.
[34] D.B. Kimmel, et al., A comparison of iliac bone histomorphometric data in postmenopausal osteoporotic and normal subjects, Bone Miner. 11 (2) (1990) 217–235.
[35] M. Ito, et al., Analysis of trabecular microarchitecture of human iliac bone using microcomputed tomography in patients with hip arthrosis with or without vertebral fracture, Bone 23 (2) (1998) 163–169.
[36] S. Boutroy, et al., In vivo assessment of trabecular bone microarchitecture by high-resolution peripheral quantitative computed tomography, J. Clin. Endocrinol. Metab. 90 (12) (2005) 6508–6515.
[37] S. Boutroy, et al., Finite element analysis based on in vivo HR-pQCT images of the distal radius is associated with wrist fracture in postmenopausal women, J. Bone Miner. Res. 23 (3) (2008) 392–399.
[38] R.M. Zebaze, et al., Intracortical remodelling and porosity in the distal radius and post-mortem femurs of women: a cross-sectional study, Lancet 375 (9727) (2010) 1729–1736.
[39] A. Cohen, et al., Assessment of trabecular and cortical architecture and mechanical competence of bone by high-resolution peripheral computed tomography: comparison with transiliac bone biopsy, Osteoporos. Int. 21 (2) (2010) 263–273.
[40] I.D. Marques, et al., Biopsy vs. peripheral computed tomography to assess bone disease in CKD patients on dialysis: differences and similarities, Osteoporos. Int. 28 (2017) 1675–1683.
[41] P.M. Chavassieux, M.E. Arlot, P.J. Meunier, Intersample variation in bone histomorphometry: comparison between parameter values measured on two contiguous

transiliac bone biopsies, Calcif. Tissue Int. 37 (4) (1985) 345–350.
[42] C. Chappard, A. Marchadier, C.L. Benhamou, Side-to-side and within-side variability of 3D bone microarchitecture by conventional micro-computed tomography of paired iliac crest biopsies, Bone 43 (1) (2008) 203–208.
[43] X. Tong, et al., Iliac crest histomorphometry and skeletal heterogeneity in men, Bone Rep. 6 (2017) 9–16.
[44] H.H. Malluche, et al., Differences in bone quality in low- and high-turnover renal osteodystrophy, J. Am. Soc. Nephrol. 23 (3) (2012) 525–532.
[45] I. Eventov, et al., Osteopenia, hematopoiesis, and bone remodelling in iliac crest and femoral biopsies: a prospective study of 102 cases of femoral neck fractures, Bone 12 (1) (1991) 1–6.
[46] D. Dempster, et al., Relationships between bone structure in the iliac crest and bone structure and strength in the lumbar spine, Osteoporos. Int. 3 (2) (1993) 90–96.
[47] T.M. Link, et al., In vivo high resolution MRI of the calcaneus: differences in trabecular structure in osteoporosis patients, J. Bone Miner. Res. 13 (7) (1998) 1175–1182.
[48] P. Messa, Skeletal fractures in patients on renal replacement therapy: how large still is the knowledge gap? Nephrol. Dial. Transplant. 31 (10) (2016) 1554–1556.
[49] S.M. Moe, T.L. Nickolas, Fractures in patients with CKD: time for action, Am. Soc. Nephrol. 11 (2016) 1929–1931.
[50] P. Evenepoel, et al., Bone biopsy practice patterns across Europe: the European renal osteodystrophy initiative—a position paper, Nephrol. Dial. Transplant. 32 (10) (2017) 1608–1613.

Received: 9 May 2018 | Accepted: 3 July 2018

DOI: 10.1111/ctr.13347

ORIGINAL ARTICLE

WILEY Clinical TRANSPLANTATION
The Journal of Clinical and Translational Research

Changes in bone microarchitecture following kidney transplantation—Beyond bone mineral density

Ashish K. Sharma[1,2] | Nigel D. Toussaint[1,2] | Grahame J. Elder[3,4] | Chamith S. Rajapakse[5] | Stephen G. Holt[1,2] | Paul Baldock[4] | Patricia L. Robertson[2,6] | Peter R. Ebeling[7] | Olivia R. Sorci[5] | Rosemary Masterson[1,2]

[1]Department of Nephrology, The Royal Melbourne Hospital, Parkville, Victoria, Australia

[2]Department of Medicine (RMH), University of Melbourne, Parkville, Victoria, Australia

[3]Department of Renal Medicine, Westmead Hospital, Westmead, Sydney, Australia

[4]Osteoporosis and Bone Biology Division, Garvan Institute of Medical Research, Darlinghurst, New South Wales, Australia

[5]Departments of Radiology and Orthopaedic Surgery, University of Pennsylvania, Philadelphia, Pennsylvania

[6]Department of Radiology, The Royal Melbourne Hospital, Parkville, Victoria, Australia

[7]Monash University, Clayton, Victoria, Australia

Correspondence: Ashish K. Sharma, Department of Nephrology, The Royal Melbourne Hospital, Grattan Street, Parkville, Vic. 3052, Australia (a.k.sharma@hotmail.com).

Funding information
AMGEN Australia

Abstract

Bone disease in kidney transplant recipients (KTRs) is characterized by bone mineral density (BMD) loss but bone microarchitecture changes are poorly defined. In this prospective cohort study, we evaluated bone microarchitecture using non-invasive imaging modalities; high-resolution magnetic resonance imaging (MRI), peripheral quantitative computed tomography (pQCT), dual energy X-ray absorptiometry (DXA), and the trabecular bone score (TBS) following kidney transplantation. Eleven KTRs (48.3 ± 11.2 years) underwent MRI (tibia), pQCT (radius) and DXA at baseline and 12 months post–transplantation. Transiliac bone biopsies, performed at transplantation, showed 70% of patients with high/normal bone turnover. Compared with baseline, 12-month MRI showed deterioration in indices of trabecular network integrity—surface to curve ratio (S/C; −15%, $P = 0.03$) and erosion index (EI; +19%, $P = 0.01$). However, cortical area increased (+10.3%, $P = 0.04$), with a non-significant increase in cortical thickness (CtTh; +7.8%, $P = 0.06$). At 12 months, parathyroid hormone values (median 10.7 pmol/L) correlated with improved S/C ($r = 0.75$, $P = 0.009$) and EI ($r = -0.71$, $P = 0.01$) while osteocalcin correlated with CtTh ($r = 0.72$, $P = 0.02$) and area ($r = 0.70$, $P = 0.02$). TBS decreased from baseline (−5.1%, $P = 0.01$) with no significant changes in BMD or pQCT. These findings highlight a post–transplant deterioration in trabecular bone quality detected by MRI and TBS, independent of changes in BMD, underlining the potential utility of these modalities in evaluating bone microarchitecture in KTRs.

KEYWORDS
bone mineral density, fracture, kidney transplantation, magnetic resonance imaging, post–transplant bone disease, trabecular bone score

1 | INTRODUCTION

Fractures are a common and serious clinical complication of the mineral and bone disorder (MBD) that is almost ubiquitous in patients with chronic kidney disease (CKD). A number of epidemiological studies have highlighted that CKD predisposes to a dramatic increase in fracture risk and resultant morbidity and mortality when compared to an age and gender-matched population without CKD.[1-4] Kidney transplantation is the optimal treatment for end-stage kidney disease (ESKD) but does not attenuate the susceptibility to fracture. Indeed, fracture risk has been reported up to 34% higher in the first 2 years post–transplantation compared to the preceding period on dialysis,[5] with a fracture incidence up to 22.5% over the first 5 years post–transplantation.[6] In addition, kidney transplant

recipients (KTRs) have higher rates of hospitalization and mortality after fracture than do people in the general population.[7] Although reductions in bone mineral density (BMD) after transplantation have been extensively reported, there is a paucity of post–transplant data regarding modifiable risk factors for fracture.[8] Improved graft and patient survival has further emphasized the importance of optimizing long-term clinical outcomes including risk of fracture and cardiovascular disease in KTRs.

Post–transplant bone disease is multifactorial, and includes effects of immunosuppressive therapy, persisting hyperparathyroidism, "hyperphosphatoninism" and the consequences of post–transplant impairment of renal function (CKD-T) superimposed on pre-existing renal bone abnormalities.[9] The diagnosis and management of post–transplant bone disease is therefore difficult, with limited validation of available diagnostic tools to evaluate changes in bone structure or predict fracture risk. Although accelerated loss of BMD in the first year after transplantation has been described as the hallmark of post–transplant bone disease,[10-12] recent studies have demonstrated a more conservative estimate of early BMD loss with long-term values nearer to average for age and gender.[13] The focus of contemporary research has been on change in bone microarchitecture post–kidney transplantation and its potential relationship to bone fragility and biomarkers.[14-18] A few studies based on histomorphometry have addressed this issue[18-21] and, more recently, studies involving non-invasive imaging, such as high-resolution peripheral quantitative-computed tomography (HR-pQCT),[15] high-resolution magnetic resonance imaging (MRI)[14,22] and the Trabecular Bone Score (TBS)[23-26] have focused on defining changes in bone microarchitecture.

In this prospective, observational study over the first 12 months following transplantation, we report changes in bone microarchitecture and bone mass that were assessed using non-invasive techniques: high-resolution MRI (tibia), dual-energy X-ray absorptiometry (DXA) to assess BMD and the TBS, peripheral quantitative computed tomography (pQCT, radius), and changes in biochemical markers.

2 | MATERIALS AND METHODS

2.1 | Study participants

All patients referred for a living donor kidney transplant at The Royal Melbourne Hospital between December 2014 and January 2016 were eligible for this study, providing they had no contraindication to MRI, and were not participating in another trial. The protocol was approved by the local ethics committee and all patients provided informed consent. A total of 27 patients planned for living donor kidney transplantation were approached for this study. Five transplant surgeries were rescheduled or canceled for clinical or logistical reasons. Fourteen of the remaining 22 patients were recruited and underwent kidney transplantation. Eleven of these patients completed follow up at 12 months. Among the exclusions, two patients moved to a different state for post–transplant care and one patient had to undergo nephrectomy after transplantation and was not included in analysis.

2.2 | Immunosuppressive therapy

Patients received induction with basiliximab and methylprednisolone (500 mg) and subsequently maintenance immunosuppression comprising tacrolimus, mycophenolate mofetil, and prednisolone. Initial prednisolone dose was 25 mg daily, tapered over 3 months to a maintenance dose of 5 mg/d. Beyond 3 months, triple immunosuppression was continued in the absence of any abnormal findings on protocol transplant biopsies (at 3 and 12 months post–transplant) or a clinical indication to the contrary determined by the treating team.

2.3 | Bone histomorphometry

Transiliac biopsies were performed using a modified Bordier trephine (Landanger) in 10 of 11 participants at the time of transplantation. The transiliac cores measuring 7 mm in diameter were analyzed by histomorphometry and micro-computed tomography (micro-CT) and were classified by Turnover (T), Mineralization (M), and Volume (V) using the Kidney Disease Improving Global Outcomes (KDIGO) recommended classification.[27] Methodology relating to bone biopsies has been described previously.[28]

2.4 | Noninvasive assessment of bone

2.4.1 | Magnetic resonance imaging

Magnetic resonance imaging images were obtained within 2 weeks preceding transplantation (baseline) with a commercial 3.0-Tesla whole-body imager (Siemens Trio, Siemens, Erlangen, Germany) and at 12 months after kidney transplantation. Participants were imaged in a feet-first prone position. MRI acquisitions were performed at the left tibial metaphysis using a three-dimensional (3D) "fast spin echo" pulse sequence readily available on any clinical MRI system requiring a scan time of 12 minutes. This was undertaken utilizing a commercially available 8-channel radiofrequency (RF) extremity coil used in clinical practice. MRI parameters include 0.273 × 0.273 × 0.6 mm voxel size, 70 × 70 × 19.2 mm field-of-view, 53 ms repetition time, 16 ms echo time, 12 averages, and echo train length of two. Raw MRI data was pre-processed via bone volume fraction (BVF) mapping and segmentation of the bone into trabecular and cortical compartments for structural measurements and topological analysis using published algorithms.[29] Topological analysis of the trabecular network was performed and two composite parameters, reported to be sensitive to microstructure of bone,[30,31] were calculated. The first of these, surface/curve ratio (S/C) is the ratio of all surface voxels to all curve voxels with the former representing plate-like elements and the latter being a marker of rod-like elements of the trabecular network. Age- and disease-related deterioration of trabecular bone involves conversion

TABLE 1 Demographic parameters at the time of transplantation (n = 11)

Variable	Values
Age at surgery (y)	48.3 ± 11.2
Gender (n of males)	8
Body mass index (kg/m^2)	26.4 ± 4.1
Cause of ESKD (n)	
Glomerulonephritis	4
Reflux nephropathy	3
Diabetes mellitus	2
Hypertension	1
Polycystic kidney disease	1
Dialysis: HD / PD / None (n)	3/4/4
Parathyroidectomy (n)	1

ESKD, end-stage kidney disease; HD, hemodialysis; PD, peritoneal dialysis.

of plate (surface) like trabeculae to rod (curve) like trabeculae. A higher S/C, therefore, indicates improved trabecular structure and strength. Trabecular deterioration also involves erosion of trabecular elements, which is measured by the Erosion Index (EI), defined as the ratio of all topological parameters (image voxel parameters representing various trabecular elements) expected to increase, to those parameters likely to decrease with network erosion caused by osteoclastic resorption. A higher ratio is consistent with greater deterioration. Both S/C and EI are derived parameters which have been validated and used in previous studies.[30,31]

2.4.2 | DXA-derived BMD and TBS

Participants underwent baseline and 12-month BMD measurements by DXA (QDR-4500 Discovery; Hologic, Waltham, MA, USA), at the lumbar spine, femoral neck and total proximal femur. BMD values were expressed in g/cm^2 and as T-scores. TBS is a novel indirect index of trabecular microarchitecture derived from pixel grayscale texture variations in the lumbar spine images acquired by DXA.[32] TBS iNsight Software (version 3.0.2.0; Medimaps, Merignac, France) was used to calculate TBS values for the lumbar spine (L1-L4). A higher TBS score is consistent with better trabecular connectivity and a reduced risk for microarchitectural damage, while a lower TBS is consistent with increased risk for microarchitectural damage. Based on results of two recent studies,[23,24] a TBS cut point of 1.37 was used to stratify patients to reduced or increased fracture risk.

2.4.3 | Peripheral quantitative-computed tomography

Three-dimensional pQCT tomographic images can be used to assess cross-sectional structure and volumetric density. We used pQCT (Stratec XCT-300; Stratec Medizintechnik, Pforzheim, Germany) at the distal radius to derive total, cortical and trabecular volumetric BMD (vBMD), cortical thickness (CtTh) and cortical area (CtA) at baseline and 12 months. All DXA and pQCT scans and TBS measurements were performed at one center by a single operator not involved in the care of study participants and blinded to other study measurements.

2.5 | Laboratory measurements

Blood samples for routine biomarkers were obtained before transplantation and at 3, 6, and 12 months post–transplantation. Serum concentrations of intact parathyroid hormone (iPTH) were determined using Architect Intact PTH (Abbott Laboratories, Abbott Park, IL, USA) chemiluminescent microparticle immunoassay (CMIA). Bone turnover markers and serum 1,25-dihydroxyvitamin D (1,25[OH]$_2$D) were also measured at baseline, 6 and 12 months. Osteocalcin (OC) and procollagen type 1 N-terminal propeptide (P1NP), markers of osteoblast activity, and the osteoclastic resorption marker beta-cross linked telopeptide (β-CTx) were assayed by an electrochemiluminescence immunoassay (Elecsys®; Roche Diagnostics, Basel, Switzerland). Serum 1,25[OH]$_2$D was measured by radioimmunoassay (Immuno-Diagnostic Systems, Boldon, UK).

2.6 | Statistical methods

Results are presented as mean (±standard deviation) for normally distributed continuous variables and as median (and interquartile range) for continuous variables with skewed distributions. Wilcoxon signed-rank test was used to assess changes in parameters between baseline and at 12 months post–transplantation. Correlation analyses using Spearman correlation coefficient were conducted to investigate associations between longitudinal changes in parameters obtained by various modalities. A two-tailed P value <0.05 was considered statistically significant. Stata statistical software package (version 11.0; Stata Corporation, College Station, TX, USA) was used for analysis.

3 | RESULTS

3.1 | Participant characteristics

Baseline demographic characteristics and potential bone modulating medications prior to and after transplantation are shown in Tables 1 and 2, respectively. The mean age of participants was 48 ± 11 years, 72.7% were male and mean body mass index of the cohort was 26.4 ± 4.1 kg/m^2. Glomerulonephritis (36.3%) was the most common cause of ESKD followed by reflux nephropathy (27.2%) and diabetes mellitus (18.1%). Seven (63.6%) participants were on dialysis (mean duration 19.4 ± 16.7 months) and four underwent pre-emptive kidney transplantation. None of the participants received anti-resorptive therapy prior to or after transplantation. There was one episode of biopsy proven acute cellular rejection treated with methylprednisolone and increased tacrolimus and mycophenolate. The remainder of participants

continued on maintenance immunosuppression, including prednisolone 5 mg daily, after their respective 3-month protocol biopsies. The mean cumulative dose of prednisolone over 12 months per patient was 3244 ± 68.6 mg.

TABLE 2 Bone modulating therapy prior to and after transplantation (n = 11)

Bone modulating therapy	At transplantation (n)	Post–transplantation (n)
Cinacalcet	1	1
Phosphate binder (CCB/NCCB)	3/5	0
Calcitriol	4	3
Cholecalciferol	3	5
Prednisolone	3	11

CBB, calcium-containing binders; NCBB, non-calcium-containing binders.

3.2 | Bone histomorphometry

Ten patients had baseline bone histomorphometry with four (40%) having evidence of high bone turnover, three normal and three low turnover, Mineralization was abnormal in four and trabecular bone volume was normal in seven and low in three. By micro-CT mean CtTh was reduced and cortical porosity was increased in all patients.[28]

3.3 | Longitudinal changes in bone microarchitecture by MRI

At 12 months there was deterioration in MRI-derived parameters of integrity of the trabecular network. S/C, indicating the plate to rod ratio of trabeculae, decreased by 16% ($P = 0.03$) from baseline. EI, which increases with trabecular deterioration, increased by 23% ($P = 0.01$; Table 3, Figure 1). There were no statistically significant differences between pre– and post–transplantation trabecular bone

TABLE 3 Bone microarchitecture parameters measured by magnetic resonance imaging (MRI), bone mineral density (BMD) determined by dual energy X-ray absorptiometry (DXA) and peripheral quantitative computed tomography (pQCT), and Trabecular Bone Score (TBS) at the time of transplantation and at 12 mo follow up

Modality	Parameter	Baseline	12 mo	*P* value
MRI (tibia)	S/C	5.5 ± 1.50	4.6 ± 1.66	0.03
	EI	0.9 ± 0.29	1.11 ± 0.34	0.01
	BV/TV (%)	10.0 ± 2.1	9.9 ± 2.4	0.76
	TbTh (μm)	125.0 ± 5.3	125.7 ± 5.0	0.33
	TbN	0.80 ± 0.14	0.77 ± 0.14	0.54
	TbS (μm)	1161.6 ± 246.3	1187.1 ± 241.1	0.72
	CtTh (mm)	2.68 ± 0.55	2.89 ± 0.64	0.06
	Total area (mm^2)	9788.8 ± 1996.3	9931.0 ± 2712.6	0.59
	Trabecular area (mm^2)	6692.2 ± 1742.4	6443.0 ± 2552.3	0.65
	Cortical area (mm^2)	3107.8 ± 692.5	3428.5 ± 811.5	0.04
DXA	LS BMD (g/cm^2)	1.02 ± 0.09	0.99 ± 0.10	0.20
	LS T-score	−0.85 (−1.2 to 0.37)	−0.9 (−1.5 to 0.15)	0.17
	FN BMD (g/cm^2)	0.70 ± 0.14	0.69 ± 0.12	0.50
	FN T-score	−1.5 (−2.4 to −0.6)	−1.6 (−2.5 to −0.9)	0.47
	TH BMD (g/cm^2)	0.86 ± 0.14	0.86 ± 0.11	0.50
	TH T-score	−0.9 (−1.7 to −0.25)	−0.6 (−1.6 to −0.25)	0.30
TBS	TBS	1.27 ± 0.11	1.21 ± 0.12	0.02
pQCT (radius)	Tb vBMD (g/cm^3)	186.8 ± 48.7	174 ± 43.5	0.07
	Ct vBMD (g/cm^3)	1164.2 ± 50.9	1161.4 ± 39.7	0.65
	Total vBMD (g/cm^3)	319.6 ± 76.4	302 ± 69.2	0.20
	CtTh (mm)	2.62 ± 0.50	2.72 ± 0.45	0.20
	Trabecular area (mm^2)	176.6 ± 29.8	175.6 ± 34.02	0.81
	Cortical area (mm^2)	92.0 ± 19.8	92.1 ± 21.3	0.72

BV/TV, trabecular bone volume; CtTh, cortical thickness; EI, erosion index; FN, femoral neck; LS, lumbar spine; S/C, surface to curve ratio; TbN, trabecular number; TbS, Trabecular separation; TbTh, trabecular thickness; TH, total hip; vBMD, trabecular and cortical volumetric bone mineral density (Tb vBMD and Ct vBMD).

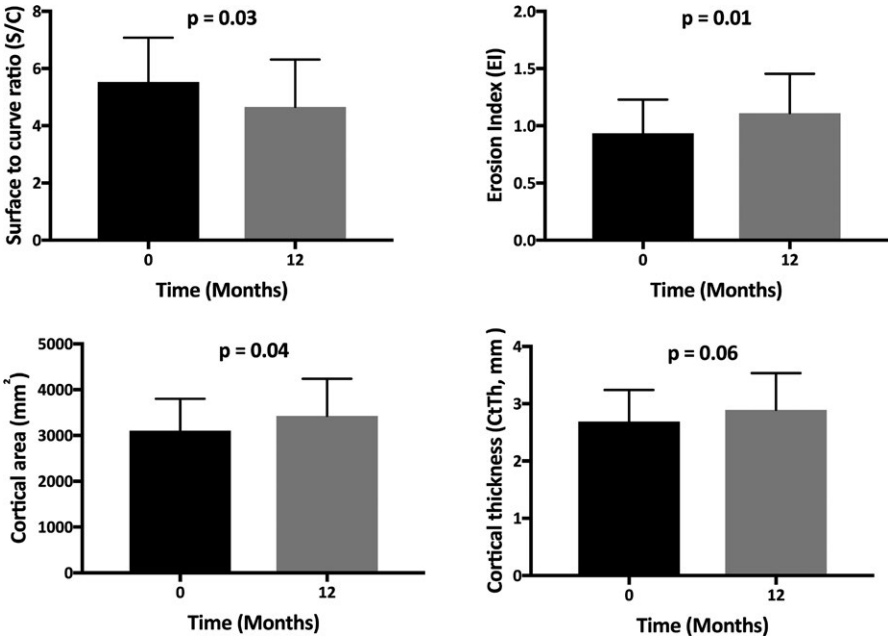

FIGURE 1 Longitudinal changes in magnetic resonance imaging (MRI)-derived parameters of bone microarchitecture

volume, trabecular number, and trabecular separation. Post–transplantation CtA increased significantly by 10.3% ($P = 0.04$) while there was a non-statistically significant 7.8% increase in CtTh ($P = 0.06$).

3.4 | Longitudinal changes in pQCT

By pQCT at the radius there was a non-significant increase in CtTh. There were no longitudinal changes in pQCT derived cortical or trabecular area or in total, cortical or trabecular volumetric BMD.

3.5 | Longitudinal changes in DXA-derived BMD and the TBS

At the time of transplantation, 80% of the study participants met BMD criteria for osteopenia or osteoporosis at the femoral neck. The median T-score at the femoral neck was −1.6 (−2.4 to −0.6), whereas T-scores at the total proximal femur and lumbar spine were in the normal range (Table 3). At 12 months, there was a 2.2% decrease in lumbar spine BMD (mean change −0.22 g/cm^2 [−0.56, 0.12]), a 2.7% decrease in femoral neck BMD (mean change −0.10 g/cm^2 [−0.39, 0.19]) and a 1.1% increase in BMD at the total hip (mean change 0.1 g/cm^2 [−0.14, 0.34]), with none of these changes reaching statistical significance.

Prior to transplantation, the mean TBS was 1.27 ± 0.11, with 9 of 11 (81.8%) patients having a TBS below 1.37. The mean TBS decreased at 12 months to 1.21 ± 0.12 ($P = 0.02$) with 10 out of 11 (90.9%) patients having a TBS lower than 1.37. The TBS at baseline and follow-up, was not significantly related to BMD or any structural parameter derived by MRI.

3.6 | Changes in biochemical markers

Baseline and 12-month follow up biochemical parameters and bone turnover markers are presented in Table 4. Immediately before transplantation, the median serum iPTH was 43.6 (16.5-57.5) pmol/L, which is within the target range recommended by the KDIGO Chronic Kidney Disease-Mineral and Bone Disorder (CKD-MBD) guidelines. At 12 months, 54.5% of patients had mild persistent hyperparathyroidism with median PTH 10.7 (7.4-17.0) pmol/L. With return of renal function, values of $1,25[OH]_2D$ rose by 78% from baseline to 6 months and remained stable within the normal reference range to 12 months. Values of bone turnover markers affected by renal function (OC, β-CTx and P1NP) fell from the pre–transplant period to 12 months as expected. On the other hand, alkaline phosphatase (ALP), which reflects osteoblast activity and is not influenced by renal function, did not change significantly from pre–transplant to 12 months. As indicated in Figure 2, mean values of serum P1NP, β-CTX and OC had all fallen toward the upper normal range by 6 months, with no statistically significant change from 6 to 12 months.

3.7 | Associations of laboratory variables to structural parameters

Pre–transplant values of serum PTH, P1NP, β-CTx, and OC were not significantly associated with any structural MRI parameters. However, at 12-months, levels of PTH correlated to S/C ($r = 0.75$; $P = 0.009$) and EI ($r = -0.71$; $P = 0.01$) but not to other structural parameters (Figure 3). OC levels at 12 months correlated to MRI derived CtTh ($r = 0.72$; $P = 0.02$) and area ($r = 0.70$; $P = 0.02$) at the tibia. OC also correlated to pQCT parameters of CtTh ($r = 0.70$; $P = 0.03$) and area ($r = 0.67$; $P = 0.05$) at the radius. On the other hand, values of serum PTH and the assayed bone turnover markers were not correlated to any BMD value or the TBS at baseline or 12 months.

3.8 | Clinical outcomes

One patient (with type 2 diabetes mellitus and PTH 65 pmol/L at baseline) was diagnosed with avascular necrosis of both hips after

Biomarker	Baseline	12 mo	*P* value
Creatinine (mmol/L)[a]	501 ± 54.3	106.2 ± 21.5	0.003
eGFR[a]	10.4 ± 2.0	67.1 ± 11.2	0.003
Calcium (mmol/L)	2.45 ± 0.13	2.47 ± 0.11	0.82
Phosphate (mmol/L)	1.98 ± 0.39	1.00 ± 0.16	0.003
iPTH (pmol/L)	43.6 (16.5-57.5)	10.7 (7.4-17.0)	0.01
ALP (IU/L)	79.0 (66.0-111.0)	84.0 (68.0-109.0)	0.79
25[OH]D (nmol/L)	63.7 ± 24.0	86.0 ± 29.4	0.14
$1,25[OH]_2D$ (nmol/L)	38.5 (20.0-72.5)	144.5 (97.0-173.7)	0.01
OC (ng/mL)	125.8 (30.8-161.7)	24.3 (20.3-38.1)	0.01
β-CTx (ng/mL)	1.08 (0.81-2.3)	0.69 (0.41-1.24)	0.02
P1NP (μg/L)	134.2 (43.0-269.2)	66.0 (42.8-117.0)	0.20

$1,25[OH]_2D$, serum 1,25-dihydroxyvitamin D; 25[OH]D, 25-hydroxyvitamin D; ALP, alkaline phosphatase; eGFR, estimated glomerular filtration rate; iPTH, intact parathyroid hormone; OC, osteocalcin; P1NP, procollagen type 1 N-terminal propeptide; β-CTx, beta-cross linked telopeptides.
[a]Values at baseline for pre–dialysis patients receiving pre–emptive transplants only (n = 4).

TABLE 4 Biochemical parameters at the time of transplantation and at 12 mo follow-up

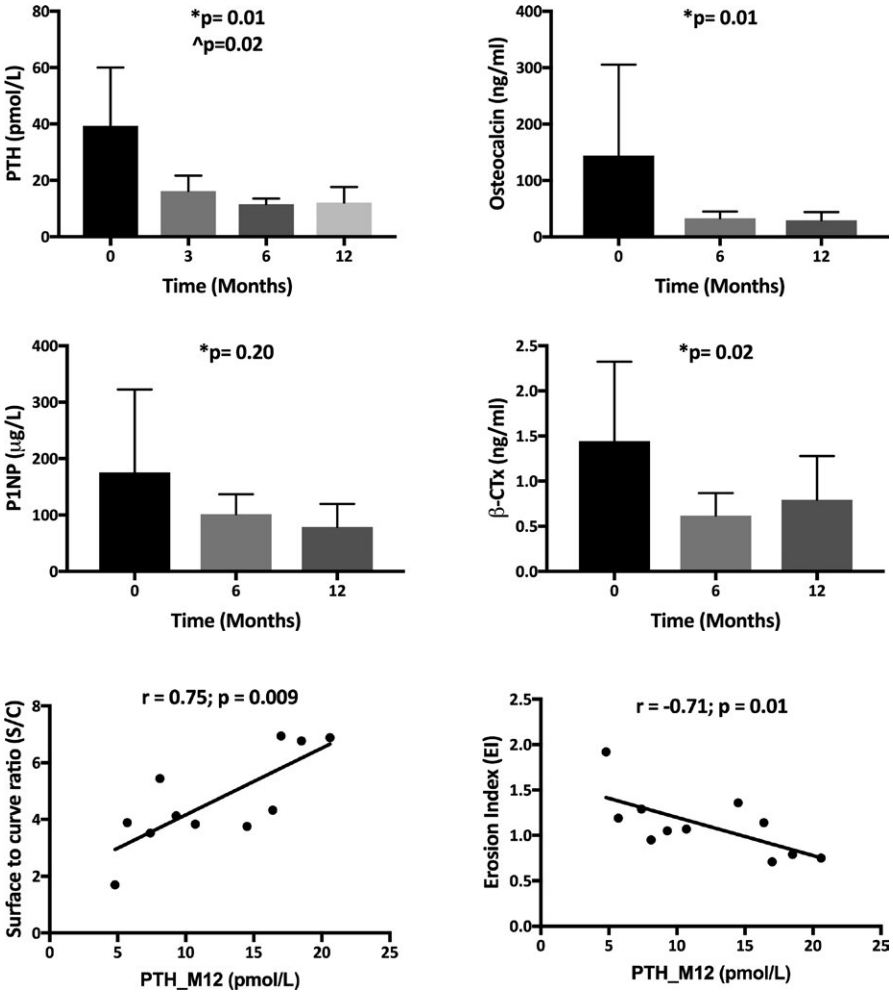

FIGURE 2 Longitudinal changes in levels (mean ± SD) of parathyroid hormone (PTH) and bone turnover markers after transplantation. *Comparison between values at baseline (0 mo) and 12 mo. There were no statistically significant changes in 6- and 12-mo levels of bone turnover markers. ^Comparison of PTH values between 3 and 12 mo. P1NP, procollagen type 1 N-terminal propeptide; PTH, intact parathyroid hormone; β-CTx, beta-cross linked telopeptides

FIGURE 3 Relationship between parathyroid hormone (PTH) levels and parameters of trabecular connectivity derived by magnetic resonance imaging (MRI) at 12 mo post–kidney transplantation

the study period completed, and subsequently sustained a spontaneous trochanteric fracture requiring total hip replacement. There were no clinically detected incident fractures during the 12-month study period.

4 | DISCUSSION

After kidney transplantation, factors contributing to deterioration in bone quality include immunosuppressive therapy, abnormalities

in mineral homeostasis, and remodeling superimposed upon pre-existing renal osteodystrophy. Although post–transplantation loss of bone mass or BMD has been well documented, changes in bone microarchitecture are not well described. In this study, we aimed to define changes in bone microarchitecture over the first post–transplant year using a combination of high-resolution imaging techniques and biochemical markers of bone turnover.

In this cohort study of 11 KTRs with predominantly high or normal turnover at baseline, changes in some MRI parameters and the TBS were consistent with deterioration in trabecular network and connectivity, while MRI suggested an improvement in cortical microarchitecture over 12 months post–transplantation. Notably, there were no statistically significant changes in BMD by DXA, despite a significant decline in the TBS to values associated with an increased fracture risk.[24] These changes in bone were accompanied by changes in biomarkers of mineral metabolism, which were concordant with published data.[33,34]

Progressive deterioration in trabecular connectivity and microarchitecture after transplantation is clinically relevant because it may increase bone fragility without quantifiable changes in bone volume. It has previously been reported that the conversion of trabecular structure from plate-like to rod-like and disruption of network connectivity adversely impacts mechanical strength of bone,[35] is associated with aging and osteoporosis[36-38] and discriminates between participants with or without fractures in imaging studies.[30,39] The observed relationship of post–transplantation PTH values to improvements in the S/C and EI measurements, likely reflects an anabolic effect of mild hyperparathyroidism on trabecular bone.[40]

The MRI-derived longitudinal improvement in cortical microarchitecture in our study is contrary to changes reported by contemporary imaging studies in kidney transplantation.[14,15] The only other MRI study to longitudinally evaluate cortical and trabecular microarchitecture in KTRs reported a decline in cortical, trabecular, and whole-bone stiffness at 6 months after transplantation in the absence of any significant corresponding changes in microarchitecture or BMD.[14] However, Iyer et al,[15] investigated bone structure changes in KTRs on an early corticosteroid withdrawal regimen and demonstrated a decrease in HR-pQCT-derived CtA (−3.9%, radius; −2.7% tibia) and thickness (−3.1%, radius; −1.9% tibia) and an increase in cortical porosity at 1-year post–transplantation. This decrease in CtTh and area was related to higher PTH levels. In comparison to the study by Iyer et al, the participants in our study had higher baseline PTH (43.7 pmol/L vs 27 pmol/L), were generally more osteopenic (mean T-score −1.5 vs −0.8) and were on traditional corticosteroid regimen. The overall results should be interpreted in the context of these differences. Participants in the present study were also significantly younger with only two (of 11) over 55 years of age compared to 27 (of 47, 57%) patients above 55 years of age in the study by Iyer et al. Notably, cortical deterioration occurs with advancing age and is more common in people above 60 years of age. Few other studies have described longitudinal changes in cortical bone post–kidney transplantation.

In contrast to previously published data about the predominance of low bone turnover in ESKD patients,[41,42] 70% of our participants had features of high or normal bone turnover at the time of transplantation, accompanied by universally thin cortices on micro-CT but with relatively preserved trabecular bone volume—an overall picture suggestive of moderate to severe secondary hyperparathyroidism. We postulate that the improvement in MRI-assessed cortical microarchitecture in our study is likely a result of suppression of excessive bone resorption and unmasking of bone modeling due to a decline in PTH levels and represents a partial correction of hyperparathyroidism-related bone changes after kidney transplantation. This release from excess remodeling and endocortical resorption may lead to net adaptive periosteal apposition and a stabilization or increase in cortical surface area and thickness.[43,44] In our study, the relationship between post–transplantation OC levels and CtTh and area at both the tibia (MRI) and the radius (pQCT) are suggestive of net bone formation. Similar to these conclusions, a recent study of paired bone biopsies at baseline and 1-year post–transplant reported significant declines in parameters of bone resorption at 1 year, with no changes in other static parameters.[18] Trabecular bone volume was also normal in most patients at baseline and only decreased minimally after transplantation. Julian et al,[10] in an early prospective histomorphometry study, also reported similar normalization of osteoclast resorption markers and resolution of hyperparathyroidism at 6 months post–transplantation.

Currently, there is no reference range for TBS for individuals with CKD because of the relative lack of studies investigating its utility in CKD[26,45] and renal transplantation.[24,25] Two studies have proposed values of the TBS to discriminate between subjects with and without fracture in CKD stages 3-4 (TBS < 1.27)[45] and in KTRs shortly after kidney transplantation (TBS < 1.37).[24] In the current study, we observed a significant decline in mean TBS at 12 months post–transplantation from a baseline score already consistent with an increased fracture risk. It is possible that the TBS is reduced early after transplantation with recovery over the longer term.[25] The longitudinal decline in TBS paralleled the MRI-derived deterioration in trabecular architecture and was unrelated to areal or volumetric BMD changes. By comparison, we observed no significant decline in BMD over 12 months. This is consistent with contemporary data showing more stable BMD long term after transplantation[13,18] and may represent a recovery after loss of bone mass early after transplant.[10]

Our study has several limitations. The small sample size limits its statistical robustness and restricts the ability to apply regression analysis to evaluate predictors of changes in bone microarchitecture. This includes the effects of bone-modifying treatments on changes in bone structure. Also, being a single-center study, the relevance of our findings to other centers is limited. Despite these limitations, our study is one of very few to explore longitudinal changes in bone structure after transplantation using high-resolution imaging.

In summary, using MRI and DXA-derived TBS in a small sample of relatively young living donor KTRs, we identified changes consistent

with a progressive deterioration in trabecular bone quality and an increased fracture risk. The lack of significant interval changes in BMD or pQCT parameters accentuates the potential importance of assessing bone health post–transplantation by alternate means. The preservation of cortical structure in our cohort, although different to available data, may represent a partial correction of bone abnormalities related to secondary hyperparathyroidism. Overall, our study highlights the heterogeneous nature of bone microarchitecture changes in post–transplant bone disease and supports further investigation of non-invasive imaging modalities in larger prospective trials to assess the evolution of histologic and structural changes in bone after transplantation. Changes in MRI parameters and the TBS may be of particular interest for detecting changes that may increase post–transplant fracture risk.

ACKNOWLEDGEMENTS

We acknowledge Amgen Australia for an unrestricted educational grant for part funding of this study. We acknowledge and thank Susan Harvey for conducting densitometry scans and the RMH radiology team for setting up and conducting the MRI scans as well as for their respective contributions and support during the study.

CONFLICT OF INTEREST

The authors of this manuscript have no conflicts of interest to disclose.

ORCID

Ashish K. Sharma http://orcid.org/0000-0002-4205-1098

REFERENCES

1. Alem AM, Sherrard DJ, Gillen DL, et al. Increased risk of hip fracture among patients with end-stage renal disease. *Kidney Int*. 2000;58(1):396-399.
2. Naylor KL, McArthur E, Leslie WD, et al. The three-year incidence of fracture in chronic kidney disease. *Kidney Int*. 2014;86(4):810-818.
3. Hansen D, Olesen JB, Gislason GH, Abrahamsen B, Hommel K. Risk of fracture in adults on renal replacement therapy: a Danish national cohort study. *Nephrol Dial Transplant*. 2016;31(10):1654-1662.
4. Tentori F, McCullough K, Kilpatrick RD, et al. High rates of death and hospitalization follow bone fracture among hemodialysis patients. *Kidney Int*. 2014;85(1):166-173.
5. Ball AM. Risk of hip fracture among dialysis and renal transplant recipients. *JAMA*. 2002;288(23):3014-3018.
6. Nikkel LE, Hollenbeak CS, Fox EJ, Uemura T, Ghahramani N. Risk of fractures after renal transplantation in the United States. *Transplantation*. 2009;87(12):1846-1851.
7. Abbott KC, Oglesby RJ, Hypolite IO, et al. Hospitalizations for fractures after renal transplantation in the United States. *Ann Epidemiol*. 2001;11(7):450-457.
8. Naylor KL, Li AH, Lam NN, Hodsman AB, Jamal SA, Garg AX. Fracture risk in kidney transplant recipients: a systematic review. *Transplantation*. 2013;95(12):1461-1470.
9. Malluche HH, Monier-Faugere MC, Herberth J. Bone disease after renal transplantation. *Nat Rev Nephrol*. 2010;6(1):32-40.
10. Julian BA, Laskow DA, Dubovsky J, Dubovsky EV, Curtis JJ, Quarles LD. Rapid loss of vertebral mineral density after renal transplantation. *N Engl J Med*. 1991;325(8):544-550.
11. Almond MK, Kwan JT, Evans K, Cunningham J. Loss of regional bone mineral density in the first 12 months following renal transplantation. *Nephron*. 1994;66(1):52-57.
12. Brandenburg VM, Politt D, Ketteler M, et al. Early rapid loss followed by long-term consolidation characterizes the development of lumbar bone mineral density after kidney transplantation. *Transplantation*. 2004;77(10):1566-1571.
13. Naylor KL, Garg AX, Hodsman AB, Rush DN, Leslie WD. Long-term changes in bone mineral density in kidney transplant recipients. *Transplantation*. 2014;98(12):1279-1285.
14. Rajapakse CS, Leonard MB, Bhagat YA, Sun W, Magland JF, Wehrli FW. Micro-MR imaging-based computational biomechanics demonstrates reduction in cortical and trabecular bone strength after renal transplantation. *Radiology*. 2012;262(3):912-920.
15. Iyer SP, Nikkel LE, Nishiyama KK, et al. Kidney transplantation with early corticosteroid withdrawal: paradoxical effects at the central and peripheral skeleton. *J Am Soc Nephrol*. 2014;25(6):1331-1341.
16. Nishiyama KK, Pauchard Y, Nikkel LE, et al. Longitudinal HR-pQCT and image registration detects endocortical bone loss in kidney transplantation patients. *J Bone Miner Res*. 2015;30(3):554-561.
17. Bonani M, Frey D, Brockmann J, et al. Effect of twice-yearly denosumab on prevention of bone mineral density loss in de novo kidney transplant recipients: a randomized controlled trial. *Am J Transplant*. 2016;16(6):1882-1891.
18. Evenepoel P, Behets GJ, Viaene L, d'Haese PC. Bone histomorphometry in de novo renal transplant recipients indicates a further decline in bone resorption 1 year posttransplantation. *Kidney Int*. 2017;91(2):469-476.
19. Monier-Faugere MC, Mawad H, Qi Q, Friedler RM, Malluche HH. High prevalence of low bone turnover and occurrence of osteomalacia after kidney transplantation. *J Am Soc Nephrol*. 2000;11(6):1093-1099.
20. Cruz EA, Lugon JR, Jorgetti V, Draibe SA, Carvalho AB. Histologic evolution of bone disease 6 months after successful kidney transplantation. *Am J Kidney Dis*. 2004;44(4):747-756.
21. Kodras K, Haas M. Effect of kidney transplantation on bone. *Eur J Clin Invest*. 2006;36(Suppl 2):63-75.
22. Link TM, Saborowski O, Kisters K, et al. Changes in calcaneal trabecular bone structure assessed with high-resolution MR imaging in patients with kidney transplantation. *Osteoporos Int*. 2002;13(2):119-129.
23. Luckman M, Hans D, Cortez N, et al. Spine trabecular bone score as an indicator of bone microarchitecture at the peripheral skeleton in kidney transplant recipients. *Clin J Am Soc Nephrol*. 2017;12(4):644-652.
24. Naylor KL, Lix LM, Hans D, et al. Trabecular bone score in kidney transplant recipients. *Osteoporos Int*. 2016;27(3):1115-1121.
25. Pérez-Sáez MJ, Herrera S, Prieto-Alhambra D, et al. Bone density, microarchitecture, and tissue quality long-term after kidney transplant. *Transplantation*. 2017;101(6):1290-1294.
26. Pérez-Sáez MJ, Herrera S, Prieto-Alhambra D, et al. Bone density, microarchitecture, and material strength in chronic kidney disease patients at the time of kidney transplantation. *Osteoporos Int*. 2017;28(9):2723-2727.
27. Moe S, Drüeke T, Cunningham J, et al. Definition, evaluation, and classification of renal osteodystrophy: a position statement from kidney disease: improving global outcomes (KDIGO). *Kidney Int*. 2006;69(11):1945-1953.
28. Sharma AK, Toussaint ND, Masterson R, et al. Deterioration of cortical bone microarchitecture: critical component of renal osteodystrophy evaluation. *Am J Nephrol*. 2018;47:376-384.

29. Rajapakse CS, Phillips EA, Sun W, et al. Vertebral deformities and fractures are associated with MRI and pQCT measures obtained at the distal tibia and radius of postmenopausal women. *Osteoporos Int*. 2014;25(3):973-982.
30. Wehrli FW, Gomberg BR, Saha PK, Song HK, Hwang SN, Snyder PJ. Digital topological analysis of in vivo magnetic resonance microimages of trabecular bone reveals structural implications of osteoporosis. *J Bone Miner Res*. 2001;16(8):1520-1531.
31. Benito M, Gomberg B, Wehrli FW, et al. Deterioration of trabecular architecture in hypogonadal men. *J Clin Endocrinol Metab*. 2003;88(4):1497-1502.
32. Silva BC, Leslie WD, Resch H, et al. Trabecular bone score: a noninvasive analytical method based upon the DXA image. *J Bone Miner Res*. 2014;29(3):518-530.
33. Evenepoel P, Claes K, Kuypers D, Maes B, Bammens B, Vanrenterghem Y. Natural history of parathyroid function and calcium metabolism after kidney transplantation: a single-centre study. *Nephrol Dial Transplant*. 2004;19(5):1281-1287.
34. Wolf M, Weir MR, Kopyt N, et al. A prospective cohort study of mineral metabolism after kidney transplantation. *Transplantation*. 2016;100(1):184-193.
35. Van der Linden JC, Homminga J, Verhaar JA, Weinans H. Mechanical consequences of bone loss in cancellous bone. *J Bone Miner Res*. 2001;16(3):457-465.
36. Seeman E, Delmas PD. Bone quality–the material and structural basis of bone strength and fragility. *N Engl J Med*. 2006;354(21):2250-2261.
37. Kimmel DB, Recker RR, Gallagher JC, Vaswani AS, Aloia JF. A comparison of iliac bone histomorphometric data in post-menopausal osteoporotic and normal subjects. *Bone Miner*. 1990;11(2):217-235.
38. Akhter MP, Lappe JM, Davies KM, Recker RR. Transmenopausal changes in the trabecular bone structure. *Bone*. 2007;41(1):111-116.
39. Boutroy S, Vilayphiou N, Roux JP, et al. Comparison of 2D and 3D bone microarchitecture evaluation at the femoral neck, among postmenopausal women with hip fracture or hip osteoarthritis. *Bone*. 2011;49(5):1055-1061.
40. Leonard MB. A structural approach to skeletal fragility in chronic kidney disease. *Semin Nephrol*. 2009;29(2):133-143.
41. Graciolli FG, Neves KR, Barreto F, et al. The complexity of chronic kidney disease-mineral and bone disorder across stages of chronic kidney disease. *Kidney Int*. 2017;91(6):1436-1446.
42. Drueke TB, Massy ZA. Changing bone patterns with progression of chronic kidney disease. *Kidney Int*. 2016;89(2):289-302.
43. Seeman E. Periosteal bone formation—a neglected determinant of bone strength. *N Engl J Med*. 2003;349(4):320-323.
44. Ahlborg HG, Johnell O, Turner CH, Rannevik G, Karlsson MK. Bone loss and bone size after menopause. *N Engl J Med*. 2003;349(4):327-334.
45. Naylor KL, Prior J, Garg AX, et al. Trabecular bone score and incident fragility fracture risk in adults with reduced kidney function. *Clin J Am Soc Nephrol*. 2016;11(11):2032-2040.

How to cite this article: Sharma AK, Toussaint ND, Elder GJ, et al. Changes in bone microarchitecture following kidney transplantation—Beyond bone mineral density. *Clin Transplant*. 2018;e13347. https://doi.org/10.1111/ctr.13347

NEPHROLOGY

Nephrology **21** (2016) 46–54

Original Article

Impact of cinacalcet pre-transplantation on mineral metabolism in renal transplant recipients

ASHISH K SHARMA,[1,2] ROSEMARY MASTERSON,[1] STEPHEN G HOLT,[1,2] SVEN-JEAN TAN,[1,2] PETER D HUGHES,[1] MELISSA CHU,[1] PAVITHRA JAYADEVA[1] and NIGEL D TOUSSAINT[1,2]

[1]Department of Nephrology, The Royal Melbourne Hospital, Parkville and [2]Department of Medicine (RMH), The University of Melbourne, Melbourne, Victoria, Australia

KEY WORDS:
calcimimetic, cinacalcet, hypercalcaemia, mineral metabolism, renal transplantation, secondary hyperparathyroidism.

Correspondence:
A/Prof Nigel Toussaint, Department of Nephrology, The Royal Melbourne Hospital, Grattan Street, Parkville, Vic. 3052, Australia.
Email: Nigel.Toussaint@mh.org.au

Accepted for publication 8 June 2015.
Accepted manuscript online 9 June 2015.

doi:10.1111/nep.12536

Conflict of interest: NDT and SGH have received honoraria and research grant funding from Amgen Australia Pty. NDT and SGH have also been members of Medical Advisory Boards for Amgen.

SUMMARY AT A GLANCE

This is a retrospective study on 532 renal transplant recipients, in which authors compared the outcomes after transplantation between those being treated with cinacalcet (n = 72) and cinacalcet-naïve counterparts before transplantation (n = 460). With the strength of a large sample size and long duration of follow up, the study observed higher post-transplant parathyroid hormone level and calcium level among those discontinuing cinacalcet.

ABSTRACT:

Aim: **Cinacalcet is effective in reducing parathyroid hormone (PTH) in patients on dialysis. Reports of biochemical profiles and other clinical outcomes in patients discontinuing cinacalcet at time of renal transplantation are limited.**

Methods: **A retrospective study assessing markers of mineral metabolism, graft and patient outcomes in renal transplant recipients to determine differences in patients discontinuing cinacalcet (C+) compared with patients not treated with cinacalcet (C–) at time of transplantation. To allow for differences between groups in pre-transplant biochemical parameters, we also analysed a matched cohort of C– with C+ recipients (2:1), matched for age, calcium and PTH levels at transplantation.**

Results: **Five hundred thirty-two recipients (460 C–, 72 C+), transplanted January 2006–December 2012, were analysed, mean age 48.0 ± 12.7 years and 64.3% were men. At a median 42.9 months follow up, there were 10 deaths (1.9%), 56 allograft loss (10.6%) and 5 parathyroidectomies post-transplant (0.8%). Median PTH immediately pre-transplant was higher in C+ *versus* C– (50.7(25.4–75.2) *versus* 28.3(13.9–49.7) pmol/L, $P < 0.001$). Twelve-month post-transplant PTH was reduced but higher in C+ (11.7(6.9–21.2) *vs* 7.2(4.6–11.2) pmol/L, $P < 0.001$). Mean calcium was higher for C+ *versus* C– at 12 months (2.50 ± 0.19 *vs* 2.43 ± 0.17 mmol/L, $P < 0.001$), with differences to 4 years post-transplant. No difference was seen in renal function, graft loss, post-transplant parathyroidectomy rate and mortality. In the matched cohort (144 C– *vs* 72 C+), similar findings were also seen.**

Conclusion: **Differences in mineral metabolism post-transplant are seen with cinacalcet pre-transplant compared with no cinacalcet. Transplant recipients discontinuing cinacalcet had higher post-transplant PTH and calcium although the clinical significance is unclear.**

Secondary hyperparathyroidism (SHPT) is associated with abnormalities in mineral metabolism and is a progressive disease, which affects a substantial proportion of patients with chronic kidney disease (CKD).[1] Mineral and bone disorder in CKD (CKD-MBD), particularly elevated levels of calcium, phosphate and parathyroid hormone (PTH), has been associated with increased morbidity and mortality in numerous studies of patients with CKD and end-stage kidney disease (ESKD) on dialysis.[2,3] At the time of renal transplantation the majority of patients with ESKD have SHPT.[4] Successful renal transplantation improves calcitriol synthesis and appears to reduce PTH levels in most cases. However resolution of SHPT is incomplete in up to 50% of renal transplant recipients at one year after

Table 1 Studies evaluating post-transplant biochemical profiles in patients discontinuing cinacalcet at the time of transplantation

Study	Year	Study design	Sample size '*n*' (on cinacalcet)	Follow up – mean (months)	Results
Torregrosa *et al*.[15]	2009	Prospective	19 (19)	6	PTH and Ca higher in 6/19† PTH and Ca unchanged in 13/19‡
Jadoul *et al*.[16]	2010	Retrospective	38 (28)	12	No change in PTH, Ca and P
Evenepoel *et al*.[17]	2012	Prospective	303 (21)	35.6 ± 15.8	PTH and Ca higher in cinacalcet-treated Higher rate of parathyroidectomy and nephrocalcinosis in cinacalcet-treated
Paschoalin *et al*.[18]	2012	Retrospective	46 (46)	12	Cinacalcet pre-transplant not associated with allograft calcification
Barros *et al*.[19]	2014	Prospective	48 (20)	6	PTH and Ca higher in cinacalcet-treated
Weekers *et al*.[20]	2015	Retrospective	97 (36)	1	Delayed graft function higher in cinacalcet-treated

†Cinacalcet dose ≥60 mg/day. ‡Cinacalcet dose = 30 mg/day. Ca, calcium; P, phosphate; PTH, parathyroid hormone.

transplantation even in the presence of good renal allograft function.[4,5] Hyperparathyroidism and hypercalcaemia post-transplantation have been associated with poorer graft outcomes,[6,7] soft tissue and vascular calcification,[8,9] and increased incidence of fractures.[10]

Calcimimetic agents increase the sensitivity of the calcium-sensing receptor (CaSR) to extracellular calcium and have been an important therapeutic option in patients with persistent SHPT despite use of standard therapies including phosphate binders and vitamin D analogues. Cinacalcet, an allosteric modulator of the CaSR, has been approved for treatment of SHPT in dialysis patients since 2004 in the United States, 2005 in Europe and 2007 in Australia. Studies have reported efficacy in suppressing PTH secretion, reducing serum calcium and phosphate levels, reducing the need for parathyroidectomy, and potentially lowering fracture rate and reducing cardiovascular hospitalization in dialysis patients.[11–13] In a large randomized placebo-controlled trial evaluating the effect of cinacalcet on clinical outcomes in dialysis participants, however, there was no statistically significant difference, according to intention-to-treat analysis, for the primary outcome, which was a composite end-point of mortality and cardiovascular end-points, perhaps related to methodological problems including drop-in and drop-out of the treatment arm and a predictably low event rate in patients aged less than 65 years.[14] In Australia, cinacalcet was approved in late 2007 for treatment of SHPT in patients with ESKD on dialysis, but not for use in renal transplant recipients and has therefore been discontinued in most patients at the time of transplantation. This potentially results in marked hyperparathyroidism and associated metabolic consequences post-transplant leading to adverse biochemical and clinical outcomes.

Few studies have attempted to evaluate the effects of discontinuing cinacalcet at the time of transplantation on mineral metabolism (Table 1).[15–19] Studies are limited by low patient numbers or lack of data concerning clinical outcomes. Most studies have found that a proportion of patients receiving cinacalcet before transplantation develop hypercalcaemia with persistent hyperparathyroidism, and in some cases, hypophosphataemia, after renal transplantation. We report a retrospective study of renal transplant recipients, transplanted over a 7 year period, assessing markers of mineral metabolism and other patient outcomes for up to 5 years of follow up. We aimed to determine differences in post-transplant biochemical parameters and long-term clinical outcomes of graft function, parathyroidectomy rates and survival in transplant recipients administered cinacalcet on dialysis prior to transplantation compared with those who were not treated with cinacalcet.

METHODS

Study design and setting

We performed a single-centre retrospective study at The Royal Melbourne Hospital (RMH), Parkville, Australia, which included all patients who received a renal transplant between 1 January 2006 and 31 December 2012. We obtained information regarding patient demographics, aetiology of ESKD, dialysis details, transplantation details (including date of engraftment, graft number, mode, immunosuppressive therapy), comorbidities (including parathyroidectomy pre-transplant), and patient outcomes such as graft loss, post-transplant parathyroidectomy and mortality from our computerized nephrology database developed in-house (Nephworks 6). Nephworks contains prospectively documented patient history, medications, comorbid events and outcomes for all dialysis and transplant patients at RMH. Blood results related to biochemical profile, namely serum levels of 25-hydroxy vitamin D (25(OH)D), calcium, phosphate, PTH, alkaline phosphatase (ALP) and creatinine, were also obtained. Patients administered cinacalcet therapy at the time of transplantation were identified and classified as cinacalcet-treated patients (C+) whereas patients not administered cinacalcet were designated cinacalcet non-treated (C−). Cinacalcet doses were retrieved and included in the analysis. Patients who received cinacalcet after renal transplantation were excluded from analysis and patients without at least 12 month follow-up data were also excluded (those who moved interstate).

Biochemical parameters

Laboratory data relating to serum PTH, calcium, phosphate, ALP and creatinine included pre-transplant levels and levels at 3, 6, 9 and 12 months post-transplantation as well as yearly thereafter to 5 years post-transplant. Serum 25(OH)D levels were available for patients at 12 months post-transplantation, but unfortunately not at the time of transplantation on all patients. All biochemistry was performed at Melbourne Health Pathology at RMH. Serum concentrations of intact PTH were determined using a solid-phase, two-site chemiluminescent enzyme-labelled immunometric assay on the IMMULITE® 2000 Analyzer (Siemens Healthcare Global, Erlangen, Germany). All other biochemical markers were measured using standard assays and analyses were performed according to the manufacturer's instructions. The estimated glomerular filtration rate (eGFR) was calculated according to the Modification of Diet in Renal Disease formula.[21] Hypercalcaemia was defined as serum calcium level >2.60 mmol/L and hyperparathyroidism a PTH level greater than the upper range of normal for the assay (>7.0 pmol/L).

Statistical methods

Results are presented as mean (±standard deviation) for normally distributed continuous variables and as median (interquartile range) for continuous variables with skewed distributions. The Kolmogorov–Smirnov test was performed to determine the distribution of variables. For differences between groups, Student's *t*-test or the Mann–Whitney *U*-test was used. For differences between periods, the paired Student's *t*-test or Wilcoxon's test for paired values was used. Given differences in demographic characteristics and baseline biochemical data between C– and C+ groups (Table 2), we performed analysis of a matched cohort of C– recipients (matching 2:1 with the C+ cohort) primarily to adjust for the differences in age, duration of dialysis and severity of SHPT at time of transplantation. Similar statistically analyses were performed to assess for biochemical changes post-transplantation as well as other clinical outcomes. For associations among variables, linear regression was used, considering variables with a *P*-value <0.05 in the univariate analysis. A *P*-value <0.05 was considered statistically significant. Stata statistical software package (version 11.0, Stata Corporation, College Station, TX, USA) was used for analysis.

RESULTS

Study population and baseline results

A total of 543 renal transplants were performed over the 7 year period. Eleven patients were excluded from analysis; two received cinacalcet following transplantation; and nine were enrolled in a randomized controlled clinical trial comparing cinacalcet and placebo in transplant recipients.[22] Demographic and baseline characteristics of our study population ($n = 532$) are shown in Table 2. Mean age of patients at the time of transplant was 48.0 ± 12.7 years and 64.3% were men. Glomerulonephritis was the predominant cause of ESKD in the cohort (29.5%) and 82.2% were undertaking dialysis at the time of transplantation (compared with 17.8% of transplants, which were pre-emptive).

Seventy-two patients, 13.5% of the total cohort (January 2006–December 2012) were taking cinacalcet at the time of transplantation. When considering only the time period after November 2007 when cinacalcet was approved for use in Australia, these 72 patients accounted for 16.8% of the cohort. The median daily dose of cinacalcet in C+ patients at

Table 2 Patient characteristics of all transplant recipients and divided according to those who were either not taking cinacalcet (C–) or administered cinacalcet (C+) at the time of transplantation

Characteristics	All ($n = 532$)	C– ($n = 460$)	C+ ($n = 72$)	*P*-value
Age at transplantation (years)	48.0 ± 12.7	47.6 ± 12.7	50.2 ± 12.4	0.01
Gender (%M)	64.3	65.9	54.2	0.05
Cause of ESKD				NS
DM	8.0	7.8	8.7	
GN	29.5	30.1	28.2	
HT	3.8	3.7	4.3	
PCKD	15.9	15.3	20.3	
Reflux	16.5	16.3	17.4	
Other	26.3	26.8	21.1	
Dialysis modality (HD/PD/pre-emptive, %)	53.8/28.4/17.8	50.1/30.3/19.6	71.5/21.1/7.4	0.03
Duration on dialysis (years)	3.41 ± 2.53	3.53 ± 2.58	2.59 ± 2.08	0.009
DM (%)	24.6	23.8	29.6	NS
IHD (%)	10.6	9.4	13.9	NS
HT (%)	71.9	71.2	76.1	NS
Parathyroidectomy (%)	13.9	14.3	11.1	NS
Donor age (years)	52.8 ± 13.4	53.2 ± 12.8	50.3 ± 16.5	0.05
Living (%)	49.4	54.1	19.4	<0.001
First graft (%)	83.2	83.2	83.3	NS
Duration of transplant (months)	45.0 ± 22.9	46.9 ± 23.1	32.3 ± 17.0	<0.001

DM, diabetes mellitus; ESKD, end-stage kidney disease; GN, glomerulonephritis; HD, haemodialysis; HT, hypertension; IHD, ischaemic heart disease; PCKD, polycystic kidney disease; PD, peritoneal dialysis.

Table 3 Biochemical parameters of mineral metabolism at time of transplantation and post-transplant in recipients who were either not taking cinacalcet (C–) or previously administered cinacalcet until the time of transplantation (C+)

Time post	Ca (mmol/l)		*P*-value	Phos (mmol/L)		*P*-value	PTH (pmol/L)		*P*-value
	C–	C+		C–	C+		C–	C+	
Pre-transplant	2.31 ± 0.23	2.22 ± 0.20	0.001	1.73 ± 0.59	1.64 ± 0.53	0.21	28.3(13.9–49.7)	50.7(25.4–75.2)	<0.001
3 months	2.43 ± 0.17	2.51 ± 0.17	<0.001	0.95 ± 0.29	0.92 ± 0.29	0.50	8.8 (5.0–14)	13.2 (8.6–24.6)	<0.001
6 months	2.44 ± 0.16	2.54 ± 0.17	<0.001	1.02 ± 0.51	0.93 ± 0.28	0.19	7.4 (4.8–11.7)	12.0 (7.5–20.1)	<0.001
9 months	2.44 ± 0.17	2.53 ± 0.15	<0.001	1.03 ± 0.35	0.97 ± 0.32	0.20	7.9 (4.6–10.8)	13.1 (7.8–21.6)	<0.001
12 months (*n* = 532)	2.43 ± 0.17	2.50 ± 0.19	0.001	1.02 ± 0.28	0.95 ± 0.41	0.07	7.2 (4.6–11.2)	11.7 (6.9–21.2)	0.005
2 years (*n* = 398)	2.43 ± 0.18	2.50 ± 0.18	0.007	1.06 ± 0.32	0.94 ± 0.28	0.02	8 (5.4–14.3)	10.7 (6.4–22.1)	0.43
3 years (*n* = 296)	2.42 ± 0.21	2.53 ± 0.17	0.006	1.07 ± 0.35	0.97 ± 0.26	0.15	6.9 (4.4–12.7)	14.4(11.3–28.7)	0.11
4 years (*n* = 155)	2.44 ± 0.18	2.52 ± 018	0.09	1.11 ± 0.35	1.16 ± 0.54	0.59	8.2 (5.5–13.6)	16.7 (8.4–52.3)	0.16
5 years (*n* = 98)	2.35 ± 0.23	2.50 ± 0.20	0.16	1.26 ± 0.56	1.21 ± 0.41	0.23	10.5 (6.0–15.9)	21.4(10.2–50.1)	0.21

Serum calcium and phosphate levels are shown as mean ± SD, and PTH levels are median (IQR). Ca, calcium; Phos, phosphate; PTH, parathyroid hormone.

time of transplantation was 60 mg (range 30–180 mg). C+ patients were older than C– patients (50.2 ± 12.4 *vs* 47.6 ± 12.7 years. $P = 0.01$).

The median PTH levels at the time of transplantation were higher in C+ *vs* C– patients (50.7(25.4–75.2) *vs* 28.3(13.9–49.7) pmol/L, $P < 0.001$). Mean serum calcium levels were statistically lower in C+ *versus* C– (2.22 ± 0.20 *vs* 2.31 ± 0.23 mmol/L, $P = 0.001$) although phosphate levels were not significantly different between groups at the time of transplantation. Mean ALP levels were greater in C+ *versus* C– patients pre-transplantation (164.5 ± 128.3 *vs* 95.0 ± 48.5 IU, $P < 0.001$).

Post-transplant biochemical parameters

Twelve months post-transplant median PTH was significantly higher in those administered cinacalcet prior to transplant (11.7(6.9–21.2) *vs* 7.2(4.6–11.2) pmol/L, $P < 0.001$) indicating persisting hyperparathyroidism, but showing marked improvement in both groups (Table 3). Mean serum calcium was also significantly higher in C+ patients at 12 months (2.50 ± 0.19 *vs* 2.43 ± 0.17 mmol/L, $P < 0.001$). Mean ALP levels were not different between groups (103.6 ± 43.9 *vs* 97.0 ± 41.6 IU, $P = 0.23$). Serum 25(OH)D levels at 12 months following transplantation did not differ between groups (57.8 ± 26.0 *vs* 51.9 ± 24.7 for C– *vs* C+, respectively, $P = 0.10$).

The proportion of all patients at 12 months post-transplant with hypercalcaemia was 17.1%, with a greater proportion in the C+ group compared with C– (25.0% *vs* 16.2%, $P = 0.06$) (Table 4). Only 31 patients had severe hypercalcaemia (serum calcium >2.80 mmol/L) at 12 months with no difference between groups ($P = 0.23$). Of all recipients at 12 months, 60.7% had high PTH levels (>7.0 pmol/L), with a significant difference between C+ and C– (76.4% *vs* 58.3%, $P = 0.003$). Differences in biochemical markers persisted post-transplant between groups, with higher post-transplant serum calcium levels in C+ patients compared with C– present to 4 years following the transplant and PTH levels significantly higher in C+ *versus* C– until 2 years post-transplant.

Table 4 Proportion of patients (%) with abnormal biochemical parameters following transplantation (6 months, 12 months and 2 years)

Biochemical parameter	All	C–	C+	*P*-value
PTH (>7.0 pmol/L)				
6 months	69.0	66.5	84.7	0.002
12 months	60.7	58.3	76.4	0.003
2 years	86.3	85.7	90.3	0.29
Calcium (>2.60 mmol/L)				
6 months	17.7	14.6	37.5	<0.001
12 months	17.1	16.1	25.0	0.06
2 years	36.5	34.6	48.6	0.02
Phosphate (<0.80 mmol/L)				
6 months	20.5	19.3	27.8	0.10
12 months	19.5	17.6	32.0	0.004
2 years	10.2	9.1	16.7	0.05

PTH, parathyroid hormone.

In relation to number of previous allografts, most transplant recipients in this study were first graft recipients (83.2%) and the proportion of these patients with high PTH and high calcium at 12 months post-transplant was 60.0% and 17.2%, respectively. For recipients with a second and third graft, 63.2% and 63.6% had high PTH and 18.4% and 10% had high calcium levels at 12 months following transplantation, respectively (not statistically different to those with a first graft).

Multivariate regression analyses with serum PTH at 12 months as the dependent variable showed independent associations with PTH level at the time of transplantation, renal function at 12 months post-transplant, and cinacalcet use pre-transplant. Serum calcium at 12 months post-transplant was independently associated with age, pre-transplant calcium, PTH and ALP levels, renal function 12 months post-transplant, and cinacalcet use at the time of transplantation.

Cinacalcet dose

Most patients ($n = 52$, 72.2%) were administered a dose of 60 mg or less prior to transplantation. Comparing the higher *versus* lower cinacalcet doses (≥60 mg *vs* <60 mg daily) the mean PTH levels were 16.4 ± 16.1 *vs* 16.0 ± 11.4 pmol/L ($P = 0.92$) and mean calcium levels were 2.57 ± 0.17 *versus* 2.47 ± 0.20 mmol/L ($P = 0.06$), respectively. Thus, for those taking more than 60 mg daily there were no statistically significant differences in serum PTH or calcium levels at 12 months compared with those prescribed lower doses.

Other clinical outcomes

At a median of 42.9 months follow up there were 10 deaths (1.9%), 56 recipients with failed grafts (10.6%) and 5 parathyroidectomies performed in recipients post-transplant (0.8%) (Table 5). There were no differences in any of these clinical outcomes between the C+ and C− groups, although the numbers of deaths and parathyroidectomies following transplantation were low.

There was no difference in renal function between the two groups, at any stage out to 5 years post-transplant, and no difference in graft failure rates in those who had received cinacalcet compared with the C− group (Table 6).

Matched cohort

As there were significant differences in the severity of SHPT between groups at the time of transplantation (and differences in some demographic parameters including age and duration of dialysis), we matched 144 C− recipients for age and biochemical markers at the time of transplantation (serum calcium and PTH) with the 72 C+ transplant recipients (matching 2:1) for assessment of outcomes (Table 7). We found similar findings as with the total transplant cohort in that post-transplant serum calcium levels were significantly higher up to 4 years and PTH levels were higher to 12 months following transplantation in those who had previously been administered cinacalcet (Table 8). Similar to the total cohort, there was no difference in serum phosphate levels following transplantation between the matched C− cohort and the C+ group. Estimated GFR was also similar in matchd C− recipients compared with C+ , with mean eGFR of 52.8 ± 21.6 *versus* 54.4 ± 24.1 mL/min/1.73 m^2 at 12 months and 50.9 ± 25.6 *versus* 48.8 ± 22.7 mL/min/1.73 m^2 at 3 years post-transplant for C− and C+ groups, respectively. Clinical outcomes were also similar with no difference between matched C− and C+ in rates of graft failure (9.2% *vs* 8.3%), post-transplant diabetes (15.1% *vs* 14.5%), post-transplant parathyroidectomy (1.0% *vs* 1.4%) and overall mortality (1.4% *vs* 1.4%).

Table 5 Outcomes of transplant recipients who were either not taking cinacalcet (C−) or previously administered cinacalcet until the time of transplantation (C+)

Outcomes	All	C−	C+	*P*-value
Graft failure (%)	10.6	10.9	8.3	0.51
Post-transplant DM (%)	12.7	12.4	14.5	0.66
Post-transplant parathyroidectomy (%)	0.8	0.7	1.4	0.50
Mortality (%)	1.9	2.0	1.4	0.74

DM, diabetes mellitus.

Table 6 Renal function (measured by MDRD eGFR) at time of transplantation and post-transplant in recipients who were either not taking cinacalcet (C−) or previously administered cinacalcet until the time of transplantation (C+)

eGFR (mL/min/1.73 m^2)	C−	C+	*P*-value
Pre-transplant	7.7 ± 5.0	6.5 ± 2.8	0.1
1 year	50.7 ± 18.7	54.4 ± 24.1	0.14
2 years	50.9 ± 24.1	53.2 ± 21.1	0.56
3 years	50.5 ± 22.2	48.8 ± 22.7	0.78
5 years	41.8 ± 22.2	47.3 ± 18.8	0.73

eGFR, estimated glomerular filtration rate; MDRD, Modification of Diet in Renal Disease.

DISCUSSION

In this single-centre retrospective study, which has larger patient numbers and longer duration of follow up than previous reported studies,[15–19] we compared the post-transplantation mineral profiles of renal transplant recipients treated with cinacalcet to those who were cinacalcet-naïve. We report differences between the two groups, mainly of higher post-transplant serum PTH and calcium in those administered cinacalcet until time of transplantation, up to 12 months and 4 years post-transplantion, respectively.

Traditional treatment for SHPT consists of dietary phosphate restriction, vitamin D analogues, and phosphate binding agents. The international Kidney Disease: Improving Global Outcomes CKD-MBD guidelines recommend parathyroidectomy in patients with severe SHPT associated with hypercalcaemia and/or hyperphosphataemia that is refractory to medical therapy.[23] Calcimimetics are relatively new

Table 7 Patient characteristics of the matched cohort of transplant recipients ($n = 216$), divided according to those who were either not taking cinacalcet (C−) or administered cinacalcet (C+) at the time of transplantation

Characteristics	C− ($n = 144$)	C+ ($n = 72$)	*P*-value
Age at transplantation (years)	49.3 ± 13.1	50.2 ± 12.4	0.52
Gender (%M)	60.7	54.2	0.36
Dialysis *versus* pre-emptive (%)	90.1/9.9	92.6/7.4	0.55
Duration on dialysis (years)	3.51 ± 2.69	2.59 ± 2.08	0.64
DM (%)	31.6	29.6	0.76
Donor age (years)	53.1 ± 13.0	50.3 ± 16.5	0.21
Duration of transplant (months)	32.6 ± 12.1	32.3 ± 17.0	0.54

DM, diabetes melltus.

Table 8 Biochemical parameters of mineral metabolism at time of transplantation and post-transplant in matched transplant recipients (n = 216) who were either not taking cinacalcet (C–, n = 144) or previously administered cinacalcet until the time of transplantation (C+ , n = 72)

Time post	Ca (mmol/l)		*P*-value	PTH (pmol/L)		*P*-value
	C–	C+		C–	C+	
Pre-transplant	2.24 ± 0.21	2.22 ± 0.20	0.32	40.9 (20.8-63.6)	50.7 (25.4–75.2)	0.29
3 months	2.41 ± 0.19	2.51 ± 0.17	<0.001	10.6 (5.2–15.4)	13.2 (8.6–24.6)	0.001
6 months	2.44 ± 0.16	2.54 ± 0.17	<0.001	7.8 (5.2–14.1)	12.0 (7.5–20.1)	<0.001
9 months	2.46 ± 0.16	2.53 ± 0.15	0.005	8.0 (4.2–11.0)	13.1 (7.8–21.6)	<0.001
12 months (n = 532)	2.43 ± 0.18	2.50 ± 0.19	0.01	7.3 (4.5–12.3)	11.7 (6.9–21.2)	<0.001
2 years (n = 398)	2.42 ± 0.15	2.50 ± 0.18	0.002	7.7 (5.0–14.5)	10.7 (6.4–22.1)	0.37
3 years (n = 296)	2.42 ± 0.21	2.53 ± 0.17	0.009	7.3 (4.4–12.7)	14.4 (11.3-28.7)	0.43
4 years (n = 155)	2.43 ± 0.18	2.52 ± 018	0.13	8.1 (4.4–17.4)	16.7 (8.4–52.3)	0.08

Serum calcium levels are shown as mean ± standard deviation, and PTH levels are median (interquartile range). Ca, calcium; PTH, parathyroid hormone.

therapeutic agents introduced for the treatment of SHPT over the last decade. Calcimimetics act by allosteric modification of CaSR on the parathyroid gland, increasing its sensitivity to extracellular levels by decreasing PTH gene expression[24,25] Cinacalcet hydrochloride remains the first and only commercially available calcimimetic approved for clinical use to date. Over the last decade a number of studies have demonstrated efficacy in lowering serum levels of PTH, calcium and phosphate with benefits including reducing the risk of parathyroidectomy, fracture, cardiovascular hospitalization, and cardiovascular death in patients over 65 years in patients on dialysis with SHPT.[11–14,26]

Persistent hyperparathyroidism is common post renal transplantation. High PTH levels, hypercalcaemia and duration on dialysis at the time of transplantation are risk factors for persistent SHPT, especially in transplant recipients with subsequent suboptimal renal function.[4] High PTH is noted in 17–60% of patients at 12 months following transplantation,[4,5] and is a major determinant of post-transplant hypercalcaemia[27] which occurs in 11–66% with casemix and differences in diagnostic criteria accounting for the wide variation.[19,28–30] Post-transplant hyperparathyroidism can result in complications of worse graft outcome,[6,7] soft tissue and vascular calcification[8,9] and increased incidence of fracture.[10] In our cohort, ~60% of transplant recipients had high PTH and ~17% had hypercalcaemia at 12 months post-transplant.

Cinacalcet is efficacious in treating SHPT not responding to standard therapy in patients on dialysis and has resulted in a decline in rates of parathyroidectomy. Parathyroidectomy is an operation with appreciable mortality and morbidity in this cohort, and not analogous to single gland parathrydroidectomy in patients with primary hyperparathyroidism. A recent paper by Ishani *et al*. describes the problems associated with parathyroidectomy in the setting of haemodialysis demonstrating the significant healthcare costs and burden of this procedure in a US ESKD cohort.[31] There is evidence however that cinacalcet is ineffective in promoting the regression of parathyroid hyperplasia particularly where the gland volume is greater than 500 mm^3 although this is controversial.[32,33]

Cinacalcet is not currently approved for use in transplant recipients and so is often discontinued at the time of transplantation or very shortly thereafter. Our retrospective cohort study determined the impact of discontination of this calcimimetic at the time of transplantation on the biochemical profile and other clinical outcomes of patients after transplantation and reports higher serum PTH and serum calcium levels, in the first 12 months and 4 years post-transplant, respectively, in patients presecribed cinacalcet prior to transplantation compared with the cinacalcet-naïve cohort. Ongoing SHPT post-transplant leads to persisting abnormalities in metabolic bone parameters but by 5 years the difference is small. Our results, in larger numbers than previous studies,[15–19] show that biochemical profiles after transplantation are relatively slow to correct although a trend in the right direction. Neverthless, use of cinacalcet prior to transplantation, and lower parathryoidectomy rates, does not seem to have any significant impact on clinical outcomes in this study.

There is limited data available regarding the effect of persistent SHPT and hypercalcaemia on long-term renal graft and patient outcomes. It has been reported that hyperparathyroidism particularly in combination with hypercalcaemia is associated with increased fracture risk[10] and progression of coronary artery calcification.[9] One study by Evenepeol *et al*. looking at protocol allograft biopsies demonstrated calcium and phosphate deposition was highly prevalent in the early post-transplant period and was related to the severity of disturbance in mineral metabolism.[34] Despite the high prevalence of calcium phosphate deposition, the clinical significance was unclear as no difference in renal function was evident at 36 months between recipients with deposition and those without. In another study from the same group, a higher incidence of nephrocalcinosis was demonstrated in recipients who had been treated with cinacalcet prior to

transplantation compared with cinacalcet-naïve patients, over a median follow up of 35 months, although there was no difference in renal allograft function between groups.[17] Our study supports these findings with no difference in eGFR at a median of 43 months post-transplant between groups despite higher PTH and calcium levels in those prescribed cinacalcet prior to transplantation.

There are several studies evaluating biochemical and clinical consequences of discontinuing cinacalcet at the time of transplantation (summarized in Table 1).[15–19] Discontinuing cinacalcet may potentially result in a rebound of PTH levels in the early post-transplant period in renal transplant recipients. Similar to our study findings, two prospective studies reported higher PTH and calcium levels post-transplant consistent with persistent hyperparathyroidism.[17,19] One of these looked at differences in the dose of cinacalcet while on dialysis and reported that ongoing or rebound hyperparathyroidism was only relevant for those receiving 60 mg daily or more.[15] Evenepoel *et al*. also showed a significantly higher parathyroidectomy rate in cinacalcet-treated patients, particularly with increasing doses, whereas graft nephrocalcinosis, although higher in cinacalcet-treated patients, did not reach statistical significance.[17] Barros *et al*., in a recently published prospective study, also reported higher PTH and calcium levels at 6 months post-transplantation, with 75% of patients taking a median daily dose of 30 mg of cinacalcet pre-transplant.[19] This study also evaluated the impact of the phosphatonin fibroblast growth factor-23 (FGF23) post-transplant, reporting higher levels in those administered cinacalcet prior to transplantation (although not statistically significantly different compared with cinacalcet-naïve patients). We found no difference in post-transplant PTH or calcium levels in recipients on higher doses of cinacalcet (>60 mg daily) compared with lower (≤60 mg daily), although the percentage of patients on higher doses was small making it difficult to draw conclusions from our data regarding the impact of cinacalcet dose.

Although cinacalcet is not currently approved for use post-transplantation there have been a number of studies of renal transplant recipients evaluating the impact of administration of this medication in this population. A recent meta-analysis including 21 studies, 15 prospective and six retrospective predominantly small observational studies with no randomized controlled trials, concluded that cinacalcet was a safe and effective treatment for post-transplant hyperparathyroidism and suggested a role for cinacalcet as an alternative to parathyroidectomy.[35] One large retrospective study reported sustained control of serum PTH, calcium and phosphate levels over three years in renal transplant recipients administered cinacalcet for persistent SHPT.[36] A more recent randomized placebo-controlled trial reported a benefit of cinacalcet in transplantation to improve post-transplant hypercalcaemia, with a 75.4 (63.8–87.1)% difference in achieving a serum calcium less than 2.55 mmol/L compared with placebo.[22] It is interesting to note that despite the effectiveness in reducing PTH levels and hypercalcaemia in this study, there was no difference in renal function between the cinacalcet and placebo arms.

Like previous retrospective studies we observed higher post-transplantation serum calcium and PTH levels along with a higher proportion of hypercalcaemia in patients receiving cinacalcet before transplantation compared with patients not on cinacalcet. Rebound or persisting hyperparathyroidism and hypercalcaemia may be a significant clinical problem as it may result in bone loss and may impair graft function either acutely, by inducing vasoconstriction, or chronically, by mediating calcification of the tubulointerstitium (nephrocalcinosis).[6,37,38] The main factors related to post-transplant hypercalcaemia are likely PTH-mediated bone resorption and recovery of calcitriol levels. Recent clinical data also support the theory that increased PTH-mediated calcium release from the skeleton is the major pathophysiological mechanism underlying post-transplant hypercalcaemia, rather than an increased renal tubular calcium reabsorption.[28] Although analysis of our data suggested no association between cincacalcet-treated patients and mortality or the need for parathyroidectomy post-transplant, the numbers of these events were too low to determine a clinically significant difference. There was also no association with allograft loss between groups, although other studies have suggested that hypercalcaemia may potentially be related to increased nephrocalcinosis and poorer graft outcomes. One previous study reported a tendency for higher eGFR in cinacalcet-treated patients;[16] however, in our cohort, there was no significant difference in renal function between groups at any stage up to 5 years post-transplant.

Recent literature has suggested that the use of cinacalcet at the time of transplantation may exacerbate kidney injury and contribute to delayed graft function following transplantation.[20] One recent retrospective study reported on 36 transplant recipients who were administered cinacalcet at the time of transplantation and, after matching with 61 recipients not on cinacalcet, found an association between cinacalcet use and delayed graft function (42% *vs* 23% for cinacalcet group *vs* controls, respectively). Unfortunately we did not have information on delayed graft function in our transplant cohort to assess for this association.

There are several limitations of our study including the retrospective nature. We have included all renal transplant patients over the study period (who had not been administered cinacalcet post-transplant); however, this cohort is likely representative of the transplant population at our centre without selection bias. Our study is also the largest reported of renal transplant recipients to date assessing the impact of cessation of cinacalcet at the time of transplantation. Indication bias is a potential limitation given the retrospective nature of this study as patients administered cinacalcet likely had more severe SHPT, compared with cinacalcet-naïve patients, which justified cinacalcet initiation

during dialysis to avoid severe complications of SHPT. We could not establish the duration of cinacalcet use in the cinacalcet-treated patients from our records and therefore the duration and degree of SHPT before transplantation. However, we performed analysis of a matched cohort of transplant recipients who had not been administered cinacalcet prior to transplantation, matching 2:1 with the cinacalcet recipients for age, duration of dialysis and degree of SHPT (serum calcium and PTH) at the time of transplantation. This analysis revealed similar findings to comparison between cinacalcet patients and cinacalcet-naïve patients in the total study group. Other limitations of our study include the lack of 25(OH)D levels at the time of transplantation, and no FGF23 and calcitriol levels at any time point, as well as no available data on fractures, bone mineral density, indications for parathyroidectomy, nor medications that may have influenced bone and mineral metabolism including bisphosphonates, phosphate binders and vitamin D analogues or vitamin D supplements.

In summary, biochemical profiles are suggestive of persisting hyperparathyroidism upon cessation of cinacalcet in patients at the time of transplantation and reinforce the need for ongoing monitoring and management of this patient subgroup. However, no significant adverse clinical outcome was noted in our cohort with the use of cinacalcet prior to transplantation and this strategy likely avoids a significant number of parathyroidectomy operations and consequent morbidity and mortality associated with this procedure. There is conflicting evidence regarding the dose–response relationship between pre-transplant cinacalcet use and SHPT on its withdrawal, which needs to be investigated and might provide a guide to risk stratification of these patients. These findings provide impetus to the need for not only larger interventional studies in this cohort but also further exploring the role of calcimimetics in transplant recipients. More studies involving continuation of cinacalcet post-transplantation are required to determine the optimal treatment of SHPT in patients listed for transplantation.

ACKNOWLEDGEMENTS

We would like to thank Janice Pickering and Jayne Amy for assisting with data collection.

REFERENCES

1. Levin A, Bakris G, Molitch M *et al*. Prevalence of abnormal serum vitamin D, PTH, calcium, and phosphorus in patients with chronic kidney disease: Results of the study to evaluate early kidney disease. *Kidney Int.* 2006; **71**: 31–8.
2. Block GA, Klassen PS, Lazarus JM, Ofsthun N, Lowrie EG, Chertow GM. Mineral metabolism, mortality, and morbidity in maintenance hemodialysis. *J. Am. Soc. Nephrol.* 2004; **15**: 2208–18.
3. Ganesh SK, Stack AG, Levin NW, Hulbert-Shearon T, Port FK. Association of elevated serum PO4, Ca× PO4 product, and parathyroid hormone with cardiac mortality risk in chronic hemodialysis patients. *J. Am. Soc. Nephrol.* 2001; **12**: 2131–8.
4. Evenepoel P, Claes K, Kuypers D, Maes B, Bammens B, Vanrenterghem Y. Natural history of parathyroid function and calcium metabolism after kidney transplantation: A single-centre study. *Nephrol. Dial. Transplant.* 2004; **19**: 1281–7.
5. Torres A, Lorenzo V, Salido E. Calcium metabolism and skeletal problems after transplantation. *J. Am. Soc. Nephrol.* 2002; **13**: 551–8.
6. Gwinner W, Suppa S, Mengel M *et al*. Early calcification of renal allografts detected by protocol biopsies: Causes and clinical implications. *Am. J. Transplant.* 2005; **5**: 1934–41.
7. Schwarz A, Mengel M, Gwinner W *et al*. Risk factors for chronic allograft nephropathy after renal transplantation: A protocol biopsy study. *Kidney Int.* 2005; **67**: 341–8.
8. Reynolds JL, Joannides AJ, Skepper JN *et al*. Human vascular smooth muscle cells undergo vesicle-mediated calcification in response to changes in extracellular calcium and phosphate concentrations: A potential mechanism for accelerated vascular calcification in ESRD. *J. Am. Soc. Nephrol.* 2004; **15**: 2857–67.
9. Mazzaferro S, Pasquali M, Taggi F *et al*. Progression of coronary artery calcification in renal transplantation and the role of secondary hyperparathyroidism and inflammation. *Clin. J. Am. Soc. Nephrol.* 2009; **4**: 685–90.
10. Perrin P, Caillard S, Javier RM *et al*. Persistent hyperparathyroidism is a major risk factor for fractures in the five years after kidney transplantation. *Am. J. Transplant.* 2013; **13**: 2653–63.
11. Block GA, Martin KJ, de Francisco AL *et al*. Cinacalcet for secondary hyperparathyroidism in patients receiving hemodialysis. *NEJM* 2004; **350**: 1516–25.
12. Cunningham J, Danese M, Olson K, Klassen P, Chertow GM. Effects of the calcimimetic cinacalcet HCl on cardiovascular disease, fracture, and health-related quality of life in secondary hyperparathyroidism. *Kidney Int.* 2005; **68**: 1793–800.
13. Lindberg JS, Culleton B, Wong G *et al*. Cinacalcet HCl, an oral calcimimetic agent for the treatment of secondary hyperparathyroidism in hemodialysis and peritoneal dialysis: A randomized, double-blind, multicenter study. *J. Am. Soc. Nephrol.* 2005; **16**: 800–7.
14. Chertow GM, Block GA, Correa-Rotter R *et al*. Effect of cinacalcet on cardiovascular disease in patients undergoing dialysis. *NEJM* 2012; **367**: 2482–94.
15. Torregrosa JV, Bergua C, Martinez de Osaba MJ, Oppenheimer F, Campistol JM. Evolution of secondary hyperparathyroidism after kidney transplantation in patients receiving cinacalcet on dialysis. *Transplant. Proc.* 2009; **41**: 2396–8.
16. Jadoul M, Banos A, Zani VJ, Hercz G. The effects of discontinuing cinacalcet at the time of kidney transplantation. *NDT Plus* 2010; **3**: 37–41.
17. Evenepoel P, Sprangers B, Lerut E *et al*. Mineral metabolism in renal transplant recipients discontinuing cinacalcet at the time of transplantation: A prospective observational study. *Clin. Transplant.* 2012; **26**: 393–402.
18. Paschoalin RP, Torregrosa JV, Barros X, Duran CE, Soler M, Campistol JM. Withdrawal of cinacalcet at the time of renal transplantation is not a risk factor for allograft calcifications in the early posttransplantation period. *Transplant. Proc.* 2012; **44**: 2379–80.
19. Barros X, Fuster D, Paschoalin R *et al*. Changes in bone mineral metabolism parameters, including FGF23, after discontinuing cinacalcet at kidney transplantation. *Endocrine* 2015; **49**: 267–73.

20. Weekers L, de Tullio P, Bovy C *et al*. Activation of the calcium-sensing receptor before renal ischemia/reperfusion excerbates kidney injury. *Am. J. Transl. Res.* 2015; **7**: 128–38.
21. Levey AS, Bosch JP, Lewis JB, Greene T, Rogers N, Roth D. A more accurate method to estimate glomerular filtration rate from serum creatinine: A new prediction equation. *Ann. Intern. Med.* 1999; **130**: 461–70.
22. Evenepoel P, Cooper K, Holdaas H *et al*. A randomized study evaluating cinacalcet to treat hypercalcemia in renal transplant recipients with persistent hyperparathyroidism. *Am. J. Transplant.* 2014; **14**: 2545–55.
23. Kidney Disease: Improving Global Outcomes (KDIGO) CKD-MBD Work Group. KDIGO clinical practice guideline for the diagnosis, evaluation, prevention, and treatment of chronic kidney disease–mineral and bone disorder (CKD-MBD). *Kidney Int. Suppl.* 2009; **113**: S1–130.
24. Levi R, Ben-Dov IZ, Lavi-Moshayoff V *et al*. Increased parathyroid hormone gene expression in secondary hyperparathyroidism of experimental uremia is reversed by calcimimetics: Correlation with posttranslational modification of the trans acting factor AUF1. *J. Am. Soc. Nephrol.* 2006; **17**: 107–12.
25. Nagano N. Pharmacological and clinical properties of calcimimetics: Calcium receptor activators that afford an innovative approach to controlling hyperparathyroidism. *Pharmacol. Ther.* 2006; **109**: 339–65.
26. Moe SM, Chertow GM, Coburn JW *et al*. Achieving NKF-K/DOQI™ bone metabolism and disease treatment goals with cinacalcet HCl. *Kidney Int.* 2005; **67**: 760–71.
27. David DS, Sakai S, Brennan BL *et al*. Hypercalcemia after renal transplantation: Long-term follow-up data. *NEJM* 1973; **289**: 398–401.
28. Evenepoel P, Van Den Bergh B, Naesens M *et al*. Calcium metabolism in the early posttransplantation period. *Clin. J. Am. Soc. Nephrol.* 2009; **4**: 665–72.
29. Ramezani M, Einollahi B, Asl MA *et al*. Calcium and phosphorus metabolism disturbances after renal transplantation. *Transplant. Proc.* 2007; **39**: 1033–5.
30. Reinhardt W, Bartelworth H, Jockenhövel F *et al*. Sequential changes of biochemical bone parameters after kidney transplantation. *Nephrol. Dial. Transplant.* 1998; **13**: 436–42.
31. Ishani A, Liu J, Wetmore JB *et al*. Clinical outcomes after parathyroidectomy in a nationwide cohort of patients on hemodialysis. *Clin. J. Am. Soc. Nephrol.* 2015; **10**: 90–97.
32. Meola M, Petrucci I, Barsotti G. Long-term treatment with cinacalcet and conventional therapy reduces parathyroid hyperplasia in severe secondary hyperparathyroidism. *Nephrol. Dial. Transplant.* 2009; **24**: 982–9.
33. Komaba H, Nakanishi S, Fujimori A *et al*. Cinacalcet effectively reduces parathyroid hormone secretion and gland volume regardless of pretreatment gland size in patients with secondary hyperparathyroidism. *Clin. J. Am. Soc. Nephrol.* 2010; **5**: 2305–14.
34. Evenepoel P, Lerut E, Naesens M *et al*. Localization, etiology and impact of calcium phosphate deposits in renal allografts. *Am. J. Transplant.* 2009; **9**: 2470–78.
35. Cohen JB, Gordon CE, Balk EM, Francis JM. Cinacalcet for the treatment of hyperparathyroidism in kidney transplant recipients: A systematic review and meta-analysis. *Transplantation* 2012; **94**: 1041–8.
36. Torregrosa JV, Morales E, Diaz JM *et al*. Cinacalcet for hypercalcaemic secondary hyperparathyroidism after renal transplantation: A multicentre, retrospective, 3-year study. *Nephrology (Carlton)* 2014; **19**: 84–93.
37. Boom H, Mallat MJ, de Fijter JW, Paul LC, Bruijn JA, van Es LA. Calcium levels as a risk factor for delayed graft function. *Transplantation* 2004; **77**: 868–73.
38. Heaf J, Tvedegaard E, Kanstrup IL, Fogh-Andersen N. Hyperparathyroidism and long-term bone loss after renal transplantation. *Clin. Transplant.* 2003; **17**: 268–74.

Hemodialysis International 2015; **19**:256–262

Assessing the utility of testing aluminum levels in dialysis patients

Ashish K. SHARMA,[1,2] Nigel D. TOUSSAINT,[1,2] Janice PICKERING,[1] Tony BEESTON,[1] Edward R. SMITH,[1] Stephen G. HOLT[1,2]

[1]*Department of Nephrology, The Royal Melbourne Hospital, Parkville, Victoria, Australia;* [2]*Department of Medicine (RMH), The University of Melbourne, Parkville, Victoria, Australia*

Abstract

Plasma aluminum (Al) is routinely tested in many dialysis patients. Aluminum exposure may lead to acute toxicity and levels in excess of ~2.2 μmol/L (60 μg/L) should be avoided. Historically, toxicity has been caused by excessive dialyzate Al but modern reverse osmosis (RO) water should be Al free. Nevertheless, many units continue to perform routine Al levels on dialysis patients. This single-center study retrospectively analyzed Al levels in plasma, raw water feed, and RO product between 2010 and 2013 using our database (Nephworks 6) with the aim of determining the utility of these measurements. Two thousand fifty-eight plasma Al tests in 755 patients (61.9% male, mean age 64.7 years) were reviewed showing mean ± SD of 0.41 ± 0.30 μmol/L. One hundred eleven (5.4%) tests from 61 patients had Al levels >0.74 μmol/L and 45 (73.8%) of these patients were or had been prescribed Al hydroxide ($Al(OH)_3$) as a phosphate binder. Seven patients had Al concentrations >2.2 μmol/L with no source of Al identified in 1 patient. One hundred sixty-six patients taking $Al(OH)_3$ (78.7% of all patients on $Al(OH)_3$) had levels ≤0.74 μmol/L, the odds ratio of plasma Al > 0.74 μmol/L on $Al(OH)_3$ was 9. The cost of plasma Al assay is $A30.60; thus, costs were $A62,974.80 over the study period. Despite RO feed water Al levels as high as 48 μmol/L, Al output from the RO was almost always undetectable (<0.1 μmol/L) with dialyzate Al levels > 2.2 μmol/L only 3 times since 2010, and never in the last 3 years. Routine unselected testing of plasma Al appears unnecessary and expensive and more selective testing in dialysis patients should be considered.

Key words: Aluminum, chronic kidney disease, contamination, dialysis, hemodialysis, phosphate binders

INTRODUCTION

Aluminum (Al) is cleared from the blood exclusively by glomerular filtration. Thus, patients with renal failure accumulate Al and are the only routine patient group likely to be at risk of Al toxicity. Al overload results in accumulation principally in the skeleton and the brain and manifests with osteomalacia (resistant to vitamin D therapy), bone and muscle pain, iron-resistant microcytic anemia, and neurologic abnormalities including speech disorders, encephalopathy and dementia.[1]

Acute Al toxicity is rare, and mostly related to Al phosphide (AlP), which is used as a pesticide. Exposure to water or ingestion of AlP causes the release of the highly toxic phosphine (PH_3) leading to rapid free radical injury, circulatory collapse, and death.[2] The Al per se only seems to be an issue if given concurrently with sodium citrate

Correspondence to: A. Sharma, MBBS, Department of Nephrology, The Royal Melbourne Hospital, Grattan Street, Parkville, Vic. 3052, Australia. E-mail: ashish.sharma@mh.org.au

DOI:10.1111/hdi.12231

which dramatically increases Al uptake, and in dialysis patients this leads to very high plasma levels ~2000 μg/L (~75 μmol/L) which can result in potentially fatal neurological toxicity.[3]

Most of the early occurrence of chronic Al toxicity was reported between 1965 and mid-1980s and primarily caused by excessive Al in dialyzate water in patients undergoing chronic hemodialysis (HD) therapy,[4] but it has also been reported after contaminated peritoneal dialysis (PD) fluid.[5] In the early days of dialysis, the preparation of dialyzate water was unsophisticated and subject to contamination from a number of sources, including the addition of Al as a flocculant to remove colloidal matter. Moreover, water purification often involved using stainless steel boilers, sometimes fitted with Al-based cathodic corrosion protection systems, leading to high Al levels in the dialyzate. Modern water preparation using reverse osmosis (RO) membrane systems, reduction in the use of Al-based phosphate binders, and the avoidance of calcium citrate means that acute or chronic Al toxicity is rarely (if ever) encountered in modern practice.[6] Al-based phosphate binders are now infrequently prescribed across the world, but apparently more in Australia/New Zealand.[6] Thus, Al-based binders[6] and Al-containing antacids now represent the major source of Al exposure in patients with end-stage kidney disease (ESKD). Aluminum can also be a contaminant present in oral and injectable medications as part of the manufacturing process,[7,8] in particular albumin products. Albumin binds Al during the purification process when passed through Al silicate filters, and thus long-term use of i.v./blood products is another potential source of excess Al.[9] There have also been reports of sepsis causing release of Al from tissue stores.[10]

The National Kidney Foundation's Kidney Disease Outcomes Quality Initiative (KDOQI) guidelines for the care of patients with ESKD recommended screening for Al toxicity with Al concentrations at least yearly, and quarterly in those receiving Al-containing medications; however, these were outlined in the guidelines as opinion-based recommendations.[11] The more recent international Kidney Disease: Improving Global Outcomes (KDIGO) Chronic Kidney Disease—Mineral and Bone Disorder (CKD-MBD) guidelines recommend avoiding long-term use of Al-containing phosphate binders and, in patients with ESKD on dialysis, dialyzate Al decontamination to prevent Al intoxication.[12] However, there are no KDIGO recommendations regarding measurement of plasma Al levels. There appears to be a low incidence of high Al levels among current dialysis patients[13] with no reported outbreaks of Al toxicity in recent literature except sporadic clusters of cases of elevated Al levels.[14]

There have only been a few retrospective studies published evaluating the frequency of abnormal plasma Al levels, the predictive value of Al testing, cut-off levels for toxicity, and the utility of routine screening in an era of Al-free dialyzate water and decreased Al-based binder administration.[13,15–17] Some investigators have advocated reevaluating the safety of Al-based phosphate binders given low demonstrated risk of toxicity and a cost benefit over contemporary first-line phosphate binders although prospective trials are lacking.[6,18]

In light of the reduction in exposure of dialysis patients to Al, an audit at our institution was undertaken to assess the requirements for continued monitoring of patients and the water quality of dialyzate. We report a single-center study assessing the frequency of abnormal Al levels in a cohort of dialysis patients over a period of 4 years with the aim of evaluating the clinical benefit of routine Al measurement.

METHODS

We performed a retrospective cohort study of dialysis patients at The Royal Melbourne Hospital (RMH), Parkville, Australia. All dialysis patients undergo routine annual surveillance of plasma Al concentrations at RMH, with biannual measurements for patients prescribed Al-based phosphate binders. We retrospectively retrieved all plasma Al levels tested for the dialysis population from January 2010 to December 2013 using our computerized nephrology database (Nephworks 6), as well as RO and water feed Al levels on all HD patients. Nephworks contains prospectively documented patient history, medications, comorbid events, and outcomes for all dialysis patients at RMH. Medical records of patients with abnormal plasma Al levels were reviewed to determine Al exposure.

Laboratory methods

Five milliliters of blood was collected into K_2-EDTA anticoagulated BD Vacutainer® (Becton, Dickinson and Company, Franklin Lakes, New Jersey, USA) Blood Collection Tubes for Trace Element Testing. This avoids significant contamination (20–60 ug/L) by the rubber stoppers made from Al silicate that are commonly used in standard evacuated blood tubes.[19] The sampling needle is not usually a problem for Al.

Plasma Al levels were measured using dual beam graphite furnace atomic absorption spectrophotometry with an AAnalyst 800 spectrophotometer (Perkin Elmer, Waltham, MA, USA) throughout the study period. The lab cut-off value for plasma Al was <0.8 μmol/L with a local

range between 1.5 and 2.0 μmol/L for patients with ESKD on Al-based binders. There is no well-defined threshold level of plasma Al concentration indicating toxicity in dialysis patients.[20] Previous studies have used different cut-off levels including 0.74 μmol/L (20 μg/L), 1.48 μmol/L (40 μg/L), 2.22 μmol/L (60 μg/L), and 3.0 μmol/L based on varying evidence and local lab parameters.[13,16–18] KDOQI guidelines recommend Al levels to be tested quarterly and be less than 0.74 μmol/L with the use of the deferoxamine (DFO) mobilization test[21] for elevated levels between 2.22 and 7.42 μmol/L (60–200 μg/L, respectively).[11] In our study, we used a cut-off value of >0.74 μmol/L to indicate abnormal levels and ≥2.2 μmol/L to indicate risk of toxicity for analysis.

We routinely undertake trace element analysis in dialyzate water collected from various sites across multiple dialysis centers. Mains water and RO output is regularly tested for Al by our service.[22] There are suggested limits of <100 μg/L (3.71 μmol/L) for large processing plants and <200 μg/L (7.42 μmol/L) for smaller plants serving 10,000 people or less.[23] We reference American National Standard ANSI/AAMI RD62:2006, which indicates maximum allowable concentration of Al in "water used to prepare dialyzate" as <10 ug/L (<0.37 μmol) for our dialysis network. We also reviewed Al levels in the dialyzate water source over this period as there are guidelines for drinking water Al content suggested by the World Health Organization (WHO).

Statistics

This is predominantly a descriptive study. Descriptive statistics are presented as mean (± standard deviation) or percentages. Data analyses were performed on individual plasma Al concentrations and not based on the mean plasma Al level per patient. Therefore, both the number of Al determinations and the number of patients are given. Mann–Whitney *U*-test was used to determine differences between patients taking and not taking Al-based phosphate binders according to Al levels. Logistic regression was used to compare differences in Al levels and Al hydroxide ($Al(OH)_3$) use over time. Stata statistical software package (version 11.0, Stata Corporation, College Station, TX, USA) was used for analysis.

RESULTS

We retrieved a total of 2058 plasma Al measurements for 755 patients over the 4-year period. The dialysis cohort had a mean age of 64 years and 62% were male (Table 1). The mean plasma Al level was 0.41 ± 0.30 μmol/L (11 ± 8.08 ug/L). A total of 211 of these patients were or had been prescribed $Al(OH)_3$ as an oral phosphate binder. Of 2058 measurements, 111 (5.4%) tests from 61 patients had Al levels greater than 0.74 μmol/L with 45 (73.8%) being on $Al(OH)_3$. These 61 patients included 47 on HD, 6 on PD, and 8 on home HD. Ten results (0.49%) were equal to or greater than 2.2 μmol/L in 7 patients out of which 6 had been prescribed $Al(OH)_3$, with no source of Al identified in 1 patient who was undergoing dialysis at home at the time and returned normal Al level on repeat testing. There was no evidence of clinical toxicity due to elevated Al levels on review of the available medical records for these patients. One hundred sixty-six patients taking $Al(OH)_3$ (78.7% of all patients on $Al(OH)_3$) had levels ≤0.74 μmol/L. The odds ratio of plasma Al > 0.74 μmol/L on $Al(OH)_3$ was 9.

$Al(OH)_3$ as a potential source of abnormal levels was identified in 45 of 61 patients (Table 2), although the cumulative Al load in patients on $Al(OH)_3$ could not be calculated given inconsistent information available regarding the dose of binders administered. In the remaining 16 patients, the abnormal results were presumed to be erroneous or a result of inadvertent exposure to Al through equipment or medications based on the lack of repeated elevated levels, levels in the nontoxic range (93.7%), and a tendency to revert to normal on repeat testing. On follow-up tests, the levels reverted to or trended toward

Table 1 Patient characteristics for all dialysis patients

Characteristics	N = 755 (%)
Age (years)[a]	63.2 ± 14.9
Gender	
Male	467 (61.9)
Female	288 (38.2)
Cause of ESKD	
DM	197 (26.1)
GN	200 (26.5)
HT	59 (7.8)
PCKD	55 (7.3)
Reflux	39 (5.2)
Other (and unknown)	205 (27.1)
Dialysis modality	
HD	582 (77.0)
PD	119 (15.8)
HHD	54 (7.2)
Duration on dialysis (mo, median [IQR])[a]	32 (61.5-9.9)

[a]At the time of the last Al level.
DM = diabetes mellitus; GN = glomerulonephritis; HD = hemodialysis; HHD = home hemodialysis; HT = hypertension; PCKD = polycystic kidney disease; PD = peritoneal dialysis; Reflux = reflux nephropathy.

Table 2 Number of patients with normal and abnormal plasma aluminum levels in relation to administration of aluminum-based phosphate binders

Al level (μmol/L)	N = 755	No $Al(OH)_3$ N = 544 (%)	$Al(OH)_3$ N = 211 (%)	P value*
<0.74	694 (91.9%)	528 (97.1%)	166 (78.7%)	<0.01
0.74–2.1	54 (7.2%)	15 (2.8%)	39 (18.5%)	<0.01
≥2.2	7 (0.9%)	1 (0.2%)	6 (2.8%)	0.01

Al = aluminum; $Al(OH)_3$ = aluminum hydroxide.
*P value for significance between subjects taking vs. not taking $Al(OH)_3$ for various Al concentrations.

normal in 47 of 61 patients (77%, including 12 patients not on $Al(OH)_3$) with Al levels >0.74 μmol/L. Out of 7 patients with Al > 2.2 μmol/L, only 1 patient had multiple elevated levels, with maximum of 3.64 μmol/L, which reverted back to normal on cessation of $Al(OH)_3$. None of the patients had Al level >7.4 μmol/L.

Al levels measured in the dialyzate water precluded any risk of exposure from that source. Despite RO feed water Al levels as high as 48 μmol/L (1300 ng/mL), Al output from the RO was almost always undetectable (<0.1 μmol/L). We have detected dialyzate Al levels >2.2 μmol/L only 3 times since January 2010, and never in the last 3 years.

The frequency of elevated plasma Al levels (>0.74 μmol/L) in patients on dialysis declined each year from 8.72% in 2010 to 2.35% in 2013, perhaps related to declining use of Al-based phosphate binders. Administration of $Al(OH)_3$ in subjects in this study declined from 31.7% to 4.75% over the same period (Table 3). The cost of single plasma Al assay is $A30.60 resulting in the total cost over the study period of $A62,974.80, or amounting to over $A1300 per month.

DISCUSSION

Al toxicity has been known to cause serious complications although the incidence of cases in the current dialysis population is very low given the elimination of Al from dialyzate water and the decreased use of Al-based phosphate binders. As we have continued to routinely measure plasma Al levels on all dialysis patients at our local center, we performed a retrospective observational study to determine the frequency of abnormal Al concentrations and assess for associations with any clinical history of toxicity, use of Al-based binders, and cost of routine measurements. We report a very low number of elevated Al levels in 755 patients over a 4-year period.

Al is ubiquitous in nature with only a tiny fraction of ingested Al absorbed and normally excreted by the kidneys. Previously, when Al was added to the dialyzate for patients undertaking HD, it would enter the body directly leading to syndromes of toxicity. However, there has been complete absence of reports of the "dialysis dementia" syndromes formerly attributed to Al toxicity in ESKD, and a substantial reduction in the prevalence of Al-related bone disease, with improvements in the quality of dialyzate water.

Plasma Al levels reflect relatively recent exposure to Al.[24,25] Monitoring Al levels might identify excessive Al intake or absorption in individual patients, aid in the recognition of accidental contamination of dialyzate with Al, and screening may potentially allow earlier recognition of Al loading with greater ability to prevent toxicity.

Table 3 Percentage of abnormal plasma aluminum levels with relationship to patients on aluminum hydroxide according to each year

Year	Patients, N	Patients on $Al(OH)_3$, N (%)*	Plasma Al levels, N	Al > 0.74 μmol/L, N (%)**	Al > 2.2 μmol/L, N (%)
2010	451	143 (31.7)	562	49 (8.7)	5 (0.9)
2011	401	46 (11.5)	524	32 (6.1)	3 (0.6)
2012	420	26 (6.2)	547	20 (3.7)	2 (0.4)
2013	363	18 (4.9)	425	10 (2.4)	0 (0.00)

Al = aluminum; $Al(OH)_3$ = aluminum hydroxide.
*P value < 0.01 for relationship between $Al(OH)_3$ administration over time, **P value < 0.01 for relationship between Al > 0.74 μmol/L over time.

Plasma Al levels, however, are not reliable predictors of chronic Al exposure and there is lack of consensus on threshold cut-off values indicating toxic levels. Historically, routine measurements of plasma Al concentrations have been recommended based on prevalent significant risk of toxicity,[15,26] but later studies have questioned the utility and cost-effectiveness of routine plasma Al measurements in all dialysis patients.[13,16–18] Many dialysis units, however, continue to measure Al levels routinely.

One study reported the incidence of abnormal Al levels in dialysis patients to be as low as 2.1%[13] while another reported an incidence of 4.2%, although the cut-off value of abnormal results in this study was 0.74 μmol/L compared to 1.48 μmol/L in the former.[16] The frequency of abnormal results in our study was 5.4% and 0.49% for results signifying risk of toxicity using the cut-offs of 0.74 and 2.2 μmol/L, respectively. This is consistent with previous studies reflecting an extremely low incidence of abnormal Al levels and greatly reduced risk of toxicity compared to the era of significant Al exposure via dialyzate water and regular use of Al-based phosphate binders.

One study from the United Kingdom argued that measuring Al levels routinely in the current era was unnecessary, although the dialysis patients in that study were not taking any Al-based phosphate binders and Al testing of the dialysis water supply achieved an acceptable minimum safety requirement.[17] Another study reported on the impact of double RO system and continued use of Al phosphate binders in a cohort of dialysis patients between 1998 and 2007.[27] This study reported a reduction in serum Al levels in patients after the new RO with no plasma Al level more than 40 μg/L (1.48 μmol/L), even with Al-based binders.

Plasma Al levels of >3.0 μmol/L have been associated with toxicity; however, defining a baseline plasma Al concentration threshold to diagnose toxic Al accumulation is difficult.[20] There is not a single report in the literature of significant Al toxicity occurring in the presence of Al levels less than 1.5 μmol/L. Elevated Al levels above 1.5 μmol/L in 1 Australian report occurred in less than 2% of patients.[6] Most elevated Al concentrations are one-off isolated levels with sustained abnormal concentrations being uncommon.[16] Therefore, consistent with our study, the literature also supports that the number of elevated Al levels is exceedingly low and often transient. There are no published data to determine whether an increase in plasma levels over time leads to tissue accumulation of Al.

Al replaces calcium at the mineralization front in bone, disturbing osteoid formation and causing low turnover bone problems. There is evidence that single measurements of serum Al show correlation with Al bone disease, with 1 study demonstrating a level greater than 100 μg/L (3.7 μmol/L) as a reliable indicator of Al deposits in bone.[28] Another reported a threefold higher risk for this complication in patients in the highest quartile of serum Al, although there was no threshold level of Al that discriminated between patients with Al bone disease and those without.[15] Another reported that a serum Al level of 60 μg/L (2.22 μmol/L) in combination with an intact Parathyroid Hormone (PTH) < 16 pmol/L provided a relatively sensitive and specific index for the detection of Al-related bone disease.[26]

The diagnosis of Al bone disease is important and some dialysis units continue to monitor Al levels regularly because of concerns that exposure may continue from medications used without knowledge such as over-the-counter antacids. Many other prescribed medications also contain hidden Al in smaller amounts.[6–8,16] One report suggested regular attention should be paid to reviewing medications known to contain significant amounts of Al that patients may be taking without knowledge of their physicians.[16] Al levels have been shown to be higher in patients receiving injectable drugs such as iron, insulin, or erythropoietin compared to those who did not receive these medications.[8]

With the move toward hemodiafiltration and the exposure to even more dialyzate water, there is the potential for increased exposure to Al from poorly maintained or failing RO membranes, so it would be important to maintain review of dialyzate Al and raw water Al levels. The problems associated with Al toxicity are not just confined to HD patients, but patients undertaking PD are also at risk. Al-based phosphate binders have been reported to contribute to toxicity in the latter population as well as non-dialyzed uremic individuals.[29,30]

The possibility of sample contamination due to extraneous sources of Al in samples needs to be considered. Al is a ubiquitous metal and contamination of plasma can occur from sources including environmental dust on the blood tubes or gloves. Considerable care is required in the storage of tubes, phlebotomy procedure, and sample preparation for the determination of Al levels to prevent contamination.

With a very low frequency of elevated total Al levels signifying risk of toxicity (0.49%) at our center and at a significant monetary cost, routine plasma Al determinations in patients at low risk are unlikely to be cost-effective. One report from the United States highlighted that the cost of Al levels may range from $40 to $100 (Spectra Laboratories) and therefore yearly costs of $32,000–$80,000 could be incurred with routine measurement for an average dialysis unit.[16]

Studies have reported that patients on dialysis taking Al-based phosphate binders with RO-treated water had no evidence of Al toxicity, and therefore arguing that the use of Al binders in the era of RO-treated dialysis water may be safe. The vast majority of dialysis patients in our cohort with abnormal plasma Al levels were taking $Al(OH)_3$ as a binder. Although only 21% of all patients on $Al(OH)_3$ had transiently elevated Al levels, this compares to only 3% of subjects not taking Al-based binders. We also report the reduction in use of $Al(OH)_3$ over time with a significantly decreased exposure to these binders being associated with a decreased proportion of patients having elevated Al levels in the more recent period.

Limitations of our study include lack of information on residual renal function, inability to accurately determine the cumulative dose of Al-based binders in individuals, and absence of DFO testing to assess total body Al load. Our study does not address the predictive value of abnormal plasma Al levels and when the frequency of abnormal levels in a population is extremely low, the utility of that test as a screening tool becomes negligible. The other consideration of Al measurement should be of cost-effectiveness, which could not be demonstrated in our study.

Plasma Al as a suitable measure of the body burden to this metal is questionable. Although there is a correlation between plasma levels and Al bone disease, the predictive value of Al concentrations for bone disease is poor. The evidence that Al is absorbed from $Al(OH)_3$ and other Al-containing compounds is indirect, and the methodology for measuring Al levels using stable isotope and mass spectroscopy is very expensive, has limited availability, and should only be performed on a small number of patients. In summary, we feel that regular unselected testing of all dialysis patients is probably unnecessary given the frequency of plasma results indicative of Al overload. The costs of such a testing strategy make it unlikely to be cost-effective. From a patient safety point of view, it makes more sense to monitor RO water levels periodically to ensure the RO is working efficiently. There is some logic in assessing Al levels in patients in whom the risk of overload is high and there is clinical suspicion of toxicity, e.g., those exposed to long-term therapy with Al-containing medications like $Al(OH)_3$, antacids, and concomitant use of any drug that augments gut absorption. Furthermore, guidelines and recommendations should be updated to reflect the reduced risk of exposure from Al-containing dialyzate. Isolated high levels are likely to be caused by contamination at the time of testing and not true Al overload. On the basis of our review, we have now moved to only perform selected testing of plasma Al on the basis of assessment of clinical risk, while routine testing of dialyzate Al is continuing.

Declaration: My coauthors and I declare no conflicts of interest. This study is not supported by any grant or funding.

Manuscript received July 2014; revised August 2014.

REFERENCES

1 Erasmus RT, Savory J, Wills MR, Herman MM. Aluminum neurotoxicity in experimental animals. *Ther Drug Monit*. 1993; **15**:588–592.
2 Perry L, et al. National toxicovigilance for pesticide exposures resulting in health care contact—An example from the UK's National Poisons Information Service. *Clin Toxicol*. 2014; **0**:1–7.
3 Kirschbaum BB, Schoolwerth AC. Acute aluminum toxicity associated with oral citrate and aluminum-containing antacids. *Am J Med Sci*. 1989; **297**:9–11.
4 Dunea G, et al. Role of aluminum in dialysis dementia. *Ann Intern Med*. 1978; **88**:502–504.
5 Gumming A, et al. Acute aluminium intoxication in patients on continuous ambulatory peritoneal dialysis. *Lancet*. 1982; **319**:103–104.
6 Mudge DW, et al. Do aluminium-based phosphate binders continue to have a role in contemporary nephrology practice? *BMC Nephrol*. 2011; **12**:20.
7 Bohrer D, et al. Drugs as a hidden source of aluminium for chronic renal patients. *Nephrol Dial Transplant*. 2007; **22**:605–611.
8 Bohrer D, et al. Role of medication in the level of aluminium in the blood of chronic haemodialysis patients. *Nephrol Dial Transplant*. 2009; **24**:1277–1281.
9 Bohrer D, et al. Influence of the glass packing on the contamination of pharmaceutical products by aluminum. Part I: Salts, glucose, heparin and albumin. *J Trace Elem Med Biol*. 2001; **15**:95–101.
10 Davenport A, et al. Sepsis: A cause of aluminum release from tissue stores associated with acute neurological dysfunction and mortality. *Clin Nephrol*. 1988; **30**:48–51.
11 National Kidney Foundation. K/DOQI clinical practice guidelines for bone metabolism and disease in chronic kidney disease. *Am J Kidney Dis*. 2003; **42**(4 Suppl 3):S1–S201.
12 Kidney Disease: Improving Global Outcomes (KDIGO) CKD-MBD Work Group. KDIGO clinical practice guideline for the diagnosis, evaluation, prevention, and treatment of Chronic Kidney Disease-Mineral and Bone Disorder (CKD-MBD). *Kidney Int Suppl*. 2009; **76**(Suppl 113):S1–S130.

13 Jaffe JA, Liftman C, Glickman JD. Frequency of elevated serum aluminum levels in adult dialysis patients. *Am J Kidney Dis*. 2005; **46**:316–319.
14 Centers for Disease Control and Prevention (CDC). Elevated serum aluminum levels in hemodialysis patients associated with use of electric pumps—Wyoming, 2007. *MMWR Morb Mortal Wkly Rep*. 2008; **57**:689–691.
15 Kausz AT, et al. Screening plasma aluminum levels in relation to aluminum bone disease among asymptomatic dialysis patients. *Am J Kidney Dis*. 1999; **34**:688–693.
16 Sandhu G, et al. Serum concentrations of aluminum in hemodialysis patients. *Am J Kidney Dis*. 2011; **57**:523–525.
17 Gault PM, Allen KR, Newton KE. Plasma aluminium: A redundant test for patients on dialysis? *Ann Clin Biochem*. 2005; **42**(Part 1):51–54.
18 Pepper R, et al. Do oral aluminium phosphate binders cause accumulation of aluminium to toxic levels? *BMC Nephrol*. 2011; **12**:55.
19 Moyer TP, Mussmann G, Nixon DE. Blood-collection device for trace and ultra-trace metal specimens evaluated. *Clin Chem*. 1991; **37**:709–714.
20 Altmann P. Aluminium toxicity in dialysis patients: No evidence for a threshold serum aluminium concentration. *Nephrol Dial Transplant*. 1993; **8**(Suppl 1):25–34.
21 Milliner DS, et al. Use of the deferoxamine infusion test in the diagnosis of aluminum-related osteodystrophy. *Ann Intern Med*. 1984; **101**:775–780.
22 CEC. *Resolution of the Council and the Representatives of the Governments of the Member States, Meeting within the Council, of 16 June 1986, Concerning the Protection of Dialysis Patients by Minimizing the Exposure to Aluminium*, 1986. Available from: http://policy.mofcom.gov.cn/english/flaw!fetch.action?libcode=flaw&id=f3558ede-4604-439a-be3a-484f1c1226ba&classcode=293;330 (accessed date: May 21, 2014).
23 WHO. *Guidelines for Drinking-Water Quality*, 4th edn. Geneva, Switzerland: World Health Organization; 2011; 564.
24 Alfrey A. Aluminum metabolism in uremia. *Neurotoxicology*. 1980; **1**:43–53.
25 Salusky IB, et al. Role of aluminum hydroxide in raising serum aluminum levels in children undergoing continuous ambulatory peritoneal dialysis. *J Pediatr*. 1984; **105**:717–720.
26 D'Haese PC, et al. Value of serum aluminium monitoring in dialysis patients: A multicentre study. *Nephrol Dial Transplant*. 1990; **5**:45–53.
27 Arenas MD, et al. [Use of the aluminum phosphate-binders in hemodialysis in the ultrapure water era]. *Nefrologia*. 2008; **28**:168–173.
28 Charhon S, et al. Serum aluminium concentration and aluminium deposits in bone in patients receiving haemodialysis. *Br Med J (Clin Res Ed)*. 1985; **290**:1613–1614.
29 Smith DB, et al. Dialysis encephalopathy in peritoneal dialysis. *JAMA*. 1980; **244**:365–366.
30 Hewitt CD, Savory J, Wills MR. Aspects of aluminum toxicity. *Clin Lab Med*. 1990; **10**:403–422.